



universität
wien

DISSERTATION

Titel der Dissertation

„Characterization of MPB2C:
A Regulator of Cell-to-cell Transport via
Plasmodesmata“

Verfasserin

Mag. Nikola Winter

angestrebter akademischer Grad

Doktorin der Naturwissenschaften (Dr.rer.nat.)

Wien, 2012

Studienkennzahl lt. Studienblatt:

A 091 490

Dissertationsgebiet lt. Studienblatt:

Molekulare Biologie

Betreuer:

Univ.-Doz. Dr. Friedrich Kragler

Acknowledgements

I want to thank Fritz Kragler for being a great mentor. He allowed me to take part in meetings and congresses from the beginning; he encouraged me to go to workshops and to get to know new methods as well as meeting established researchers and international fellow students in the field. - And all this despite that I was not an easy student and for both of us it was not always easy to work together in the stressful lab routine. Thank you!

I want to thank my lab mates: Daniela Fichtenbauer, Kornelija Pranjic, Eva Klopff, Gregor Kollwig, Shoudung Zhang - it was fun to work together, we became friends, and I will always remember the "old days" with a warm feeling. I want to thank the members of the institute of biochemistry at the University of Vienna and colleagues at the MFPL, Erna Huber, Harald Nierlich, Gabriele Permoser, Andreas Hartig, Andreas Bachmair, Cecile Brocard, Prabhavathi Talloji, Maria Granilshikova, members of the Hartig, Bachmair, Teige and Ammerer lab, and Maria Bauer, former member in the lab of Fritz Pittner.

Furthermore I want to thank Tobias Sieberer, who by offering a position in his lab to me spared me from existential anxiety or the embarrassment of being "unemployed" during the fifteen months it took me to fight against my pride and my exaggerated expectations in order to get this thesis written. Maybe I would not have written it at all otherwise. Thanks go also to the members of the Sieberer lab Olena Poretska, Wenwen Huang, Karin Zwerger and Clemens Uanschou, and from earlier times Christine Marizzi.

I want to thank my reviewers and my PhD committee for their patience and helpful advice.

I want to thank David Jackson and his welcoming and helpful lab team, especially Alexander Goldshmidt and Xianfeng Morgan Xu, for the opportunity to visit the famous and inspiring Cold Spring Harbor Laboratories and for teaching me RNA *in situ* hybridization.

I thank my family, especially my mother Dorothea Winter, for their support and encouragement and my friends, especially Julia Burkart, for thoughtful conversations and for sharing ups and downs during our similar experiences in approaching a career in natural sciences. I want to thank Monika Bachler. I am grateful for the emphatic and personal advice of Freda Meissner-Blau to finish this thesis.

And I appreciate that, born in Europe, in Austria, I had the opportunity to attend university and to graduate without having to go into debts for obtaining a higher education. I see this as a precious gift and as a mandate to deal with it in a responsible way.

Abstract

Characterization of MPB2C, a regulator of cell-to-cell transport via plasmodesmata

MPB2C (MOVEMENT PROTEIN BINDING PROTEIN 2C) is a plant-specific, microtubules-associated protein that was shown to specifically interfere with the cell to cell movement of two very different factors: the *Tobacco mosaic virus* movement protein (TMV MP) essential for the spread of viral infection, and the homeodomain transcription factor KNOTTED1 (KN1) which is involved in stem cell initiation and maintenance. TMV MP and KN1 are able to specifically facilitate their own transport into neighboring cells via plasmodesmata by temporarily altering the size exclusion limit of these dynamic membranous channels that connect plant cells.

The aim of this study was to characterize the function of MPB2C in a developmental context and to gain insight into the significance of homeodomain protein cell-to-cell movement by analyzing plants overexpressing, misexpressing or lacking MPB2C.

The endogenous expression domain of *MPB2C* in *Arabidopsis* overlaps with or flanks the expression domains of genes encoding non-cell autonomous homeodomain proteins, STM and KNAT1/BP, respectively, in the vegetative and inflorescence shoot apical meristems, in gynoecia and in the abscission zone of siliques. This strongly supports the hypothesis of MPB2C being involved in regulation of cell-to-cell transport of these transcription factors *in planta*. Interaction of MPB2C with these proteins was confirmed by bimolecular fluorescence complementation. Yet *MPB2C* is also expressed in other tissues, which suggests a broader scope of MPB2C function beyond the interaction with STM and KNAT1/BP.

Various transgenic plant lines were established that ectopically overexpress *MPB2C*, and two different methods were applied in attempts to create *MPB2C* silencing lines. Furthermore two *MPB2C* point mutants and a T-DNA insertion line were analyzed. No *MPB2C* knock-out lines could be confirmed or established; this could indicate that MPB2C is an essential factor for plant growth. Occasional phenotypic alterations indicating altered stem cell homeostasis or homeodomain protein function in plants with modified *MPB2C* expression were observed. With one *MPB2C* overexpression construct plants resembling *knat1/bp* mutants were obtained. This shows that MPB2C function is important in the regulation of homeodomain proteins beyond meristems in more differentiated tissues as well. The regulatory processes in stem cell domains seem to be robust and they are redundant, hence the malfunction of one component might be largely balanced by others.

The MPB2C protein was shown to be prone to degradation in native cell extracts, but it could be stabilized by adding proteasome inhibitors. A link to proteasomal degradation might be provided via KNB1, a novel protein that interacts with MPB2C and the homeodomain proteins STM and KNAT1/BP. In our working model MPB2C, with the help of KNB1, regulates STM and KNAT1 protein levels and their availability for intercellular transport.

Charakterisierung von MPB2C, einem Protein, das den interzellulären Transports via Plasmodesmen reguliert

MPB2C (MOVEMENT PROTEIN BINDING PROTEIN 2C) ist ein pflanzenspezifisches, Mikrotubuli-assoziiertes Protein, das, wenn es überexprimiert wird, den interzellulären Transport zweier sehr unterschiedlicher Faktoren spezifisch verhindert: Es sind dies einerseits das Tabakmosaikvirus Movement Protein (TMV MP), das für die Ausbreitung der viralen Infektion in der Pflanze verantwortlich ist, und andererseits der Transkriptionsfaktor KNOTTED1 (KN1), der eine wichtige Rolle in der Stammzellbildung und -erhaltung spielt. TMV MP und KN1 vermitteln spezifisch ihren eigenen Transport in benachbarte Zellen über Plasmodesmen, indem sie das Größenausschlusslimit dieser dynamischen membranösen interzellulären Verbindungskanäle zwischen Pflanzenzellen temporär vergrößern.

Ziel dieser Arbeit war es, die Funktion von MPB2C in einem entwicklungsspezifischen Zusammenhang zu charakterisieren und so Einsicht in die Rolle des direkten interzellulären Transports von Homöodomänenproteinen zu erlangen. Dazu wurden Pflanzen mit veränderten Expressionsmengen oder -domänen von MPB2C hergestellt und untersucht.

Die endogene Expressionsdomäne von MPB2C in *Arabidopsis* überlappt mit jener des nicht-zellautonomen Homöodomänenproteins STM und grenzt an die Expressionsdomäne von KNAT1/BP in vegetativen und reproduktiven Apikalmeristemen, im Gynoeceum und der Bruchzone zwischen Früchten und Blütenstielen. Das bekräftigt die Hypothese, dass MPB2C *in planta* an der Regulation des direkten interzellulären Transports dieser Transkriptionsfaktoren beteiligt ist. Die Interaktion zwischen MPB2C und diesen Proteinen wurde durch bimolekulare Fluoreszenz- Komplementation bestätigt. MPB2C wird aber auch in anderen Geweben (z.B. in Wurzelspitzen) exprimiert, was weitere endogene Funktionen von MPB2C nahelegt, welche über die Interaktion mit STM und KNAT1/BP hinausgehen.

Es wurden verschiedene transgene Pflanzenlinien etabliert, die *MPB2C* überexprimieren, und mit zwei verschiedenen Methoden wurde versucht, silencing Linien zu etablieren. Weiters wurden zwei Punktmutanten und eine T-DNA Insertionslinie untersucht. Es konnte jedoch keine *MPB2C* Knockout-Linie bestätigt oder etabliert werden; das könnte darauf hindeuten, dass MPB2C essentiell ist und daher Knockout-Pflanzen nicht überlebensfähig sind. Gelegentlich zeigten einzelne transgene Pflanzen mit veränderter *MPB2C* Expression phänotypische Veränderungen, die auf eine gestörte Stammzellhomöostase oder beeinträchtigte Funktion von Homöodomänenproteinen hinweisen. Ein Überexpressionskonstrukt löste einen Phänotyp aus, welcher der *knat1/bp* Mutante ähnelt. Das zeigt, dass MPB2C nicht nur in Meristemen sondern auch in differenzierteren Geweben an der Regulation von Homeodomänenproteinen beteiligt ist. Die regulatorischen Mechanismen im Stammzellbereich direkt scheinen sehr robust zu sein, und sie sind redundant, sodass die Fehlfunktion einer Komponente großteils kompensiert werden kann.

MPB2C unterliegt in Zellaufschlüssen dem proteosomalen Abbau. Eine Verbindung zum Proteasom-vermittelten Abbau könnte KNB1 liefern. KNB1 ist ein nicht charakterisiertes Protein, das mit MPB2C und mit den Homöodomänenproteinen STM und KNAT1/BP interagiert. In unserem Arbeitsmodell moduliert MPB2C gemeinsam mit KNB1 die Funktion von STM und KNAT1/BP, indem sie deren Verfügbarkeit für den interzellulären Transport beeinflussen.

Abbreviations:

aa	amino acids
ABA	abscisic acid
Ala	alanine
Arabidopsis	<i>Arabidopsis thaliana</i>
AZ	abscission zone
BELL	BEL1-like
bHLH	basic helix-loop-helix transcription factor
BiFC	bimolecular fluorescence complementation
bp	base pairs
CaMV	<i>Cauliflower mosaic virus</i>
Col	Columbia (ecotype)
DNA	deoxyribonucleic acid
ER	endoplasmic reticulum
F1, 2, 3	... indicates <i>filial</i> generations of plants resulting from crosses
GA	gibberellic acid
GFP	green fluorescent protein
GUS	β-glucuronidase
HD	homeodomain
kDa	kilo Daltons
KNOX	KNOTTED1-like homeobox
Ler	Landsberg <i>erecta</i> (ecotype)
LRR-RLK	leucine-rich repeat receptor-like kinase
NAA	1-naphthaleneacetic acid , a synthetic auxin analog
NaCl	sodium chloride
NCAP	non-cell-autonomous protein
NCATFs	non-cell autonomous transcription factors
NLS	nuclear localization signal
nt	nucleotides
ORF	open reading frame
ORMV	oilseed rape mosaic virus
RFP	red fluorescent protein
mRFP	monomeric RFP
RT	room temperature
RNA	ribonucleic acid
mRNA	messenger RNA
miRNA	micro RNA
siRNA	short interfering RNA
SAM	shoot apical meristem
SEM	scanning electron microscope
T1, 2, 3	...indicates generations of <i>transformed</i> plants
TALE	three amino acid loop extension
TF	transcription factor
TMV	tobacco mosaic virus
tobacco	<i>Nicotiana tabacum</i>
UTR	untranslated region
YFP	yellow fluorescent protein

Gene abbreviations:

ACR4	<i>ARABIDOPSIS CRINKLY4</i>
AS1, 2	<i>ASYMMETRIC LEAVES1, 2</i>
ATH1	<i>ARABIDOPSIS THALIANA HOMEBOX GENE1</i>
BOP1, 2	<i>BLADE ON PETIOLE1, 2</i>
BRI1	<i>BRASSINOSTEROID INSENSITIVE 1</i>
CmPP16	<i>C. maxima</i> PHLOEM PROTEIN 1
CR4	<i>CRINKLY4</i>
CRR	<i>CRINKLY4-RELATED</i>
CUC1, 2	<i>CUP-SHAPED COTYLEDONS1, 2</i>
ER	<i>ERECTA</i>
GLO	<i>GLOBOSA</i>
HAE	<i>HEASA</i>
HSL2	<i>HEASA-LIKE2</i>
IDA	<i>INFLORESCENCE DEFICIENT IN ABSCISSION</i>
KN1	<i>KNOTTED1</i>
KNAT	<i>KNOTTED1-like in Arabidopsis thaliana</i>
KNAT1/BP	<i>KNOTTED1-like in Arabidopsis thaliana1</i>
KNB1	<i>KNOTTED1 BINDING PROTEIN 1</i>
LFY	<i>LEAFY</i>
MPB2C	<i>MOVEMENT PROTEIN BINDING PROTEIN 2C</i>
PAS	<i>PASTICCINO</i>
PME	<i>PECTIN METHYLESTERASE</i>
p35S	<i>CaMV 35S promoter</i>
PNF	<i>POUNDFOOLISH</i>
PNY	<i>PENNYWISE</i>
SHR	<i>SHORTROOT</i>
SIEL	<i>SHORTROOT-INTERACTING EMBRYONIC LETHAL</i>
STM	<i>SHOOT MERISTEMLESS</i>
TMV MP	<i>TMV movement protein 30</i>

Nomenclature: Genes are written in *italic* fonts.

p indicates a promoter

:: signifies a gene (right side) under a promoter (left side),

- separates fusion proteins,

>> indicates transactivation.

e.g.: *pPROMOTER::GENE-TAG*

or: *pPROMOTER >>GENE-TAG*

Disclaimer: I tried to identify all holders of the rights of published figures and schemes re-used in this work, and I asked for permission to use these materials in my thesis. In case I might still have unintentionally violated some copyrights I ask to be informed.

Contents

1	Preface	1
2	Introduction	4
2.1	What is life? Definition of terms and concepts.....	4
2.2	No life without communication	6
2.2.1	Multicellular life – more than the sum of its parts	6
2.3	Communication via Plasmodesmata modulated via MPB2C	7
2.4	Signaling molecules and routes of intercellular signaling	7
2.5	Plasmodesmata (PD)	8
2.5.1	PD structure and components	8
2.5.2	PD transport routes and regulation	11
2.5.3	Transcription factors on the move - Plasmodesmata in development.....	15
2.6	KNOX homeodomain proteins – the medium is the message	17
2.6.1	KNOX Homeodomain proteins in plant development	18
2.6.2	Meristem identity from the KNOX perspective - STM	19
2.6.3	Inflorescence architecture from the KNOX perspective – KNAT1/BP	21
2.7	The role of MPB2C in regulation of cell-to-cell transport.....	27
2.8	Addendum 1: The role of cell-wall modifying Pectin Methylesterases in development with regard to plasmodesmal transport.....	29
2.9	Addendum 2: Apoplasmic and symplasmic signaling seems to be interlinked via receptor like kinases	29
3	Results.....	32
3.1	The <i>MPB2C</i> gene and its expression	32
3.1.1	Expression domains of <i>MPB2C</i> in a developmental context	33
3.1.2	<i>MPB2C</i> promoter activity is largely consistent with MPB2C protein localization in seedlings and floral tissues	35
3.1.3	<i>MPB2C</i> is expressed in root and shoot apical regions in seedlings.....	35
3.1.4	<i>MPB2C</i> is expressed in guard cell precursors	36
3.1.5	<i>MPB2C</i> is expressed in vegetative and inflorescence shoot apical meristems.....	36
3.1.6	<i>MPB2C</i> is highly expressed in young carpels and in the abscission zone	44
3.1.7	<i>MPB2C</i> and <i>KNB1</i> are co-expressed in a number of tissues	44
3.1.8	Auxin and Gibberellic Acid, but Absciscic Acid increase <i>MPB2C</i> promoter activity	44
3.2	The MPB2C protein.....	46
3.2.1	MPB2C is plant specific and does not belong to a multi-gene family in <i>Arabidopsis</i>	46
3.2.2	<i>MPB2C</i> encodes a protein with a predicted central coiled-coil domain.....	46
3.2.3	Predicted subcellular localization of the MPB2C protein	47
3.2.4	Dynamics of MPB2C–GFP/RFP subcellular localization	51
3.2.5	The N-terminus of MPB2C is involved in subcellular localization and aggregate formation	52

3.2.6	Deletion of the MPB2C coiled-coil region reduces the tendency to form aggregates	56
3.3	MPB2C <i>in vivo</i> interactions	56
3.3.1	MPB2C homodimerizes and interacts with KNB1	56
3.3.2	MPB2C and KNB1 interact with KNAT1/BP	56
3.3.3	The MEINOX domain of KNAT1/BP is not essential for interaction with MPB2C and not necessary for interaction with KNB1 in BiFC assays	57
3.3.4	The KNAT1/BP MEINOX domain is sufficient but not essential for homodimerization	57
3.3.5	Co-expression of <i>MPB2C</i> and <i>KNAT1/BP</i> with <i>KNB1</i> reduces KNB1 protein levels	60
3.3.6	The central part of the predicted coiled-coil region of MPB2C is not essential for protein-protein interactions	60
3.3.7	MPB2C(delta 178-229), like full-length MPB2C fusion proteins, interferes with KN1 homeodomain cell-to-cell movement	60
3.3.8	Summary: MPB2C protein-protein interactions	61
3.4	Detection of the endogenous MPB2C protein via a peptide antibody	62
3.4.1	MPB2C protein is sensitive to proteasomal degradation	63
3.5	No knock-out line of <i>MPB2C</i> is available	64
3.5.1	<i>MPB2C</i> polymorphisms do not alter phenotypic appearance	64
3.5.2	T-DNA insertion line SALK 90101C	64
3.5.3	<i>MPB2C</i> TILLING point mutation lines	66
3.5.4	Overexpression of an artificial micro RNA reduces MPB2C protein levels only partially	69
3.5.5	No <i>MPB2C</i> knock-out could be obtained based on a hairpin RNA approach	69
3.6	Developmental effects of altered <i>MPB2C</i> expression in <i>Arabidopsis</i>	71
3.6.1	Protein levels of MPB2C are only moderately elevated when expressed from the 35S promoter 71	
3.6.2	N-terminal or C-terminal fusion proteins to MPB2C have different phenotypic effects	72
3.6.3	Ectopic overexpression of <i>MPB2C</i> leads to occasional fasciation	72
3.6.4	Ectopic overexpression of <i>MPB2C(delta 1-58)</i> partially mimics the <i>bp-1/pny</i> phenotype	76
3.6.5	The number of unfertilized ovules is increased in plants overexpressing <i>MPB2C</i>	76
3.6.6	Embryo defects were observed in plants with altered <i>MPB2C</i> expression	80
3.6.7	Expression of <i>MPB2C</i> from the <i>KNAT1/BP</i> promoter might cause embryo patterning defects .	81
3.7	Combined overexpression of <i>MPB2C</i> and <i>KNB1</i> does not alter shoot apex development	82
3.8	Down-regulation of <i>MPB2C</i> in <i>KNB1</i> - overexpressing plants had no obvious effect on development ..	83
3.9	Summary Results	85
4	Discussion – Summary and Outlook	85
4.1	Phenotypic effects of altered <i>MPB2C</i> expression	86
4.1.1	Expected results upon altered <i>MPB2C</i> expression	86
4.1.2	<i>MPB2C</i> down-regulation	86
4.1.3	Expected effects of ectopic <i>MPB2C</i> expression	87

4.1.4	<i>MPB2C</i> misexpression phenotypes manifest in different developmental stages	88
4.2	<i>MPB2C</i> function in the context of homeodomain protein action	88
4.2.1	Does <i>MPB2C</i> regulate <i>STM</i> or <i>KNAT1/BP</i> in the vegetative shoot apex?	89
4.2.2	<i>MPB2C</i> and the link towards proteasomal degradation	90
4.2.3	Fasciation – a potential sign of cytokinin imbalance at the shoot apical meristem	92
4.2.4	A role of <i>MPB2C</i> in female gametogenesis?	93
4.2.5	<i>MPB2C</i> function during embryo patterning – the “hydra”-like phenotype.....	94
4.2.6	A role for <i>MPB2C</i> during internode patterning and pedicel development.....	95
4.2.7	<i>MPB2C</i> without the N-terminal hydrophobic domain is functional	97
4.3	<i>MPB2C</i> function in the context of <i>KNOX</i> genes - and beyond	99
4.3.1	<i>MPB2C</i> , <i>KONX</i> and stomatal development	99
4.3.2	The function of <i>MPB2C</i> in roots remains elusive.	99
4.3.3	<i>MPB2C</i> and <i>KNB1</i>	100
4.3.4	Is <i>MPB2C</i> involved in plant defense?	100
4.4	<i>MPB2C</i> and apoplasmic transport - plant hormones.....	101
4.4.1	Auxin	101
4.4.2	Gibberellins	102
4.4.3	Cytokinin	102
4.4.4	The <i>pas</i> mutants –a connection between <i>MPB2C</i> and lipid rafts?	103
4.4.5	Lipid rafts – a common feature in cell-to-cell transport of homeodomain proteins in animals and in plants?	104
5	Material and Methods	109
5.1	DNA Protocols- Cloning.....	109
5.1.1	<i>E. coli</i> strains	109
5.1.2	Bacterial growth.....	109
5.1.3	<i>E. coli</i> transformation.....	109
5.1.4	Plasmid isolation from <i>E. coli</i>	110
5.1.5	Cloning	110
5.2	RNA protocols	111
5.2.1	RNA extraction	111
5.2.2	RNA <i>in situ</i> hybridization.....	111
5.3	Protein Protocols	112
5.3.1	<i>In silico</i> Protein sequence analysis.....	112
5.3.2	Antibodies	113
5.3.3	Native Protein extraction with proteasome inhibitor.....	113
5.3.4	Protein extraction via Trizol and Acetone precipitation	114
5.3.5	Western blot	114
5.4	Plant Protocols.....	114

5.4.1	Plant growth conditions.....	114
5.4.2	Plant ecotypes.....	115
5.4.3	Transgenic lines.....	115
5.4.4	MPB2C SALK line	116
5.4.5	MPB2C TILLING lines	116
5.5	Agrobacterium strain	116
5.5.1	Agrobacterium-mediated transformation of <i>Arabidopsis thaliana</i>	116
5.5.2	Agrobacterium infiltration of <i>Arabidopsis thaliana</i>	117
5.5.3	Genomic DNA isolation from <i>Arabidopsis</i>	117
5.5.4	Plant pre-treatment with proteasome inhibitor	117
5.5.5	Induction of plants with ethanol.....	117
5.6	Histology	118
5.6.1	GUS staining.....	118
5.7	Microscopy	118
5.7.1	Fluorescence microscopy.....	118
5.7.2	Light microscopy	119
5.7.3	Scanning electron microscopy	119
5.7.4	Digital Photography	119
5.8	Software.....	119
6	Appendix A: RNA <i>in situ</i> hybridization lab protocol.....	120
7	Appendix B – Protein Sequences used for alignment	128
7.1	Species relation of MPB2C homologs	128
7.2	Protein Sequences used for Alignment:	128
7.3	(TAIR) Accession numbers	130
8	Appendix C Primers used	131
9	Appendix D Transgenic Arabidopsis lines	132
10	Appendix E: Raw data trichome count	135
11	References	137
12	Curriculum Vitae	154

1 Preface

My motivation to study molecular biology was to understand what “life” is. What I learned in the past years during my studies and in the lab was less an answer to this question. Rather did I learn a lot about what “scientific knowledge” means and how researchers in natural sciences established methods to achieve the causal explanation of observed phenomena agreed upon by scientific peers. I also learned that the scientific career requires the researcher to leave the lab at some point and to dedicate lots of time and energy to acquiring funding instead of continuing to do what one was trained for during university education.

I chose to work on exploring the function of MPB2C because this protein is involved in regulation of intercellular transport – where coordination and communication meet defense against pathogens, at the point where ingenuity and vulnerability of multicellular organisms meet. Moreover I was fascinated by the finding of French researchers that the non-cell-autonomous homeodomain proteins with which MPB2C interacts also moved between animal cells – despite they have no plasmodesmata (Ruiz-Medrano, Xoconostle-Cazares et al. 2004; Tassetto, Maizel et al. 2005)! And above all, MPB2C could also interfere with HD movement in animal cells – despite that their cytoskeleton functions in very different ways than in plants. I saw this as a possibility to gain more insight into the mechanism of cell-to-cell transport across plasmodesmata, and my idea was that it might have to do with membranes, because that is what animal and plant cells have in common. And there was evidence that the domain responsible for non-cell-autonomous homeodomain protein internalization directly interacts with membranes and promotes receptor-independent endocytosis-mediated internalization (Barany-Wallje, Keller et al. 2005) whereas HD secretion was associated with vesicles enriched in cholesterol and sphingolipids (Dupont, Prochiantz et al. 2007). This special lipid composition is a defining feature of lipid rafts, membrane micro domains, which recently were also postulated to be also associated with plasmodesmata (Raffaele, Bayer et al. 2009). Beside the aspect of cell-to-cell transport and mechanisms of integration of individual cells as functional parts into the organism, the link to stem cells via interaction of MPB2C with one of the stem cell identity genes, *SHOOTMERISTEMLESS*, opened the perspective to gain insight into the most exciting processes in multicellular life: the emergence of complexity out of uniformity, the beginning of cellular differentiation at the borders of meristems.

So, what is life?

If the method to answer this is looking for causes and consequences the answer might be: Life is a robust network of intertwined signaling cascades with feed-forward and feedback loops based on internally determined genetic programs which provide a rich repertoire of ways to react to external cues. Life is constant information processing. The language used in molecular biology bears many terms borrowed from engineering to describe the processes of life. Organisms are described as if they were complex machines with sensors and regulators and switches and regulatory networks. - If life is nothing else than a complicated mechanistic process, we will understand it one day. But this is not what I was curious about. Of course it is fascinating to discover how evolution led to the development of the most elaborate solutions for regulatory processes which are all together integrated into one functional unit, an animal, a plant, a bacterium, or an alga. But there are more skilled minds and people with better memories than mine to understand such processes in detail. These other scientists will dissect all the intricate causal relationships, probably they will be supported by computers, which we need in order to process the incredible amounts of data we are

able to gather today with the advent of all the –omics approaches and other methods of quantitative genetics and biology. But this is not what amazed me when I was asking what life is, and when I decided to study biology.

There exist other definitions of life which deny a simple mechanistic or materialistic explanation. They leave more space for the awe in face of the mystery that life seems to be. Living organisms are autopoietic (Humberto Maturana), open systems maintaining a dynamic equilibrium far from a thermodynamic equilibrium they are one form of dissipative systems (Ilya Prigogine). Life is not only a complicated but a complex phenomenon, complexity being an emergent property. That sounds promising and mysterious in the first place. But do these concepts really explain anything more than the mechanistic perspective does? Or are they just less precise and hence leave open some space for imagination, for associations evading quantification and therefore cannot be addressed by natural sciences? Then they would be no different from the mysterious concept of a *vis vitalis*, the vital force proposed by animist philosophers. On the other hand if they help in their vagueness to direct the attention of curious people to aspects which were neglected so far by natural sciences because they become only visible in an integrated approach which does not get lost in details, then they will stimulate new hypotheses, new experimental approaches, and new ways of measuring. However, if they then can be broken down into quantifiable and measurable aspects, natural sciences will step in and integrate these new aspects into the mechanistic world view. That kind of knowledge gives us security and provides us with the power to intervene and to predict the outcome of manipulations of the systems we can grasp with the means of logic and causality.

So, what is life? I did not find a comprehensive answer, but my search for it during my studies and during my work in the lab led me away from this question. I leave this task to philosophers and theologians, maybe also to lawyers. What relevance, what consequence does it have to find an answer to it at all? Is it not more appropriate to leave the big question aside and to enjoy asking more modest questions, which to solve renders science so rewarding, not to say addictive? This is the art of natural science: To pose the right questions, which are not trivial but precise enough in order to be answered or broken down into smaller questions which can be addressed experimentally.

Another question became more urgent to me in the past years. Not: “What *is* life?” but: “What is the *meaning* of life?” - Another question for philosophers and theologians? I do not think so. I rather think it is the mission and duty for every person to find their own answer to this question, this, in my humble opinion is the foundation of human dignity. Having found ones answer will allow a person to grow to their highest potential for the sake of their own wellbeing and for the sake of all other beings. So, what is the purpose of my life? I feel that the answer has much to do with people and how we relate to ourselves, to each other and to our planet. Science does not stand separate from everything else. Science is embedded in society, in the economic, political and social framework. Competition, mass production (“publish or perish”), and the requirement for economic profitability are defining features of academic life today. - Are these the criteria for good science? Good to know that loyalty, cooperation and even friendship do still exist among some scientist, as I have learned from my supervisor and his way to relate to his colleagues in the field - but this is not at all valued in the current system. Competition leads to keeping results jealously secret instead of sharing findings and material freely and generously – what a waste of time, energy and human potential! Universities being forced (or even volunteering) to implement liberal economic rules - this results in mass production of information rather than knowledge. This means chopping results into bits and pieces in order to get as many publications as possible out of the scientific projects and the project leaders

and the members of the research teams. Consequently findings are diluted out of context and contributing to a huge not even remotely comprehensible ever-growing flood of information. Where does the noise start and where does the signal (knowledge) end? Maximizing economic profitability results in patents on life; in journals which sell knowledge (mostly resulting from publicly funded research) back to the research community and *de facto* prevent public access to this knowledge, and in decisions for funding of proposals promising to be economically exploitable.

This is not the environment in which I want to work. I do not want to waste my energy on this struggle for survival (and I perceive this not just as a metaphor). I am ready to give what I can but I also demand a humane environment for scientists. Funding and publishing should not strictly follow economic rules. I want to do good research in an inspiring and collaborative environment, and I want to contribute to the creation of better working conditions for researchers. However, I still do not know where to start. Definitely not by going into politics. But staying in academia would mean to accept the given system. And even if I tried to do meaningful research, which research do we actually need? Do we need to improve crops for poor countries - when people do not starve or suffer malnutrition because there is not enough food on the planet, but rather because of the unfair distribution of resources and the oppressive dependencies which globalization has created? Do we need to develop drought resistant crops – as long as the insane economic growth paradigm requires ever raising rates of production and consumption that inevitably result in growing waste and greenhouse gas emissions inciting climate change?

The economic paradigm dominating society, politics, science, and culture must change. And it does. A new way of thinking is already emerging, e.g. with the growing movement in support of open access publishing. This paradigm shift will affect all aspects of our life, and I hope still that I will find a way to experience it and promote it while being a scientist. I hope to find my “niche”, to find people and a place where I can contribute with my talents and the skills which I serendipitously had the opportunity to acquire, and I long to find this place rather today than tomorrow. My hope is to find a way to reconcile my rejection of the current scientific environment with my vision of a more fruitful environment and the passion and joy that I found in doing science.

2 Introduction¹

2.1 What is life? Definition of terms and concepts

Despite the fact that physics and chemistry are obviously sufficient as mental tools to explain individual processes of life by – according to the analytical approach of natural sciences – taking the biochemical processes that occur in living organisms into parts, the discussion among scientists about a definition of life is still ongoing (Koshland 2002; Greener 2008). The search for extraterrestrial life (McKay 2004) or the discovery of novel life forms on earth not corresponding to current definitions of life (Wolfe-Simon, Switzer Blum et al.), efforts of synthetic biology to create life *de novo* and questions about the origin of life demand the re-thinking of our definition of life. Since this definition is a man-made mental concept it lies upon the scientific community to agree on what we call “life” at a given time and to adapt our understanding of “life” constantly as our knowledge grows.

The reductionist strategy of focusing on single aspects, which are then quantifiable and can be individually varied under laboratory experimental setups, was the basis that allowed scientists to discover and describe general processes that occur in living organisms. But a pure reductionist and materialist epistemic approach to the definition of life falls short because it is static and because life is considered an emergent phenomenon (Macklem 2008). Systems theory has developed as a discipline to complement the reductionist approach towards the definition of life by establishing a more holistic and dynamic perspective. To exemplify the difference between a reductionist and a holistic approach: The focus on the hereditary material as the key feature of life in the past 150 years led to the establishment of molecular genetics. If Gregor Mendel had not decided to selectively focus on isolated traits and ignore other observations he would have not been able to formulate the principles of genetic inheritance. The novelty of his approach was to restrict his research to distinct attributes instead of taking into account the entire complex organism, and to evaluate his results statistically. This approach was necessary to establish modern biology as a powerful sub-discipline of natural sciences that expanded scientific knowledge from early descriptive approaches to the modern causal understanding of processes in life on the molecular level. However, the more details about mechanisms became clear the more grew the need to integrate this knowledge again into a holistic model of what constitutes life. Back to the example of the hereditary material: By the year 2001 when the first draft of the human genome sequence was published (Venter, Adams et al. 2001), (Lander, Linton et al. 2001) the public disappointment was conspicuous: It became obvious that is not the sheer number of protein-coding genes that makes humans “the pride of creation (or evolution)” which we are (at least often from our point of view...). The number of protein-coding genes in humans is only five times larger than that in *E. coli* and in the same order of magnitude as in many animals and plants. The number of human genes is even exceeded by organisms considered to be of lower complexity, like grape (Pertea and Salzberg 2010).

This “insult” was soon countered by the reasoning that the number of protein coding genes does obviously not account for the complexity of an organism (Carroll 2001; Pertea and Salzberg 2010). Recent findings on the importance of gene regulation and the effects of environmental influences on genes, summarized under the term epigenetics unraveled a much more dynamic perspective on the

¹ To the impatient reader: Please skip this and start at page 7 with chapter 2.3 Communication via Plasmodesmata modulated via MPB2C.

essentials of life. Hence – without a prior reductionist approach focusing on genes we would not have reached the point where we realized that genes are only one physical component of a dynamic complex system that relies not only on its components but on the implications of the coaction between these components². As Erwin Schrödinger stated in his essay “What is life”:

“It is by avoiding the rapid decay into the inert state of 'equilibrium' that an organism appears so enigmatic” (Schrödinger 1944)

All living organisms maintain a state of low entropy, i.e. a state of order, against the second law of thermodynamics which says that systems tend towards an equilibrium state of maximal entropy. Maintaining a constant state of low entropy requires borders, requires inside and outside, self and non-self. Phospholipids due to their amphipatic nature, a charged hydrophilic head group and their hydrophobic tail of fatty acid hydrocarbon chain(s), spontaneously form lipid bilayers in water which build spheres that reseal their surface when disturbed. This lipid bilayer is the basic container or “chemical reaction tube” for all life. The membrane creates and protects identity, but at the same time it is a barrier in two directions, and it is the interface between the organism and the environment. And because life represents a form of dynamic equilibrium, a constant interaction between inside and outside – metabolism in the first place - is vital. Metabolism (whose purpose rather than exchange of matter, as Schrödinger ponders, is the uptake of negative entropy (Schrödinger 1944)) is the most basic relationship between an organism and its environment. This interface also sets the framework for what a living organism can be.

Speaking of negative entropy the concept of information cannot be omitted. In-formation requires content (something con-tained, something distinct from the environment) to be available in a certain *form* and to be recognized as such or to be efficacious in some form on its environment. Among available definitions “*Information = Data + Meaning*” is short and catchy – but “meaning” requires an instance to recognize “meaning”. Therefore I consider one other definition more useful, because it is comprehensive but still does not depend on the concept of a conscious mind:

“Information is any type of pattern that influences the formation or transformation of other patterns.”³

The *form* of that influence may be called a signal. Signals only exist in the context in which they can be perceived. Signal transduction is a linear process in which information is encoded, transmitted, received and decoded. True communication takes place when linear signal transduction becomes closed via a feedback loop. The flow and exchange of information is essential for the establishment and maintenance of complex dynamic systems that maintain a flexible equilibrium on the basis of self-organization. So I would like to slightly modify the declaration “Life is communication” (Günther Witzany) into: “No life without communication”.

² With “system” I mean a set of elements related to and dependent from each other and interacting in a manner that they can be seen as an integrated whole distinct from their environment. A system has a defined inner organization (patterns) through which it emerges, functions and maintains itself.

³ Wikipedia, 11.7.2012 <http://en.wikipedia.org/wiki/Information>

2.2 No life without communication

Communication is a “pattern” of the living system which is essential for the integrated regulation of internal and external processes. A new system emerges when organisms establish a new relationship to their environment beyond linear signal transduction or stimulus and response reaction. This happens when organisms start to communicate with each other in their habitat. This interaction can adopt different degrees of intensity the most intense extreme is when individual cells give up their autonomy in order to become part of a bigger whole, the emergence of a multicellular organism. Identity shifts from individual cells to cell associations, tissues, and organs. Cells no longer need to perform all functions in order to survive and to reproduce, they can differentiate and specialize, but at the same time they become dependent from the other cells in the organism.

This very short summary of the story of phylogenesis, the evolution from unicellular to multicellular life, is also recapitulated in a certain sense during the ontogenesis of each individual multicellular organism that once derived from a single zygote. This totipotent stem cell divides, and the daughter cells are still genetically identical but they activate differential genetic programs and specialize in order to fulfill certain functions but not others. This happens once in the life of a higher animal, where all organs are pre-established during embryogenesis. And it happens continually during the lifetime of a plant, where totipotent undifferentiated stem cells are continually reproduced in the shoot and root apical meristems that supply the plant constantly with cells. As this process continues, cells are gradually displaced from the stem cell niche (Laux 2003) and start to differentiate. Every cell that forms any postembryonic structure in a plant is a direct offspring of a stem cell in a primary or secondary meristem. Of course this generative process relies on the exchange of intercellular signals for coordinated growth.

2.2.1 Multicellular life – more than the sum of its parts

Even bacteria, a life form which chose a survival tactic based on innumerable autonomous individual cells with a fast clonal reproduction, developed means of communication. Be it the exchange of genetic information via horizontal gene transfer or coordinated growth mediated by signaling via quorum sensing. So communication makes sense in evolution, even for the unicellular mavericks. Communication allows the individuals to join forces in certain situations in which single cells on their own have less chance to survive or to occupy new niches within an ecosystem. The positive effects of de-centralized information exchange between equivalent autonomous individual cells can be further increased by specialization of individuals within the collective. In doing so the collective acquires emergent properties - properties different in quality from and exceeding the properties of the individuals. Complexity rises with the number of the interactions between different components/entities. This is the beginning of a new super-organism formed by the cells that started to interact and specialize. There is of course a price to pay for the individual cells: a loss of autonomy up to a degree of specialization where a single cell no longer can survive outside the collective. Life forms in between these two stages are for instance represented by different members of the volvocine algae. There is the unicellular organism *Chlamydomonas reinhardtii*, then there exists the cell colony of 16- 32 individual cells partially differentiated forming *Eudorina*, and there is the form of a multicellular organism consisting of specialized cells called *Volvox carteri* (Kirk 2005; Miller 2010).

It has been suggested that certain genomic changes had led to multicellularity e.g. the increase in the number of SNARE genes necessary for vesicular transport (Sanderfoot 2007; Kloepper, Kienle et al.

2008)⁴ or the advent and differentiation of homeotic genes of the *HOX* cluster, which are essential for eukaryotic body plan establishment (Derelle, Lopez et al. 2007). Recent research suggests that no particular genetic changes led to evolution of multicellularity. Rather the genetic premises were given and hence multicellularity developed many times independently in evolution in all three kingdoms (Bonner 1998) whereas other lineages with the same genetic potential stayed single-celled. It is within this field where cell identity (Homeobox genes) and intercellular signaling (intimately linked with the lipid membranes which are the interface between organism and environment) - hence core features of multicellular organization - meet, where the subject of this thesis is located.

2.3 Communication via Plasmodesmata modulated via MPB2C

In contrast to most animal cells, plant cells are immobile within the organism because they are separated and encased by rigid cell walls mainly consisting of polysaccharides. Still, most plant cells are directly interconnected via plasmodesmata providing a cytoplasmic and membranous continuum. Our group is interested in the regulatory mechanisms of symplasmic signal transduction via plasmodesmata and the role of plasmodesmal signaling in coordination of neighboring cells and tissues during development. **MOVEMENT PROTEIN BINDING PROTEIN 2C** (MPB2C) is involved in the regulation of selective movement of homeodomain transcription factors, which play key roles in development. By further characterizing MPB2C we aimed to gain more insight into the selective plasmodesmal transport route and its role in development.

In this introduction I will first outline the possible routes for plant intercellular signal transduction and the signaling molecules involved. Then I will summarize current knowledge about plasmodesmata, their structure and function in signaling. Subsequently I will introduce **KNOTTED LIKE HOMEBOX** (KNOX) homeodomain proteins and by the example of two non-cell autonomous members of this family, **SHOOTMERISTEMLESS** (STM) and **KNOTTED1 LIKE IN ARABIDOPSIS THALIANA 1/BREVIPEDICELLUS** (KNAT1/BP), I will recapitulate long known and brand new findings about their roles in development. After this, I will summarize what is known about the role of MPB2C in plasmodesmal transport and what the scope of this thesis will be.

2.4 Signaling molecules and routes of intercellular signaling

As stated previously, cells within multicellular organisms need to communicate with each other. The signals used by plants are chemical or electric in their nature. Molecular signals range in their dimensions from gases such as ethylene to large ribonucleoprotein complexes. Some signals function over large distances to convey messages between plants or even between plants and other species, like the sesquiterpenes and other volatiles emitted upon herbivore attack (Pare and Tumlinson 1999) or small secondary metabolites in root exudates that mediate plant-plant or plant-microbe communication in the rhizosphere (Bais, Park et al. 2004). Other molecules - proteins, RNAs and metabolites - act as systemic signals within the plant traveling the phloem [reviewed by (Turgeon and Wolf 2009)] like the famous florigen FLOWERING LOCUS T, or they are transported directly from cell to cell like auxin (Cande and Ray 1976). Then there are short- range signals acting over the distance of a few cells like the peptide ligand **CLAVATA3** (Fletcher, Brand et al. 1999; Rojo, Sharma et al. 2002;

⁴ This is however controversial. In green plants an expansion of SNARES involved in endosomal trafficking occurred at the same time when multicellularity arose. This might have been the basis for polarization of cells as prerequisite for cellular differentiation. Other researchers argue against this postulate pointing out that *Drosophila* and *Caenorhabditis* have about the same number of SNARE genes as *Saccharomyces*.

Lenhard and Laux 2003), which is produced in the shoot apical meristem and binds its ligands CLAVATA1 and CLAVATA2 in order to confine the meristematic domain, or like the homeodomain transcription factor **KNOTTED1** (KN1), which moves from cell to cell via plasmodesmata in the shoot apical meristem and even transports its own mRNA (Jackson 1994; Lucas, Bouché-Pillon et al. 1995).

The signal range is one possibility to classify signals; another one is the kind of the signaling molecules. Some molecular signals have been assigned the status of hormones (Santner and Estelle 2009), others are referred to as peptide ligands (Matsubayashi 2003) or polypeptide hormones (Ryan and Pearce 2001). Other signals like mRNAs (Lucas, Yoo et al. 2001), miRNAs (de Felippes, Ott et al. 2011) or proteins like KN1 (Lucas, Bouché-Pillon et al. 1995) or SHORT ROOT (Helariutta, Fukaki et al. 2000) acting as transcription factors [for reviews see: (Kurata, Okada et al. 2005; Wu and Gallagher 2011)] are not merely messengers activating receptors at the cell surface in order to elicit an intracellular signal transduction cascade, but they themselves are active in the target cells. Recently even lipids have been proposed to function as long-range signals transferred via the phloem (Benning, Tamot et al. 2012).

How do cells emit and perceive molecular signals? There are two possibilities: either the signal must cross membrane(s) or not. The **apoplastic** route implies secretion of the signaling molecule into the intercellular space, the apoplast, and its docking to an appropriate receptor at the surface of the same or another cell. Whether a cell can receive such an apoplastic signal depends on the presence of surface receptors and the diffusion range of the signaling molecules in the extracellular space. The **symplasmic** route does not require the signal to cross membranes, because signals are transmitted directly via gap junctions in animals or via **plasmodesmata** (PD) in plants. PD channels provide a continuum of cytoplasm, plasma membrane and endoplasmic reticulum between neighboring cells. Thus, plants can be regarded as supracellular entities (Strasburger 1882; Tangl 1884; Lucas, Biao Ding et al. 1993; Lucas and Lee 2004). Nevertheless, there is still room for privacy of individual cells, as the PD aperture size, the so-called **size exclusion limit** (SEL), of these membranous tubes can be regulated in higher plants in order to allow receptor-mediated directed and selective transport of certain macromolecules, whereas small solutes can diffuse freely [for extensive reviews see (Haywood, Kragler et al. 2002; Heinlein 2002; Lucas and Lee 2004; Ruiz-Medrano, Xoconostle-Cazares et al. 2004)].

2.5 Plasmodesmata (PD)

The progress in PD research is well documented by countless reviews that continuously reported the state-of-the-art knowledge about PD structure, function and biogenesis (Robards 1975; Robards 1990; Lucas, Biao Ding et al. 1993; Epel 1994; Overall and Blackman 1996; Kragler, Lucas et al. 1998; Crawford and Zambryski 1999; Heinlein and Epel 2004; Lucas and Lee 2004; Maule 2008; Lucas, Ham et al. 2009; Xu and Jackson 2010; Burch-Smith and Zambryski 2012). Here, I will follow the methodological approaches in PD research in order to give the reader an impression from which kind of questions⁵ our current knowledge about PD has arisen.

2.5.1 PD structure and components

In 1879 Eduard Tangl, professor of botany at the University of Czernowitz, Bukowina (today: Ukraine) published his observation of “a continuous protoplasmic body” between the cells of the endosperm

⁵ Each experiment is based on a certain question. The methods available at a given time facilitate but also confine the kind of experiments which can be done and hence the questions which can be answered.

(see Figure 1 A) of various plants. In 1884 in his report “On the theory of protoplasmic continuity in plant tissues”, he described a “traumatropic” re-arrangement of nuclei in epidermal onion cells in response to wounding, even if they were more than 3- 5 cells apart from the incision. He considered this as evidence for a connection between the cells facilitating information exchange (Tangl 1884). Early work was entirely based on microscopic observations, and since PD are below the resolution limit of light microscopy, new methods were required to further investigate these structures.

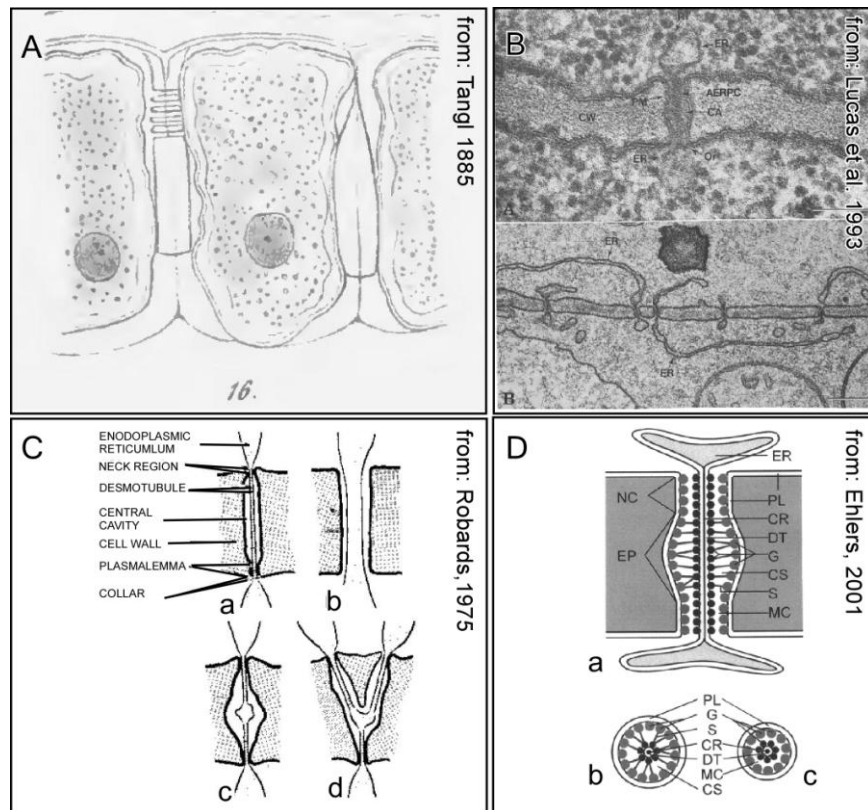


Figure 1: Models of Plasmodesmal Structure

A: Drawing from Eduard Tangl. The picture shows endosperm cells from rye during germination, and connections across the cell wall can be seen. Picture from: (Tangl 1885). **B:** Electron microscopy allowed a resolution high enough to discriminate substructures of PD, and the intimate connection between PD and ER was observed. In the upper picture a single plasmodesma connecting two root cells separated by the cell wall. The lower picture shows the continuity of ER strands across PD. Pictures from: (Lucas, Biao Ding et al. 1993). **C:** First PD schemes showed PD as seen in early electron microscopic pictures. The ER was mostly found “appressed” or constricted (a), and unstricted ER was only seen during early stages of cell plate formation (b). Some PD formed central cavities (c), and other PD were branched (d). Picture from: (Robards 1975). **D:** The PD pore harbors not only the desmotubule membrane but also globular (G) and spoke like (S) proteins connecting the plasma membrane (PL) with the desmotubule (DT). These proteins not only stabilize PD, they also restrict the available space for molecules in the cytoplasmic sleeve (CS) to small 2.5nm microchannels (MC). The CS widens in the central cavity (EP) and is narrow at the neck constriction (NC) whose diameter is dynamically modified via callose deposition in the surrounding cell wall. The cytoskeletal components allow dilation (b) and constriction (c) of the plasmodesma. Scheme from: (Ehlers and Kollmann 2001).

Established in the late 1950ies, the first break-through technology allowing major advances in PD research was electron microscopy (see Figure 1B to D). Naturally, at that time research was still rather descriptive than manipulative. It was also observed that PD are not evenly distributed across cell walls but instead often accumulate in “pitfields”, whereas some cell walls have no PD at all. Different forms of PD were described: simple PD, PD with “median nodules” forming cavities, and “anastomosed”⁶ PD were discerned (see Figure 1C). Continuous membranous structures between

⁶ later these Y-, X- and H- shaped PD were called “branched”

two cells which are observed within the central duct were identified to be derived from the **endoplasmic reticulum** (ER). This central membrane tubes within PD were named “appressed ER”, or also “**desmotubule**”⁷. PD evolution was investigated by means of comparative description. The appressed ER was discovered to be a feature acquired by the green land plants (Cook, Graham et al. 1997). Improved fixation methods and other technical advances allowed better resolution, and other substructures became visible: globular particles and radial “spokes” between desmotubule and plasmalemma, which later were proposed to be helically arranged actin filaments with myosin spokes connecting the plasma membrane and the desmotubule (Overall and Blackman 1996) (see also Figure 1D). First estimates of PD dimensions were made, but they were inconsistent (Robards 1975), and, surprisingly, they are still debated today (Burch-Smith and Zambryski 2012). The biogenesis of PD was investigated, leading to the discrimination between primary PD, which form during cytokinesis between dividing cells when the ER becomes “trapped”⁸ in the phragmoplast, the newly formed cell plate; secondary PD by contrast are inserted *de novo* into the cell wall of neighboring cells. Secondary PD can establish connections between cells which are not of clonal origin and which may even belong to different tissues. About 100 years after Tangl, in the 1970ies and 1980ies, new methods apart from microscopy were established: electrophysiological measurements of PD conductivity were performed; callose formation upon wounding was investigated, and hydraulic conductivity of PD and their density was measured and compared between different species. In early studies it was also observed that plant viruses were associated with and could modify PD. The interaction between viruses and plasmodesmata became an intense and fruitful field of research, and many insights into PD function are derived from these studies which are not summarized here. For recent reviews on this topic please see (Benitez-Alfonso, Faulkner et al. 2010; Niehl and Heinlein 2011; Schoelz, Harries et al. 2011).

Identification of the molecular components of PD proved to be a challenge. Biochemical approaches such as detergent or protease treatment led to the conclusion that the desmotubule must be intimately linked to proteins whereas the plasma membrane lining the PD is sensitive to a certain degree to detergent treatment, which confirms its lipid nature (Tilney, Cooke et al. 1991). In some plants, interference with actin polymerization by cytochalasin D treatment increased PD aperture in the neck region and dilated the desmotubule indicating that the cytoskeleton is involved in PD organization [discussed by (White and Barton 2011)]. Biochemical experiments revealed the existence of plasma membrane microdomains enriched in sphingolipids and sterols. Such microdomains are also called “membrane rafts”, as they are thought to establish liquid crystalline (“liquid ordered”, L_0) lateral compartments in the more fluid (“liquid disordered”) surrounding membrane and to facilitate the sorting and clustering of certain membrane-targeted molecules (discussed in detail below). Evidence is accumulating that also PD membranes might be associated with such rafts [recently reviewed by (Mongrand, Stanislas et al. 2010; Maule, Benitez-Alfonso et al. 2011; Tilsner, Amari et al. 2011)], see also Figure 2 B).

For a long time biochemical approaches to isolate PD were only of limited success, because of the intimate association of PD with the cell wall and with membranes. The distinction between cell wall components and *bona fide* PD constituents was almost impossible. **Immunologic** approaches were used successfully in order to identify PD components: Antibodies were raised against PD-enriched

⁷ in allusion to the term “microtubule”, because of the extremely compact form of this structure (Robards et al. 1975; Tilsner et al. 2011)

⁸ The notion of ER becoming “trapped” is debated, because the ER in this process might not play such an entirely passive role as this term suggests (Boevink et al. 1998; Sparkes et al. 2009).

cell wall fractions (Epel 1996), viral movement proteins [in the hope of recognizing similar plant endogenous PD transported proteins, (Xoconostle-Cazares, Xiang et al. 1999)], or against proteins associated with gap junctions in animals (Yahalom, Warmbrodt et al. 1991)⁹. Later, **genetic screens** were performed to identify PD-localized proteins (Thomas, Bayer et al. 2008), proteins interacting with viral movement proteins (Huang, Andrianov et al. 2001) or with other endogenous proteins known to move via PD (Xoconostle-Cazares, Xiang et al. 1999). Such proteins were cloned and used as baits in order to identify endogenous components of the PD transport machinery. In fact, *MPB2C* was originally identified in this way: A cDNA library was screened in a modified yeast-two-hybrid screen (CytoTrap System) for proteins interacting with the ***Tobacco mosaic virus movement protein*** (TMV MP30) (Kragler, Curin et al. 2003). In a different approach, a cDNA library randomly tagged with fluorescent protein was screened to identify PD-located proteins (Escobar, Haupt et al. 2003). Forward genetics was also applied by mapping mutations leading to increased or decreased capacity of PD-mediated intercellular transport. Of course these mutants were not easy to characterize since altered PD permeability was expected to cause severe phenotypes or even be embryo or seedling lethal. Therefore the harvest of these efforts was rather meager: Nine such mutants were reported so far, and only five of them were characterized: *increased size exclusion limit (ise) 1 and 2*, encoding RNA helicases (Kobayashi, Otegui et al. 2007; Stonebloom, Burch-Smith et al. 2009); of the five isolated *gfp arrested trafficking (gat)* mutants, *gat1* encoding an m-type thioredoxin was characterized (Benitez-Alfonso, Cilia et al. 2009); furthermore *cct8*, which codes for a chaperonin subunit (Xu, Wang et al. 2011; Fichtenbauer, Xu et al. 2012); and finally *decreased size exclusion limit1 (dse1)*, a point mutation in a gene encoding a putative WD40 protein (Xu, Cho et al. 2012). Surprisingly none of these genes encoded structural components of PD, neither did they localize at PD. Apparently PD transport is not only regulated at PD but also in other parts of the cell. Recently, this prompted Tessa Burch-Smith and Patricia Zambryski to proclaim a “paradigm shift” and to propose the “organelle-nucleus-plasmodesmata” (ONP) model taking into account various intracellular but also extracellular signaling processes involved in PD regulation (Burch-Smith and Zambryski 2012)].

Finally in 2011, with the help of a method allowing the enzymatic removal of cell wall components, the **PD proteome** comprising the surprisingly high number of about 1300 proteins was published (Fernandez-Calvino, Faulkner et al. 2011). Current knowledge about PD-localized proteins and the respective references is reviewed in: (Oparka 2004; Fernandez-Calvino, Faulkner et al. 2011; Burch-Smith and Zambryski 2012). Now, despite that many of the players are known (actin, myosin, calreticulin, pectin methyl esterases, peroxidases, callose-synthesizing glucan synthase-like (GSL) proteins and a callose-degrading β -1,3-glucanase, receptor-like kinases, Rab-like proteins, remorin, ...etc.), the exact functional relations among these PD components are still not understood. It is still unclear how many different transport routes exist, how they are regulated, and what renders a factor mobile. A lot remains to be done in this regard (Maule, Faulkner et al. 2012).

2.5.2 PD transport routes and regulation

In 1975 even the role of PD was not clear, and scientists were discussing where and how transport across PD occurred – whether the passage of molecules happened within the cytoplasmic sleeve or within the lumen of the appressed ER -, and how transport was regulated.

⁹ A homology between gap junctions and PD was postulated, which despite similarities at the level of in transport regulation did not prove to be the case on a structural level (Robards 1990).

“If the ER constitutes the symplasm, then plant cells have the opportunity for intercellular transport of materials without the constant crossing of membranes [...] There are therefore good a priori arguments for supposing that plasmodesmata are functional in symplastic transport. There remain difficulties to reconcile with such a role: plasmodesmata often separate cells of quite different types [...], and they must therefore be functionally selective; further, individually or together, they need to be capable of sustaining bidirectional fluxes [...]. It is important to know whether plasmodesmata are, at least to some extent, open continuities from cell to cell which will allow the free interchange of ions and molecules, or whether the symplastic pathway is indeed confined to the cavity of the ER.” (Robards 1975)

Initiated by the discovery of green fluorescent protein (GFP) by Roger Tsien, fluorescence microscopy opened up new possibilities in topology and, thus, in PD research: The PD pore size was determined not by gauging structures but by testing PD permeability in living cells. The PD **size exclusion limit** (SEL) for free diffusion of molecules between cells was established by observing the intercellular movement of fluorescent tracers in the cytoplasm either via pressure microinjection (Wolf, Deom et al. 1989; Waigmann and Zambryski 1995) or ionophoretic microinjection, or by expressing various forms of fluorescent proteins in single cells after microprojectile bombardment of expression vectors (Oparka, Roberts et al. 1999). Also non-invasive methods were established like dye loading experiments such as diffusion-based dye loading (Duckett, Oparka et al. 1994; Kim, Hempel et al. 2002; Christensen, Faulkner et al. 2009), or by expressing fluorescent proteins via tissue-specific promoters in transgenic plants (Kim, Cho et al. 2005). This work established the notion of so-called “symplasmic domains” in which certain cells are more intimately connected than others. Like the SEL itself, these symplasmic domains vary between tissues and change in the course of development (Crawford and Zambryski 2001; Kim, Cho et al. 2005; Kim and Zambryski 2005).

For a long time research focused on the cytoplasmic transport, and only few articles on transport via the membranous parts of PD were published. In the past years, the latter has come back into the focus of research again (Oparka 2004; Gallagher and Benfey 2005; Kragler 2007; Tilsner, Amari et al. 2011). The free movement of molecules across PD was not only tested in the cytoplasm, but also via the plasma membrane (Grabski, De Feijter et al. 1993), the ER membrane (Grabski, De Feijter et al. 1993; Martens, Roberts et al. 2006) or via the ER lumen (Cantrill, Overall et al. 1999; Barton, Cole et al. 2011). Surprisingly only the outer leaflet of the plasma membrane seems to provide a barrier inhibiting lateral diffusion of molecules across PD. It was not unequivocally shown whether the inner membrane leaflet allows lateral diffusion or not [discussed by (Tilsner, Amari et al. 2011)] but the dense coverage of globular proteins and the “spokes” between desmotubule (the appressed ER) and the plasma membrane within the channel rather argue against lateral diffusion of proteins attached to the inner leaflet of the plasma membrane across PD. Fluorescent reporters were also targeted to certain subcellular domains like the ER or the cytoskeleton, which prevented intercellular movement. Interestingly, nuclear targeting was not sufficient to abolish movement of molecules up to 40 kDa (Crawford and Zambryski 2000).

Much of the early research on PD function originates from studies with viral movement proteins. The dynamic nature of the PD SEL was soon discovered. The SEL does not only change in the course of development, and it does not only differ between tissues; the SEL can change even within one single cell, which means that PD can be actively opened (gated) to facilitate intercellular transport. Thus, indeed both modes of PD transport postulated by the research community exist: one is the non-targeted diffusion-driven movement of small molecules, and the other is targeted, **selective**

transport which allows even molecules considerably larger than the basal SEL to pass through PD. Hence, PD are not rigid or static pores in the cell wall but highly flexible dynamic channels which can be gated and which are equipped with mechanisms to identify their cargo and to mediate selective transport. Huge ribonucleoprotein complexes – endogenous as well as of viral origin –selectively target and move through PD. This seems to be facilitated by chaperone- assisted unfolding and refolding (Kragler, Monzer et al. 1998; Kragler, Monzer et al. 2000; Aoki, Kragler et al. 2002; Xu, Wang et al. 2011; Fichtenbauer, Xu et al. 2012). Transport is not only selective but also **directional**, at least between certain tissues: The same protein (GFP-KN1) moved from the mesophyll to the epidermis but not in the reverse direction in the leaf, whereas no such directionality was observed within the shoot apical meristem (Kim, Yuan et al. 2002; Kim, Yuan et al. 2003). Asymmetry in PD transport was even observed for molecules which move by diffusion (Christensen, Faulkner et al. 2009).

Biochemical treatments with cytoskeleton depolymerizing or stabilizing agents revealed that some transport routes require intact **cytoskeletal** components (reviewed by (White and Barton 2011)), treatment with chemicals that interfere with vesicle trafficking showed that some transport routes involve components of the **endomembrane system** [reviewed by (Oparka 2004; Gallagher and Benfey 2005; Tilsner, Amari et al. 2011)]. Genetic approaches revealed that phosphorylation (Wagmann, Chen et al. 2000; Lee, Taoka et al. 2005), glycosylation (Taoka, Ham et al. 2007), GPI anchors (Simpson, Thomas et al. 2009) or transmembrane domains [of PD-localized proteins (Thomas, Bayer et al. 2008) and of PD transport regulators (Lee, Yoo et al. 2003)] are important for PD targeting or for the regulation of cell-to-cell movement of some proteins [reviewed in (Oparka 2004; Rim, Huang et al. 2011)].

However, no conserved “**zip code**” for PD targeting or gating could be identified. Although several protein motifs involved in PD transport or PD targeting have been described (Chen, Sheng et al. 2000; Aoki, Kragler et al. 2002; Kim, Rim et al. 2005; Taoka, Ham et al. 2007; Thomas, Bayer et al. 2008), there is no common motif among all tested non-cell-autonomous proteins [see also review by (Kragler 2007)]. For instance, one of the identified sequences seems to be context-dependent: In motif swapping experiments, a highly conserved C-terminal sequence of the non-cell-autonomous heat shock cognate 70 (Hsc70) chaperone could confer non-cell autonomy upon a closely related human Hsp70 chaperone but not upon GFP (Aoki, Kragler et al. 2002). In contrast, the sequence necessary and sufficient for selective cell-to-cell transport of the homeodomain protein KN1 could confer non-cell-autonomy upon unrelated proteins (Kim, Rim et al. 2005). KN1 was the first transcription factor in plants identified to move from cell to cell via PD. A modified KN1 with three Lysine- to Alanine substitutions N-terminally adjacent to the homeodomain (KN1 M6) lost the capacity to move (Lucas, Bouché-Pillon et al. 1995). However, it took ten more years to identify a sequence of 70 amino acids length including the homeodomain and the N-terminal adjacent region with an NLS (KN₁₂₅₆₋₃₂₆) which was shown to be necessary and sufficient for selective PD transport (Kim, Rim et al. 2005). Interestingly, the KN1 M6 mutation not only abolished cell-to-cell movement of KN1, it also almost completely abolished interaction with MPB2C (Winter, Kollwig et al. 2007). Transmembrane domains seem to be another way to target PD. Thomas et al. (Thomas, Bayer et al. 2008) identified a PD-localized protein, PDLP1, targeted to PD via the secretory pathway. The transmembrane domain of PDLP1 was sufficient to confer PD localization to a citrine variant of YFP. As discussed by (Tilsner, Amari et al. 2011), vesicle fusion takes place in the proximity of PD but not within PD, so two signals must exist within the PDLP1 transmembrane domain, one for vesicle

membrane targeting and fusion with the plasma membrane in the proximity of PD, and a second signal for lateral diffusion and anchoring within the PD membrane.

There are many seemingly contradictory findings on PD transport, e.g.:

- Co-existence of free diffusion regulated via the PD pore size with selective targeting and gating of PD;
- The finding that large as well small molecules can cross PD either via the cytoplasmic sleeve or via the ER membrane or the ER lumen;
- Association with certain cytoskeletal components which can enhance or block movement;
- Mobility of some proteins seems to be regulated via phosphorylation and glycosylation, and for other proteins binding to pectin methylsterases (PMEs) is essential for transport despite that PMEs would rather be expected to modify extracellular cell wall components;
- RNA and proteins seem to have PD targeting signals whereas for others the overall structure including size seems to be decisive.

These findings now converge into the bigger picture which shows the coexistence of different routes for PD targeting and PD passage, which are regulated in various ways. These recent findings will allow scientists to disentangle the various observations by sorting them and assigning them to different kinds of PD transport routes. Figure 2A shows a model of intracellular routes targeting non-cell-autonomous proteins (NCAPs) for PD transport, and Figure 2B depicts a model mapping the different membranes and membrane subcompartments in PD.

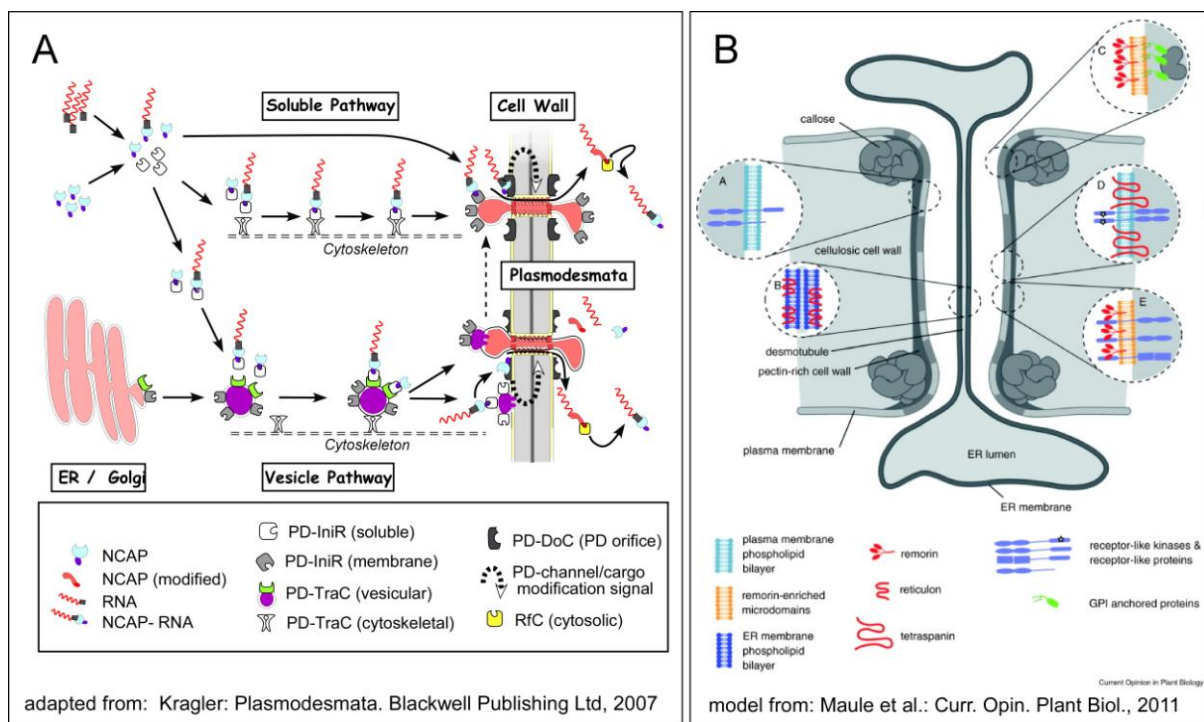


Figure 2: Current Models of Plasmodesmal Transport and Membrane Composition

A: The model shows two routes of selective NCAP transport towards PD. One is the soluble pathway, and the other is a vesicle-mediated pathway. Both routes are associated with the cytoskeleton and they require the following steps: (1) recognition of the NCAP in the cytoplasm, (2) transfer along the cytoskeleton towards PD where PD receptors recognize NCAPs (3) and trigger a PD/cargo modification signal which subsequently mediates transport (4). In the target cell re-folding of the partially unfolded transported NCAP is required (5). NCAP: non cell autonomous protein; PD-IniR: PD initial receptor; PD-TraC: PD transport complex; PD-DoC: PD docking complex, RfC: refolding chaperone. Model adapted from: (Kragler 2007). **B:** Structural model of a plasmodesma with emphasis on the membrane subcompartments (cytoskeletal elements are omitted, compare with Figure 1 D). The pectin- and callose- enriched (= cellulosic) cell wall is lined by the plasma membrane which is compartmentalized by tetraspanins or by membrane rafts providing platforms for accumulation of

receptor like kinases and GPI-anchored proteins. The strong curvature of the appressed ER membrane is mediated by reticulons. Model from: (Maule, Benitez-Alfonso et al. 2011).

2.5.3 Transcription factors on the move - Plasmodesmata in development

Although it was evident that cell-to-cell communication is essential for multicellular plants, Anthony Robards in his review 1975 cited the bleak statement of his colleagues a few years earlier:

...“we cannot assign any role to the plasmodesmata with any confidence” (Robards 1975)

37 years later, how much confidence do we have now in assigning roles to PD? The initial prognosis that PD transport was essential for plants has been confirmed by the isolation of embryo and seedling lethal PD mutants (Kobayashi, Otegui et al. 2007; Benitez-Alfonso, Cilia et al. 2009; Stonebloom, Burch-Smith et al. 2009; Xu and Chua 2010; Koizumi, Wu et al. 2011; Xu, Cho et al. 2012). We know that diffusion in younger tissues is less restricted than in most differentiated tissues; that water, ions, lipids, solutes, peptides and proteins, and even ribonucleoprotein complexes containing mRNA and small siRNA and miRNA can cross PD. An astonishingly large part of proteins known to move via PD are **transcription factors** (TFs) [reviewed by: (Haywood, Kragler et al. 2002; Wu, Dinneny et al. 2003; Cilia and Jackson 2004; Oparka 2004; Ruiz-Medrano, Xoconostle-Cazares et al. 2004; Gallagher and Benfey 2005; Kurata, Ishida et al. 2005; Kurata, Okada et al. 2005; Wu and Gallagher 2011)]. And conversely, a considerable portion of TFs belonging to various protein families such as homeobox, GRAS, MYB, MADS box, bZIP, and bHLH proteins has been found to be capable of cell- to-cell movement (Lee, Colinas et al. 2006; Rim, Huang et al. 2011). These findings prompted Bill Lucas and colleagues to ask whether transcription factors might have been non-cell-autonomous by default and only became restricted in their movement or entirely cell autonomous during evolution, especially after the insertion of the ER-derived desmotubule into PD (Lucas, Ham et al. 2009). The function of non-cell-autonomous TFs in patterning processes has been shown in various contexts, here some examples are given:

- The movement of the small bHLH transcription factor **TARGET OF MONOPTEROS7** (TM07) expressed in the embryo proper is the signal moving into the adjacent suspensor in order to specify the embryonic root meristem (Hamann, Mayer et al. 1999; Schlereth, Moller et al. 2010).
- In roots, endodermis specification is dependent on the movement of **SHORTROOT** (SHR), a GRAS family TF (Nakajima, Sena et al. 2001), whereas root hair formation depends on **CAPRICE** (CPC), a non-cell-autonomous Myb-like DNA-binding domain protein (Wada, Kurata et al. 2002).
- In the shoot apical meristem and in inflorescence meristems, the stem-cell identity promoting homeodomain transcription factor **WUSCHEL** (*WUS*) moves from the rib meristem/organizing center into the central and peripheral zone of the meristem where it activates transcription of **CLAVATA3** (CLV3), which encodes a secreted peptide that upon binding to its receptors **CLAVATA1 & 2** (CLV1 & 2) restricts in turn *WUS* expression (Yadav, Perales et al. 2011).
- Stomatal patterning in the epidermis has also been associated with PD transport: The basic helix-loop-helix transcription factor **SPEECHLESS** (SPCH) is required for asymmetric epidermal cell divisions necessary for the initiation of the stomatal cell lineage (MacAlister, Ohashi-Ito et al. 2007). The cell-to-cell movement of SPCH is regulated via callose deposition at PD via **GLUCAN SYNTHASE-LIKE 8** (GSL8) (Guseman, Lee et al. 2010) and via an unknown

mechanism dependent on the glycosyltransferase-like protein, **KOBITO1** (Kong, Karve et al. 2012).

- In leaves, trichome spacing is coordinated by **GLABRA 3** (GL3)- mediated trapping and depletion of the non-cell autonomous, trichome-identity-promoting WD40 repeat protein **TRANSPARENT TESTA GLABRA1** (TTG1) (Bouyer, Geier et al. 2008).
- In flowers, two MADS-box transcription factors, **DEFICIENS** and **GLOBOSA** (GLO) regulate stamen and petal identity in a non-cell autonomous fashion (Perbal, Haughn et al. 1996), and movement of **LEAFY** (LFY) is required for activation of homeotic genes involved in patterning of the floral meristem (Sessions, Yanofsky et al. 2000).
- Correct patterning of abaxial pedicel cell identity depends on the movement of the homeodomain transcription factor **KNAT1/BP** into cells beyond its expression domain (Douglas, Chuck et al. 2002; Venglat, Dumonceaux et al. 2002; Kim, Yuan et al. 2003)

Intriguingly, the role of cell-to-cell movement of the first non-cell-autonomous TF in plants described, the homeodomain protein **KNOTTED1** (Lucas, Bouché-Pillon et al. 1995), is still not fully understood (see below). The routes and regulation mechanisms of several other non-cell autonomous transcription factors have been described. Obviously these molecules use different transport routes: It was suggested that LFY or SPCH movement, similar to free GFP, is based on diffusion and can be regulated by altering the SEL (Wu, Dinneny et al. 2003; Kong, Karve et al. 2012). The movement of SHR in roots between stele and endodermis via PD can also be suppressed by decreasing the SEL upon increased callose synthesis (Vaten, Dettmer et al. 2011). This suggests that SHR moves via the cytoplasmic sleeve, but interestingly SHR (like the non-cell autonomous transcription factors CPC, TMO7 and AGAMOUS-LIKE 21) was observed to bind to an endosome-associated protein, **SHORTROOT-INTERACTING EMBRYONIC LETHAL** (SIEL), and hypomorphic SIEL alleles impaired SHR movement (Koizumi, Wu et al. 2011). In other words, at least in the case of SHR, an endosome-associated factor (SIEL) is important for cytoplasmic cell-to-cell movement of SHR.

The **KNOX class I** (KNOX I) homeodomain transcription factors KN1, STM and KNAT1/BP move in a selective and directed manner, and actively alter the PD size exclusion limit (Lucas, Bouché-Pillon et al. 1995; Kragler, Monzer et al. 2000; Kim, Yuan et al. 2003). Their transport route is also thought to occur via the cytoplasmic sleeve, but as STM did not interact with the endosome-associated, movement-promoting SIEL (Koizumi, Wu et al. 2011), STM and by inference probably KNOX I trafficking seems to be regulated in a way distinct from SHR. Results from the lab of David Jackson corroborate the idea that SHR and KNOX I proteins use distinct trafficking routes via PD, since mutations in the *CCT8* gene coding for a chaperonin abolished KNOX I movement but not SHR movement (Xu, Wang et al. 2011).

The difficulty in identifying the role of cell-to-cell movement for KNOX class I function lies in the fact that the domain necessary and sufficient for movement is part of the homeodomain, which mediates DNA- binding and hence is pivotal for KNOX I function as transcription factors. Therefore an experimental approach is needed to interfere with KNOX I movement but not with their activity as transcriptional regulators. One such approach was to generate GUS-KNOX fusion proteins. The large N-terminal GUS protein impairs KNOX I cell-to-cell movement but does not abolish KNOX I function as transcriptional regulators. Such GUS-KNOX I fusion proteins expressed from different promoters were used for complementation assays. Expression of cell autonomous *GUS-KNAT1* from the ubiquitous 35S promoter did fully complement the *bp* phenotype. But when GUS-KNAT1 was expressed from the endogenous *KNAT1/BP* promoter in *bp* mutants, only the stem elongation

phenotype but not the pedicel angle and epidermal patterning phenotypes in *bp* mutants were complemented (Rim, Jung et al. 2009)¹⁰. Hence, KNAT1 movement itself seems not to be essential for its function, but KNAT1 is required to be present in tissues outside its expression domain. Other results support the notion that at least for certain STM functions protein movement itself is necessary: First, whereas expression of a movement-competent GFP-KN1 fusion protein from the *STM* promoter did rescue the strong *stm-11* mutant, a cell autonomous GUS-KN1 fusion protein, even when expressed from the *35S* promoter, was only able to partially rescue *stm-11* mutants (Kim, Yuan et al. 2003). Second, in *CCT8* chaperonin co-suppression lines, STM cell-to-cell movement was impaired, and plants failed to continue shoot growth after germination similar to strong *stm* mutants (Xu, Wang et al. 2011). Interestingly, despite that cell autonomous GUS-KNOX I fusion proteins were obviously functional and could complement KNOX I mutants at least partially, no KNOX I overexpression phenotypes were triggered by these movement-incompetent constructs, neither with *p35S::GUS-KN1/stm-11* (Kim, Yuan et al. 2003) nor with *p35S::GUS-BP/bp-3* (Rim, Jung et al. 2009).

The recently described *gorgon* (*gor*) mutant with an arginine to lysine mutation at position 53 of the STM homeodomain might open another possibility to investigate KNOX I function (Takano, Niihama et al. 2010). This missense mutation caused continuous enlargement of the primary meristem, a phenotype which in other experiments was associated with KNOX overexpression. But *STM^{gor}* is not a hypermorphic allele: First, in contrast to wild type *STM*, *STM^{gor}* depends on the presence of *PNY*. Second, like the movement incompetent GUS-KNOX I fusion proteins (Kim, Yuan et al. 2003; Rim, Jung et al. 2009), *STM^{gor}* did not cause typical KNOX overexpression phenotypes when ectopically expressed. Although the mutation was assumed to affect DNA binding specificity or affinity, this has not been tested yet. It also remains to be tested whether *STM^{gor}* is still able to move via PD or not.

We reasoned that MPB2C might provide a third way to approach the question of how important KNOX I movement is. MPB2C was shown to bind KNOX I proteins and to interfere with KN1 homeodomain-mediated cell-to-cell movement when overexpressed in leaves (Winter, Kollwig et al. 2007). MPB2C did not interact with a KN1 variant lacking the homeodomain, and even the change of three amino acids in the *KN1 M6* mutant, which abolished KN1 movement (Lucas, Bouché-Pillon et al. 1995), also abolished interaction with MPB2C (Winter, Kollwig et al. 2007). Therefore, as a cellular protein interfering with KNOX I transport, MPB2C seemed to be an attractive tool in order to investigate the importance of KNOX I cell-to-cell movement during development.

2.6 KNOX homeodomain proteins – the medium is the message

Homeodomain (HD) proteins are transcriptional regulators with a common 60 amino acid sequence, the homeodomain, which mediates DNA binding. They are encoded by so-called homeotic genes, “master genes”, which are essential for patterning and development in all higher organisms. Homeodomain proteins regulate the establishment of the body plan in sponges, vertebrates, plants and fungi (Gehring, Affolter et al. 1994). A HD gene subclass, the **TALE** (three amino acid loop extension) family, is conserved among plants and animals (Burglin 1997). In plants, TALE proteins comprise the **KNOX** (KNOTTED1-like homeobox) and **BELL** (BEL1-like) subfamily, which can homo- and heterodimerize (Bellaoui, Pidkowich et al. 2001) in various combinations (Hackbusch, Richter et al. 2005). In plants, KNOX-BELL interaction is thought to regulate subcellular localization (Bhatt, Etchells et al. 2004; Cole, Nolte et al. 2006; Lee, Lin et al. 2008; Rutjens, Bao et al. 2009) and target-

¹⁰ for a detailed description of the *knat1/bp* mutant please see chapter 2.6.3

DNA binding affinity (Smith, Boschke et al. 2002) of the dimers. Interestingly, some of these homeotic master regulators are NCAPS. They can selectively move from cell to cell in animals (Prochiantz 2000) and in plants (Lucas, Bouché-Pillon et al. 1995; Kim, Yuan et al. 2003; Kim, Rim et al. 2005). In other words: as mobile transcription factors, they themselves are the signal and the message at the same time. Non-cell-autonomous homeodomain proteins in plants belong to the KNOX class I subfamily, and they have been shown to move selectively across PD. Additionally, similar to some viral movement proteins they form ribonucleoprotein complexes and mediate the transport of their own mRNA. However, it is not known why these proteins move and why they transport their own mRNA instead of being expressed in a larger domain. Of the four KNOX class I proteins encoded by the *Arabidopsis* genome (the classification of KNOX genes follows below), only STM and KNAT1/BP were shown to move from cell to cell, whereas KNAT2 and KNAT6 did not; neither did KNAT3, which belongs to KNOX class II (Kim, Rim et al. 2005). These results are derived from experiments in leaf tissues where these genes are not expressed endogenously. Interestingly, inter-tissue movement was unidirectional in the leaf – KNOX I proteins moved from mesophyll to the epidermis but not in the other direction - whereas movement was possible between all layers in all directions in the shoot apical meristem (Kim, Yuan et al. 2003; Kim, Rim et al. 2005). This suggests that other cellular components are involved in the tissue-specific regulation of KNOX I movement across PD. MPB2C might be one of these factors (Winter, Kollwig et al. 2007).

2.6.1 KNOX Homeodomain proteins in plant development

KNOX transcription factors in plants are involved in various patterning events during development: in shoot apical meristem initiation and maintenance, in establishing floral meristem architecture, in leaf patterning, pedicel and abscission zone formation, and in the patterning of floral organs [reviewed by: (Chan, Gago et al. 1998; Hake, Smith et al. 2004; Hay and Tsiantis 2010)]. Together with their respective BELL interacting proteins they are thought to integrate diverse signaling events on a gene regulatory level [see e.g. (Wu and Smith 2012)]. *Arabidopsis* encodes eight “classical” KNOX genes and *KNATM* (Magnani and Hake 2008), which lost the homeodomain. KNOX genes fall into two classes based on their sequence homology (Chan, Gago et al. 1998; Hake, Smith et al. 2004). KNOX I genes (*STM*, *KNAT1/BP*, *KNAT2*, and *KNAT6*) are expressed in the shoot apical meristem and in other distinct domains, whereas KNOX class II genes are expressed more broadly (see Table 1).

gene	Accession	expression domains	references
STM	At1g62360	from the globular embryo onwards in shoot vegetative, inflorescence, floral and axillary meristems, carpels	(Barton 1993; Endrizzi, Moussian et al. 1996; Long, Moan et al. 1996; Long and Barton 1998; Long and Barton 2000; Bhatt, Etchells et al. 2004; Scofield, Dewitte et al. 2007; Takano, Niihama et al. 2010)
KNAT1 /BP	At4g08150	heart stage embryo, shoot vegetative, inflorescence meristems, stem (cortex), lateral root base, pedicel, abscission zone, style	(Lincoln, Long et al. 1994; Chuck, Lincoln et al. 1996; Douglas, Chuck et al. 2002; Venglat, Dumonceaux et al. 2002; Mele, Ori et al. 2003; Smith and Hake 2003; Truernit, Siemering et al. 2006; Ragni, Belles-Boix et al. 2008)
KNAT2	At1g70510	Embryo, root, shoot vegetative meristem, floral meristems, carpel primordia, replum, internode-pedicel junction, floral abscission zone	(Lincoln, Long et al. 1994; Dockx, Quaedvlieg et al. 1995; Pautot, Dockx et al. 2001; Venglat, Dumonceaux et al. 2002; Ragni, Belles-Boix et al. 2008; Li, Pi et al. 2011)
KNAT3	At5g25220	expressed in most tissues; not in the root tip	(Serikawa, Martinez-Laborda et al. 1996; Truernit, Siemering et al. 2006)
KNAT4	At5g11060	almost every organ; root vasculature	(Serikawa, Martinez-Laborda et al. 1996; Truernit, Siemering et al. 2006)
KNAT5	At4g32040	almost every organ; flanks of lateral roots, boundary between cell division and elongation	(Serikawa, Martinez-Laborda et al. 1996; Truernit, Siemering et al. 2006)
KNAT6	At1g23380	Embryo: meristem, boundary maintenance; root, shoot vegetative meristem, flower, carpel, internode-pedicel junction, floral abscission zone	(Dean, Casson et al. 2004; Belles-Boix, Hamant et al. 2006; Ragni, Belles-Boix et al. 2008)
KNAT7	At1g62990	Xylem	(Zhong, Lee et al. 2008)
KNATM	At1g146760	boundaries of cotyledon primordia, leaf primordia, lateral domains of flower meristems, base of gynoecium/abscission zone, adaxial proximal side of mature lateral organs	(Magnani and Hake 2008)

Table 1: KNOX genes in Arabidopsis.

Table modified from: (Hamant and Pautot 2010)

2.6.2 Meristem identity from the KNOX perspective - STM

STM is an essential gene. Strong *stm* mutants arrest growth after germination, because they fail to establish a **shoot apical meristem** (SAM) (Barton 1993). Weaker *stm* alleles are able to resume growth after a phase of growth arrest and initiate a post-embryonic SAM via activity of other genes (Clark, Jacobsen et al. 1996; Endrizzi, Moussian et al. 1996). *STM* is also required for meristem identity in the reproductive phase (Kanrar, Onguka et al. 2006; Scofield, Dewitte et al. 2007; Smith, Ung et al. 2011). In flowers, *STM* conveys carpel identity (Scofield, Dewitte et al. 2007). The vegetative SAM in *stm* mutants can be rescued by the expression of *KNAT/BP1*, and *KNAT2* can replace *STM* function in carpel formation, which shows that these closely related genes display a certain functional redundancy while maintaining special functions as well (Byrne, Simorowski et al. 2002; Scofield, Dewitte et al. 2008). Consistent with this, ectopic overexpression of *STM*, *KNAT1/BP*, *KNAT2* and *KNAT6* yields similar phenotypes of reduced growth due to inhibited cell expansion and cell differentiation, aberrant leaf shapes like lobed leaves and ectopic meristematic tissue, and floral patterning abnormalities. All these phenotypes can be traced back to inhibition of differentiation programs (Lincoln, Long et al. 1994; Chuck, Lincoln et al. 1996; Pautot, Dockx et al. 2001; Dean, Casson et al. 2004).

STM establishes the shoot meristem in the embryo and then prevents cells from entering into differentiation programs. The *STM* expression domain defines the meristem region, and the *STM* promoter is often used as a SAM marker. The cells which are - through continuous but slow division of the stem cells - replaced from the stem cell niche enter regions which provide an environment that no longer promotes stem cell fate but triggers the initiation of differentiation programs. In vegetative shoot meristems most displaced cells assume the identity of rosette leaf primordia budding from the meristem in a spiral phylotactic pattern. Sites of lateral organ initiation can be identified even before any visible morphological changes as regions at the shoot apex with local

auxin maxima and the absence of *STM* expression (Heisler, Ohno et al. 2005). After floral transition, the SAM is converted into the inflorescence meristem which now produces phytomers, secondary inflorescences (branches) and eventually flower meristems instead of rosette leaves. All new aboveground organs of the reproductive stage are derived from the inflorescence meristem, where the inflorescence architecture is patterned. Units forming the modular structure of the inflorescence are called phytomers, each consisting of an internode (the stem), a cauline leaf, and an axillary meristem (Steeves and Sussex 1989). In contrast to stem cells of the vegetative, inflorescence and floral meristem, stem cells of the axillary meristems are initiated *de novo*. The flower meristem gives rise to the floral organs: four sepals, four petals, six stamens and a gynoecium or carpel consisting of two valves which fuse to enclose two strands of placental tissue branching out to the ovules in *Arabidopsis*. The placental tissue is supplied with nutrients via vascular strands in the replum separating the two strands of placental tissue. The flower stalks are called pedicels and provide the junction between flowers and the stem. After fertilization, the organs of the three outer floral whorls – sepals, petals and stamen – are shedded via controlled reduction in cell-to-cell adhesion in the so-called abscission zone at the junction between the floral organs and the pedicel. After fertilization the gynoecium is called silique and remains attached to the pedicel until the seeds are ripe. Then dehiscence takes place, where lignified cells at the valve margins enter senescence and become dry. This creates tensions triggering the detachment of the two valves from the replum so that the mature seed are released (Ferrandiz, Pelaz et al. 1999; Roberts, Elliott et al. 2002). After floral transition *STM* expression remains active in the central regions of the inflorescence meristem and in tissues of the floral meristem which give later rise to the gynoecium (Schofield, Dewitte et al. 2007). *STM* is not active in the gametes and becomes re-activated during the globular stage of the embryo when the SAM of the new plant is established (De Smet, Lau et al. 2010).

Whereas several factors involved in control of *KNOX* gene expression are known [for reviews please see: (Ori, Eshed et al. 2000; Carraro, Peaucelle et al. 2006; Hay and Tsiantis 2010)], no comprehensive screen for *STM* target genes has been published so far. *STM* plays a role in hormone regulation in the SAM [reviewed by (Shani, Yanai et al. 2006)] by directly regulating the expression of genes involved in **gibberellic acid** (GA) biosynthesis and degradation in order to maintain low GA levels in the SAM (Tanaka-Ueguchi, Itoh et al. 1998; Hay, Kaur et al. 2002; Jasinski, Piazza et al. 2005). *STM* induces cytokinin biosynthesis genes. Increasing cytokinin levels either via exogenous application or through increased biosynthesis partially rescued *stm* mutants (Yanai, Shani et al. 2005). Well-studied regulators of *STM* expression are the NAC domain transcription factors **CUP SHAPED COTYLEDONS** (CUC) 1 and 2, which initiate *STM* expression in the embryo, where *STM* subsequently maintains *CUC* gene expression (Aida, Ishida et al. 1999). *STM* represses expression of the transcription factor **ASYMMETRIC LEAVES 1** in the SAM whereas in lateral organs, in the absence of *STM*, AS1 and AS2 in turn repress *KNAT1/BP*, *KNAT2* and *KNAT6* (Ori, Eshed et al. 2000; Semiarti, Ueno et al. 2001; Phelps-Durr, Thomas et al. 2005; Guo, Thomas et al. 2008). *STM* interacts with BEL1-like homeodomain proteins (Hackbusch, Richter et al. 2005), which themselves regulate *KNOX* gene expression, like e.g. **SAWTOOTH** 1 and 2 (Kumar, Kushalappa et al. 2007). Polycomb group chromatin remodeling complexes are involved in direct repression of *KNOX* class I genes (Xu and Shen 2008).

This is only a short non-comprehensive overview of what is known about *STM*. However, it is still a mystery why *STM* selectively moves from cell to cell, and why the protein probably transports its own mRNA. *KN1* in maize is not expressed in the outermost layer of the SAM, in which no *KN1* mRNA but *KN1* protein was detected (Jackson 1994). Although a non-cell autonomous effect of *KN1* was already known for long time (Hake and Freeling 1986), this difference in *KN1* mRNA and protein

localization in fact prompted Sarah Hake, Bill Lucas, David Jackson, and colleagues to investigate whether the KN1 protein itself can traffic from cell to cell – which it does (Lucas, Bouché-Pillon et al. 1995). However, *STM* in *Arabidopsis* is expressed in all meristem layers (Long, Moan et al. 1996) – so if at all: Where does STM move in *Arabidopsis*, and why? KNOX movement has been suggested to help integrate the meristem and coordinate developmental programs in adjacent cells (Kim, Yuan et al. 2003). But it is also possible that STM movement in the *Arabidopsis* shoot apex is not essential: *stm* mutants could be partially rescued with a movement-deficient *GUS-KN1* construct expressed from the 35S promoter. A significant difference between overexpression of movement- incompetent GUS-KN1 and movement- competent GFP-KN1 was that GUS-KN1 despite high expression levels did not trigger phenotypes typical for ectopic KNOX overexpression (Kim, Yuan et al. 2003).

2.6.3 Inflorescence architecture from the KNOX perspective – *KNAT1/BP*

KNAT1/BP is expressed in the peripheral zone of the vegetative SAM and after floral transition at the base of the inflorescence meristem, in the cortex of internodes, and in pedicels. *KNAT1* is highly expressed in nodal regions and in the abscission zone (Lincoln, Long et al. 1994; Douglas, Chuck et al. 2002; Douglas and Riggs 2005; Shi, Stenvik et al. 2011). This correlates well with the *knat1/bp* mutant phenotype: reduced internode length, short pedicels (hence the name *brevipedicellus*), downward-oriented siliques, reduced apical dominance, achlorophyllous cell files on epidermal internode cells overlying vascular tissue beneath of pedicels. These achlorophyllous stripes consist of differentiation-defective cells with aberrant epidermal patterning which show ectopic deposition of lignin. Moreover, *bp* plants develop bulgy structures in the abscission zone which are associated with premature shedding of floral organs (Lincoln, Long et al. 1994; Chuck, Lincoln et al. 1996; Venglat, Dumonceaux et al. 2002; Mele, Ori et al. 2003; Wang 2006; Shi, Stenvik et al. 2011). Unlike *STM*, *KNAT1* is not essential for shoot apex initiation or maintenance.

It was known that the function of *KNAT1* in internode patterning relies upon interaction with the BEL1-like homeodomain transcription factor **PENNYWISE** (PNY, also called **BELLRINGER**, **REPLUMLESS**, **VAMAANA**, or **BLH9**) (Byrne, Groover et al. 2003; Roeder, Ferrandiz et al. 2003; Smith and Hake 2003; Bhatt, Etchells et al. 2004; Cole, Nolte et al. 2006). Both mutants cause aberrant internode patterning and result in reduced internode length. Characteristic for *pny* mutants is the irregular internode patterning leading to stems with regions of clustered siliques and regions with no siliques at all. In *pny/knat1* double mutants internodes are even shorter whereas plants have still downward-pointing siliques and clusters of siliques (Smith and Hake 2003; Bhatt, Etchells et al. 2004). This additive phenotype suggests that each gene product functions also in contexts where the other one is not required. Consistent with this, the expression domains of both genes overlap at the periphery of the inflorescence meristem, in stems and pedicels but differ in other tissues. Furthermore, PNY like two other BEL1-like HD proteins, **POUND-FOOLISH** (PNF) and **ARABIDOPSIS THALIANA HOMEBOX GENE1** (ATH1), interacts with STM, and these three BELL genes act redundantly in establishing the embryonic SAM, in vegetative SAM maintenance, and in establishment and maintenance the inflorescence meristem (Rutjens, Bao et al. 2009; Ung, Lal et al. 2011). This is what makes KNOX proteins “master” transcriptional regulators: their combinatorial potential. It is thought that the combination of KNOX and BELL transcription factors available in a given tissue leads to activation or repression of a certain set of genes, and that the same KNOX gene product regulates the expression of different target genes in the presence of other BELL interaction partners (Ragni, Truernit et al. 2007).

So, the interaction between KNAT1 and PNY is necessary for correct internode patterning, but how to explain the downward-pointing pedicels or the achlorophyllous stripes in *bp* mutants? The observed interaction of PNY with *KNAT6* (Bhatt, Etchells et al. 2004) and *KNAT2* (Ragni, Belles-Boix et al. 2008) draws a line from gene regulation during internode patterning to the other hitherto unexplained *bp* mutant features. Recent research shed light on an entire interlinked molecular network involved in internode patterning, pedicel development and establishment of the abscission zone. Apart from KNAT1/BP the characters in this (inter)play are as follows: **KNAT2** and **KNAT6**, two other *KNOX class I* genes; **ATH1**, another BEL1-like homeodomain protein (Quaedvlieg, Dockx et al. 1995; Gomez-Mena and Sablowski 2008; Li, Pi et al. 2011), **BLADE ON PETIOLE (BOP) 1** and **2**, two BTB-ankryin transcriptional co-regulators involved in lateral organ boundary organization (Ha, Kim et al. 2003; Hepworth, Zhang et al. 2005; Ha, Jun et al. 2007); and the peptide ligand **INFLORESCENCE DEFICIENT IN ABSCISSION (IDA)** with its receptor kinases **HAESA (HAE)** and **HAESA LIKE2 (HSL2)**; just to mention it: the levels of auxin and ethylene also regulate abscission (Patterson 2001; Taylor and Whitelaw 2001), but these plant hormones will not be discussed here.

2.6.3.1 *KNAT1/BP and abscission zone patterning*

A feature of KNAT1/BP which remained undiscovered for quite a long time is that it acts as a negative regulator of floral organ abscission (Wang 2006; Shi, Stenvik et al. 2011). The common function of KNAT1 seems to lie in patterning organ boundaries, mostly by restricting expression domains of genes promoting cell differentiation in these zones. The establishment of pedicel orientation and abscission zone patterning seem to be interlinked, since plants with abscission defects often also show abnormal expression of genes involved in pedicel orientation. This correlation is corroborated by the finding of a vestigial abscission zone between internode and pedicel (Stenvik, Butenko et al. 2006). Abscission defects are observed in the following mutants: *bop1/2* (McKim, Stenvik et al. 2008), *kna2/6* (Shi, Stenvik et al. 2011), *ath1* (Gomez-Mena and Sablowski 2008), and in *ida* mutant plants (Butenko, Patterson et al. 2003). All these genes are part of the KNAT1 interaction network.

Abscission zone differentiation can be divided into four consecutive stages (Patterson 2001): I) differentiation of **abscission zone (AZ)** cells; II) acquiring the competence to respond to abscission signals; III) cell wall loosening through pectin degradation and cell expansion; IV) separation of the organ and formation of a lignified protective layer. Transition to stage II depends on the function of *BOP1* and *2*, which are necessary for cells to become competent to respond to abscission signals (McKim, Stenvik et al. 2008). As the name suggests, *BOP1* and *BOP2* are also involved in leaf patterning: *BOP1* directly binds to and activates the promoter of *AS2*, encoding a LOB domain transcription factor promoting adaxial leaf cell fate specification in *Arabidopsis*. *AS2* together with the Myb domain transcription factor *AS1*¹¹ represses *KNAT1*, *KNAT2* and *KNAT6* in the leaf (Ori, Eshed et al. 2000; Semiarti, Ueno et al. 2001; Ha, Kim et al. 2003; Ha, Jun et al. 2007; Guo, Thomas et al. 2008; Jun, Ha et al. 2010). Overexpression (Xu, Xu et al. 2003) or gain of function (Li, Pi et al. 2011) of *AS2* caused *bp*-like pedicel phenotypes, but the endogenous situation seems to be different in inflorescences. *BOP1/2* do not seem to activate *AS2* in pedicels, because *KNAT1* expression was not increased in *bop1/2* mutants (Khan, Xu et al. 2012). In fact, *AS2* is extremely low expressed in pedicels and stems and only weakly in nodes (Lin, Shuai et al. 2003; Yamaguchi, Yamaguchi et al. 2012). Moreover, in contrast to the situation in leaves, *BOP1/BOP2* do not repress but activate *KNAT6* expression (but not *KNAT2* expression). Consequently, the *p35S::BOP2* phenotype is rescued in *kna6* (but not in *kna2*) mutant plants (Khan, Xu et al. 2012). *KNAT1* in combination with PNY

¹¹ which itself is repressed by STM in the shoot apical meristem (Byrne, Barley et al. 2000)

restricts the expression of *KNAT2* and *KNAT6* in pedicels and internodes to the abscission zone and the junction between stem and pedicel, respectively. In *bp* and in *pnv* mutants the expression domains of *KNAT2* and *KNAT6* extend to slightly different degrees into the entire pedicel and into the stem (see Figure 3). Accordingly, the *knat6* (but not the *knat2*) mutant can rescue the *pnv* phenotype and partially rescues the *bp* phenotype. The *bp* phenotype is completely rescued in *bp/knat2/knat6* or *bp/knat2/knat6/pnv* and partially rescued in *bp/knat6* or *bp/knat6/pnv* mutants (Ragni, Belles-Boix et al. 2008).

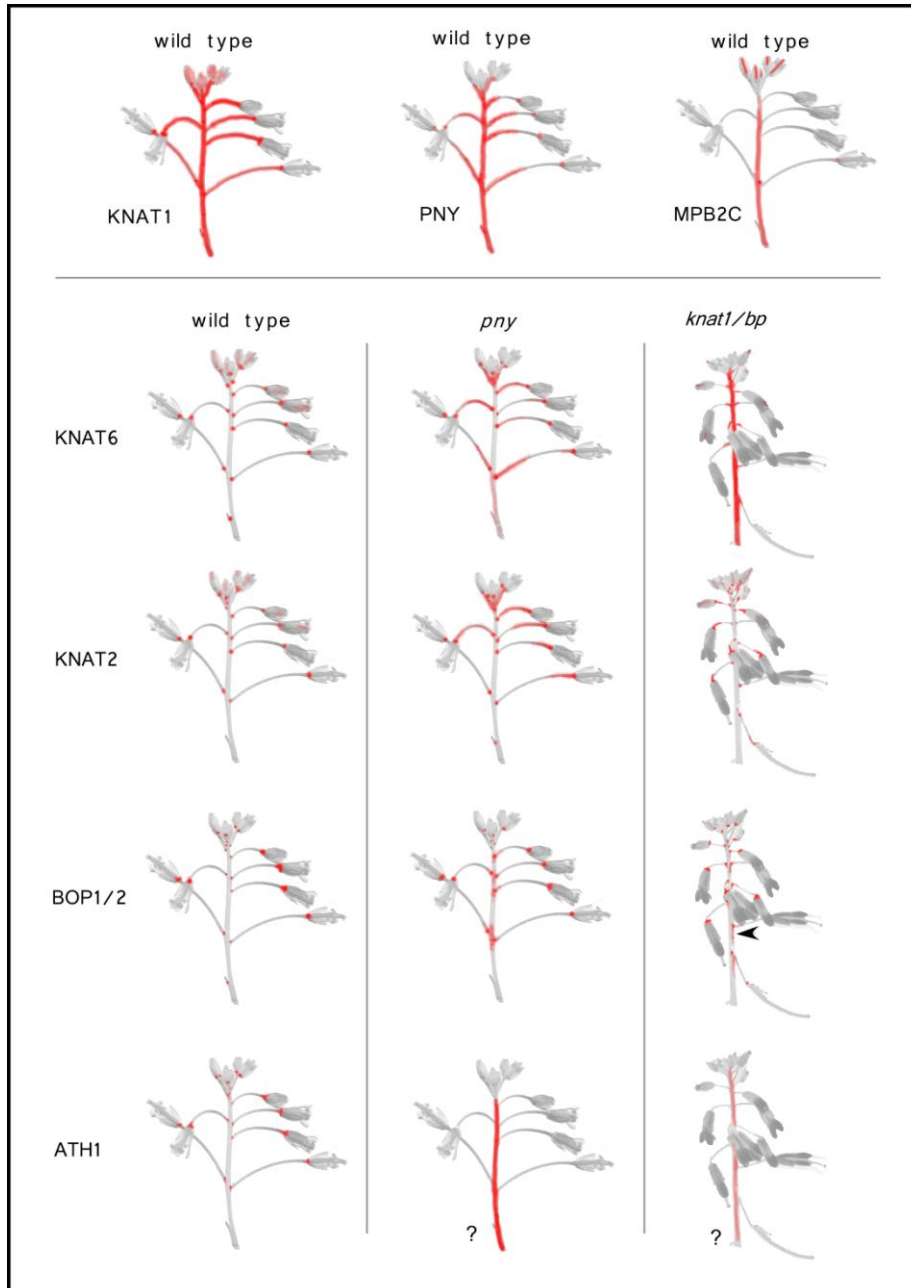


Figure 3: Altered expression domains in pedicels and stems of *bp* and *pnv* mutants

In wild type plants *KNAT1* and *PNY* are expressed in stems, pedicels, nodes and the abscission zone. *MPB2C* is strongly expressed in carpels and weakly in internodes subtending flowers after anthesis. *MPB2C* expression is upregulated in the abscission zone around and after abscission of sepals and petals (not shown, see Figure 13). Expression of *KNAT2*, *KNAT6*, *BOP1*, *BOP2*, and *ATH1* are restricted to nodes and to the abscission zone. In *bp* and *pnv* mutants the expression zones of these genes extend to different degrees into pedicels and internodes. Data for *KNAT1* and *PNY* expression are derived from GUS stains published by (Douglas, Chuck et al. 2002) and (Roeder, Ferrandiz et al. 2003), respectively. *MPB2C* expression domains in inflorescences were published in (Winter, Kollwig et al. 2007) and this thesis. Data for *KNAT6* and *KNAT2* expression are derived from GUS stains published in (Ragni, Belles-Boix et al. 2008). Data for *BOP1* and *BOP2* expression are

derived from GUS stains in (Khan, Xu et al. 2012). The arrowhead shows extension of *BOP1/2* expression into regions basipetally of nodes corresponding to the reported achlorophyllous stripes in *bp* mutants (Douglas, Chuck et al. 2002). *ATH1* expression in wild type was reported by (Dockx, Quaedvlieg et al. 1995) and (Gomez-Mena and Sablowski 2008). For *ATH1* expression in *bp* and *pnv* mutants only qRT-PCR data from internode tissue are available. Kahn et al. reported significantly increased *ATH1* levels in *bp* mutants and very strong upregulation of *ATH1* expression in *pnv* mutants (Khan, Tabb et al. 2012).

KNAT1 also has a direct effect on *BOP1/2* expression: Similar to the *KNAT2* and *KNAT6* expression domains, the expression domains of the *BOP1* and *2* genes are expanded in *bp* and in *pnv* mutants, and the ectopic expression of *BOP2* in *bp* mutants in cell files of internodes beneath pedicel junction exactly correlates with the achlorophyllous ectopically lignified stripes observed in *bp* mutants (Khan, Xu et al. 2012). So, *BOP1/2* expression is regulated by *KNAT1*, and the genes act (whether directly or indirectly) in an antagonistic manner on common target genes, like on *KNAT2* and *KNAT6* or on lignin biosynthetic genes (Khan, Xu et al. 2012). Like *knat2/knat6* double mutants, the *bop1/2* double mutant completely rescues the *pnv* phenotype and is able to rescue the *bp* pedicel phenotype (Butenko, Shi et al. 2012). Interestingly, *PNY* as well as *KNAT1* were shown to regulate the expression of cell wall modifying pectin methyl esterases. So, apart from an indirect effect via repression of abscission-promoting genes *KNAT2* and *KNAT6*, *KNAT1* and *PNY* might also have a direct effect on abscission (see Addendum 1: The role of cell-wall modifying Pectin Methyl esterases in development with regard to plasmodesmal transport).

2.6.3.2 *KNAT1/BP and pedicel patterning*

BOP1/2 overexpression causes downward-oriented pedicels and clustered siliques similar to the phenotype of *pnv/bp* mutants (Ha, Jun et al. 2007; Khan, Xu et al. 2012). As mentioned previously, *BOP1/2* does not act on *KNAT1* on a transcriptional level in pedicels but rather seems to interfere with *KNAT1* function via antagonistic action on common target genes. Consistent with this, *KNAT1* expression is not altered in *bop1/2* mutants (Khan, Xu et al. 2012). In *bp/bop1/2* triple mutants the *bop1/2* abscission defect is still visible but the pedicel orientation phenotype caused by the *bp* mutation is suppressed (Khan, Xu et al. 2012), which puts *BOP1/2* downstream of *KNAT1/BP* in pedicel patterning. So, if the main function of *KNAT1* in pedicel patterning is to repress *BOP1/2* (and hence to interfere with activation of *KNAT2*, *KNAT6* and *ATH1*), then absence of *BOP1/2* no longer requires *KNAT1* function. Derepression of *KNAT2* and *KNAT6* seems to be the cause for the pedicel orientation phenotype in *bp* mutants, because *knat2/knat6* double mutants also rescue the *bp* pedicel orientation phenotype (Ragni, Belles-Boix et al. 2008). However, overexpression of *KNAT6* alone is not sufficient to cause downward-oriented pedicels (Khan, Xu et al. 2012). Here, it would be interesting to see if co-overexpression of *KNAT6* with its BELL partner *ATH1* (see below) results in downward-oriented siliques, and/or if *KNAT2* needs to be co-expressed.

Another player in signaling during abscission zone formation is *IDA*, encoding a peptide ligand which binds the two receptor-like kinases *HAE* and *HSL2*. They in turn activate a MAP kinase signaling cascade (Butenko, Patterson et al. 2003; Cho, Larue et al. 2008; Stenvik, Tandstad et al. 2008), which eventually leads to activation of *KNAT2* and *KNAT6* transcription (Butenko, Shi et al. 2012). Abscission is absent in *ida* mutants, whereas overexpression of *IDA* causes premature organ shedding and ectopic abscission of pedicels, branches and cauline leaves through activation of vestigial abscission zones (Stenvik, Butenko et al. 2006). *IDA*, *HAE* and *HSL* are expressed in the abscission zone (Butenko, Patterson et al. 2003), whereas the five *IDA-like* genes (*IDL1* to *5*) in *Arabidopsis* are expressed in other tissues like e.g. in cotyledon vasculature, guard cells of young seedlings, at the adaxial base of the pedicel, and in the funiculus (Stenvik, Tandstad et al. 2008). Note that *MPB2C* is also expressed in

these tissues [(Winter, Kollwig et al. 2007) and this work]. IDA signaling promotes abscission, and KNAT1 acts downstream of IDA, since *bp* mutants rescue the *ida* abscission defect (Shi, Stenvik et al. 2011). Like *BOP1/2*, *IDA* is not involved in KNAT1 transcriptional regulation, since *KNAT1* is not upregulated in *ida* mutants. But *KNAT2* expression is strongly reduced, and *KNAT6* is absent in the abscission zone of *ida* mutant plants, indicating increased KNAT1 activity - or impaired BOP1/2 function. The authors speculate that IDA could trigger a KNAT1 post-translational modification, which might regulate its movement and by this way interfere with KNAT1 function (Shi, Stenvik et al. 2011; Butenko, Shi et al. 2012). However, *p35S::IDA* plants have no downward-oriented siliques (Stenvik, Tandstad et al. 2008), as would be expected if KNAT1 movement was abolished like in the *bp*-rescue experiments with *pKNAT1::GUS-KNAT1/bp-3* plants expressing a movement-incompetent form of KNAT1 (Rim, Jung et al. 2009) described below. Moreover, earlier experiments showed that abscission defects in *bop1/2* mutants are epistatic to the premature abscission phenotype caused by *p35S::IDA* (McKim, Stenvik et al. 2008). This rather directly places BOP1/2 and not *KNAT1/BP* downstream of IDA signaling. So it remains to be shown if and how IDA or BOP1/2 act on KNAT1 (see model in Figure 4). Apart from ERECTA, IDA is the second receptor-like kinase which is involved in KNAT1 signaling (please see Addendum 2: Apoplasmic and symplasmic signaling seems to be interlinked).

The BEL1-like homeodomain transcription factor **ATH1** is expressed in vegetative and floral meristems and at organ boundaries (Gomez-Mena and Sablowski 2008). ATH1 physically interacts with STM, KNAT1, KNAT2 and KNAT6 (Hackbusch, Richter et al. 2005; Cole, Nolte et al. 2006; Li, Pi et al. 2011). ATH1 together with two other BEL1-like homeodomain proteins PNY and PNF plays a role in vegetative SAM maintenance, probably via redundant interaction with STM, because *ath1/pny/pnf* triple mutants mimic *stm* mutants (Rutjens, Bao et al. 2009). At the transition to flowering, *ATH1* is down-regulated, and overexpression of *ATH1* interferes with internode and pedicel elongation. *ath1* mutants show defects in abscission zone patterning, and they do not shed floral organs (Gomez-Mena and Sablowski 2008). *ATH1* is upregulated in *pny* and *bp* mutants, and conversely the *pny* phenotype is rescued completely, and *bp* phenotype partially in *ath1* mutants, but less efficiently than in *knat6* mutants (Khan, Tabb et al. 2012). Partial rescue in *bp/ath1* double mutants indicates that *ATH1* might not be the only BELL co-factor for *KNAT2* and *KNAT6* in pedicel patterning. BOP1/2 activity not only induces expression of *KNAT6* but also of *ATH1*. All three genes are co-expressed in the abscission zone and at the junction between stem and lateral organs. In these tissues, *ATH1* as a BELL co-factor interacts with *KNAT2* (Li, Pi et al. 2011) and with *KNAT6* (Li, Pi et al. 2011; Khan, Tabb et al. 2012). The KNOX-BELL heterodimerization with *ATH1* seems to be a central feature for *KNAT2* and *KNAT6* function in these tissues, since the *ath1* mutation suppresses the *p35S::BOP2* phenotype (Khan, Tabb et al. 2012) and the *bp*-like pedicel phenotype of AS2-gain of function plants (Li, Pi et al. 2011). Interestingly, *ATH1* acts back on *KNAT1* expression: *KNAT1* expression in the base of flower buds, the future abscission zone, but not in pedicels is reduced in *ath1* mutants (Gomez-Mena and Sablowski 2008).

The pedicel is not a simple radially symmetric structure. It consists of distinct domains which are determined through different factors. It has a proximal and a distal identity as well as distinct adaxial lateral and abaxial cells (Douglas, Chuck et al. 2002, Douglas, 2005 #1143; Douglas and Riggs 2005). The angle between pedicel and internode results from coordination of cell differentiation and elongation between the adaxial and the abaxial side of the pedicel and the establishment of a border between pedicel and stem. *LEAFY* seems to be a key regulator in mediating adaxial pedicel fate by restricting the elongation of adaxial cortical cells at the pedicel base, probably via activation of other

adaxial cell fate genes like *REVOLUTA* and *PHABULOSA* (Yamaguchi, Yamaguchi et al. 2012). In *bp* mutants, the distal abaxial and lateral cells of the pedicel do not properly differentiate. The expanding and differentiating adaxial cells outgrow the abaxial cells, which in turn results in the downward-bending of the organ (Douglas and Riggs 2005). *KNAT1* together with *PNY* restricts *BOP1/2* and *KNAT2/6* expression to the adaxial nodes and to the abscission zone. Ragni et al. showed ectopic activity of the *KNAT2* promoter in distal regions of pedicels in *bp* mutants (Ragni, Belles-Boix et al. 2008). Interestingly, a movement-incompetent GUS-*KNAT1* fusion protein expressed from the *KNAT1* promoter could rescue the short internode phenotype in *bp* plants but not the pedicel-orientation phenotype. However, when expressed from the ubiquitous 35S promoter, GUS-*KNAT1* could rescue all *bp*- associated phenotypes (Rim, Jung et al. 2009). This indicates that *KNAT1* protein must be present in cells where the gene is not expressed endogenously, but *KNAT1* movement itself does not seem to be necessary for *KNAT1* function. However, here again, as described for the analogous experiment with *STM* (Kim, Yuan et al. 2003), the ubiquitous expression of movement-incompetent GUS-*KNAT1* did not trigger *KNAT1* overexpression phenotypes (Rim, Jung et al. 2009).

We obtained *bp/pny* like phenotypes in *Arabidopsis* lines transgenic for *p35S::MPB2C(delta 1-58)-RFP* indicating compromised function of these proteins upon ectopic expression of *MPB2C* which might either prevent movement of *KNAT1* or trigger degradation of *KNAT1*. Figure 4 shows a model of the regulatory interactions during pedicel and abscission zone patterning possibly involving *KNAT1*. However, the big question still remains unanswered: Why is *KNAT1* not simply expressed in all cells where its presence is required?

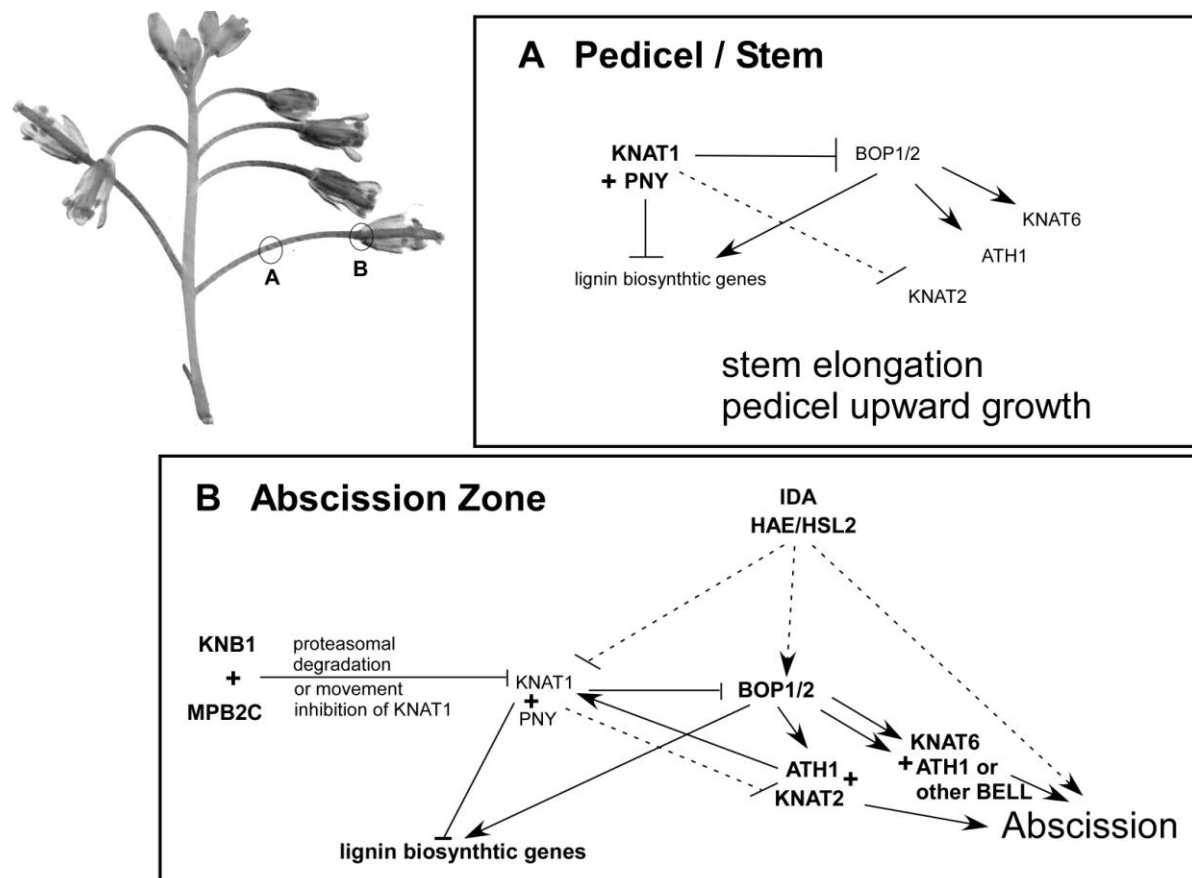


Figure 4: Pedicel and abscission zone patterning model

A: In the stem and pedicel KNAT1 and PNY repress the expression of *BOP1/2*, *KNAT2*, *KNAT6* and *ATH1*. This allows stem and pedicel growth and correct pedicel patterning resulting in wild type inflorescence patterning and upward oriented pedicels. **B:** In the abscission zone when organ shedding is initiated, *KNAT1* and *PNY* are still expressed, but MPB2C and KNB1 might interfere with KNAT1 movement or trigger KNAT1 degradation. Whether they interact with PNY is unknown. *BOP1/2* genes are no longer repressed, and BOP1/2 proteins can activate *KNAT2*, *KNAT6* and *ATH1* transcription which in turn activate transcription of genes necessary for abscission. ATH1 is probably the BELL co-factor for KNAT2 and KNAT6 in the abscission zone, but KNAT6 might function independently of ATH1, possibly by interacting with another BELL protein (Li, Pi et al. 2011). Furthermore IDA/HAE/HSL2 are expressed in abscission zones. Binding of the ligand IDA to its receptors HAE/HSL2 activates a MAP kinase cascade which eventually leads to activation of KNAT2 and KNAT6 transcription. IDA-signaling might interfere with KNAT1 function on a post transcriptional level. Alternatively, IDA/HAE/HSL2 signaling might even activate BOP1/2. Also, IDA might activate abscission via another pathway in parallel, because not all 35S::IDA abscission zone patterning defects were rescued in *knat2/knat6* mutants (Shi, Stenvik et al. 2011). Patterning defects occur, when the abscission zone- specific signaling situation is active in stems and pedicels. This leads to reduced internode and pedicel length and to downward-oriented siliques. Inversely, when pedicel-specific signaling is activated in abscission zones, floral organs are no longer shed. The signaling network in nodes seems similar to the situation in the abscission zone, but a difference between abscission zone and node signaling is that IDA HAE/HSL2 are not expressed in nodes and hence abscission is not initiated in nodes except when IDA is ectopically expressed there (Stenvik, Butenko et al. 2006). Hypothetic interactions (discussed in the literature but not experimentally proven) are shown as dashed lines except for the activation of BOP1/2 via IDA which is my own speculation. Interaction on the protein level is shown as “+”, active factors are shown with bold letters.

2.7 The role of MPB2C in regulation of cell-to-cell transport

MPB2C was discovered in a membrane-based yeast two-hybrid interaction screen as a protein from a *Nicotiana tabacum* cDNA library interacting with the **Tobacco Mosaic Virus movement protein** (TMV MP-30)(Kragler, Curin et al. 2003). MPB2C was shown to co-localize with TMV MP at microtubules and to interfere with TMV MP cell-to-cell movement via plasmodesmata (Kragler, Curin et al. 2003). The search for potential plant endogenous interaction partners of MPB2C identified the KNOX class 1 transcription factors KN1, STM (Winter, Kollwig et al. 2007), and KNAT1/BP [(Fichtenbauer 2011) and this work]. These homeodomain proteins can selectively traffic from cell to cell via PD (Kim, Yuan et al. 2003). But MPB2C did not interact with other homeodomain proteins like BEL1 or with other non-cell autonomous proteins like SHR, GLO, LFY or **C. maxima PHLOEM PROTEIN 1** (CmPP1) (Fritz Kragler, pers. comm.). So, MPB2C specifically interacts with a subset of proteins that engage in specific and selective cell-to-cell trafficking. Furthermore, MPB2C interacts with a novel protein, the plant specific **KNOTTED BINDING PROTEIN1** (KNB1) which binds certain TALE proteins and triggers KNOX protein degradation upon interaction. *KNB1* is a single copy gene in *Arabidopsis* and encodes a 16kDa protein with a predicted coiled coil domain (Fichtenbauer 2011).

Overexpression of *MPB2C* was shown to interfere with the spread of viral infection (Ruggenthaler, Fichtenbauer et al. 2009; Fichtenbauer 2011; Cho, Cho et al. 2012), presumably via sequestration of the viral movement protein to microtubules and thus preventing the viral ribonucleoprotein complex from arriving at and passing through PD. Additionally, MPB2C was shown to interfere with KNOX homeodomain-mediated cell-to-cell movement in leaves when overexpressed in transgenic *Arabidopsis* plants (Winter, Kollwig et al. 2007). How is MPB2C as a cytoskeleton- associated protein involved in the regulation of macromolecular cell-to-cell transport via PD? The presence of MPB2C homologs in multicellular land plants but not in evolutionary more ancient organisms or in other kingdoms correlates with the occurrence of the appressed ER within PD (Lucas, Biao Ding et al. 1993; Lucas, Ham et al. 2009). The appressed ER (or desmotubule) in the center of the cytoplasmic sleeve offers a membranous route for transport. Unlike PD in green algae lacking the appressed ER, fully diversified PD in higher plants allow strict regulation of cell-to-cell transport and selective non-cell-autonomous protein (NCAP) trafficking. This process involves transport of the protein cargo to the PD, selective docking at the PD, selective temporal modification of the PD size exclusion limit,

chaperone-facilitated unfolding of the NCAP before the passage through PD and subsequent re-folding in the target cell (Haywood, Kragler et al. 2002; Ruiz-Medrano, Xoconostle-Cazares et al. 2004; Kragler 2007; Lucas, Ham et al. 2009; Xu, Wang et al. 2011) (see also Figure 2 A).

This elaborate mechanism can be regulated on many levels and allows the physical exchange of macromolecules which can also act as signaling molecules between neighboring cells. Protein size, intracellular localization and protein levels were shown to affect the cell-to-cell movement of various **non-cell autonomous transcription factors** (NCATFs) (Rim, Huang et al. 2011). In contrast to the size of a protein, intracellular localization and protein levels are no mere intrinsic property of a protein, since they are depending on the particular cellular environment. This might explain tissue-specific differences in cell-to-cell movement behavior of some NCATFs (Kim, Yuan et al. 2003), depending on the presence and activity of interacting and modifying proteins which vary in different cells and tissues. Intracellular localization depends on the presence of receptors, but also on targeting peptides, retention signals, membrane anchors, protein modifications, protein processing etc. The effects of transport and localization motifs can be modified by cleavage or by conformational changes, which mask or unmask such peptides, or via protein modifications like the attachment of GPI anchors or myristoylation, mediating membrane association. Other modifications like phosphorylation or ubiquitination can influence protein stability, association with other proteins, or subcellular localization. Interaction with other proteins of course can also change intracellular localization, like e.g. BELL-KNOX heterodimerization, which mediates nuclear localization (Cole, Nolte et al. 2006). Protein abundance can be regulated on different levels: transcription rates, mRNA stability, alternative splicing, translation rates, and protein stability. All these changes are dependent on protein /or and RNA interactions.

MPB2C seems to be involved in several of these regulatory mechanisms via protein-RNA interactions and protein-protein interactions: MPB2C, like KN1 or TMV MP, binds RNA (Winter, Kollwig et al. 2007); *MPB2C* overexpression alters the subcellular localization of TMV MP (Kragler, Curin et al. 2003) and of KNOX homeodomain proteins by recruiting them to microtubules and preventing their access to PD (Winter, Kollwig et al. 2007). Furthermore it is shown in this work that MPB2C itself is subject to degradation via the 26S proteasome pathway. MPB2C may also direct its interaction partners towards proteasomal degradation, as suggested by the observed reduction of KNB1 levels upon co-expression with *MPB2C* and *STM* or *KNAT1* during transient expression via agroinfiltration (this work), in yeast (Fichtenbauer 2011) and in plants (Fritz Kragler, personal communication). By manipulating MPB2C we wanted to learn more about the importance of this symplasmic transport route in patterning processes during *Arabidopsis* development. In this work, we aimed at gaining insight into the importance of PD transport during development with a special focus on the role of MPB2C in KNOX I homeodomain protein movement and function. Evidence from previous work was corroborated according to which movement of STM in the shoot apex might not impair its function, but movement of KNAT1 or its stability in pedicels is required for correct pedicel patterning.

2.8 Addendum 1: The role of cell-wall modifying Pectin Methylesterases in development with regard to plasmodesmal transport

Recently, PNY has been shown to regulate the expression of a **pectin methylesterase** (*PME*). PNY represses *PME5* (At5g47500) expression in the apical meristem and activates *PME5* expression in the internodes (Peaucelle, Louvet et al. 2011). Earlier, the expression of *PME3* (At3g14310) has been shown to be down-regulated in the *bp-9* mutant (Mele, Ori et al. 2003). These results were explained from a mechanistic perspective, but maybe there is also a signaling perspective in it, too.

Arabidopsis encodes 66 (Tian, Chen et al. 2006; Peaucelle, Louvet et al. 2008) *PME* genes. PMEs are involved in loosening of the plant cell wall, and they play roles in various physiologic and developmental processes. Some *PMEs* are expressed in many tissues, others are expressed highly specific (Pelloux, Rusterucci et al. 2007). PMEs are involved in cell separation events during root tip elongation, organ outgrowth at the shoot apex (Peaucelle, Louvet et al. 2008), fruit softening or dehiscence of dry fruits [although their potential role in abscission zone formation is controversial (Sexton 1982)]. PMEs play a role in pollen tube growth, leaf growth polarity and internode elongation [reviewed by (Micheli 2001; Pelloux, Rusterucci et al. 2007; Wolf, Mouille et al. 2009; Wolfe-Simon, Switzer Blum et al. 2011)]. Overexpression of a fungal *PME* in tobacco led to decreased internode length due to reduced cell expansion (Hasunuma, Fukusaki et al. 2004). Furthermore, some PMEs are enriched in cell walls around plasmodesmata (Morvan 1998; Faulkner, Akman et al. 2008), and two PMEs (At1g53840 and At3g14300) were identified in the PD proteome (Fernandez-Calvino, Faulkner et al. 2011). Interestingly, cell-to-cell movement of TMV MP and other viral movement proteins requires binding to a *PME* in tobacco whose most closely related homolog in *Arabidopsis* is *PME3* (At3g14310) (Dorokhov, Makinen et al. 1999; Chen, Sheng et al. 2000), the gene whose expression depends on KNAT1. It was speculated that PMEs can act as a chaperone but this has been rebutted again. Christine Faulkner and Andy Maule summarize:

*“What PD-specific role PME has in the absence of viruses remains to be ascertained.”
(Faulkner and Maule 2011)*

However, with KNAT1 and PNY involved in regulation of *PME* expression and KNAT1 moving through plasmodesmata, it will be interesting to test whether KNAT1 movement, like TMV MP movement also depends on PMEs, and whether there exists a feedback loop in form of a *PME*-based mechanism of KNAT1 movement control.

2.9 Addendum 2: Apoplastic and symplasmic signaling seems to be interlinked via receptor like kinases

In some papers the measurement of the angle between pedicel and stem was used to quantify the degree of impaired KNAT1/BP function in individual mutants. The “classical” *bp* phenotype would show pedicels with angles larger than 90°, whereas “mild” or “partially rescued” phenotypes would show perpendicular pedicels with angles close to 90°. However, it is important to take into account in which ecotype the experiments were performed. The “classical” *bp* phenotype with downward-oriented pedicels is only observed in Landsberg *erecta* (*Ler*), whereas pedicels are rather perpendicular in *bp* mutants in the Columbia (*Col*) background (Douglas and Riggs 2005)¹². *Ler* harbors a mutant *erecta* gene. **ERECTA** (*ER*) encodes a **leucine-rich repeat receptor-like kinase** (LRR-

¹² Note also that *stm* mutations in *Ler* are more severe than in *Col*.

RLK) (Torii, Mitsukawa et al. 1996). LRR-RLKs are transmembrane proteins with a cytoplasmic kinase domain and represent a large gene family (*Arabidopsis* encodes 216 *LRR-RLKs*) (Shiu and Bleecker 2001). Some LRR-RLKs are known to play important roles in patterning during development (Dievart and Clark 2004) e.g. CLV1, which regulates meristem size (Clark, Williams et al. 1997); HAE and HSL2, the receptors involved in abscission zone maturation (Jinn, Stone et al. 2000; Stenvik, Tandstad et al. 2008); and **BRASSINOSTEROID INSENSITIVE 1** (BRI1), the receptor for brassinosteroids (Li and Chory 1997). Interestingly, despite that LRR signaling itself implies already intercellular signaling - cell-membrane-localized receptors bind extracellular ligands and transmit the extracellular signals into intracellular signals - in several cases a second non-cell autonomous signal, a transcription factor moving symplasmically via plasmodesmata, is also part of the regulatory circuits (see Table 2).

An interesting connection between apoplastic signaling received via receptor-like kinases and symplasmic signaling via plasmodesmata might be provided by **ARABIDOPSIS CRINKLY4** (ACR4). The maize homolog of this RLK **CRINKLY4** (CR4) was shown to be localized at PD connecting aleurone cells (Tian, Olsen et al. 2007). *Arabidopsis* encodes ACR4 and four **CRINKLY4-RELATED** (CRR) proteins (Cao, Li et al. 2005), which are expressed in different tissues. *ACR4* is expressed throughout development in various tissues, among which are embryos, vegetative and floral meristems, root tips and ovules (Gifford, Dean et al. 2003; Cao, Li et al. 2005). In *Arabidopsis* ACR4 intracellular localization was described to be at the plasma membrane and in form of bodies within the cytoplasm (Gifford, Dean et al. 2003). The microscopic resolution in these experiments was not high enough to test whether ACR4 was also localized at PD, but the fluorescence pattern was similar to that of CR4-YFP in maize (Tian, Olsen et al. 2007). So it remains to be shown by high-resolution fluorescence or electron microscopy whether ACR4 is localized at PD. ACR4 was not reported in the PD proteome (Fernandez-Calvino, Faulkner et al. 2011). However, other PD-localized RLKs were identified in the PD proteome, and they were confirmed to reside at PD upon transient expression. The authors conclude:

“The frequency (from a very limited survey) with which these proteins were identified suggests that the PD may represent a receptor-rich domain and points to a previously unrecognised potential for cell-to-cell communication to be influenced by factors in the extracellular environment. (Fernandez-Calvino, Faulkner et al. 2011).

So tissue organization might be dependent on both, apoplastic and symplasmic signaling, and they might directly feed back onto each other.

process	LRR-RLK	ligand	secondary non-cell autonomous signal	literature
stomatal patterning	ERECTA	EPIDERMAL PATTERNING FACTORS EPF1 & EPF2	SPEECHLESS (bHLH transcription factor)	(Shpak, McAbee et al. 2005; Guseman, Lee et al. 2010; Lee, Kuroha et al. 2012)
meristem organization	CLAVATA1	CLAVATA3	WUSCHEL (HD transcription factor)	(Mayer, Schoof et al. 1998; Lenhard and Laux 2003; Yadav, Perales et al. 2011)
abscission zone patterning	HAESA/HAESA LIKE2	INFLORESCENCE DEFICIENT IN ABSCISSION	KNAT1/BP (HD transcription factor)	(Jinn, Stone et al. 2000; Stenvik, Tandstad et al. 2008; Shi, Stenvik et al. 2011)
cell division, differentiation, development, morphogenesis	BRASSINOSTEROID INSENSITIVE 1	Brassinosteroids	unknown; evidence for a signal: in the root, expression of a QC marker gene, the MADS-box gene AGL42, depends on a BRI1-mediated signal from the epidermis (Hacham, Holland et al. 2011)	reviewed by (Clouse 2011; Witthoft and Harter 2011)

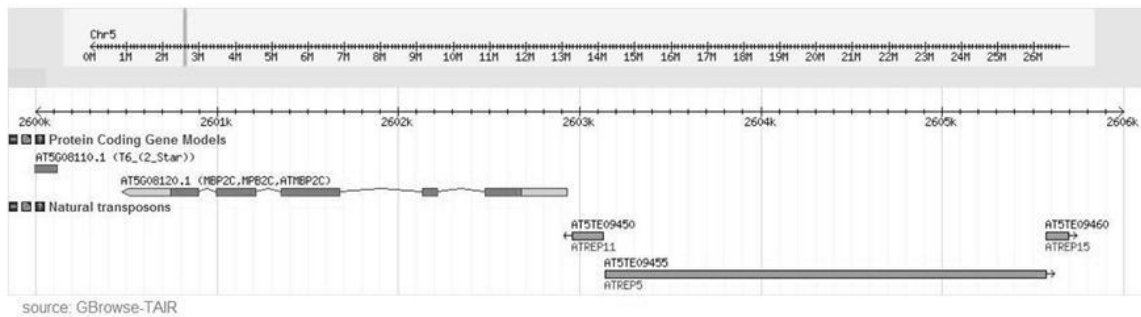
Table 2: Examples showing coupling of apoplastic and symplasmic signaling

3 Results

3.1 The *MPB2C* gene and its expression

MPB2C (TAIR Accession: At5g08120) is a single-copy gene in *Arabidopsis*. It is located on chromosome five on the complement strand. The transcript of 1499 nucleotides encompasses five exons, and *Arabidopsis* cDNA collection libraries suggest there is only one splice variant with a protein encoding sequence of 981 nucleotides translated into 326 amino acids. The protein has a predicted molecular weight of 37.3 kDa. The intergenic region upstream of *MPB2C* spans 3.2 kb. This region harbors three transposable elements (see Figure 5). These repetitive sequences are probably the reason for the failure of previous attempts to clone the entire upstream region.

Transposons upstream of *MPB2C*



Locus	TAIR accession	Coordinates	Length	Orientation	Identity
MPB2C	At5g08120	2600474 – 2602927	2 454 bp	complement	gene
ATREP11	At5te09450	2602958 – 2603131	174 bp	complement	RC/helitron transposon
ATREP5	At5te09455	2603143 – 2605574	2 432 bp	forward	RC/helitron transposon
ATREP15	At5te09460	2605575 – 2605698	124 bp	forward	transposon
BIM1	At5g08130	2606200 – 2610250	4 051 bp	complement	gene

Figure 5: Genomic locus of *MPB2C*

MPB2C is encoded on the complement strand on chromosome 5. The gene has five exons. The intergenic region upstream *MPB2C* harbors three transposons: *ATREP11*, *ATREP5* and *ATREP15*. Annotation of the transposable elements shown in the table was visualized by using GBrowse-TAIR¹³.

In order to identify the promoter region of *MPB2C*, a sequence spanning just 496 bp upstream of the *MPB2C* start codon had been cloned into the binary vector pKGWFS7 (Karimi, Inze et al. 2002). This vector provides a promoterless GFP-GUS reporter protein, which can also serve as a C-terminal tag. In our lab, GFP from this vector was never detected, no matter which promoter or promoter::protein sequence was cloned upstream into the vector (Kollwig 2010; Fichtenbauer 2011). β -glucuronidase (GUS) is an enzyme encoded by the *uidA* gene that cleaves the glucoside 5-bromo-4-chloro-3-indolyl- β -D-glucuronic acid (X-Gluc), a colorless substrate, into 5-bromo-4-chloro-3-indoxyl, which is then oxidized into 5,5'-Dibrom-4,4'-dichlor-indigo, a blue dye. With the help of this enzymatic reaction, expression domains of a gene of interest can be stained blue by expressing the enzyme under the respective promoter and then incubating tissues with the GUS substrate X-Gluc (Jefferson, Kavanagh

¹³ GBrowse is a web-based server application developed by the Generic Model Organism Database project (GMOD) <http://gmod.org>

et al. 1987). *pMPB2C::GFP-GUS* (internal name of the construct and transgenic lines: 2-1-C) and was shown to yield a specific expression pattern in GUS reporter assays, see also: (Winter, Kollwig et al. 2007), which correlated well with *in silico* predicted expression patterns (see Figure 6) and tissue-specific detection of *MPB2C* transcripts via RT-PCR (done by Shoudong Zhang, Kragler Lab). One of the transposons, *ATREP11*, is included within this upstream regulatory sequence. Only 29 nucleotides separate *ATREP11* and the first nucleotide of the *MPB2C* 5' untranslated region. 278 nucleotides separate *ATREP11* from the start codon of *MPB2C*. Apart from promoters, other sequences like enhancer regions or elements within introns (Rose and Beliakoff 2000) can affect gene expression and transcript stability. Furthermore, the *MPB2C* protein appeared to be sensitive to proteasomal degradation in protein extracts from *Arabidopsis* (see chapter 3.4.1). Therefore we compared the GFP-GUS readout for *MPB2C* promoter activity with the signal obtained from a *MPB2C*-GFP-GUS fusion protein expressed from the endogenous promoter. In parallel, *MPB2C* transcripts were localized via RNA *in situ* hybridization, for comparison with the results from the GUS reporter lines.

3.1.1 Expression domains of *MPB2C* in a developmental context

As *MPB2C* interacts with the homeodomain of the meristem-specific transcription factors *KN1*, *STM* (Winter, Kollwig et al. 2007) and *KNAT1/BP* [(Fichtenbauer 2011) and this work], we analyzed the *MPB2C* tissue-specific expression in the shoot apical region, where *STM* and *KNAT1* are expressed (Lincoln, Long et al. 1994; Long, Moan et al. 1996) and active as transcriptional regulators. *In silico* data derived from microarray and high-throughput expression assays suggest medium- to low-range expression levels of *MPB2C* in a number of distinct tissues including the shoot apical meristem (SAM) during various developmental stages except for dormant seeds. *MPB2C* expression peaks in the SAM and in developing inflorescences which supports the notion that *MPB2C* plays a role in *STM* and *KNAT1* regulation (see Figure 6).

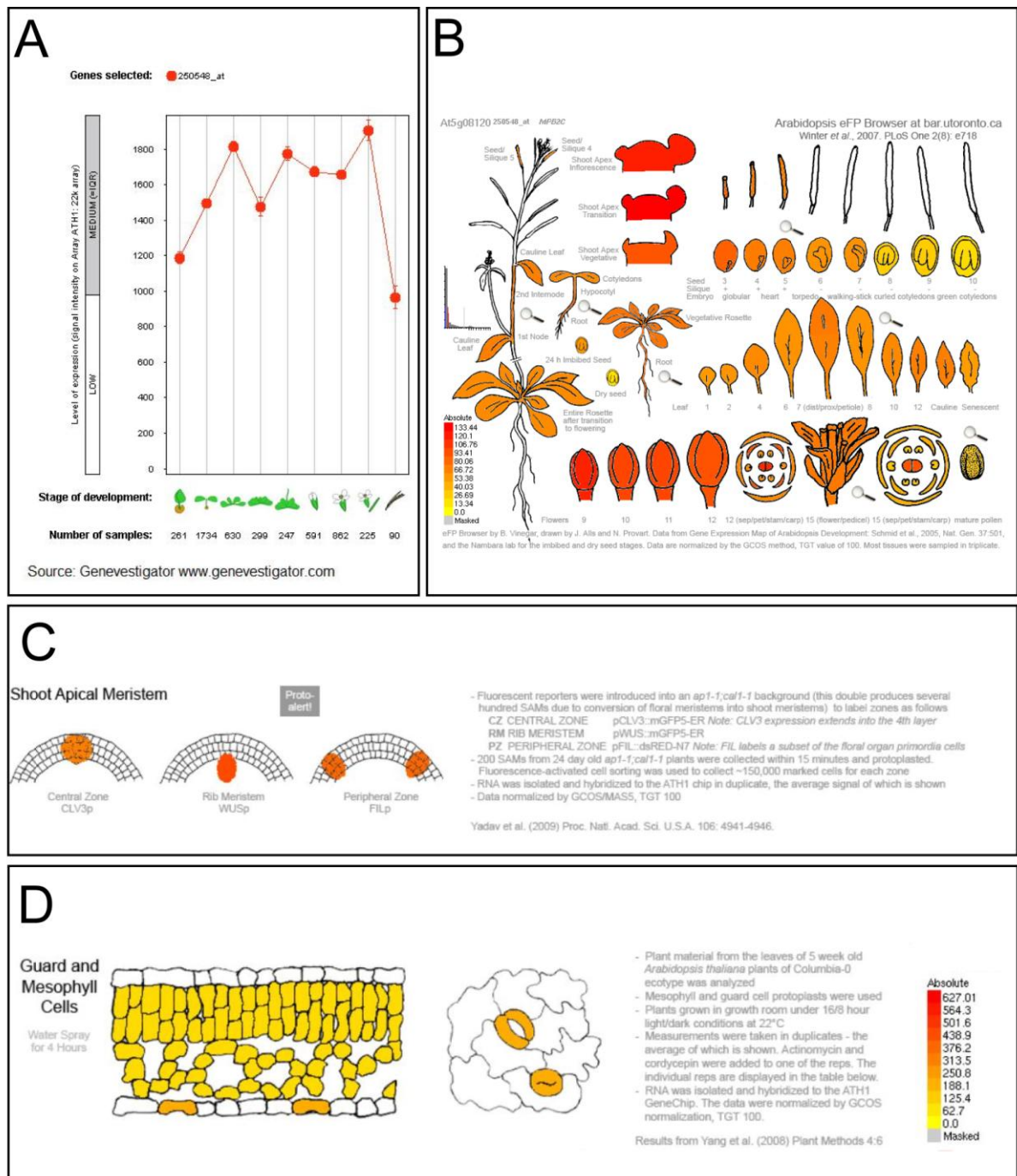


Figure 6: In silico models for MPB2C gene expression

Various online tools are available to visualize published microarray data. **A:** The Geneinvestigator software (Hruz, Laule et al. 2008) visualizes results obtained from Affymetrix Arabidopsis ATH1 genome 22k array – in which MPB2C has the probe set ID: 250548_at. In the course of development, MPB2C expression is medium to low in relation to the average gene expression under the various experimental settings. **B to D:** Another online visualization tool is the eFP browser (Winter, Vinegar et al. 2007), which again shows MPB2C expression throughout plant life. The absolute expression levels peak in the shoot apex and in immature flowers. **C:** MPB2C is expressed in all zones of the shoot apical meristem, in the central zone, the rib meristem and in the peripheral zone (expression data derived from RNA isolated from meristem-subdomains hybridized to the ATH1 microarray (Yadav, Girke et al. 2009)). **D:** MPB2C mRNA was detected in mesophyll cells and in guard cells (expression data derived from (Yang, Costa et al. 2008), who performed a guard cell-specific microarray by using the pGC1 promoter). MPB2C promoter activity in the shoot apical meristem and in guard cells could be experimentally confirmed in the here presented work (see Figure 10 and Figure 9, respectively).

3.1.2 *MPB2C* promoter activity is largely consistent with *MPB2C* protein localization in seedlings and floral tissues

To investigate *MPB2C* expression, a reporter construct was generated by cloning a 2.4 kb genomic fragment of *MPB2C* comprising the putative promoter region 496 bp upstream of the start codon and the genomic sequence containing the *MPB2C* open reading frame until just before the stop codon into vector pKGWFS7 to obtain the construct *pMPB2C::MPB2C-GFP-GUS* (internal name: 58). Of over 100 independent transgenic *pMPB2C::MPB2C-GFP-GUS* reporter lines, 11 lines were chosen for closer expression analysis in the T2 (see Table 3). First the staining pattern was compared to plants harboring only the *pMPB2C::GFP-GUS* reporter (Winter, Kollwig et al. 2007). In general, the variability of the tissue-specific GUS signal between and within the *pMPB2C::MPB2C-GFP-GUS* lines was considerably lower than in *pMPB2C::GFP-GUS* lines. Between different independent lines transgenic for *pMPB2C::MPB2C-GFP-GUS*, a range of GUS stain intensities was observed, but tissue-specific expression was consistent throughout the analyzed 11 lines, i.e. signals in a certain tissue in different lines were strong, weak or absent, but there was no line which showed a pattern completely different than in other lines.

Some differences in the expression domains between the two different reporter constructs were observed: In *pMPB2C::GFP-GUS* lines, seven day old seedlings had more often a strong GUS signal in the vasculature of the cotyledons and in the hypocotyl vasculature, and a less intense signal in the root tip and in lateral root primordia (compare in Figure 7 E with F and G with H). Interestingly, also the mRNA *in situ* localization yielded a signal in the vasculature of seedling hypocotyls in contrast to *pMPB2C::MPB2C-GFP-GUS* (compare panel A and B in figure Figure 10), which might indicate that the *MPB2C* protein has a high turnover rate in the vasculature of aboveground tissues, whereas it might be lower expressed but more stable in primary and secondary root meristems. No *MPB2C* mRNA *in situ* localization data are available for roots. In inflorescences of the first *pMPB2C::MPB2C-GFP-GUS* transgenic generation (T1), we observed results similar to those from *pMPB2C::GFP-GUS* lines: A signal was detected in carpels, and additionally weak GUS activity in internodes and pedicels of some plants was observed. Additionally, at the time of floral organ abscission and in subsequent stages, strong GUS activity was observed in the abscission zone. Since at the time when these experiments were done, the focus of my work was on vegetative meristems, no comparative follow-up GUS stain in inflorescences of T2 plants of all lines was done, only T2 plants of line 58-1 and 58-7 were stained, and individual plants showed the same GUS pattern as their parents.

3.1.3 *MPB2C* is expressed in root and shoot apical regions in seedlings

An overview of *MPB2C* expression patterns observed in seedlings of eleven independent transgenic lines is given in Table 3.

line tissue	58-1	58-2	58-3	58-4	58-5	58-6	58-8	58-9	58-10	58-11	58-12	2-1-C
root tip	+++++	++++	+++	+++	++++	++	+++	+++	+++	++++	++++	+/-
root vasculature	+++	++	++	-	++	-	++	+	++	++	++	+
lateral root primordia	++++	+++	-	-	-	-	-	-	-	+++	-	-
hypocotyl (vasculature)	+/-	-	-	+/-	-	-	-	-	-	-	-	++
shoot tip (incl. young true leaves)	+++++	+++	+++	+++	+++	++	+++	+++	+++	+++	+++	+++
cotyledons	+++	++	-	-	-	-	-	-	-	-	-	++

Table 3 *MPB2C* promoter activity

GUS intensity in ten day old T2 seedlings transgenic for *pMPB2C::MPB2C-GFP-GUS* grown on selective agar plates under long day conditions was compared. Between 10 and 20 individual seedlings per line were examined, and the average signal

intensity in different expression domains viewed under the binocular microscope was judged arbitrarily. For comparison, the expression pattern of the reference line 2-1-C for *pMPB2C::GFP-GUS* is shown in the last column.

Very strong GUS activity could be seen at the shoot tip, including the first true leaves (Figure 7A, B, C, E, I). In nine of eleven lines, no GUS signal was observed in cotyledons. Individual plants from two lines showed GUS activity, mainly in the vasculature of cotyledons (Figure 7A, B). Generally there was no signal in the hypocotyl, only in two out of eleven independent lines a weak signal was observed in the hypocotyl vasculature (Figure 7 A, B, E). In the root, *MPB2C* was expressed most strongly in the meristematic zone – which is characterized by small cells overlaid by the root cap (Dolan, Janmaat et al. 1993) (see Figure 7 and Figure 8). There was no signal in the distal two layers of the columella, and a weak signal in the proximal cell files, as well as in the lateral root cap. A stronger signal was detected in the cells of the epidermal layer within the meristematic zone, and a weaker signal appeared in the cortex and endodermis in this region. The strongest signal was in the procambium, the progenitor cells for all future vascular tissues. More proximal of the root tip, the strong GUS signal continued into the stele which represents the mature vascular tissue. This signal decreased proportional to the distance from the root tip eventually disappearing entirely (compare e.g. Figure 8D, a more distal part of the root with still a strong vascular signal with Figure 8E, depicting a more proximal part of the root with no GUS activity in the vasculature). In some plants with general stronger GUS signal, the GUS reporter could be detected throughout the root in vascular tissues (compare Figure 7A and B). In three out of eleven independent lines, a strong GUS signal was detected in lateral root primordia from the earliest stages (Malamy and Benfey 1997) of cell divisions in pericycle cells onwards (Figure 8B to E). The intensity of the GUS signal reached a maximum at the stage of lateral root emergence. By the stage of meristem activation, the uniformly strong area of GUS activity in the lateral root primordium observed in prior stages changed, and expression in the proximal region decreased whereas high GUS activity remained in the procambium of the lateral root tip analogous to the pattern observed in the primary root tip (cf. Figure 7). Notably, we also observed a local maximum of GUS activity in lateral root primordia of *p::KNB1::KNB1-GFP-GUS* reporter lines [see Figure 14 and (Fichtenbauer 2011)] and *pKNB1::GFP-GUS* lines (Kollwig 2010).

3.1.4 *MPB2C* is expressed in guard cell precursors

In expanding true leaves, a gradient of *MPB2C* expression was observed the signal was ubiquitous and strong in the proximal part and decreased towards the leaf tips. In the distal parts, the signal became restricted to the vasculature. In a line with very high levels of GUS activity (line 58-1), a signal was observed in immature stomatal cells of cotyledons and true leaves (see Figure 9). *MPB2C* promoter activity was detected in early meristemoid stages. It increased gradually with differentiation peaking after the symmetric division of the guard mother cells. In mature stomata, the signal was hardly detectable (Figure 9).

3.1.5 *MPB2C* is expressed in vegetative and inflorescence shoot apical meristems

MPB2C expression (*pMPB2C::MPB2C-GFP-GUS*) was detected throughout the vegetative shoot apex including all three meristematic layers (consistent with microarray data) and incipient leaf primordia. This result was confirmed via RNA *in situ* hybridization (see Figure 10). The strongest signal in the SAM was observed in young seedlings. After floral transition, a weak *MPB2C* mRNA signal throughout the entire apical region of inflorescence and in floral meristems was detected *in situ* (see Figure 10E and Figure 12). The overall signal in reproductive meristems was much weaker than in seedlings. Of these weak signals, floral meristems right before the onset of floral organ primordia differentiation showed the highest *MPB2C* mRNA accumulation. Analogous to the vegetative stage, leaves

surrounding the inflorescence showed a signal, especially in the vasculature and in adaxial lateral parts of the leaf blade (see transversal section in Figure 12C). A weak signal was detected in the stem cortex. An even weaker signal than with RNA *in situ* hybridization was obtained in the GUS reporter approach. Hardly any signal could be detected in *pMPB2C::MPB2C-GFP-GUS* inflorescence meristems (Figure 12D). A very faint signal was detected in the cortical region of the stem, in axillary buds (inset in Figure 12D) and in leaves surrounding the inflorescence. Interestingly, contrary to these results, high amounts of MPB2C protein were detected in protein extracts of inflorescences with the specific antibody (see Figure 26B). This suggests a second peak of *MPB2C* expression in the course of development in tissues other than meristems.

Figure 7

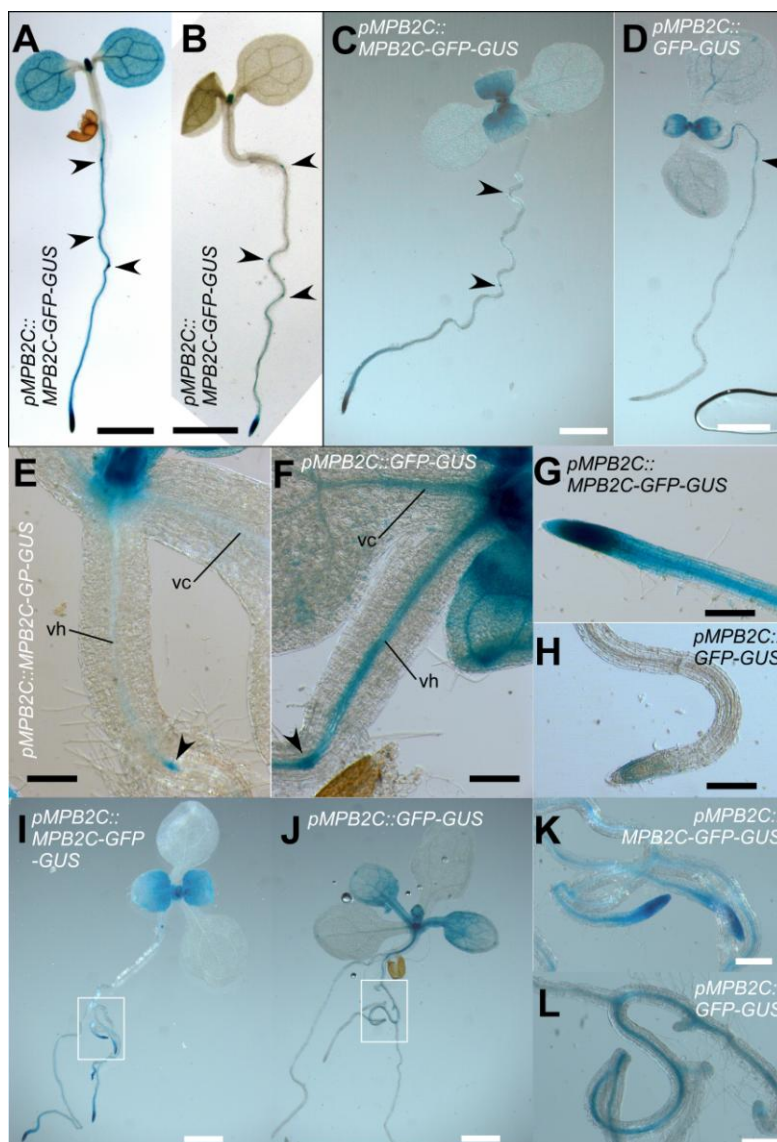


Figure 7: *MPB2C* expression in seedlings

A, B: Three day old seedlings transgenic for *pMPB2C::MPB2C-GFP-GUS* (vector pKGWFS7) grown under long day conditions on agar plates. **A:** Plant showing a strong overall GUS signal (line 58-1) seen in 2 of 11 lines. **B:** Plant (line 58-2) with GUS signal representing the average strength in 9 out of 11 lines, except for the signal in lateral root primordia, which was only observed in 3 lines. *MPB2C* expression domains did not vary much. Only the signal strength differed considerably between independent lines. Expression was strongest in the root tip, in lateral root primordia (arrowheads), and in leaf primordia. *MPB2C-GFP-GUS* expression was observed in the vasculature of the root with decreasing intensity towards the hypocotyl. Promoter activity in the cotyledons, mainly in the vasculature, was only observed in plants with overall high GUS signal strength. **C to L:** Seven day old agar plate- grown seedlings stained for GUS-activity. Two different reporter constructs were

compared: **C, E, G, I, K:** *pMPB2C::MPB2C-GFP-GUS* (vector pKGWFS7, line 58-2) versus **D, F, H, J, L:** *pMPB2C::GFP-GUS* (vector pKGWFS7, line 2-1-C). Both constructs showed expression in true leaves (**C** to **F**) – whereby the signal in expanding leaves decreased towards the leaf tip, where it eventually became restricted to the vasculature. **D, F:** The signal in the cotyledon vasculature (vc) was stronger in the line expressing only the GFP-GUS reporter without translational fusion to *MPB2C*, and this construct also produced a signal in the hypocotyl vasculature (vh), compare **E** with **F**. Both constructs showed GUS activity in the root tip, the root vasculature, and in lateral root primordia (arrowheads in **C, D, E, F**). The signal in the root and root tip was much stronger in the reporter construct including the *MPB2C* protein (**C, G**). Scale bars: A- D, I, J: 1mm; E to H, K, L: 200µm.

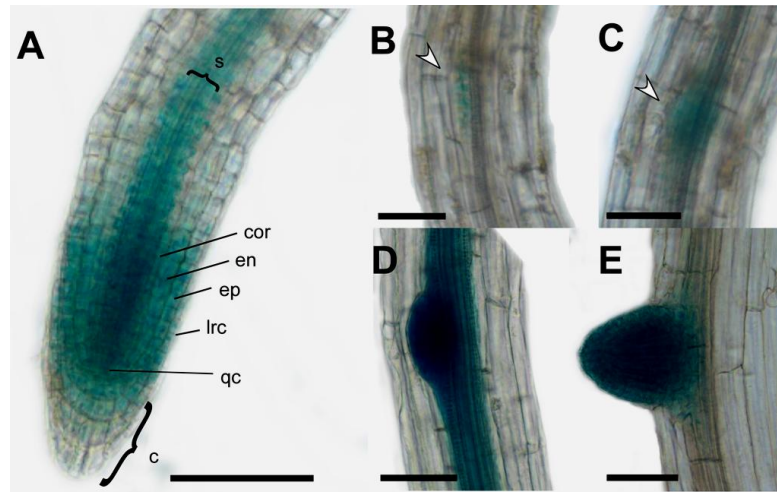


Figure 8: *MPB2C* expression domains in seedling roots

A: *pMPB2C::MPB2C-GFP-GUS* (line 58-2) was detected in the root tip in seven-day old agar plate- grown seedlings. The strongest signal was detected in the procambium, the immature vascular tissue in the meristematic zone. All other tissues in the meristematic zone also showed *MPB2C* promoter activity: the quiescent center (qc), stele (s), cortex (cor), endodermis (en), epidermis (ep) and in the lateral root cap (lrc). In the elongation zone, the signal was restricted to the stele. **B** to **E:** shows lateral root primordia of different individual plants of line 58-2 in order to represent different developmental stages. *MPB2C* expression was detected from first stages of anticlinal cell division in the pericycle (**B**, stage I) throughout later stages (**C**: stage III, **D**: stage V) until the stage of emergence, when the lateral root is fully differentiated (**E**). Stages of development were classified after (Malamy and Benfey 1997). Note the strong promoter activity of *MPB2C* in the vasculature of the root in **D** – this vascular signal was strong in distal regions, and it decreased towards the hypocotyl. Scale bars A: 100µm, B to E: 50µm.

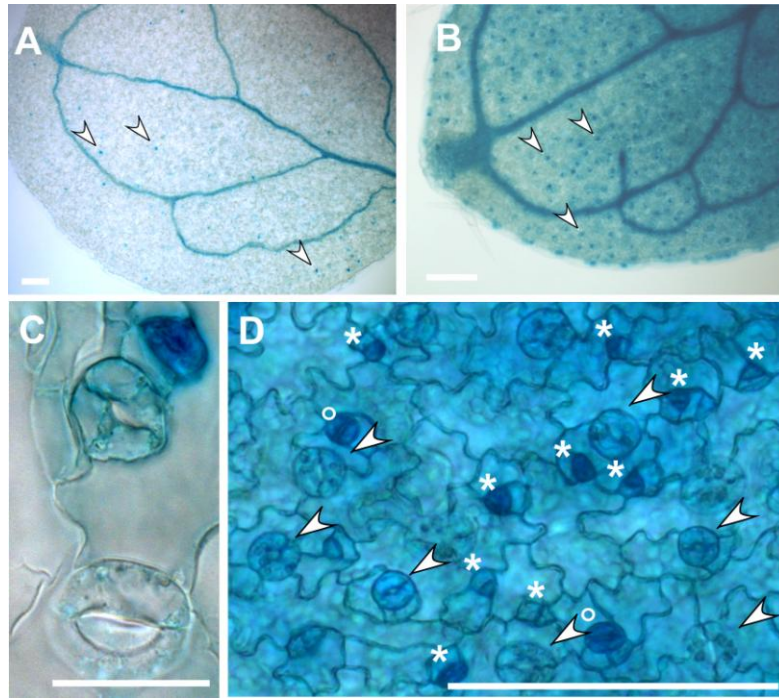


Figure 9: *MPB2C* expression in leaves of seedlings

7 day old seedlings transgenic for *pMPB2C::MPB2C-GFP-GUS* (line 58-1) grown on agar plates. **A** and **C**: cotyledon, **B** and **D**: first true leaf. **A, B**: The *MPB2C* promoter is mainly active in the vasculature of cotyledons (A) and young leaves (B), and in this line with high overall GUS activity, spots in the epidermis are visible (arrowheads in A and B). **C, D**: Close-up examination revealed that immature, but not mature guard cells display high *MPB2C* promoter activity **C**: In a close-up of the cotyledon epidermis, three stomata in different developmental stages are visible. A mature stoma (lowest) shows very faint blue-stained probably cytoplasmic structures, which were not determined. The young stoma in the middle shows weak GUS activity, and the immature guard cell pair (top) shows strong GUS activity. **B, D**: In expanding true leaves, the *MPB2C* promoter is highly active in the vasculature. A gradient of decreasing GUS signal towards the more differentiated distal part of the leaf is visible (B). **D**: Aside from the GUS signal in epidermal pavement and mesophyll cells, higher *MPB2C* expression levels were observed in guard cells. A weak GUS signal was detected in triangle-shaped meristemoids and guard mother cells (*). In the course of stomatal differentiation, the signal increased, peaking in immature guard cells (°). In mature stomatal cells (arrowheads) the signal was either weak or absent. For orientation, a scheme of the stereotypic division model for stomatal spacing can be seen in: (Golz and Hudson 2002). Scale bars: A, B, D: 50µm; C: 25µm.

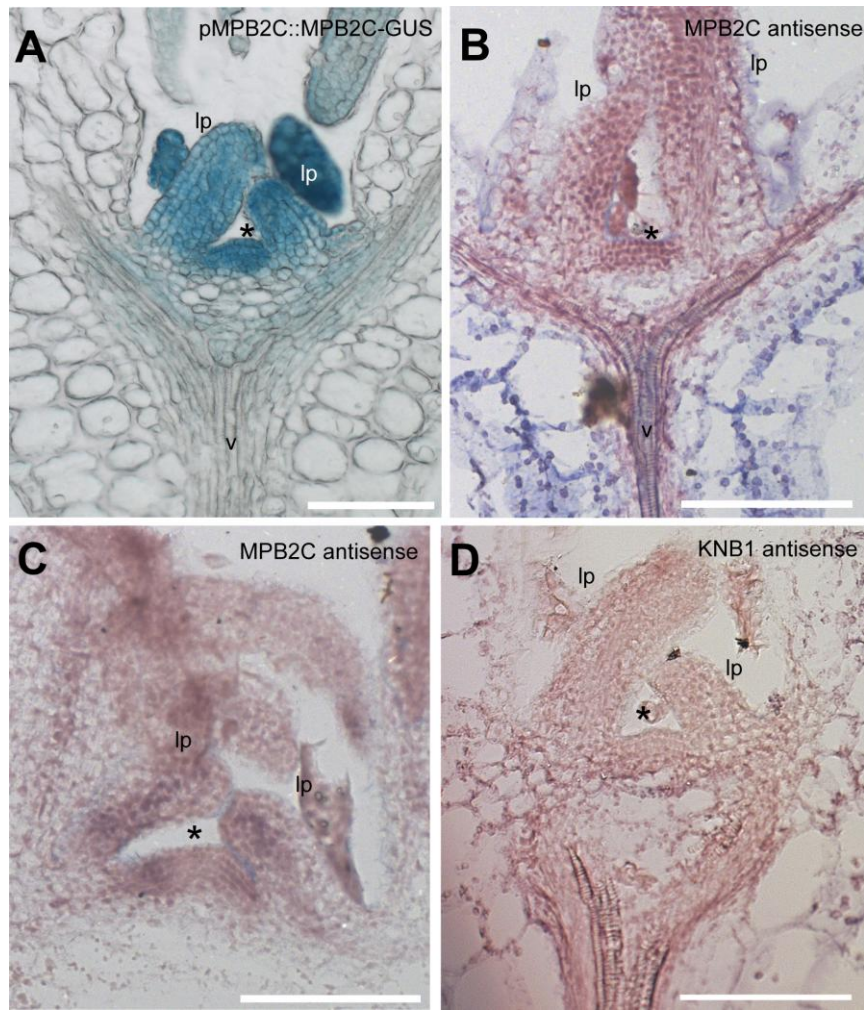


Figure 10: *MPB2C* and *KNB1* expression in the vegetative shoot apex

A: *MPB2C* promoter activity in line 58-1 transgenic for *pMPB2C::MPB2C-GFP-GUS*. This experiment was done by Kornelija Pranjić. **B, C:** *MPB2C* mRNA localization detected by *in situ* RNA hybridization. **D:** *KNB1* mRNA localization. **A, B:** In seedlings grown on agar plates (two true leaves), both detection methods confirmed *MPB2C* promoter activity in the shoot apical meristem (asterisk) and in developing leaf primordia (lp). The vascular signal (v) was only obtained by *in situ* RNA localization (B, probe: M4). **C:** A similar expression pattern was also observed in older plants prior to floral transition. Note that *MPB2C* expression in developing leaves is stronger on the adaxial side. The plant was grown ca. 4 weeks on soil under short day conditions, and then shifted to long day conditions for 4 days to induce flowering, but this plant shows still the morphology of a vegetative apex. (Probe M4). **D:** The *KNB1* antisense probe showed expression in leaf primordia (lp), in the SAM (asterisk) and in the vasculature in a seedling grown in parallel with the plant shown in **B**. Scale bars: 100 μm.

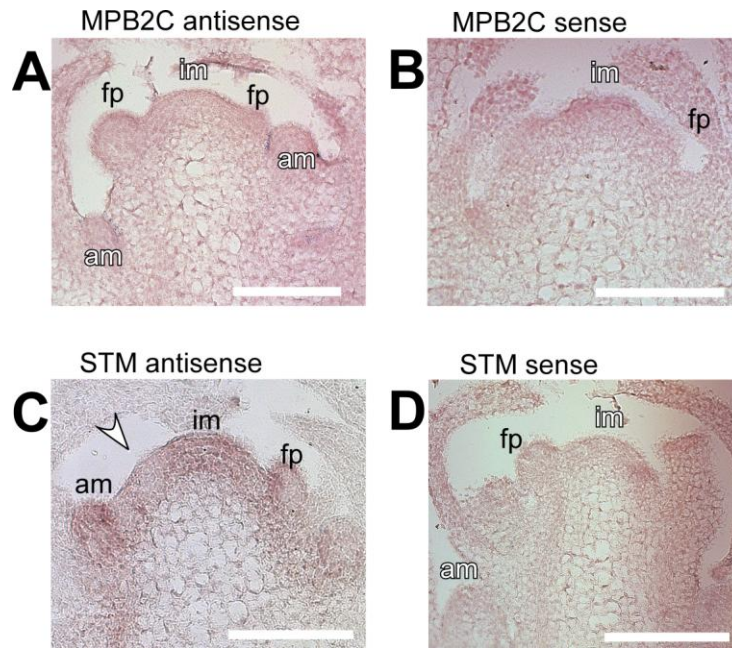


Figure 11: MPB2C and STM expression during floral transition

A: Shortly after transition from the vegetative to reproductive stage (prior to stem elongation) *MPB2C* mRNA with probe M2 (note that this probe always produced a weaker signal than probe M4) was not detected in significant amounts in the inflorescence meristem (im), in floral primordia (fp) and in axillary meristems (am). **B:** *MPB2C* sense probe as negative control. **C:** In this stage, *STM* transcript was detected in the inflorescence and in axillary meristems. In contrast to *MPB2C*, *STM* expression is excluded from regions of lateral organ formation (arrowhead indicates an incipient floral primordium), and expression remains absent in the more differentiated floral primordium (fp). **D:** *STM* sense probe as negative control. Scale bars: 100 μm.

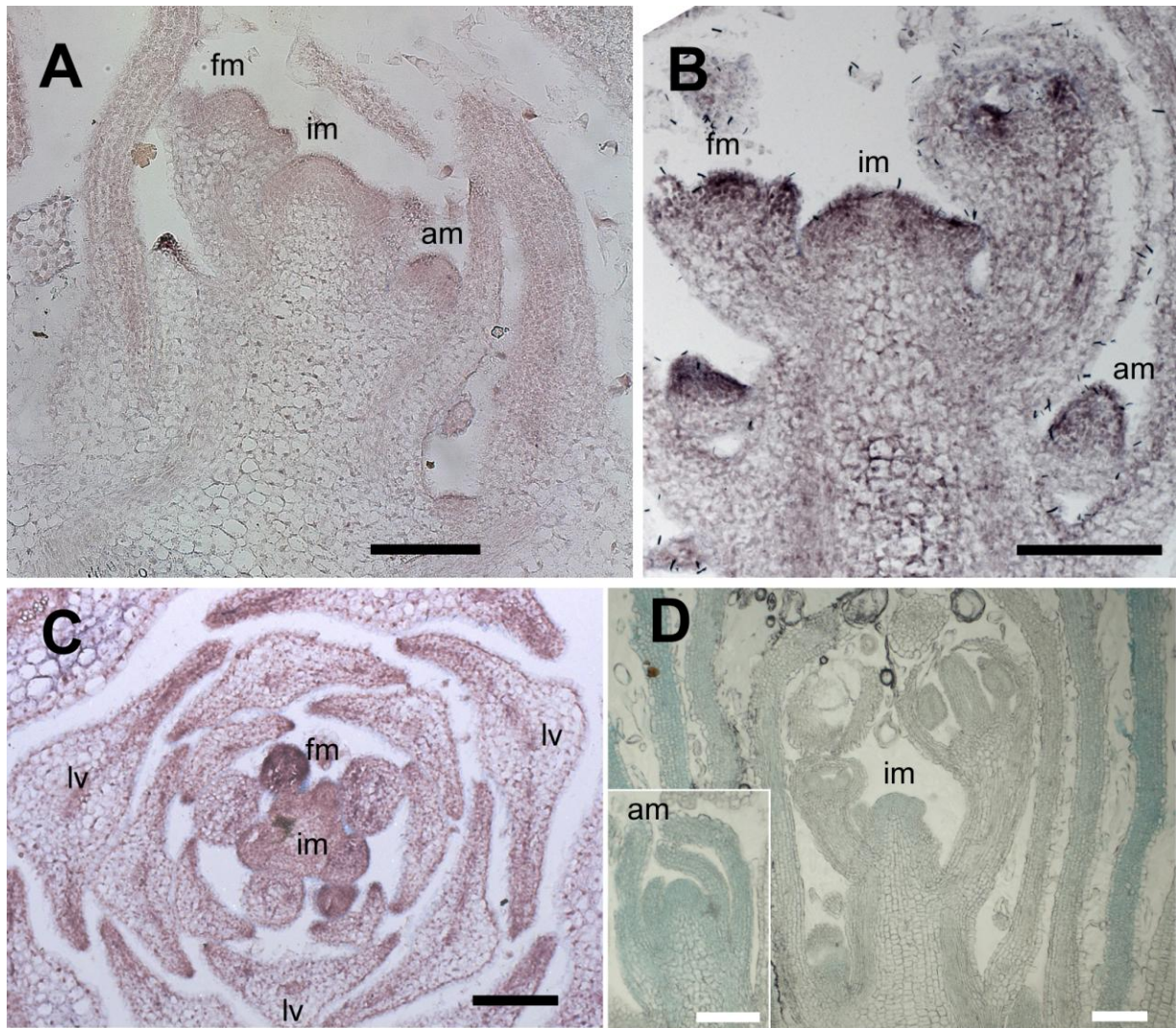


Figure 12: *MPB2C* expression in the reproductive shoot apex

MPB2C RNA *in situ* hybridization of longitudinal (A, B) and transverse (C) sections of *Arabidopsis* shoot apices after floral transition. D shows a longitudinal section of a comparable apex in the *pMPB2C::MPB2C-GFP-GUS* reporter line 58-1. These plants were grown on soil under long day conditions for four weeks. A to C: After floral transition at the onset of internode elongation, weak *MPB2C* promoter activity was detected by RNA *in situ* hybridization (probe M4) throughout the apical region. B: After a prolonged detection reaction, the signal in the inflorescence meristem (im), in floral meristems (fm) and in axillary meristems (am) became more clear. The signal in floral meristems was stronger than in the inflorescence meristem (visible in A, B and C). C: In leaves enclosing the inflorescence, a signal was detected mostly in the vasculature (lv) and in adaxial and lateral regions (visible in A and the cross-section C). D: The overall low expression was at the detection limit of the GUS reporter system. The *pMPB2C::MPB2C-GFP-GUS* reporter (line 58-1) showed a weak GUS signal in leaves surrounding the inflorescence and in axillary meristems (inset in D). The faint signal in the inflorescence meristem was barely detectable. Alternatively this could indicate that the *MPB2C* protein (in this case *MPB2C-GFP-GUS*) is not stable in these regions. Scale bars: 100µm; im: inflorescence meristem, fm: floral meristem, am: axillary meristem, lv: leaf vasculature.

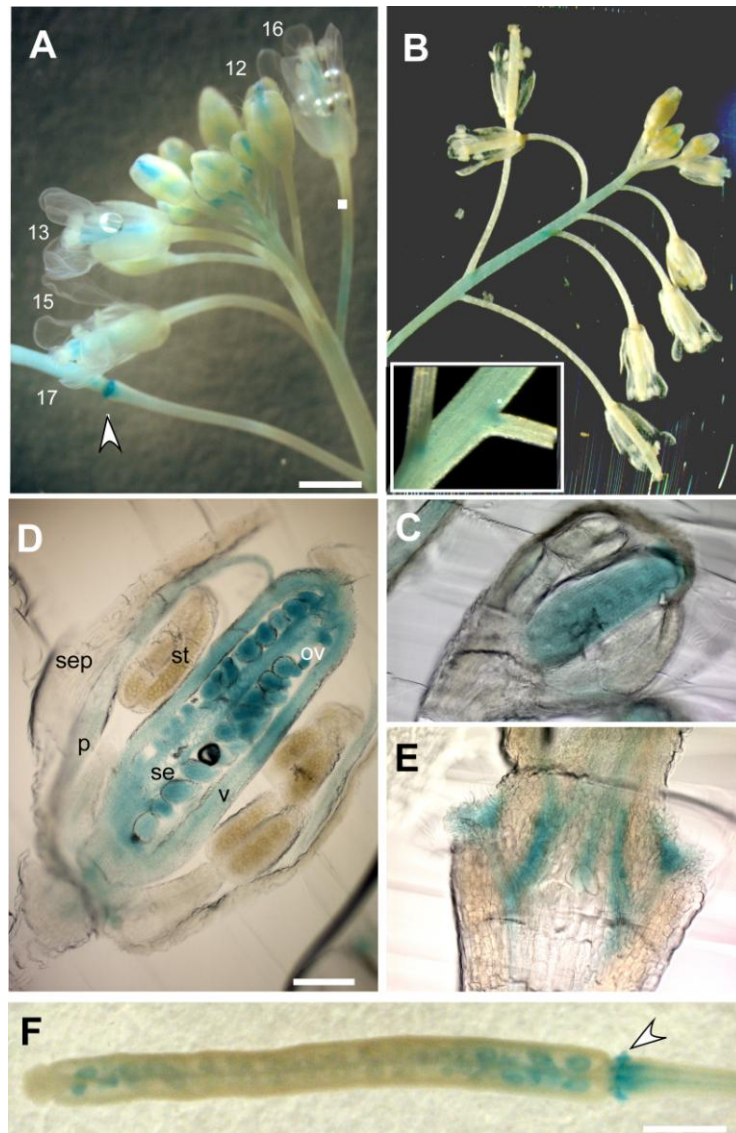


Figure 13: Expression of *MPB2C* in floral organs

Plants transgenic for *pMPB2C::MPB2C-GFP-GUS* were grown on soil in the greenhouse under long day conditions. **A, B:** In flowers (**A:** line 58-16, T1 plant; **B:** line 58-1, T2 plant), GUS activity was detected in carpels throughout all stages of flower development until fertilization (strong signal in A, very faint signal in B). Weak GUS activity was observed in single pedicels (see pedicel of stage 16 flower in A, marked by a white square) or in internodes of terminal inflorescences in B. In internodes, stronger expression was observed at the adaxial regions of the pedicel-stem junction (inset in B showing an internode from a different plant of the same line grown in parallel). **C:** In young flowers (approx. stage 6), *pMPB2C::MPB2C-GFP-GUS* was expressed throughout the gynoecium. **D:** In stage 12 flowers right before anthesis, *MPB2C-GFP-GUS* expression was visible in valves (va), ovaries (ov), the septum (se), and a weak signal was visible in petals (p). Note that this was a line with an overall strong GUS signal. No GUS signal was detected in sepals (se) and stamens (st) or in the style and stigma. After fertilization, the expression domain became restricted to developing seeds. **E:** *pMPB2C::MPB2C-GFP-GUS* was expressed in the abscission zone (see also arrowheads in A and F), a domain where *MPB2C* and *KNAT1/BP* expression overlap. **F:** In mature siliques, only few seeds showed a GUS signal, and no signal was observed in other parts of the silique. The *MPB2C* promoter was still active in the abscission zone. Scale bars: 1mm A, F; 100µm D.

3.1.6 *MPB2C* is highly expressed in young carpels and in the abscission zone

In the course of floral tissue differentiation, the *pMPB2C::MPB2C-GFP-GUS* and *pMPB2C::GFP-GUS* yielded strong GUS activity in the gynoecium. Until the stage of fertilization, expression was observed in most parts of the gynoecium: valves, ovules, placenta and septum, but not in the stigma and style or in tissues of the outer floral whorls (Figure 13, see also (Winter, Kollwig et al. 2007)). Only in lines with overall strong GUS signal, a weak expression in petals prior to anthesis (Figure 13B) was observed. After fertilization, the GUS signal became gradually restricted to developing seeds, and by stage 16/ 17¹⁴, *MPB2C* was no longer expressed in valves and in the septum. At this stage a new and strong expression domain was observed in the abscission zone (Figure 13A, E and F). In the abscission zone, *MPB2C* is co-expressed with *KNAT1* and *KNB1*. In maturing seeds within green siliques after stage 17, expression of *pMPB2C::MPB2C-GFP-GUS* was no longer detectable, consistent with *in silico* data (Figure 6).

3.1.7 *MPB2C* and *KNB1* are co-expressed in a number of tissues

In seedlings as well as in flowers, co-expression of *MPB2C* with *KNB1* was observed [see also (Fichtenbauer 2011)]. *KNB1* was expressed in seedling shoot and root tips, in secondary root buds, in the cotyledon vasculature and in root vascular tissue, in expanding true leaves, in carpels and after fertilization in developing seeds and in the abscission zone of siliques (Figure 14). In seedlings, *KNB1* expression seemed to be generally stronger than expression of *MPB2C* – more independent transgenic lines showed a stronger overall signal, especially often also in cotyledons beyond the vasculature.

3.1.8 Auxin and Gibberellic Acid, but Absciscic Acid increase *MPB2C* promoter activity

Plants of the *pMPB2C::MPB2C-GFP-GUS* reporter line 58-1 when grown under long day conditions on agar plates supplemented with different substances. Presence of the synthetic auxin α -Naphthalene acetic acid (NAA) and of gibberellic acid increased the *MPB2C* promoter activity in cotyledons, leaves, in the hypocotyl and in roots. No changes were observed when plants were grown on plates supplemented with absciscic acid or Tween-20. Growth on 100mM NaCl triggers osmotic stress. Plants grown under this condition had a retarded development and displayed a weaker GUS signal in cotyledons and expanding leaves (Figure 15). These experiments were done by Kornelija Pranjic in the Kragler Lab.

¹⁴ numbers according to (Smyth, Bowman et al. 1990)

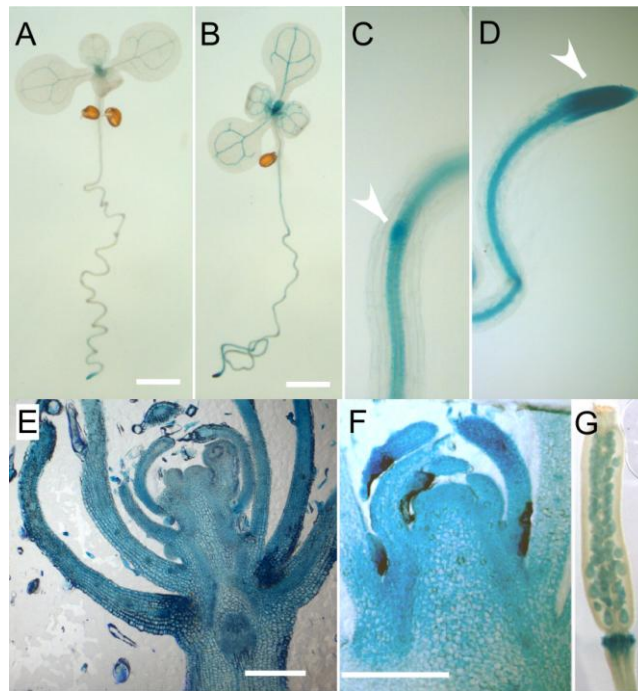


Figure 14: Expression of *KNB1* largely overlaps with *MPB2C* expression

A to D (C and D are close-ups of the plant shown in B): Line 38-23 (from Daniela Fichtenbauer, Kragler Lab) transgenic for *pKNB1::KNB1-GFP-GUS* seven days after germination grown on agar plates under long day conditions. Both plants, one with a lower overall signal (**A**) as well as a plant with stronger GUS signal (**B**), show *pKNB1::KNB1-GFP-GUS* expression in the shoot and root tips, in cotyledon vasculature and in expanding leaves, in lateral root primordia (arrowhead in **C**) and in the root tip (arrowhead in **D**) as well as in the root vasculature (B, C, D). **E**: A longitudinal section through a ca. 4 week old plant grown under long day conditions on soil transgenic for *pKNB1::GFP-GUS* (line A4-10 from Gregor Kollwig, Kragler lab) was detected in leaves surrounding inflorescences, and in the stem, especially in the cortex and epidermal regions. The signal was barely detectable in floral primordia and in the inflorescence meristem. **F**: Axillary meristem of a plant transgenic for *pKNB1::KNB1-GFP-GUS* (line 38-1 from Daniela Fichtenbauer, Kragler lab). The signal was detected throughout axillary buds including the meristematic region. In the main inflorescence a pattern similar to *pKNB1::GFP-GUS* was observed (not shown). *KNB1* expression in carpels of unfertilized flowers was strong [data not shown, see (Fichtenbauer 2011)]. **F**: Line 38-1 shows expression in maturing seeds and in the abscission zone. Plants in pictures E to G were grown on soil under long day conditions. Scale bars: A, B: 1mm; E: 200µm, F: 100µm.

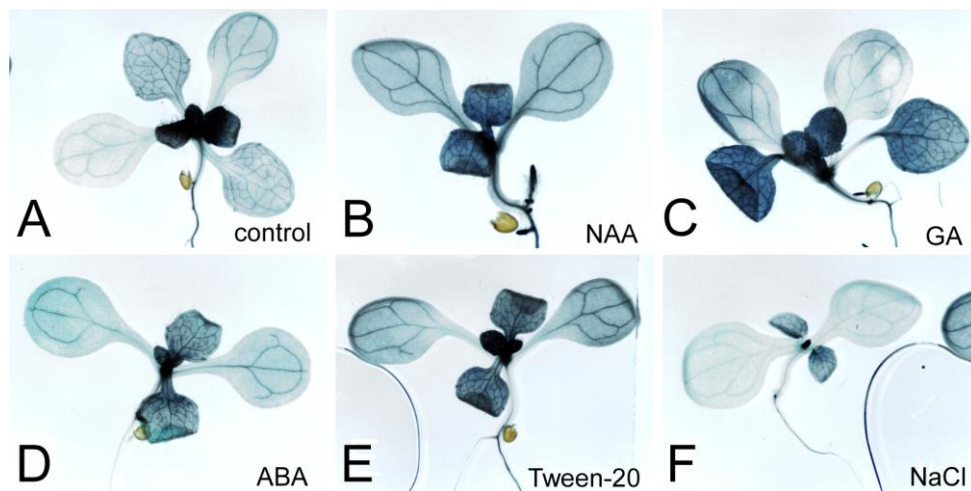


Figure 15: Effect of external application of hormones on *MPB2C* promoter activity

A- F: 7 day old plants transgenic for *pMPB2C::MPB2C-GFP-GUS* (line 58-1) grown under long day conditions on agar plates including 3% sucrose, except for the Tween-20 and the NaCl plates. Compared to the control plant (**A**), growth on 5µM NAA (**B**) and 5µM gibberellic acid (**C**) increased the strength of the GUS reporter signal in leaves, in the hypocotyl and in roots.

Plates supplemented with 10µM abscisic acid (D) or 0,2% Tween-20 (E) showed no altered *MPB2C-GFP-GUS* expression levels. Growth under osmotic stress on 100mM NaCl (F) resulted in retarded growth and hence a reduced GUS signal in cotyledons. Experiment performed and pictures taken by Kornelija Pranjic, Kragler Lab.

3.2 The MPB2C protein

3.2.1 MPB2C is plant specific and does not belong to a multi-gene family in *Arabidopsis*

A simple standard BLAST (Altschul, Gish et al. 1990) search of the MPB2C protein sequence against a non-redundant protein database yielded homologous proteins across embryophyta (land plants). The size of the proteins varied between 215 and 497 amino acids. The identity scores ranged from 96% to 42% for eudicotyledonous plants, from 38% to 31% (E- value <0.001) for monocotyledonous plants, and proteins with an identity between 23% and 21% (E- values between 0.1099 and 0.0108) were retrieved for non- spermatophytes (seed plants). The evolutionary most ancient homolog was found in the moss *Physcomitrella patens* belonging to the bryophytes (non- vascular plants). There were no significant hits for non-plant proteins (E- value >1), see also (Kragler, Curin et al. 2003; Cho, Cho et al. 2012). In this search against protein databases, no homologous protein from angiosperms was retrieved, but this might be due to incomplete data sets for angiosperm proteins in the available public databases. A query in which a translated nucleotide database was searched using the AtMPB2C protein sequence with the tblastn algorithm yielded two mRNA sequences coding for homologous proteins from spruce with identities of 30% for *Picea glauca* and 37% for *Picea sitchensis* *MPB2C-related proteins*. As far as data about the genomic location were available, the exon/intron structure of five exons was conserved for most genes, except for the *Physcomitrella* locus and the locus of one *Selaginella* gene with 6 exons each. The alignment of putative MPB2C homologs (see Figure 16 and Appendix B – Protein Sequences used for alignment) was used as input for the construction of a phylogenetic tree (Figure 17) to allow an estimate for the significance of the retrieved proteins. Indeed, the proteins fell into clades roughly representing phylogenesis: There was a clade for monocotyledonous and a clade for dicotyledonous plants, the translated gymnosperm sequences fell into a separate clade, and the sequences from *Selaginella* (lycophytes) and finally *Physcomitrella* (bryophytes) were assigned to most distant clades. A gene duplication event seems to have occurred in monocotyledonous plants yielding two clades for the MPB2C paralogs within the monocot clade. In *Selaginella* also two homologous proteins were found.¹⁵

3.2.2 MPB2C encodes a protein with a predicted central coiled-coil domain

Based on software prediction tools, only a coiled-coil region but no functional domains can be assigned to the MPB2C protein sequence. As described previously, an N- terminal conserved hydrophobic region (boxed in Figure 16) seems to be important for subcellular localization (Kragler, Curin et al. 2003), see also chapter 3.2.5. According to the Conserved Domain Database at NCBI (Marchler-Bauer, Anderson et al. 2009), a domain of unknown function DUF812 (pfam 005667) and regions with similarity to chromosome segregation protein SMC were assigned to MPB2C, both spanning the central part of the protein – roughly between amino acids 120 and 250. This part is also predicted to form a coiled-coil structure.

¹⁵ Note added in proof: A recent publication reported three MPB2C genes in maize and duplicated MPB2C genes not only in monocotyledonous but also in some dicotyledonous plants, e.g. in *Glycine max* or in *Nicotiana benthamiana* (Cho et al., 2012). So, as expression databases become more and more complete, maybe more MPB2C paralogs will be discovered.

A coiled-coil is a structural motif characterized by alpha helices that coil around each other forming a superhelix. Such motifs often mediate protein-protein interaction. Coiled-coils are characterized by heptad repeats with apolar amino acids at positions **a** and **d** and often charged residues at positions **e** and **g** (Lupas 1996). A central coiled-coil region in the MPB2C protein sequence is predicted by various domain prediction algorithms. Based on the Lupas method (Lupas, Van Dyke et al. 1991), the region between amino acids 182 and 244 has the highest probability to fold into a coiled-coil. In the Arabi-COIL database (Rose, Manikantan et al. 2004), a coiled-coil domain is predicted between amino acids 126- 221. With the algorithm Paircoil2 (McDonnell, Jiang et al. 2006) the region between amino acids 126 and 253 yields the highest score for a coiled-coil domain. Alignment with the coiled-coil domain predicted for NtMPB2C (Kragler, Curin et al. 2003) yields a region of 46% identity and 72% similarity between amino acids 125 and 240 of AtMPB2C. Two well conserved regions of two and twelve phased heptad repeats typical for coiled-coils can be found between amino acids 139-152 and 170-253, respectively (boxed in red in the alignment in Figure 16, see also (Ruggenthaler, Fichtenbauer et al. 2009)). Note that there are two highly conserved exceptions in the heptad pattern which might be responsible for specific interactions, e.g. with RNA (Fritz Kragler unpublished): There are two positively charged lysines instead of apolar residues at the **d** positions of heptad 3 (K187) and heptad 6 (K208) of the second conserved region (amino acids highlighted in blue in Figure 16).

In conclusion: MPB2C is predicted to fold into a coiled-coil structure in its central region between amino acids 125 and 253. This structural motif might facilitate interaction with other molecules. We tested this hypothesis by constructing MPB2C(delta 178-229), a *MPB2C* deletion mutant lacking a part of the putative coiled-coil region. The subcellular localization (chapter 3.2.6) and protein-protein interactions in bimolecular fluorescence assays (chapter 3.3.6) of this truncated protein were tested and compared with full-length MPB2C. This mutant form did not abolish interactions completely but led to less specific interactions, probably because the first coiled-coil stretch was not affected by the deletion.

3.2.3 Predicted subcellular localization of the MPB2C protein

Although endogenous MPB2C was immunolocalized at microtubules in leaf epidermal protoplasts (Kragler, Curin et al. 2003), algorithms predict a potential nuclear localization signal in this protein. A region (aa 94- aa 110) upstream of the predicted coiled-coil domain seems to meet the criteria for a bipartite nuclear localization signal (NLS) (Raikhel 1992):

- two adjacent basic amino acids,
- a spacer region of any 10 residues,
- at least three basic residues (Arg or Lys) in the five positions after the spacer region.

A simple nuclear localization signal in this region is conserved in MPB2C homologs except for the homolog from *Picea glauca* (underlined in Figure 16B). Still, this predicted NLS awaits experimental testing.

Apart from the immunolocalization in protoplasts, the subcellular localization of MPB2C–fluorescent fusion proteins in plant cells at microtubules (Kragler, Curin et al. 2003; Winter, Kollwig et al. 2007) argues against the functional relevance of this predicted NLS. Moreover, the MPB2C-GFP-GUS fusion protein was not observed in nuclei of tissues examined in the promoter studies - in contrast for instance to KNB1-GFP-GUS, which was seen in nuclei of cotyledon epidermal cells (Fichtenbauer

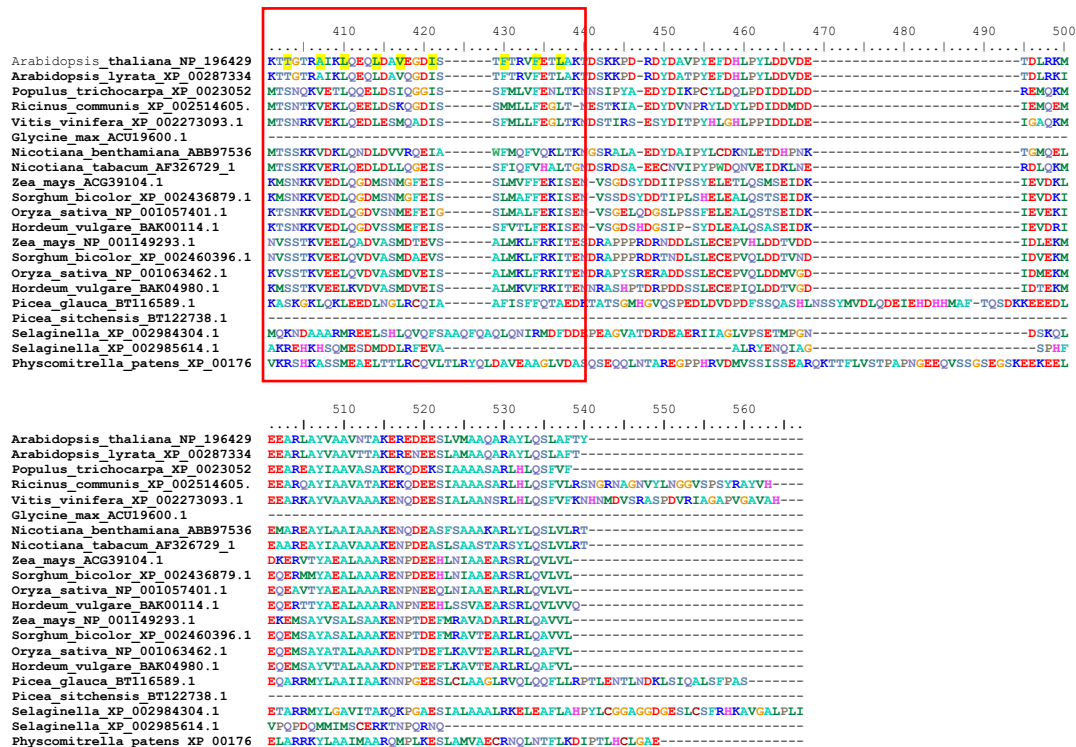
2011). Furthermore, *MPB2C* expressed in yeast or in animal cells was found in the cytoplasm and not in the nucleus (Fritz Kragler, personal communication). Either the NLS is structurally masked, or this sequence has another function. Such regions with an accumulation of positively charged residues could also mediate interaction with nucleic acids, and *MPB2C* was shown to bind RNA (Winter, Kollwig et al. 2007).

[illegible]

Sequence logo for the PTH101 binding site. The x-axis shows positions 110 to 200. The y-axis shows the log-odds of a nucleotide being at a position. The logo highlights a conserved sequence: MYEQQQHFMFLQSDSG---FGDDSSWLAGDGD---LRLSPHQQAAGTNSGNGNIDRLRLKIDVEMVFLPIHBMHKEKRS---FKRGRSMYTKM. A box highlights the sequence PTH101 CS94728 G79A.

Arabidopsis thaliana NP_196429
 Arabidopsis lyrata XP_00287334
 Populus trichocarpa XP_0023052
 Ricinus communis XP_002514605
 Vitis vinifera XP_002273093.1
 Glycine max ACU19600.1
 Nicotiana benthamiana AB997536
 Nicotiana tabacum AF326729.1
 Zea mays AGC39104.1
 Sorghum bicolor XP_002436879.1
 Oryza sativa NP_001057401.1
 Hordeum vulgare BAK00114.1
 Zea mays NP_001149293.1
 Sorghum bicolor XP_002460396.1
 Oryza sativa NP_001063462.1
 Hordeum vulgare BAK04980.1
 Picea glauca BT116589.1
 Picea sitchensis BT122738.1
 Selaginella XP_002984304.1
 Selaginella XP_002985614.1
 Physcomitrella patens XP_00176

[illegible]



B

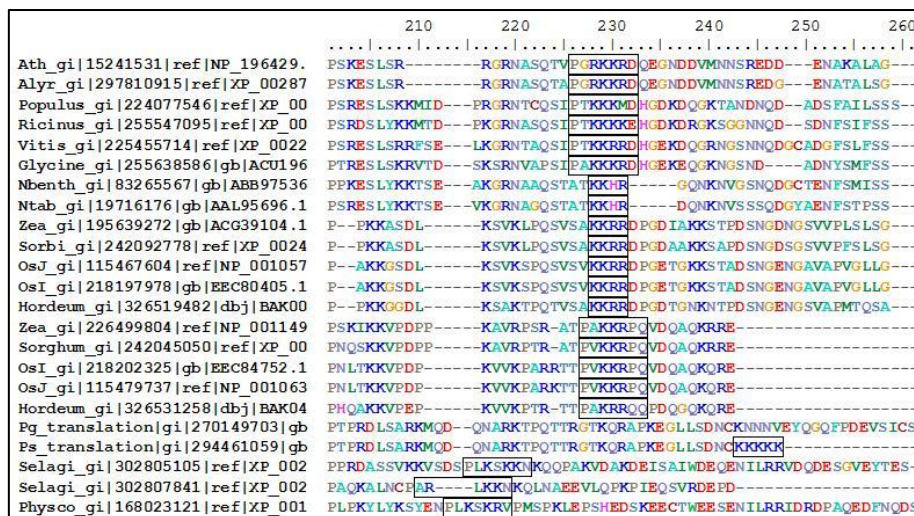


Figure 16: Alignment of the MPB2C protein

A: BLAST (Altschul, Gish et al. 1990) search of protein sequences similar to MPB2C from *Arabidopsis thaliana* yielded homologous proteins throughout the realm of land plants. A: Protein sequences from representative species were aligned using ClustalW2 (Goujon, McWilliam et al.). Boxed in black is the hydrophobic region close to the N-terminus of NtMPB2C described by (Kragler, Curin et al. 2003). The putative coiled-coil regions are boxed in red, and the hydrophobic residues at positions a and d of the heptad repeats are marked yellow. The two highly conserved exceptions of this heptad pattern (residues K187 and K208 in the *Arabidopsis thaliana* sequence) are highlighted in blue instead of yellow. Locations of TILLING point mutations (see chapter 3.5.3) are indicated. B: Close-up of the amino acids predicted as putative bipartite nuclear localization signal (boxed).

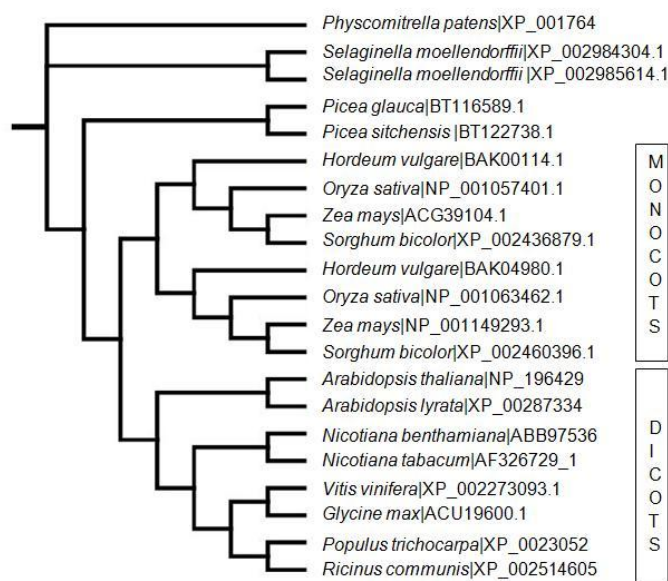


Figure 17: Phylogenetic Tree of MPB2C protein

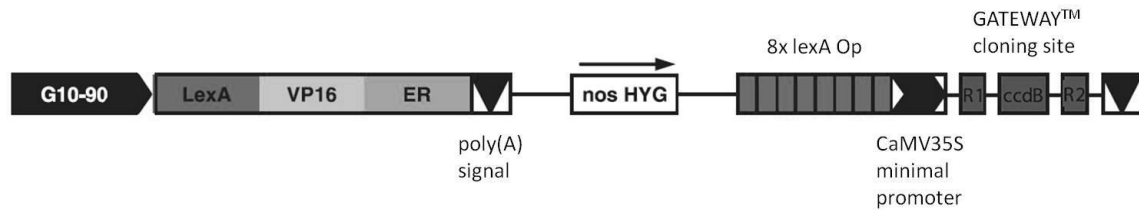
A representative selection of protein sequences homologous to *AtMPB2C* was used as an input for the construction of a phylogenetic tree by ClustalW2 (Goujon, McWilliam et al.). The tree was visualized with the software Mesquite 2.75 (Maddison 2011). Unique accession numbers of the proteins are indicated (see also Appendix B – Protein Sequences used for alignment).

3.2.4 Dynamics of MPB2C–GFP/RFP subcellular localization

MPB2C was previously described to be cell-autonomous and to appear in a cytosolic punctate pattern along microtubules. These findings are based on immunofluorescence analysis of *NtMPB2C* localization in protoplasts derived from *N. tabacum* leaf tissue (Kragler, Curin et al. 2003), transient overexpression of *NtMPB2C-RFP* in epidermal cells of *N. tabacum* (Kragler, Curin et al. 2003), transient and 35S promoter-driven overexpression of *GFP-AtMPB2C* in epidermal leaf cells of *A. thaliana* (Ruggenthaler, Fichtenbauer et al. 2009) and transient overexpression of *AtMPB2C-GFP* or – *RFP* in *N. benthamiana* epidermal leaf cells (Winter 2007; Winter, Kollwig et al. 2007).

MPB2C fused to a C-terminal fluorescent protein tag has a strong tendency to build large aggregates when expressed from the strong viral 35S promoter. Only very early during transient expression the characteristic punctate pattern along microtubules could be observed. In cells with strong expression, mobile clusters of the fusion protein appeared soon, and after 48 hours, MPB2C appeared almost exclusively in large immobile aggregates (Winter 2007). Whereas MPB2C-GFP (derived from the binary gateway vector pEarleyGate103) could readily be detected in transient expression assays in *N. benthamiana* leaves, the same fusion protein could not be detected in transgenic *Arabidopsis* plants, neither via confocal microscopy nor via Western blot analysis although the expression of the construct was confirmed via RT-PCR (Winter 2007). The same situation was true for *p35S::MPB2C-RFP* cloned into the binary Gateway® vector pBat-TL-K-RFP. A second different *MPB2C-RFP* fusion protein was cloned into vector pMDC7 (Curtis and Grossniklaus 2003). In order to prevent steric hindrance, an Alanine linker was inserted between MPB2C and mRFP1. The resulting *pG10-90::XVE>>pOlexA-46::MPB2C-Ala-mRFP1* cassette allowed estradiol-inducible expression of MPB2C-Ala-RFP. XVE, an artificial transcription factor including an estrogen receptor is expressed from the strong synthetic G10-90 promoter (a *CaMV35S* promoter enhanced by a G-box motif (Ishige, Takaichi et al. 1999)). The gene of interest is under the control of an artificial promoter,

*OlexA*₄₆, followed by a minimal 35S promoter. In the presence of β -estradiol, XVE can enter the nucleus and activate transcription from *pOlexA*₄₆ (see also Figure 18).



Scheme modified with permission from: Moore et al., The Plant Journal 2006

Figure 18: Scheme of the cassette allowing estradiol inducible overexpression

The estradiol inducible MPB2C-Ala-mRFP1 fusion protein could be detected in transient expression assays in *N. benthamiana* epidermal leaf cells and in transgenic *Arabidopsis* plants (see Figure 19). In ten day old transgenic seedlings, MPB2C-Ala-mRFP1 was detected as early as three hours after induction with estradiol. In leaf tissues of transgenic plants, MPB2C-Ala-mRFP1 was observed in the expected punctate pattern along microtubules (Figure 19A), B, whereas in roots the fusion protein was visible in form of small bodies (Figure 19 I, J), or the fluorescent signals appeared diffuse in the cytoplasm and in nuclei (Figure 19 K, L). The latter cytoplasmic and nuclear signal was also observed in transient assays and was considered to be an artifact due to overexpression. In transient expression and in transgenic plants, MPB2C-Ala-mRFP1 was located in the cytoplasm in small bodies and in filamentous or reticulate structures, which were in proximity to the endoplasmic reticulum, but they did not co-localize with an ER-marker (Figure 19C to H).

3.2.5 The N-terminus of MPB2C is involved in subcellular localization and aggregate formation

The hydrophobic motif close to the N-terminus (boxed in the NtMPB2C sequence in the alignment, Figure 16) described by (Kragler, Curin et al. 2003) is well conserved among gymnosperms and angiosperms. Yet it is only present in one of the two *MPB2C* subclades in monocotyledonous plants. The N-terminal region of MPB2C is thought to be involved in directing the protein to discrete structures along microtubules generating the characteristic punctate pattern. Deletion of this conserved hydrophobic region at the N-terminus of NtMPB2C led to a change in subcellular localization towards a continuous decoration of microtubules which became visible as filaments, whereas the formation of aggregates was strongly reduced (Kragler, Curin et al. 2003). Interestingly fusion of GFP to the N-terminus of AtMPB2C had the same effect (Ruggenthaler, Fichtenbauer et al. 2009), see also chapter 3.6.2. The fusion protein might interfere with correct folding of the N terminus or hinder folding or at least weaken heterodimer formation. Therefore fusion proteins were attached only to the C-terminus of MPB2C in this work, except for the split YFP system cloned via binary vectors pCI112 and pCI113, which was only available in form of N-terminal fusion proteins connected via a glycine linker and a Myc tag to the protein of interest.

Earlier experiments showed that a larger deletion of the N-terminus affecting the predicted coiled-coil domain of NtMPB2C resulted in the loss of a distinct subcellular localization. This truncated fluorescent fusion protein was detectable as a diffuse background signal in the cytoplasm (Kragler, Curin et al. 2003). Analogous to the deletion constructs in tobacco, two different N-terminal deletion constructs were generated in AtMPB2C (Figure 20). One construct, AtMPB2C(delta 1-58), lacking the

first 58 amino acids, started from the middle of the conserved hydrophobic domain. In the second construct, AtMPB2C(delta 1-117) the entire region N-terminal to the predicted coiled-coil motif was deleted. AtMPB2C(delta 1-58)-RFP was located along microtubules in a more continuous manner than the full-length protein, and large aggregates were not observed. This correlates with NtMPB2C(delta 1-66) in tobacco (Kragler, Curin et al. 2003). The observed shift in subcellular localization caused by the loss of the hydrophobic domain might occur because interaction of MPB2C with vesicles forming the characteristic punctate pattern along microtubules is interrupted by this deletion. AtMPB2C(delta 1-117)-GFP could not be detected in transient expression assays, which suggests that this deletion destabilizes the fusion protein.

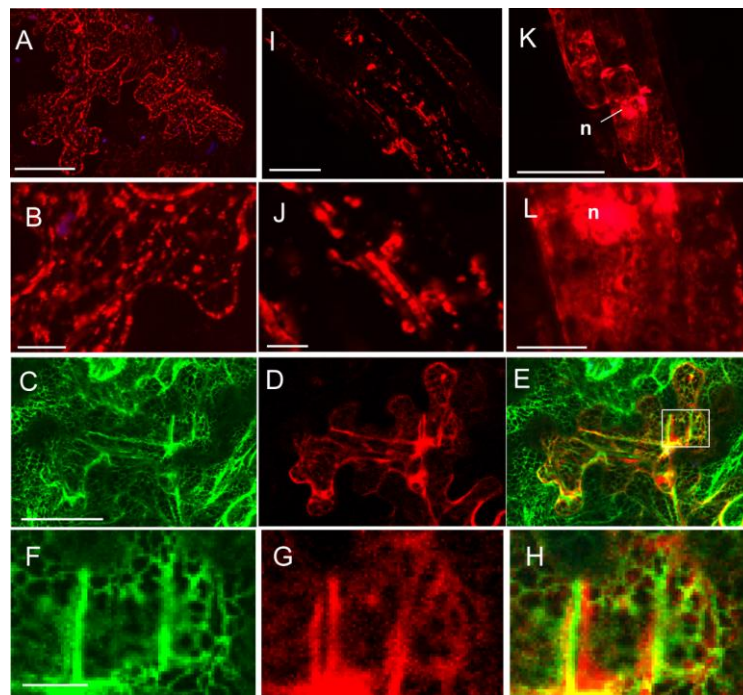


Figure 19: Subcellular localization of MPB2C-Ala-mRFP1

A, B, I to L: Confocal images taken by F. Kragler show transgenic *Arabidopsis* plants harboring the construct *G10-90::XVE>>pOlexA₄₆::MPB2C-Ala-mRFP1* (in binary vector pMDC7) after 2 days of induction with β -estradiol. **B to H:** Confocal images of leaf epidermal pavement cells in *N. benthamiana* line 16C 48 hours after agrobacterium-mediated infiltration and β -estradiol-induction with the same construct as above (*G10-90::XVE>>pOlexA₄₆::MPB2C-Ala-mRFP1*). **A and B** (magnified): MPB2C-Ala-mRFP1 was seen in the cytoplasm in small aggregates along filamentous/reticulate structures. However, these structures did not represent the endoplasmatic reticulum, as shown in **C to H**: Transient expression of MPB2C-Ala-mRFP1 (red channel in D, G, and the merged pictures E and H) in the *N. benthamiana* line 16C which constitutively expressed ER-targeted GFP (green channel in C, F, and the merged pictures E and H) showed close association but no co-localization between GFP and RFP in the merged picture (E, H). Pictures C to H show a confocal Z-stack at the surface of an epidermal cell where the reticulate structure of the cortical ER can be seen. Pictures F to H show a magnified detail (boxed in E) from the pictures above. The green and the red signal are close, but they do not overlap. The yellow signal is only visible in regions of high signal strength of both constructs, and probably results from bleeding through of the channels but does not represent co-localization. **I to L:** In roots of transgenic *Arabidopsis* expressing MPB2C-Ala-mRFP1, the signal appeared in form of small clusters (**I, J**) or more diffuse in spherical or torus-shaped bodies in the cytoplasm and occasionally in nuclei (**n**) (**K, L**). The nuclear signal seen in K and L (labeled with n) might be an artifact due to overexpression and/or degradation of the fusion protein and unspecific nuclear accumulation. Scale bars: A, C, I, K: 50 μ m; B, F; J, L: 10 μ m; red: MPB2C-Ala-mRFP1, green: ER-GRP, blue: chloroplast autofluorescence; n: nucleus.

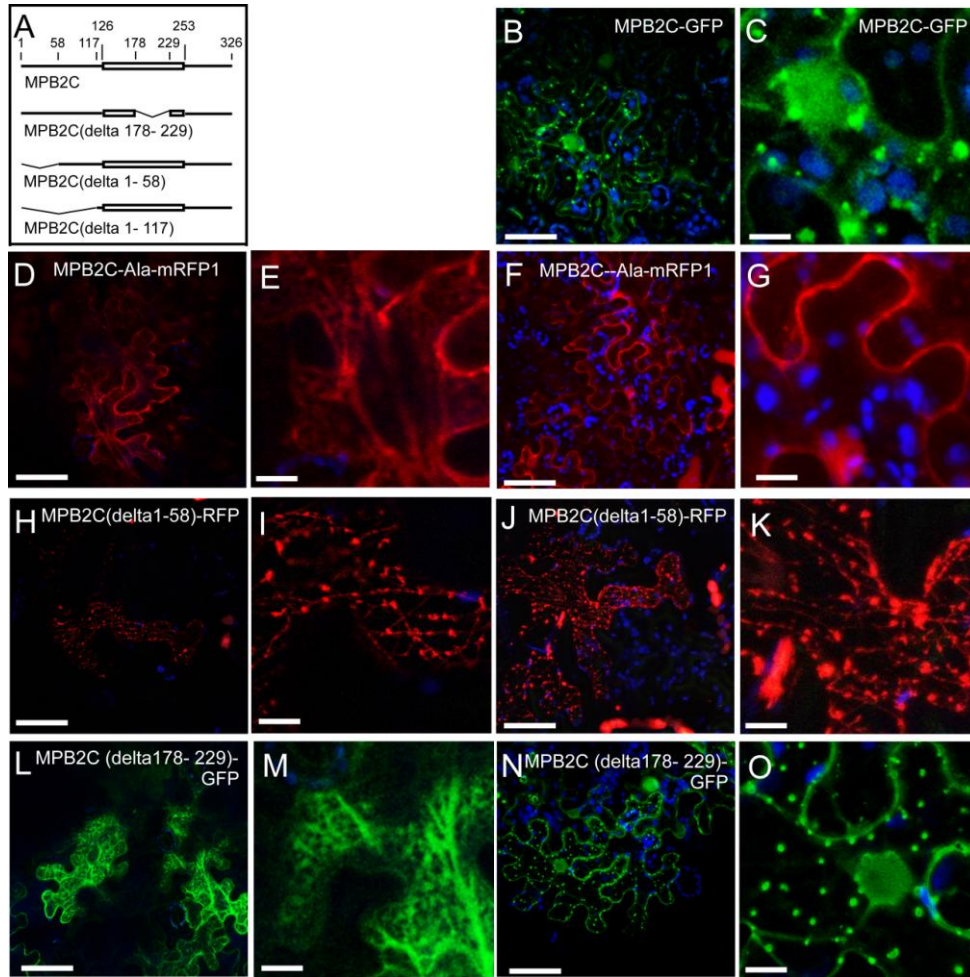


Figure 20: Subcellular localization of MPB2C full length and domain deletion constructs

A: Scheme of deletion constructs generated in this work. The box represents the predicted coiled-coil region of MPB2C. **B to O:** Transient expression of different MPB2C- fusion protein constructs in *N. benthamiana* epidermal cells 24 to 48 hours post infiltration. **B, C:** *p35S::MPB2C-GFP* (vector pEarleyGate103); **D to G:** β -estradiol induced *pG10-90::XVE>>pOlexA₄₆::MPB2C-Ala-mRFP* (vector pMDC7, construct L); **H to K** (pictures taken by F. Kragler): *p35S::MPB2C(delta1-58)-RFP* (in vector pBat-TL-K RFP, construct Q); **L to O:** *p35S::MPB2C(delta178-229)-GFP* (vector pEarleyGate103, construct 55). Pictures B, C, F, G, J, K, N and O show merged Z-stacks at the nuclear plane. Pictures D, E, H, I, L and M show merged Z-stacks close to the cell surface. Scale bars: B, D, F, H, J, L, and N: 50µm, C, E, G, I, K, M and O: 10µm; green: GFP fusion proteins, red: RFP fusion proteins, blue: chloroplast autofluorescence.

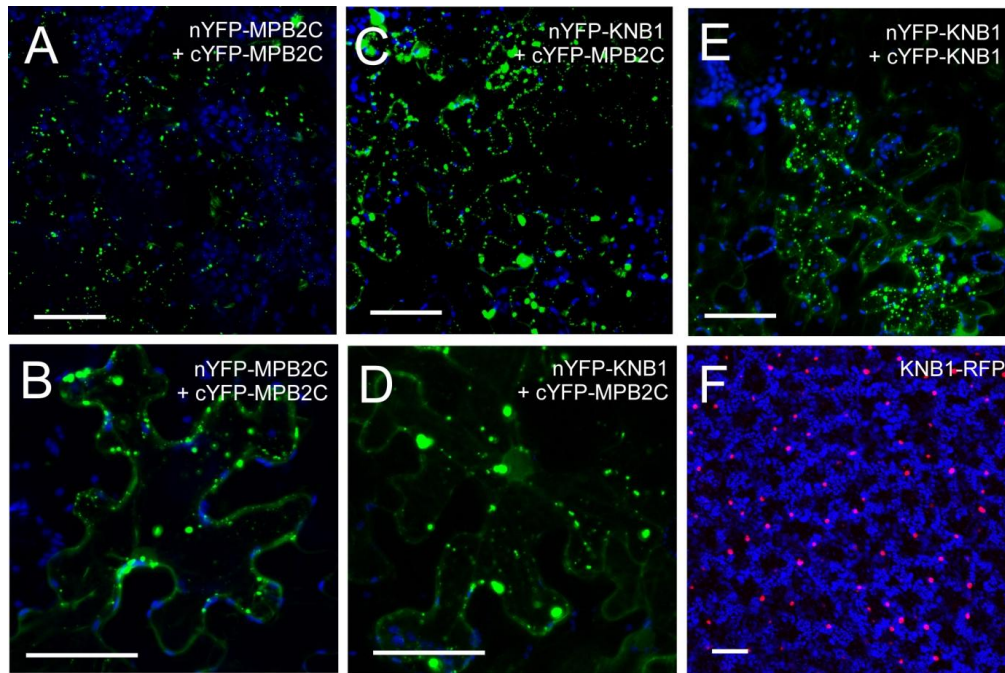


Figure 21: Interactions of MPB2C and KNB1 in bimolecular fluorescence complementation assays

Pictures are derived from transient co-expression of split YFP fusion proteins 24 hours after infiltration in *N. benthamiana*. The green signal in **A** to **E** represents reconstituted YFP fluorescence through interaction of the fusion proteins. **A, B:** n/cYFP-MPB2C forms homodimers. The cytosolic aggregates resemble the signal obtained with MPB2C-GFP. **C, D:** cYFP-MPB2C and nYFP-KNB1 interact forming cytosolic aggregates. **E:** n/c-YFP-KNB1 homodimerizes in the split YFP system forming cytosolic aggregates. **F:** KNB1-RFP was detected in nuclei (co-localization of this fusion protein with DAPI-stained nuclei was shown by (Fichtenbauer 2011)), whereas interaction between nYFP-KNB1 with cYFP-MPB2C (**C, D**) or n/c-YFP-KNB1 homodimerization (**E**) were observed mostly in the cytoplasm. Scale bars **A** to **E**: 50µm, **F**: 100µm; green: reconstituted YFP, red: RFP fusion proteins, blue: chloroplast autofluorescence.

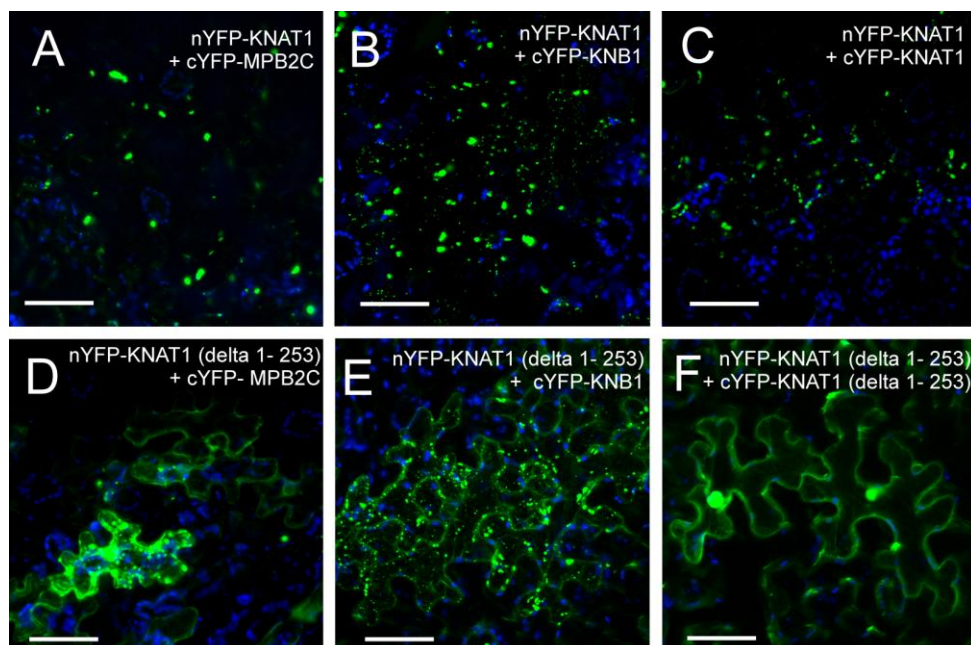


Figure 22: KNAT1/BP interactions in bimolecular fluorescence complementation assays

nYFP-KNAT1 interacts with cYFP-MPB2C (**A**), cYFP-KNB1 (**B**) and with cYFP-KNAT1 (**C**). The KNAT1 C-terminus including the ELK, NLS and homeodomain [=KNAT1 (delta 1- 253)] is sufficient to give a positive interaction signal with cYFP-MPB2C (**D**) and cYFP-KNB1 (**E**) when fused to nYFP. **F:** Fluorescent signals suggesting homodimerization of n/cYFP-KNAT1 (delta 1- 253) were detected in nuclei, not in the cytoplasm, where a high diffuse background was observed. The MEINOX motif deletion completely abolished clustering (compare **F** to **C**). Scale bars: 50µm; green: reconstituted YFP signal, blue: chloroplast autofluorescence

3.2.6 Deletion of the MPB2C coiled-coil region reduces the tendency to form aggregates

MPB2C(delta 178-229) is lacking a large part of the predicted coiled-coil domain (Figure 20A). We tested whether this deletion would alter subcellular localization of MPB2C. MPB2C(delta 178-229)-GFP showed a subcellular localization similar to full-length MPB2C-GFP (compare Figure 20B, C to L, M, N, O), but the tendency to form large aggregates was reduced. Hence, subcellular localization is not mediated via sequences within the deleted coiled-coil stretch. As the coiled-coil region was expected to play a role in protein-protein interactions, the next step was to investigate MPB2C protein interactions in general and the effect of the partial coiled-coil deletion on interaction.

3.3 MPB2C *in vivo* interactions

In order to study interaction of MPB2C with other proteins *in planta*, bimolecular fluorescence complementation (BiFC) assays with agrobacterium-mediated transient expression in *N. benthamiana* leaves were performed. AtMPB2C and potential interaction partners – some of which had been identified previously in yeast-two hybrid and protein overlay assays - were cloned into the binary vectors pCL112 and pCL113 as C-terminal fusion proteins either to the N-terminal (nYFP) or the C-terminal (cYFP) half of a split YFP. Upon interaction of the proteins of interest, the two halves of the split YFP protein were approached close enough to reconstitute YFP, which then emitted a fluorescent signal upon excitation at 488nm. Confocal images were taken 24 or 48 hours post infiltration.

3.3.1 MPB2C homodimerizes and interacts with KNB1

The homodimerization of MPB2C observed in yeast two-hybrid interaction assays (Kragler, Curin et al. 2003) could be confirmed *in planta* (Figure 21A, B). In the split YFP assays 24 hours after infiltration, small bodies became visible in the cytoplasm forming large aggregates in later stages of transient expression. A diffuse cytoplasmic and nuclear background signal was also observed (Figure 21B). MPB2C interacted with KNB1, a novel protein identified in our lab as an interaction partner of KN1 (Fichtenbauer 2011) (Figure 21C, D). Like MPB2C, KNB1 also interacted with itself in the split YFP system (Figure 21E). Interestingly, an interaction of KNB1 with itself or with MPB2C was detected in the cytoplasm, whereas KNB1-GFP and KNB1-RFP in transient expression assays and in transgenic plants were detected in nuclei and not in the cytoplasm (compare Figure 21D and E). Maybe the KNB1 split YFP fusion proteins could not form homodimers competent to translocate into the nucleus because of conformational changes or because KNB1 dimers were only formed in the cytosol whereas KNB1 remained monomeric in the nucleus. This is interesting in regards to KNB1 interaction with homeodomain proteins which themselves need to be nuclear localized in order to function as transcription factors. Could KNB1 interaction interfere with homeodomain protein gene regulation?

3.3.2 MPB2C and KNB1 interact with KNAT1/BP

Previously MPB2C had been shown to specifically interact with the viral movement protein TMV-MP (Kragler, Curin et al. 2003), and with the homeodomain proteins KN1 and STM (Winter, Kollwig et al. 2007). Hence, the question whether MPB2C also interacted with KNAT1 was standing to reason. KNAT1 is the closest ortholog in *Arabidopsis* of KN1 from maize, and of all KNOX proteins it has the highest sequence similarity to STM. Like STM, KNAT1 also moves between cells and tissue layers (Kim, Yuan et al. 2003; Kim, Rim et al. 2005), and KNAT1 partially rescued *stm-11* mutants when expressed from the *AtML1* promoter (Kim, Yuan et al. 2003). In BiFC assays, MPB2C showed strong interaction with KNAT1 building cytosolic clusters (Figure 22). KNAT1 also interacted with KNB1

(Figure 22B), consistent with the yeast-two hybrid results (Fichtenbauer 2011). Interestingly, similar to KNB1, full-length KNAT1 showed homodimerization in the cytosol, and no nuclear YFP could be observed (Figure 22C).

3.3.3 The MEINOX domain of KNAT1/BP is not essential for interaction with MPB2C and not necessary for interaction with KNB1 in BiFC assays

A KNAT1 mutant version, KNAT1 (delta 1-253), lacks more than half of the protein including the MEINOX domain, which is located at amino acid positions 133- 236. The homeodomain, the NLS and the ELK domain in the C-terminal part of the protein remain intact (Fichtenbauer 2011). Interaction of MPB2C with this truncated version of KNAT1 was observed in the split YFP assay (Figure 22D). This finding is consistent with earlier results in which the interaction of MPB2C with the KNOX proteins KN1 and STM was dependent on the presence of the homeodomain but not of N-terminal domains (Winter, Kollwig et al. 2007). In yeast two-hybrid assays, the deletion of the KNAT1 MEINOX domain completely abolished interaction with KNB1 (Fichtenbauer 2011). But in the split YFP system, co-infiltration of nYFP-KNAT1 (delta 1-253) with cYFP-KNB1 did give a signal in form of discrete small clusters (Figure 22E). However, apart from the clusters, a high diffuse cytoplasmic background signal was observed. This diffuse signal was present in all combinations with KNAT1 (delta 1-253) and also in combinations with MPB2C(delta 178– 229). As described previously (Winter, Kollwig et al. 2007), discerning weak signals from background in this split YFP system was sometimes difficult since the difference was subtle. Such weak diffuse cytoplasmic signals were interpreted as background unless additional clearly localized signals were visible, i.e. clusters or a nuclear signal. For KNB1 and KNAT1 (delta 1- 253), this interpretation was backed up by co-immunoprecipitation experiments, where interaction of KNB1-RFP with YFP-KNAT1 (delta 1-253) was strongly reduced but not completely absent compared to interaction of KNB1-RFP with full-length YFP-KNAT1 (Fichtenbauer 2011).

3.3.4 The KNAT1/BP MEINOX domain is sufficient but not essential for homodimerization

The MEINOX domain of KNOX proteins is thought to mediate protein-protein interactions between KNOX and BELL homeodomain proteins, both being members of the KNOX TALE protein family (Bellaoui, Pidkowich et al. 2001). But the MEINOX domain does not seem to be essential for homodimerization of KNOX proteins. It was reported that both, the homeodomain and the MEINOX domain, might mediate homodimerization of KNOX proteins (Muller, Wang et al. 2001; Nagasaki, Sakamoto et al. 2001). In the split YFP system, n/cYFP-KNAT1 homodimerization yielded a strong signal visible as large cytoplasmic aggregates (Figure 22C). Homodimerization of the truncated n/cYFP-KNAT1 (delta 1- 253) lacking the MEINOX domain resulted in a diffuse cytoplasmic and a strong nuclear signal, but no aggregates were observed (Figure 22F), suggesting that interaction was substantially weakened. Of all combinations in the split YFP system used in this work, only the deletion in KNAT1 (delta 1- 253) changed the subcellular localization of the observed homo-interaction signal, in this case from cytosolic to nuclear. Whether the nuclear signal is a background resulting from crowding of the fusion proteins in the nuclei and cytosol remains to be shown. The nuclear signal might also represent genuine interaction: The absence of the MEINOX domain in n/cYFP-KNAT1 (delta 1- 253) strongly reduced homodimerization in the cytosol, but, speculating, in the presence of DNA, the DNA-interacting homeodomains of these truncated proteins might have come close enough to reconstitute YFP fluorescence.

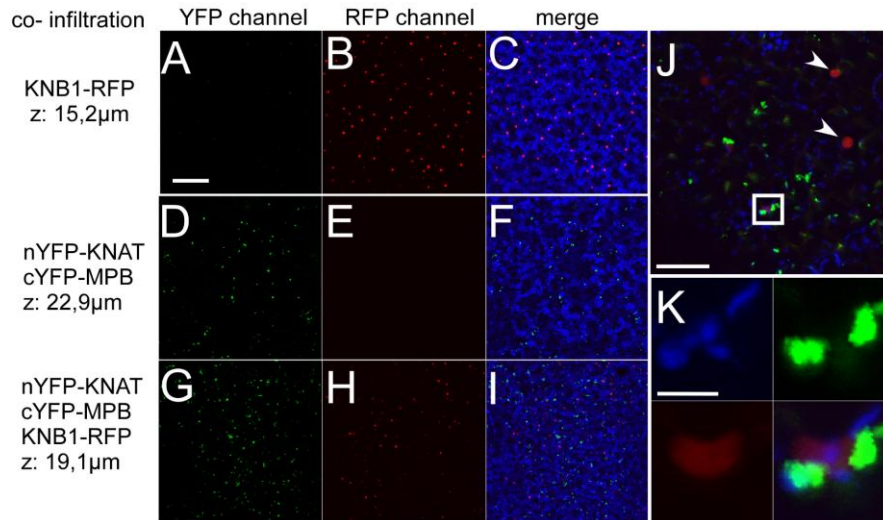


Figure 23: Triple co-expression of *MPB2C*, *KNAT1/BP* and *KNB1*

A, B, C: Confocal stack of KNB1-RFP infiltration. **D, E, F:** Confocal stack if nYFP-KNAT1 and cYFP-MPB2C co-infiltration. **G, H, I:** Confocal stack of triple infiltration with KNB1-RFP, nYFP-KNAT1 and cYFP-MPB2C. **J** and close-up **K:** Magnification of triple infiltration. The presence of KNB1-RFP did not interfere with interaction of KNAT1 and MPB2C (compare **D** to **G**). But KNB1-RFP levels were strongly reduced when all three proteins were expressed in the same cell (compare **B** to **H**). Picture **J** shows stronger KNB1-RFP signals in cells with no co-expression of nYFP-KNAT1 + cYFP-MPB2C (arrowheads). The weaker KNB1-RFP signal in co- expressing cells (boxed in **J**) is only visible in nuclei when magnified (**K**, bottom row). **K:** The nuclear KNB1-RFP is flanked by two clusters of nYFP-KNAT1 + cYFP-MPB2C (right). The four pictures in **K** show each channel separate and the merged picture (lower right). Scale bars A to I: 200μm; J: 50μm; K: 10μm. Stack size (z value) is indicated to allow comparison of signal intensities. A, D, G: YFP channel; B, E, H: RFP channel; C, F, I, J, K: merged images; blue: chloroplast autofluorescence.

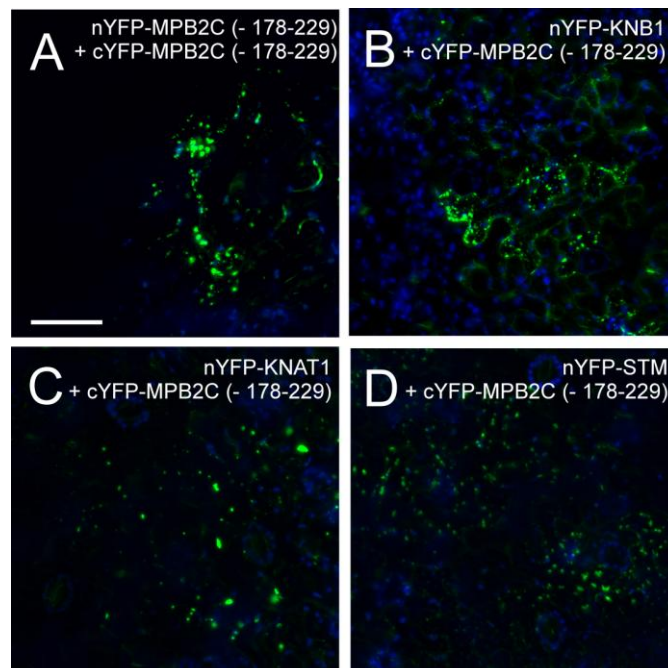


Figure 24: MPB2C(delta 178-229) interactions

cYFP-MPB2C(delta 178-229) interacted with nYFP-MPB2C(delta 178-229) (**A**), with nYFP-KNB1 (**B**), nYFP-KNAT1 (**C**) and nYFP-STM (**D**) in BiFC assays. Scale bar: 50μm; green: reconstituted YFP fluorescence, blue: chloroplast autofluorescence.

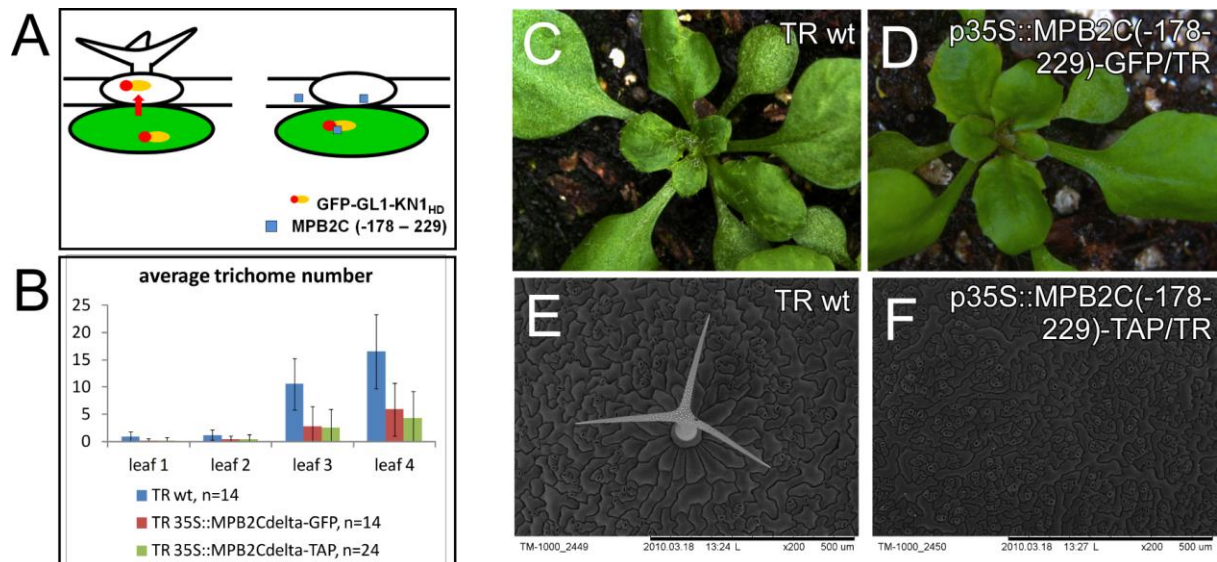


Figure 25: MPB2C(delta 178-229) interferes with KN1_{HD} cell-to-cell movement

A: Outline of the principle underlying the trichome rescue reporter line generated to track KN1_{HD} cell-to-cell transport by (Kim, Rim et al. 2005). Trichome-less *glabrous1* (*gl1*) mutants were transformed to express the fusion protein GFP-GL1–KN1₂₅₆₋₃₂₆ from the subepidermal *Arabidopsis* RuBisCO small subunit 2b (*RbcS2b*) promoter. The *KN1* homeodomain (KN1_{HD} or KN1₂₅₆₋₃₂₆) allowed the fusion protein to move from mesophyll, where *pRbcS2b* is active, into the epidermis, where GFP-GL1–KN1₂₅₆₋₃₂₆ acts as a transcription factor and functionally complements the *gl1* mutation. Therefore, trichomes are formed (left). Co-expression of *MPB2C* or *MPB2C*(delta 178- 229) from the 35S promoter interferes with the movement of GFP-GL1–KN1₂₅₆₋₃₂₆ into the epidermis, and no trichomes are formed (right picture). **B:** Chart showing the average trichome number on the first four leaves of independent T1 plants transgenic for *p35S::MPB2C(delta 178-229)-GFP* (red, n=14) and *p35S::MPB2C(delta 178-229)-TAP* (green, n= 24) and the untransformed trichome rescue line (blue, n= 14). *p35S::MPB2C(delta 178-229)-tag* interfered significantly with trichome formation (Students T test: $p < 0.05$). The average number of trichomes was reduced to 29% and 25% of TR wt levels in T1 lines transgenic for *p35S::MPB2C(delta 178-229)-GFP* and for *p35S::MPB2C(delta 178-229)-TAP*, respectively. **C, D:** Binocular microscope pictures, and **E, F:** scanning electron microscope pictures of untransformed trichome rescue plant and plants with reduced trichome number. **D:** *p35S::MPB2C(delta 178-229)-GFP* (T1 plant 55-2/TR); **F:** *p35S::MPB2C(delta 178-229)-TAP* (T1 plant 56-16/TR).

	TR wt, n=14	TR 35S::MPB2C(-178-229)-GFP, n=14	TR 35S::MPB2C(-178-229)-TAP, n=24
leaf 1	0,86 +/- 0,95	0,14 +/- 0,4 $p = 0.02$	0,17 +/- 0,64 $p = 0.02$
leaf 2	1,21 +/- 0,97	0,43 +/- 0,6 $p = 0.019$	0,38 +/- 0,92 $p = 0.015$
leaf 3	10,57 +/- 4,69	2,86 +/- 3,6 $p = 0.000052$	2,54 +/- 3,45 $p = 0.000014$
leaf 4	16,50 +/- 6,78	5,93 +/- 4,9 $p = 0.000083$	4,29 +/- 4,97 $p = 0.0000074$

Table 4: Effect of MPB2C(delta178-229)-GFP/-TAP on KN1_{HD} movement in the trichome reporter line

The average trichome number in TR plants transgenic for *p35S::MPB2C(delta 178- 229)-GFP* or *p35S::MPB2C(delta 178-229)-TAP* was significantly reduced (p values indicated) in all leaves compared to the untransformed parental TR line. Two out of 14 T1 plants transgenic for *p35S::MPB2C(delta 178- 229)-GFP/TR* (plants 55-10 and -13), and 8 out of 24 T1 plants transgenic for *p35S::MPB2C(delta 178- 229)-TAP/TR* (plants 56-3, -10, -14, -17, -19, -21, -23, -24) had no trichomes at all on the first four leaves.

3.3.5 Co-expression of *MPB2C* and *KNAT1/BP* with *KNB1* reduces *KNB1* protein levels

Based on the observed interactions of *MPB2C*, *KNAT1* and *KNB1* in all combinations, we asked whether these proteins interact in form of a large complex or whether interaction was temporally and/or spatially separated. Therefore the effect of *KNB1* expression on co-expressed *MPB2C* and *STM* or *MPB2C* and *KNAT1* was tested in the split YFP system and in parallel in yeast three-hybrid assays (Fichtenbauer 2011). The interaction of nYFP-*KNAT1* with cYFP-*MPB2C* or nYFP-*STM* with cYFP-*MPB2C* was not hindered upon co-expression of *KNB1*-RFP (Figure 23 shows interaction with *KNAT1*). However, the signal intensity of *KNB1*-RFP seemed weaker when *MPB2C* and *KNAT1* or *STM* were co-expressed. This is consistent with results from the yeast three-hybrid screen, where presence of *MPB2C* prevented a positive readout of the interaction between *KNB1* and *KNAT1*, and with Western blots assays, which revealed that *KNB1* protein amounts were reduced in the presence of *MPB2C* (Fichtenbauer 2011). Hence the proteins seem to act destabilizing on each other, and if a trimeric *MPB2C*-*KNB1*-*KNOX I* complex is formed, then it might have no long half life in the cell.

3.3.6 The central part of the predicted coiled-coil region of *MPB2C* is not essential for protein-protein interactions

In BiFC assays all interactions observed with the *MPB2C* full length protein were also observed with *MPB2C*(Δ 178-229). The truncated protein formed less aggregates, and a stronger cytoplasmic background signal were observed indicating that the interactions were weaker. Thus despite the deletion of a large part of the predicted coiled-coil domain, *MPB2C*(Δ 178-229) was still able to form homodimers and heterodimers with *KNB1*, *KNAT1* and *STM* (Figure 24). This result was surprising because the coiled-coil domain was expected to provide a structural core to the protein and to mediate protein-protein interactions. The reduction of aggregates and clusters and the shift towards a more equal cytoplasmic localization of the signal indicates a reduced capacity of *MPB2C*(Δ 178-229) to homodimerize or multimerize. However, protein-protein interaction was obviously not completely abolished by this deletion. Consistent with this was the finding that *MPB2C*(Δ 178-229) still interfered with *KN1* homeodomain- mediated cell-to-cell transport (see chapter 3.3.7).

3.3.7 *MPB2C*(Δ 178-229), like full-length *MPB2C* fusion proteins, interferes with *KN1* homeodomain cell-to-cell movement

Overexpression of *MPB2C*(Δ 178-229)-*tag* in transgenic plants had the same effect as overexpression of full-length *MPB2C*-*tag* in the trichome rescue reporter system: Cell-to cell-movement of the *KN1* homeodomain was impaired. In the lab of David Jackson (CSHL), a transgenic *Arabidopsis* line was designed to use trichome formation as a readout for the cell-to-cell movement of the *KN1* homeodomain (Kim, Rim et al. 2005). Overexpression of *MPB2C*-*tag* in this so-called trichome rescue line reduced or completely abolished trichome formation. The interaction of *MPB2C* with the *KN1* homeodomain interfered with the cell-to-cell movement of the latter (Winter 2007; Winter, Kollwig et al. 2007). Overexpression of *MPB2C*(Δ 178-229)-*GFP* or *MPB2C*(Δ 178-229)-*TAP* had a strong negative effect on trichome formation and hence on the movement of the *KN1* homeodomain. Trichomes on leaves 1- 4 were significantly reduced compared to the untransformed trichome rescue line (see Figure 25, Table 4, and Appendix E: Raw data trichome count). Interestingly, the reduction of was trichomes was even stronger than in plants overexpressing full length *MPB2C*-*tag* (Winter 2007), where trichomes on leaves 1& 2 were on average reduced to 49% (n= 21 T1 plants) of TR wt compared to *MPB2C*(Δ 178-229)-*tag* lines with an average reduction to 19% (n= 38 T1 plants) of TR wt.

These findings are consistent with the observation that MPB2C(delta 178-229) did behave similar to full length MPB2C in other experimental setups:

1. There was no difference in yeast-three hybrid interaction assays between full length MPB2C and MPB2C(delta 178-229) (Fichtenbauer 2011);
2. MPB2C(delta 178- 229) still formed homodimers and interacted with KNB1, KNAT1, and STM in split YFP assays (see chapter 3.3.6);
3. Plants overexpressing MPB2C(delta 178- 229) occasionally showed fasciation, which was also observed in plants that overexpressed full length MPB2C (see chapter 3.6.3).

3.3.8 Summary: MPB2C protein-protein interactions

- MPB2C interacts with MPB2C, KNB1, STM and KNAT1 in the split YFP system.
- Transient co- overexpression of MPB2C, KNB1 and STM or KNAT1 reduces protein levels of KNB1.
- Deletion of a large part of the MPB2C putative coiled-coil domain in MPB2C(delta 278-229) does not substantially alter the subcellular localization and does not completely abolish homodimerization or protein-protein interactions with KNB1, KNAT1 and STM and with the KN1_{HD} in the trichome rescue reporter system.

The results of observed interactions in the BiFC system are summarized in Table 5.

	MPB2C	MPB2C (delta 178-229)	KNB1	STM	KNAT1/BP	KNAT1/BP (delta 1- 253)
MPB2C	++ punctae, aggregates, background in cytoplasm/ nucleus	n.dX	++ cytoplasmic aggregates, background in cytoplasm/ nucleus	++ cytoplasmic aggregates no background	+++ cytoplasmic aggregates no background	++ cytoplasmic punctae, background in cytoplasm/ nucleus
MPB2C (delta 1-117)	-	n.d.	-	-	-	n.d
MPB2C (delta 178-229)	X	++ cytoplasmic aggregates, background in cytoplasm/ nucleus	++ cytoplasmic aggregates, background in cytoplasm/ nucleus	+ cytoplasmic aggregates, background in cytoplasm/ nucleus	++ cytoplasmic aggregates, no background	-/+ background in cytoplasm/ background or signal in nucleus
KNB1	X	X	++ cytoplasmic punctae, aggregates, background in cytoplasm/ nucleus	+ cytoplasmic aggregates, background in cytoplasm/ nucleus	+++ aggregates no background	++ aggregates, background in cytoplasm
KNAT1/BP	X	X	X	X	+++ aggregates no background	n/a
KNAT1/BP (delta 1- 253)	X	X	X	X	X	-/+ background in cytoplasm/ background or signal in nucleus

Table 5: Summary of protein interactions in bimolecular fluorescence complementation assays.

Definitions:-: no signal, -/+ weak or background signal, +: positive signal, ++: strong signal compared to split YFP-GUS co-infiltrations as negative controls; n/a: not analyzed, X: redundant.

3.4 Detection of the endogenous MPB2C protein via a peptide antibody

Three antibodies against MPB2C are available. A polyclonal antibody raised in rabbit against recombinant NtMPB2C described by (Kragler, Curin et al. 2003), a second polyclonal antibody targeting full-length AtMPB2C (Winter, Kollwig et al. 2007), and a polyclonal peptide antibody targeting the 22 C-terminal amino acids of MPB2C used in this work. As was observed with the polyclonal antibody raised against the whole protein, the polyclonal peptide antibody as well detected MPB2C at a higher apparent molecular mass than expected (at about 45 kDa instead of the calculated 37.3 kDa). Evidence for the specificity of the antibody came from the observation that the band was absent in plants from SALK line 90101C in which a T-DNA insertion caused a truncated form of MPB2C lacking the 51 C-terminal amino acids and hence also the epitope for the peptide antibody (see figure Figure 28 and chapter 3.5.2). Furthermore, the intensity of the band was decreased in lines overexpressing an artificial micro RNA (aMIR) targeting MPB2C mRNA (see Figure 26 A and chapter 3.5.4). Consistent with the GUS reporter lines for MPB2C promoter activity and the *in silico* data, the MPB2C protein could be detected in seedlings and leaf tissues, yet the highest amounts of MPB2C protein were detected in floral tissues (Figure 26 B).

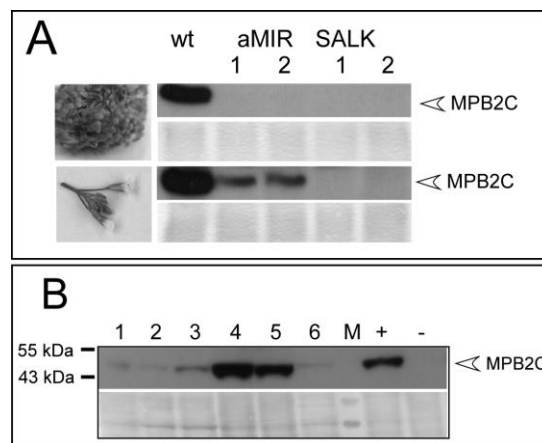


Figure 26: MPB2C Antibody specificity and tissue specific detection of MPB2C protein accumulation

A: The specificity of the C-terminal peptide antibody was confirmed using MPB2C miRNA-mediated silencing lines and the T-DNA insertion line SALK_90101C. Compared to wild type (lane 1), plants overexpressing an artificial micro RNA targeting MPB2C showed reduced levels of MPB2C protein in Western blots (lanes 2 and 3). MPB2C in plants homozygous for T-DNA insertion in line SALK_90101C was not detected with the C-terminal peptide antibody (lanes 4 and 5), because the epitope was deleted by the T-DNA insertion (see also Figure 28). In the upper picture extract from seedlings five days after germination grown in liquid medium were blotted. The lower picture shows a Western blot on protein extracts from inflorescences. Here, MPB2C levels in aMIR_MP2C lines were decreased by 60- 80%. Note that MPB2C protein levels were generally lower in seedling extracts, but a faint signal in the aMIR_MP2C lines was detected after overnight exposure with high sensitivity films (not shown). wt: wild type; aMIR: *p35S::aMIR_MP2C* lane 2: line A6-32_6-28; lane 3: line A6-32_1-1-1; SALK: SALK_90101C lane 4: line 7-1 (homozygous), lane 5: line 4-1 (homozygous); numbers indicate independent lines pooled (seedlings) or different individual plants (inflorescence tissues). **B:** Western blot showing MPB2C protein abundance in samples from different tissues. Consistent with *in silico* and expression data, MPB2C protein was detected throughout plant life, but the highest levels were detected in floral tissues (lanes 4 and 5). Lane 1: seedlings, lane 2: rosette leaves, lane 3: cauline leaves, lane 4: flower buds, lane 5: flowers after fertilization, lane 6: senescent leaves. M: marker, "+": positive control (wt), "-": negative control (SALK line). The respective Ponceau stained blots are shown below the exposed films in as loading controls.

3.4.1 MPB2C protein is sensitive to proteasomal degradation

When extracted under native conditions (but with a standard protease inhibitor cocktail included), AtMPB2C protein could hardly be detected on Western blots if the samples had been frozen for storage between extraction and Western blot. However, this was not the case after extraction under denaturing conditions with the Trizol reagent (Invitrogen), removal of RNA and subsequent acetone precipitation followed by resuspension in buffer (see Material and Methods). With this procedure MPB2C could be detected even after weeks of storing the samples at -20°C and even after repeated thawing and freezing. Hence we concluded that MPB2C might be susceptible to a proteolytic activity in native protein extracts, which was absent in extracts derived from the denaturing isolation protocol with Trizol/acetone. In order to test whether the destabilization was due to proteasomal degradation of MPB2C, we applied proteasome inhibitors. Infiltration of plant material with the proteasome inhibitors MG132 and Epoxomicin followed by protein extraction under native conditions including the proteasome inhibitors indeed increased the MPB2C signal in Western blots (Figure 27). As a control for proteasome inhibitor efficacy an *Arabidopsis* line named R-GUS (a gift from Andreas Bachmair, MFPL) was used (Figure 27 A). This line expressed a GUS reporter protein, which was modified to be sensitive to proteasomal degradation (Garzon, Eifler et al. 2007). Under our conditions, three times more R-GUS protein was detected in the presence of proteasome inhibitors than without. Endogenous MPB2C accumulated 50 times more with proteasome inhibitors applied than without (Figure 27 B).

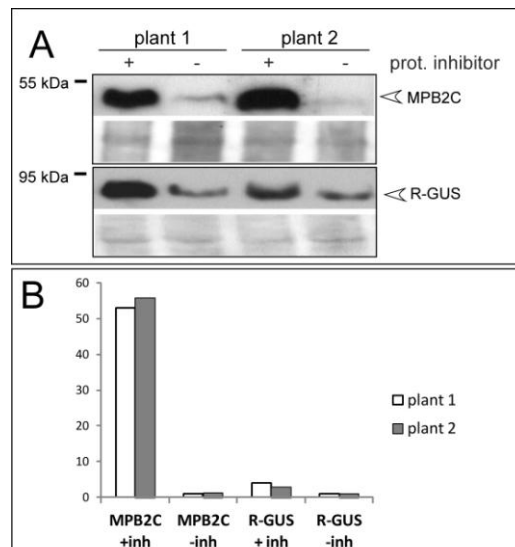


Figure 27: MPB2C protein is sensitive to proteasomal degradation

A: Upper panel: MPB2C was unstable when extracted under native conditions, but protein levels could be stabilized when proteasome inhibitors (100 μM MG132, 5 μM Epoxomicin) were applied before and during protein extraction. Lower panel: Effective proteasomal inhibition was monitored by samples from a reporter line named R-GUS (Garzon, Eifler et al. 2007), expressing GUS with an N-terminal arginine residue which, according to the N-end rule, triggers immediate ubiquitination and proteasomal degradation of the protein. The same protein extracts (from floral tissue) were used for detection of MPB2C and R-GUS. MPB2C was detected with the C-terminal peptide antibody, whereas R-GUS was detected with an anti-HA antibody, see also Materials and Methods. **B:** The band intensity of the Western blots in A were quantified using ImageJ and normalized to the Ponceau stained blots. The average signal of MPB2C and R-GUS without proteasome inhibitors was set to 1, respectively. Presence of proteasome inhibitors increased the MPB2C signal over 50 times. The abundance of R-GUS was increased over three times in the presence of proteasome inhibitors compared to extraction without inhibitors.

3.5 No knock-out line of *MPB2C* is available

So far, no knock-out line for *MPB2C* has been described. (Ruggenthaler, Fichtenbauer et al. 2009) reported that they could not regenerate transformants with a silencing construct. Neither had previous attempts in the lab of F. Kragler succeeded in confirming *MPB2C* SALK T-DNA insertion knock-out lines. Therefore different approaches were undertaken to study the effect of reduced *MPB2C* protein levels in plants. Two TILLING point mutations and one SALK T-DNA insertion leading to a truncated *MPB2C* protein were closer examined, furthermore two different *MPB2C* silencing approaches via an artificial micro RNA and a hairpin construct were pursued.

3.5.1 *MPB2C* polymorphisms do not alter phenotypic appearance

When the experiments were planned, 30 polymorphisms for *MPB2C* were documented by the platform TAIR (The Arabidopsis Information Resource, <http://www.arabidopsis.org/>), see Table 6). Five polymorphisms (PERL) were naturally occurring nucleotide substitutions found in different ecotypes. PERL0875214 was in the promoter, and the other four polymorphisms could be predicted to have no severe effect on the protein structure as they did not lead to changes in conserved amino acids. PERL0875206 is a silent mutation, and PERL0875204, PERL0875203, PERL0875201 as well as PERL0875200 resulted in exchanges of amino acids with similar characteristics regarding charge/hydrophobicity and size of the side chains and/or they were in non-conserved regions. The other 25 polymorphisms had been artificially created either by EMS mutagenesis (TILLING lines) or by T-DNA insertion (SALK and SAIL lines). Two TILLING lines were closer examined (see chapter 3.5.3). Of the 6 T-DNA insertions, two were located in the promoter region, one was located 39 nucleotides downstream of the stop codon, and the other two were located within introns. One intron mutant line was closer examined (see chapter 3.5.2).

3.5.2 T-DNA insertion line SALK 90101C

Three T-DNA insertion lines for the *MPB2C* locus had been reported by the SALK Institute (Alonso, Stepanova et al. 2003): lines SALK_120810, SALK_090101 and GK-135C08. But these insertions were located within introns (see Table 6). Only in line SALK_90101C, the T-DNA was inserted exactly at the border between the fourth exon and the fourth intron (see Figure 28 B). This mutation will produce a truncated form of *MPB2C* consisting of 275 amino acids specific for *MPB2C* and 22 random amino acids resulting from the T-DNA insertion (see alignment in Figure 28A). Hence this mutant *MPB2C* protein is predicted to lack 51 amino acids at the C-terminus. Therefore this line was examined more closely, and the T-DNA insertion in line SALK_90101C could be confirmed by genomic PCR and sequencing. The T-DNA was inserted in the antisense direction, i.e. the left border was located at the 3' end (relative to the *MPB2C* locus) of the insertion, and the right border was at the 5' side of the insertion. In Western blots no signal for the *MPB2C* protein was detected with the peptide antibody (see figure Figure 26A and Figure 28C). Apparently, indeed a truncated form of *MPB2C* was produced lacking the C-terminal epitope used to raise the peptide antibody (underlined in the wt sequence in Figure 28A). As expected, no developmental or phenotypic abnormalities were observed in line SALK_90101C, as this mutation did not affect conserved domains. However, this line was useful as a control for the specificity of the peptide antibody recognizing the C-terminal 22 amino acids.

Germplasm	Name	Region	Mutation	Mutation
not an ABRC stock	SAIL_331_C02.v1	promoter	T-DNA insertion	-520 nt
Polymorphism	PERL0875214	promoter	T → C	-387 nt
TILLING CS91435	ATMPB2C_165F6	exon 1	C → T	S43=
TILLING CS94720	ATMPB2C_202C3	exon 1	C → T	L52=
Polymorphism	PERL0875206	exon 1	G → A	V57=
TILLING CS88807	ATMPB2C_121F1	exon 2	C → T	S91=
TILLING CS94728	ATMPB2C_202C4	exon 2	G → A	G79D
TILLING CS96221	ATMPB2C_221G8	exon 2	C → T	S91F
TILLING CS89694	ATMPB2C_154H7	exon 3	G → A	E164=
TILLING CS91285	ATMPB2C_185C2	exon 3	G → A	R143K
TILLING CS95591	ATMPB2C_213B2	exon 3	G → A	K108=
Polymorphism	PERL0875204	exon 3	A → G	I191V
Polymorphism	PERL0875203	exon 4	A → G	K220R
Polymorphism	PERL0875200	exon 5	T → C	V310A
Polymorphism	PERL0875201	exon 5	G → C	R284T
N530629	SALK_030629.48.80.x	3'UTR	T-DNA insertion	STOP +39 nt
TILLING CS86834	ATMPB2C_110A1	intron	substitution	
TILLING CS86897	ATMPB2C_110A7	intron	substitution	
TILLING CS87004	ATMPB2C_112G3	intron	substitution	
TILLING CS87320	ATMPB2C_117A3	intron	substitution	
TILLING CS90185	ATMPB2C_161C2	intron	substitution	
TILLING CS91431	ATMPB2C_165B6	intron	substitution	
TILLING CS92988	ATMPB2C_176E2	intron	substitution	
TILLING CS93475	ATMPB2C_182A3	intron	substitution	
TILLING CS92218	ATMPB2C_195E4	intron	substitution	
TILLING CS92393	ATMPB2C_197D7	intron	substitution	
TILLING CS95934	ATMPB2C_217B4	intron	substitution	
CS27951	SALK_120810.43.25.x	intron 2	T-DNA insertion	
CS27941	SALK_090101.53.15.x	intron 4	T-DNA insertion	
CS412896	GK-135C08-012755	intron 4	T-DNA insertion	

Table 6: MPB2C Polymorphisms

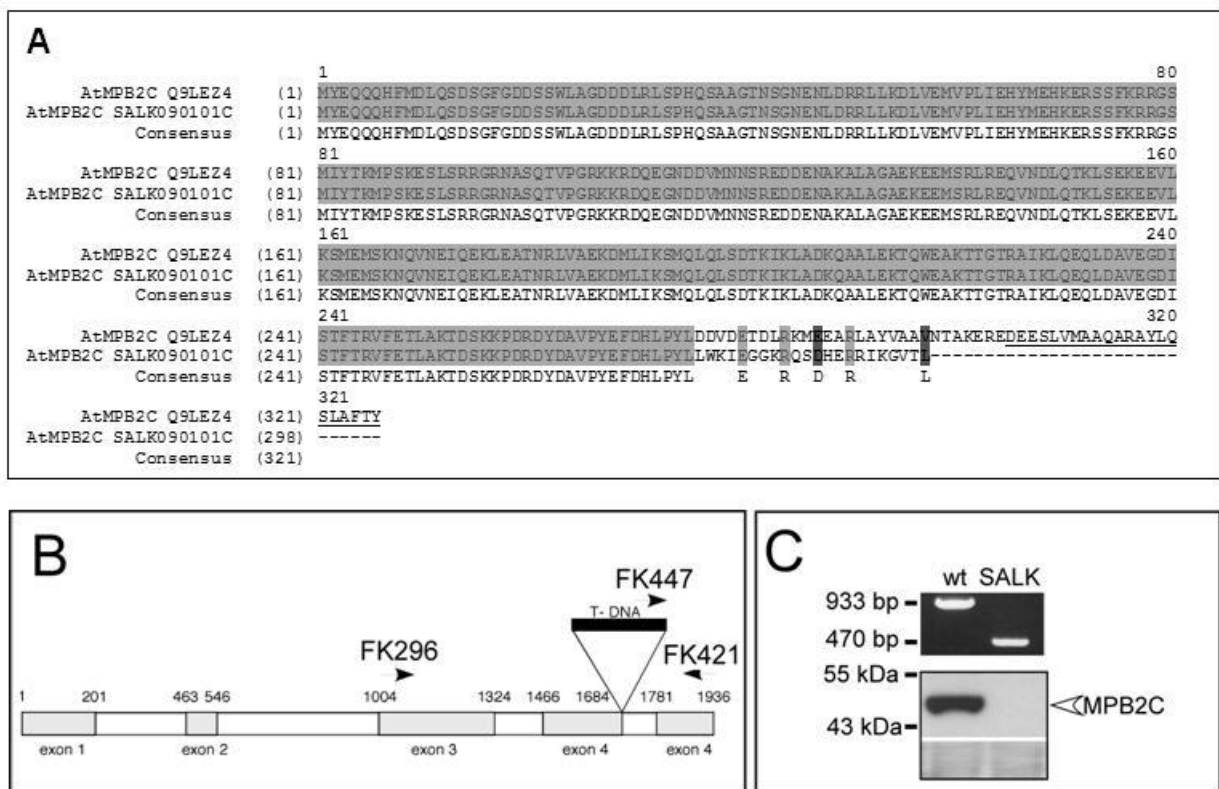


Figure 28: MPB2C T-DNA insertion line SALK_90101C

A: Alignment of full length MPB2C with the truncated protein resulting from T-DNA insertion in line SALK_90101C. The peptide antibody was raised against the C-terminal 22 amino acids of MPB2C (underlined). Line SALK_90101C lacks the C-terminal 51 amino acids, and additional 22 non-related amino acids encoded by the T-DNA were inserted instead. **B:** Scheme of the *Arabidopsis* MPB2C gene showing the insertion point in line SALK_90101C. T-DNA is inserted at the exon/intron border after the fourth exon. The insertion was confirmed by genomic PCR with three primers FK296, FK447, FK421, whose binding sites are indicated in B. **C:** Genomic PCR with these three primers in wild type plants produced an amplicon of 933 nucleotides with primers FK296 and FK470 (upper panel, first lane). In the presence of the T-DNA insert, a PCR product of 470 nucleotides was obtained with primers FK447 and FK421 (upper panel, second lane). Genomic PCR confirmed a plant homozygous for the T-DNA insertion (upper panel) which on Western blots lacks the band at ~45 kDa with the peptide antibody (lower panel).

3.5.3 MPB2C TILLING point mutation lines

19 nucleotide substitutions resulted from a TILLING (Till, Reynolds et al. 2003) service order by our laboratory at the Seattle TILLING collection in the initial phase of the project. Eleven nucleotide mutations were located in introns, five resulted in silent mutations within exons, and three resulted in amino acid exchanges within protein coding regions of MPB2C (see Table 6). The guanine- to adenine mutation in exon 2 of ATMPB2C_202C4 was translated into an amino acid exchange at position 79. A small uncharged glycine (G) was replaced by a negatively charged aspartic acid (D) residue within a stretch of conserved amino acids. This glycine is conserved in dicotyledonous plants but not in monocots (see also Figure 16). The associated TILLING line CS94728 was chosen for further analysis. A guanine to adenine mutation in exon 3 in TILLING line CS91285 resulted in arginine (R) 143 to lysine (K) mutation. This amino acid exchange could not be considered to be severe, since both amino acids have positively charged side chains and are hydrophilic. This position is conserved in dicotyledons and in several orthologs within one clade the two monocot clades. No arginine is found in *Zea mays* at this position. TILLING line CS91285 was later reported to carry also a mutation in the gene AT4G16390 (*SUPPRESSOR OF VARIATION 7*), which codes for a pentatricopeptide repeat protein involved in chloroplast biogenesis. As this initial mutant M3 line showed an interesting phenotype and the additional mutation was not known at the time of the experiments, it was further

analyzed. TILLING line CS96221 had serine (S) to phenylalanine (F) substitution at position 91. Serine is conserved at this position in dicotyledons. This amino acid exchange could have steric effects due to the benzyl group of phenylalanine or effects on charge since serine is a polar residue, and phenylalanine is nonpolar. However, TILLING line CS96221 was not further analyzed because M3 plants did not show an obvious phenotype.

In a pre-screen both TILLING lines CS94728 and CS91285 showed similar phenotypes that at first seemed to correlate with the respective point mutations (Figure 29). However, after backcrossing of these lines to Columbia wild type for three generations it became obvious that the phenotypes did not co-segregate with the respective TILLING mutation (see Figure 30). Some observed phenotypes might be explained by the *erecta* mutation which causes compact growth. This mutation was present in “big mama”, the plant whose seeds were used to create the original TILLING collection (Till, Reynolds et al. 2003). The mutation had seemingly no effect on plant growth or the presence of MPB2C protein, since MPB2C could be detected via Western blot in both TILLING lines - although at lower levels especially in line CS94728 compared to wild type (Figure 29D).

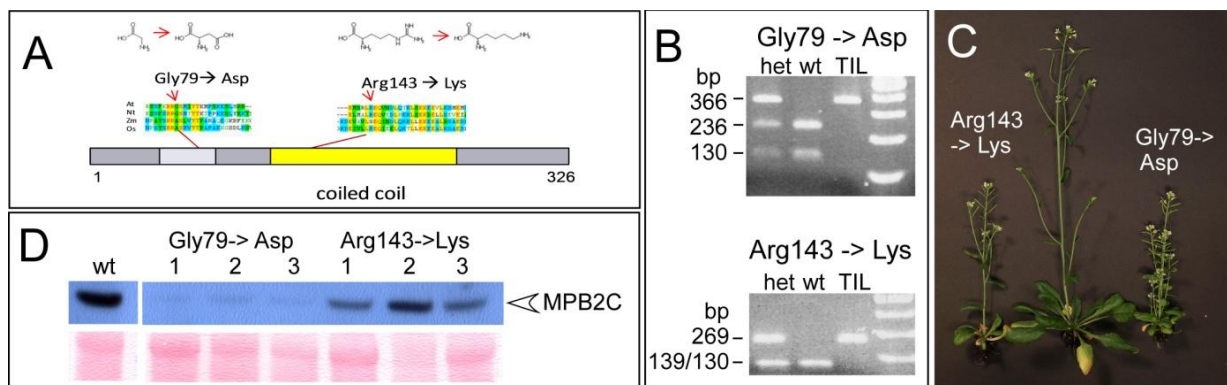


Figure 29: MPB2C TILLING Lines

A: Scheme showing the location of EMS mutagenesis- induced TILLING point mutations and associated amino acid changes in the MPB2C protein (light grey: hydrophobic domain, yellow: predicted coiled-coil region). The alignment shows that both amino acid changes are located in regions conserved between *Arabidopsis thaliana*, *Nicotiana tabacum*, *Zea mays* and *Oryza sativa*. Gly79 is conserved between At and NtMPB2C, whereas maize and rice have an alanine, another small nonpolar amino acid residue at this position. Arg143 is conserved between At-, Nt- and OsMPB2C amidst a highly conserved region. **B:** TILLING mutations could be detected via differential restriction digest patterns of PCR- amplified genomic regions. Restriction digest with NlaIV (line CS94728) or DdeI (line CS91285) allowed to discern plants homozygous (TIL) or heterozygous (het) for the respective mutation or without mutation (wt). **C:** The photo shows the observed phenotypes of homozygous TILLING lines CS91285 (Arg143→Lys) (left) and CS94728 (Gly79→ Asp) (right) before they were back-crossed into wild type Columbia (plant in the middle). **D:** MPB2C protein levels were reduced in inflorescence tissues in line CS94728 (Gly79→ Asp) and to a lesser degree in line CS91285 (Arg143→Lys) compared to wild type.

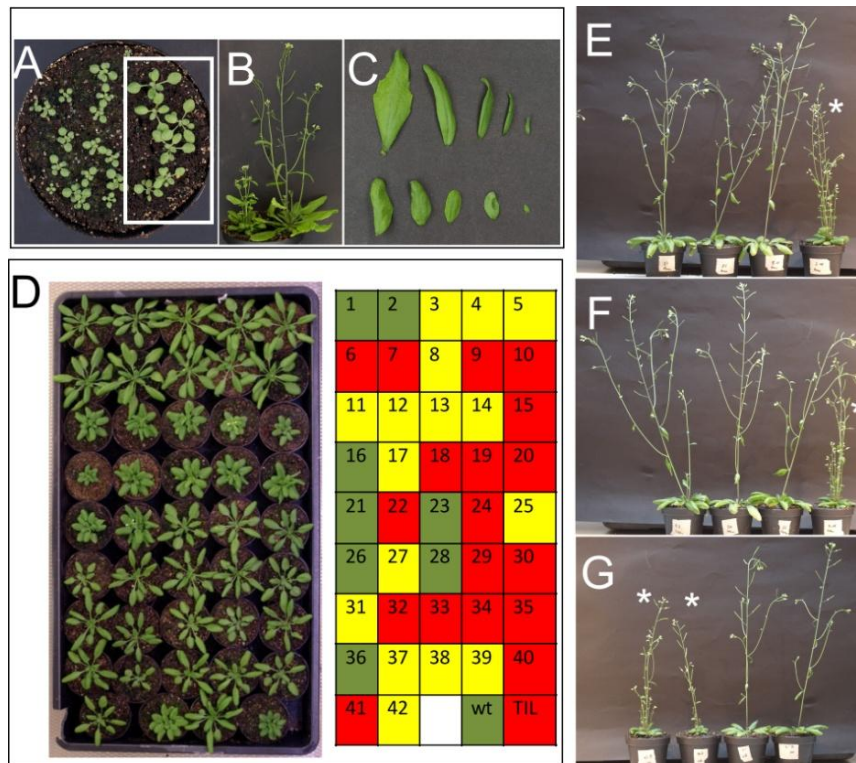


Figure 30: *MPB2C* TILLING mutation CS94728 (Gly79→ Asp)

A to C: Before back-crossing to wild type Columbia, a phenotype seemed to be associated with the point mutation Gly79→Asp. **A:** Two weeks after germination, plants of the TILLING line (left side) were smaller than wild type (boxed) when grown in the same pot. **B:** Adult TILLING plant (left) grown in the same pot with wild type (right), showing a remarkable difference in overall plant size. **C:** Cauline leaves of adult TILLING plants (lower row) were shorter and had a more rounded shape compared with leaves of a wild type control plant (upper row). **D:** After three round of back- crossing into Columbia wild type, it became obvious that the observed phenotype was not co-segregating with the TILLING point mutation. At the right side the schematic representation of the tray shows the result of genomic analysis: yellow-colored fields represent heterozygous plants, homozygous wild type plants are represented by green fields, and plants homozygous for the point mutation are indicated in red. Back- crossed plants are numbered and control plants are labeled wt for Columbia wild type and TIL for a parental plant homozygous for the point mutation. **E- G:** After bolting, the phenotype (marked by asterisks) occurred in plants that were homozygous (**E**) or heterozygous (**F**) for the point mutation, and in plants that were homozygous for the wild type *MPB2C* allele (**G**).

3.5.4 Overexpression of an artificial micro RNA reduces MPB2C protein levels only partially

An artificial micro RNA targeting the *MPB2C* transcript (aMIR_MPB2C) had been produced earlier (Winter 2007). Briefly, the backbone of miR164b was modified to target a sequence from the second exon of *MPB2C* (5'-TTAAGCGGCGTGGTTCATGATCT), and this aMIR_MPB2C was ectopically overexpressed under the viral 35S promoter. Ten independent transgenic lines could be recovered, and the presence of the processed micro RNA was verified via RNA gel blot. In three independent transgenic lines (lines A6-32 #1, #6, and #9) *MPB2C* protein levels were reduced to between 20% and 60% of wild type *MPB2C* levels (see Figure 26 A). Nevertheless, no phenotypic abnormalities were observed in these plants. Maybe a reduction of *MPB2C* was not sufficient to trigger knock-out phenotypes.

3.5.5 No *MPB2C* knock-out could be obtained based on a hairpin RNA approach

In a parallel approach, an inducible hairpin construct was generated using the binary vector pOpOff2hyg (Wielopolska, Townley et al. 2005) to trigger *MPB2C* gene silencing. Despite countless attempts to obtain more transgenic plants, only three independent lines could be isolated. This might indicate that the construct could be adverse to plant growth. Out of these three lines resistant to the selection marker hygromycin, only two lines expressed the GUS reporter construct upon induction with 10μM dexamethasone. This GUS reporter included in the vector backbone was placed under the same inducible promoter to allow monitoring the promoter activity (Figure 31 B). In protein extracts from seedlings of all three transgenic lines grown without induction, lower *MPB2C* protein levels were observed compared to wild type (Figure 31 C). Upon dexamethasone induction higher *MPB2C* levels (approaching wild type levels) were detected in the two lines that showed GUS activity, and no change was observed in line 43-2 which did not show a GUS signal. This result was contrary to the expected effect: Wild type *MPB2C* levels were expected to be found in non-induced plants, whereas reduced *MPB2C* levels were expected in induced plants expressing the hairpin construct. In protein extracts from older plants or from inflorescences of adult individual plants, a reduction of *MPB2C* protein could be observed in line 43-1 but not in line 43-2. Line 43-3 was not tested. However, no phenotypic alterations were observed in these lines (Figure 31D).

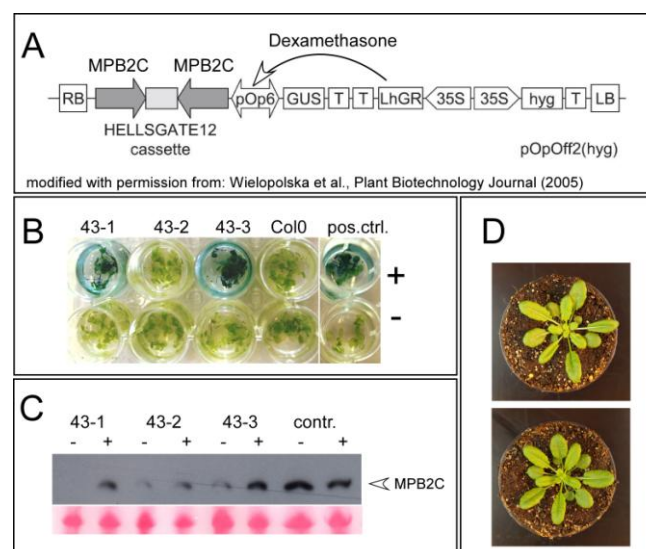


Figure 31: *MPB2C* hairpin siRNA approach

A: Scheme of the pOpOff2 hyg T-DNA cassette: *RB*: right border; *MPB2C*: *MPB2C* cDNA in sense and then antisense direction spaced by an intron; *pOp6*: artificial bidirectional promoter consisting of six operons in tandem targeted by the artificial transcription factor *LhGR*; *GUS*: β glucuronidase reporter gene; *T*: terminator; *LhGR*: artificial transcription factor that only in the presence of dexamethasone enters the nucleus and activates transcription from the *pOp6* promoter; *35S*: viral 35S promoter; *hyg*: hygromycin B phosphotransferase gene conferring resistance to hygromycin B; *LB*: left border; scheme modified from (Wielopolska, Townley et al. 2005) and the CSIRO website (CSIRO_Website) **B:** Only two of the three independent lines transgenic for the *MPB2C* hairpin silencing construct showed GUS reporter activity upon induction with 10 μ M dexamethasone: lines 43-1 and 43-3 (blue staining in A). Upper row: induced plants, lower row: control treatment of the same lines grown in parallel with DMSO. An estradiol-inducible GUS reporter line (*pMDC7-GUS*) was included as control for the GUS staining (pos. ctrl.). **C:** Compared to DMSO- control treatment (-), *MPB2C* protein levels were increased upon induction (+) in lines 43-1 and 43-3 that also showed activation of the GUS reporter. **D:** Induced plants of line 43-1 (upper pot) did not differ phenotypically from control plants grown under the same conditions (lower pot).

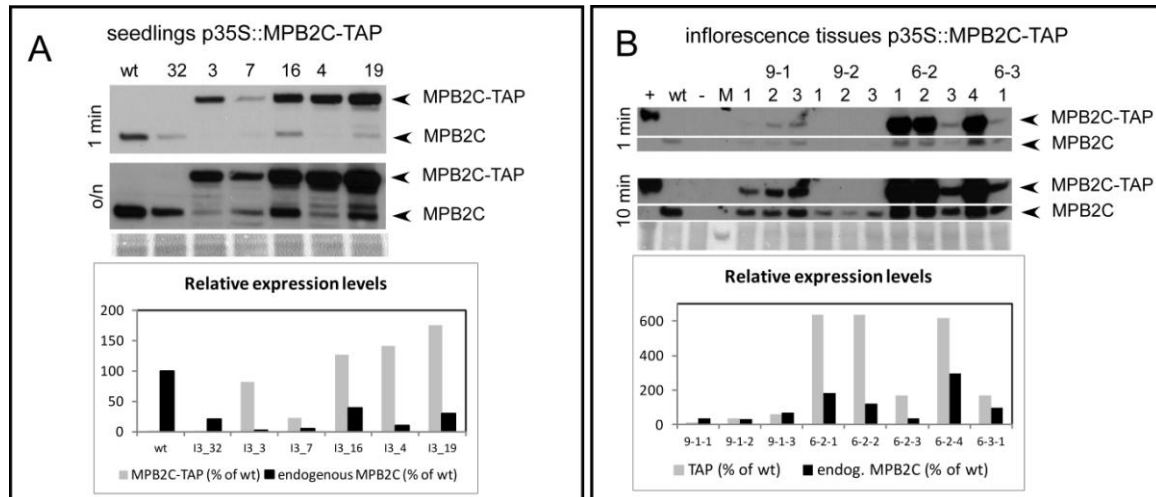


Figure 32: Protein expression levels in *p35S::MPB2C-TAP* lines

Endogenous MPB2C and MPB2C-TAP levels varied in different independent lines transgenic for *p35S::MPB2C-TAP* (construct name: I3). **A:** Western blot on protein extracts from two week old soil-grown and BASTA-selected T2 seedlings from different independent lines. Endogenous MPB2C was detected in all lines upon longer exposure (lower panel, background bands are appearing). Still all transgenic lines had lower endogenous MPB2C levels than the wild type. The diagram shows protein levels (all signals were normalized to the Ponceau stain shown below the Western blots) relative to endogenous MPB2C in wild type (= 100%). Lines I3_16, I3_4 and I3_19 were genuine overexpression lines with slightly higher levels of MPB2C compared to wild type, whereas MPB2C levels were decreased in lines I3_32, I3_3, and I3_7 in comparison to wild type plants. **B:** Protein extracts from inflorescence tissues of individual T4 plants from two independent lines (line I3_9 and I3_6) show that different T2 lines were not homogenous in MPB2C-TAP expression (compare line I3_9-1 with a weak signal with line I3_9-2 that shows no MPB2C-TAP). In the T2 seedlings assay shown in A, I3_9 had a weaker endogenous MPB2C level than wt and an equal level of MPB2C-TAP, whereas line I3_9 was a strong overexpression line. In the T4, individual plants had similar levels of protein expression (exception: plant I3_6-2-3 with a low transgene expression compared to the high transgene expression of its siblings). Protein levels were normalized to the signal observed by Ponceau protein stain and quantified relative to the endogenous MPB2C signal in the wild type plant (= 100%). wt: wild type, numbers indicate individual *p35S::MPB2C-TAP* plants, M: marker.

3.6 Developmental effects of altered *MPB2C* expression in *Arabidopsis*

In order to obtain information about the function of *MPB2C* in a developmental and multicellular context, transgenic *Arabidopsis* lines were established in which *MPB2C-tag* or *MPB2C(delta 178-229)-tag* or *MPB2C(delta 1-58)-tag* were expressed driven by different promoter systems. In a first attempt, plants were transformed with *MPB2C* overexpression constructs based on the strong viral 35S promoter. Occasional fasciation of stems aside, no consistent phenotypic changes could be observed in 40 independent lines in Columbia background transgenic for *p35S::MPB2C-TAP* (construct name: I3, see below). Subtle phenotypic alterations in lines transgenic for various *MPB2C* overexpression constructs were erratic and not reproducible in subsequent generations. The only exception was a phenotype similar to *bp-1* and *pnv* mutants in two independent lines transgenic for *MPB2C(delta1-58)-RFP* (see chapter 3.6.4). As an alternative approach to constitutive overexpression, lines with inducible expression either under a 35S-derived promoter or under different plant endogenous, meristem subdomain- specific promoters were established. We used the estradiol- inducible cassette on pMDC7 (Curtis and Grossniklaus 2003) and an ethanol- inducible transactivation system, where meristem-subdomain specific promoter driver lines can be combined with effector lines harboring the gene of interest (see Figure 41). This allowed inducible tissue-specific expression of the gene of interest. *pWUS*, *pKNAT1*, *pSTM*, and *pAtML1* driver lines (a generous gift from Partick Laufs, INRA, France) were transformed with *MPB2C* or *KNB1* effector constructs. Note that due to time constraints only a limited number of resulting transactivation lines could be analyzed in the T1. Transgenic lines used and established during this or previous work are summarized in Appendix D Transgenic *Arabidopsis* lines.

3.6.1 Protein levels of *MPB2C* are only moderately elevated when expressed from the 35S promoter

Plants transformed with *MPB2C* fusion proteins under the viral 35S promoter cloned with binary vectors from the pEarleyGate series (Earley, Haag et al. 2006) did not show stable phenotypic alterations. The overexpression of *MPB2C-GFP* (vector pEarleyGate103) in transgenic lines could not be verified on the protein level, neither via Western blots nor via confocal microscopy, although expression was confirmed by RT-PCR and a fluorescent signal was detected upon agroinfiltration of this construct (see Figure 20 B and C). Furthermore, trichome rescue lines transgenic for *p35S::MPB2C-GFP* showed reduced trichome rescue efficiency (Winter 2007), which indicates that *MPB2C-GFP* was functional in hindering cell-to-cell movement of the GFP-GL1-KN1_{HD} reporter construct, despite that *MPB2C* itself was not detectable in these lines. These lines were not further analyzed.

The overexpression of *p35S::MPB2C-TAP* (vector pEarleyGate205) could be confirmed via Western blot. Of 33 independent transgenic lines tested, 19 lines were true overexpressing lines i.e. they showed increased levels of *MPB2C-TAP* protein compared to endogenous *MPB2C* (example given in Figure 32). Thirteen lines showed equal levels of the fusion protein and endogenous *MPB2C*, and one line showed only expression of the endogenous protein. The levels of *MPB2C-TAP* in these independent lines were only moderately elevated. In pools of two week-old plants, total *MPB2C-TAP* reached less than twice the expression level of endogenous *MPB2C* in the wild type. Figure 32A shows typical examples for varying protein levels in extracts from seedlings of independent transgenic lines. In inflorescence tissues, where endogenous *MPB2C* expression was highest, maximum overexpression rates in individual T4 plants were six times the endogenous *MPB2C* protein

level detected in control plants (Figure 32B). Individual plants from lines with strong expression often varied considerably in their expression level (compare e.g. plant 6-2-2 with 6-2-3 in Figure 32B). This is probably the reason why the detected level of transgene overexpression in pooled seedlings was apparently lower, whereas in fact this represented only the average of individual plants with varying expression levels. Note that endogenous MPB2C levels were often lower in transgenic plants compared to endogenous MPB2C levels in wild type plants.

In general, MPB2C-TAP overexpressing plants displayed no consistent phenotypic changes other than occasional and non-heritable fasciation compared to wild type control plants. Germination rate, root length, overall growth rates and developmental timing, main shoot height, and the number of paraclades or floral patterning were indistinguishable from wild type plants (data not shown).

3.6.2 N-terminal or C-terminal fusion proteins to MPB2C have different phenotypic effects

Phenotypic alterations in *MPB2C*-overexpressing plants like clockwise twisting of leaves, broadened petioles and stomatal patterning defects described by (Ruggenthaler, Fichtenbauer et al. 2009) were not observed in the lines generated in this work (see e.g. the scanning electron microscope pictures of the leaf surface with no stomatal clusters in an *MPB2C* over-expressing plant in Figure 25F). This might be explained by the different fusion constructs used: In the lab of Elisabeth Waigmann (Ruggenthaler, Fichtenbauer et al. 2009), MPB2C had an N-terminal GFP tag (GFP-MPB2C), whereas we used C-terminally tagged MPB2C. The reason for our choice was to prevent interference of an N-terminal fusion protein with N-terminal domains of MPB2C, because the N-terminus seems to be important for correct subcellular localization of the protein. It had been shown that deletion of the MPB2C N- terminus including the hydrophobic domain resulted in stronger accumulation along microtubules (Kragler, Curin et al. 2003) (see chapter 3.2.5). Indeed, Ruggenthaler et al. described the subcellular localization of GFP-MPB2C as “*continuous decoration of microtubules*” – a pattern which was not observed for endogenous MPB2C in immunostained leaf tissue- derived protoplasts (Kragler, Curin et al. 2003). Such a pattern was never observed with full-length MPB2C-GFP or MPB2C-RFP but it was readily observed with N-terminal mutants such as *MPB2C(delta1-58)*-RFP (see chapter 3.2.5).

3.6.3 Ectopic overexpression of *MPB2C* leads to occasional fasciation

Occasionally stems with fasciated growth were observed in *MPB2C* overexpression lines when plants were grown at 17°C (Figure 33). Fasciation

“...typically involves broadening of the shoot apical meristem, flattening of the stem and changes in leaf arrangement. The term fasciation comes from the Latin fascis meaning a bundle. (...) In linear fasciation, the stem is flattened and the shoot apical meristem (SAM) is enlarged and flattened as a ribbon (Ecole 1970). As a result the shoots have a bilateral symmetry instead of a central one.” (Iliev and Kitin 2011).

Fasciation arises through an imbalance between stem cells and differentiating cells at the boundary of the shoot apical meristem resulting in an enlarged and asymmetrical meristem. Genetic as well as environmental influences can trigger fasciated growth. However, this phenotype with low penetrance could not be correlated with expression levels of the transgene. Due to the low frequency of observed fasciation, *MPB2C* expression levels could only be quantified in protein extracts from inflorescence tissues after the phenotype had been detected, i.e. many days after the

initiating stage of fasciation at the inflorescence meristem. It is conceivable that most of the time effects of *MPB2C* overexpression could be balanced by endogenous factors. But susceptibility to factors disturbing meristem regulation was seemingly increased in *MPB2C* overexpression plants. Unknown factors could be the final trigger to manifest a latent vulnerability in balancing disturbances in coordination of cell identity at the shoot apical meristem caused by *MPB2C* overexpression.

Evidence for a role of environmental factors as final triggers of fasciation was found when plants were grown at 17°C. The decreased growth rate at a lower temperature was reported to enhance fasciation phenotypes (Leyser 1992). Supporting the specificity of the phenotype was the occurrence of fasciation at the same low and erratic frequency in *Arabidopsis* and *N. tabacum* plants transgenic for *p35S::NtMPB2C* and *p35S::delta N-NtMPB2C* (F. Kragler, unpublished). Furthermore fasciation was not observed in any control plants grown under the same conditions (including antibiotic selection). However, stem fasciation was not observed in progeny of these plants, even when they were grown again at 17°C. Hence, additional yet unknown factors seem to play a key role in triggering the *MPB2C* facilitated fasciation phenotype.

Apart from mild fasciation in *p35S::MPB2C-TAP* plants (Figure 33A), three cases of strong fasciation were observed in three independent T1 plants transgenic for three different constructs:

- *p35S::MPB2C(delta178-229)-GFP* (plant 55-1), one out of six independent T1 plants, Basta-selected (Figure 33C);
- *p35S::MPB2C-RFP* (plant M13), one out of 14 independent T1 plants, kanamycin- selected (Figure 33D);
- *p35S::MPB2C(delta 1-58)-RFP* (plant Q15), one out of 15 independent T1 plants, kanamycin-selected (Figure 33E).

Bolting was delayed in these plants, and single inflorescence stems and flowers showed a disturbed radial symmetry. Cross-sections of stems were oval instead of a circular, but the patterning of tissue layers and the structure of vascular bundles was not affected (Figure 33B). In plants M13 and Q15 the endogenous *MPB2C* protein levels were strongly decreased compared to control plants. However, several other independent plants transgenic for the same constructs with decreased endogenous *MPB2C* levels did not show this phenotype (Figure 35). Presence of *MPB2C* mRNA was confirmed in all these lines (F.K. personal communication). The RFP fusion protein could not be detected in any of these plants, neither via confocal microscopy nor via Western blot using *MPB2C*- (this work) and RFP- (F.K. pers. comm.) specific antibodies. As in all other cases of fasciation, this phenotype was not heritable and appeared occasionally in different individual plants of independent lines in subsequent generations (F.K. pers. comm.).

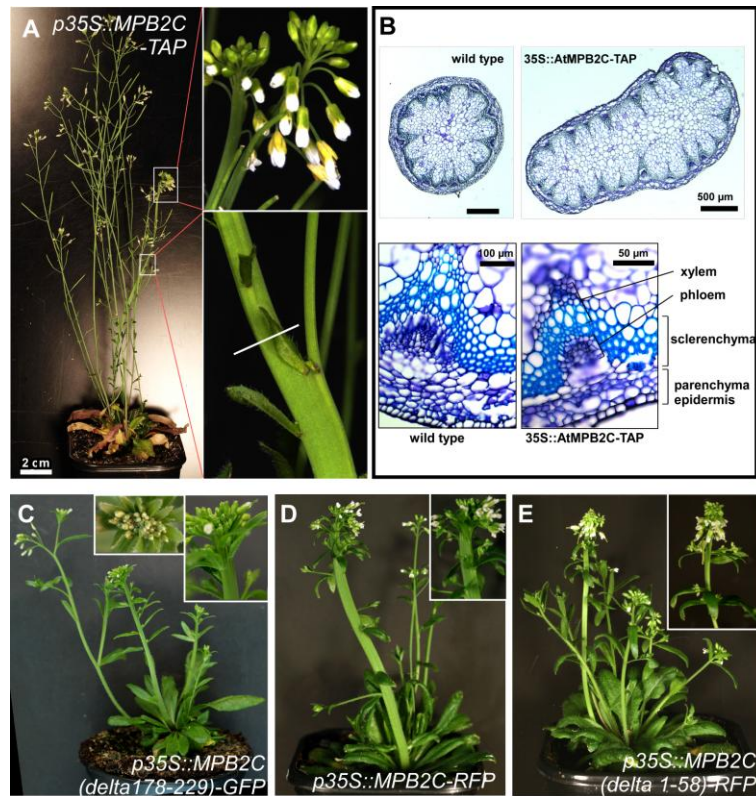


Figure 33: Fasciation in plants overexpressing different MPB2C-fusion protein variants

A, B: Fasciated stem and inflorescence of a plant transgenic for *p35S::MPB2C-TAP* (in vector pEarleyGate205). The white line in the lower close-up shows the region of the section shown in B. **B:** Toluidine blue stained cross sections of wild type (left) and *p35S::MPB2C-TAP* stems (right) show that tissue layers in fasciated stems are not affected. Note that sklerenchyma cell walls appear thicker in the *p35S::MPB2C-TAP* plant than in wild type, but this is an artifact caused by section thickness and focus. **C, D, E:** Single T1 plants transgenic for different MPB2C overexpression constructs showed fasciated stems. **C:** *p35S::MPB2C(delta178-229)-GFP* (vector pEarleyGate103), plant 55-1; **D:** *p35S::MPB2C-RFP* plant M13 (vector pBat-TL-K-RFP); **E:** *p35S::MPB2C(delta 1-58)-RFP*, plant Q15 (vector pBat-TL-K-RFP).

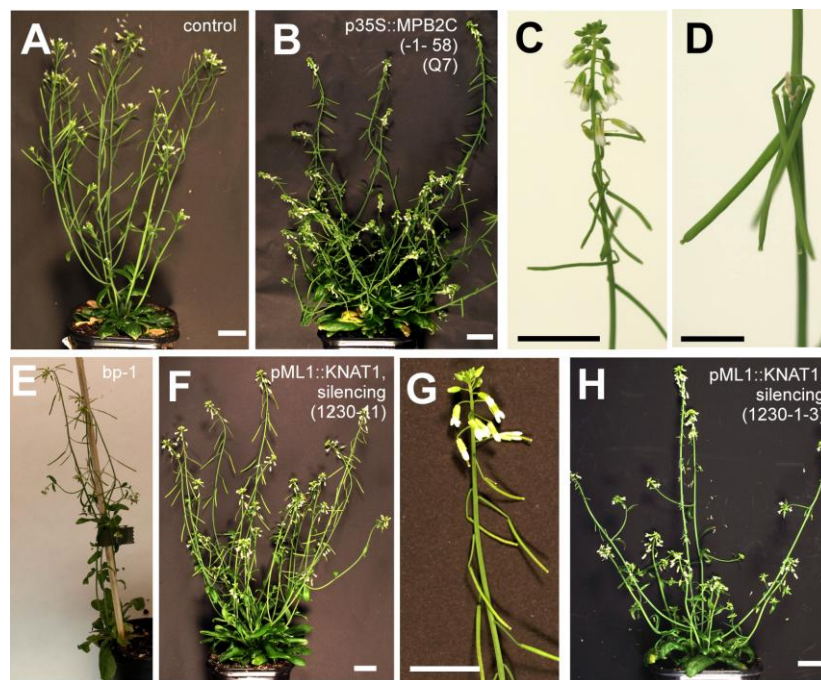


Figure 34: Some *p35S::MPB2C(delta1-58)-RFP* plants resemble *bp-1/pny* mutants

In contrast to control plants (**A**), T1 plant Q17 transgenic for *p35S::MPB2C(delta 1-58)-RFP* (**B** and close-ups **C** & **D**) showed a phenotype similar to the *KNAT1* mutant *bp-1* (**E**, F2 plant of *bp-1* (in *Ler*) crossed to *Col* wt). A similar phenotype was

observed in plants transgenic for *pAtML1::YFP-KNAT1* which apparently showed spontaneous silencing as judged from absent YFP fluorescence (F with close-up G and H). The angles of paraclades were larger (compare B and H with A), pedicels were shorter (as in *bp-1*) and bent (C, D) leading to downward-pointing siliques (compare B to H with A). Irregular internode spacing leading to clustered siliques (D) was not observed in *bp-1* or *KNAT1*-silencing plants but in *pry* mutants. Scale bars: A, B, F, H: 2 cm; C, D, G: 1 cm.

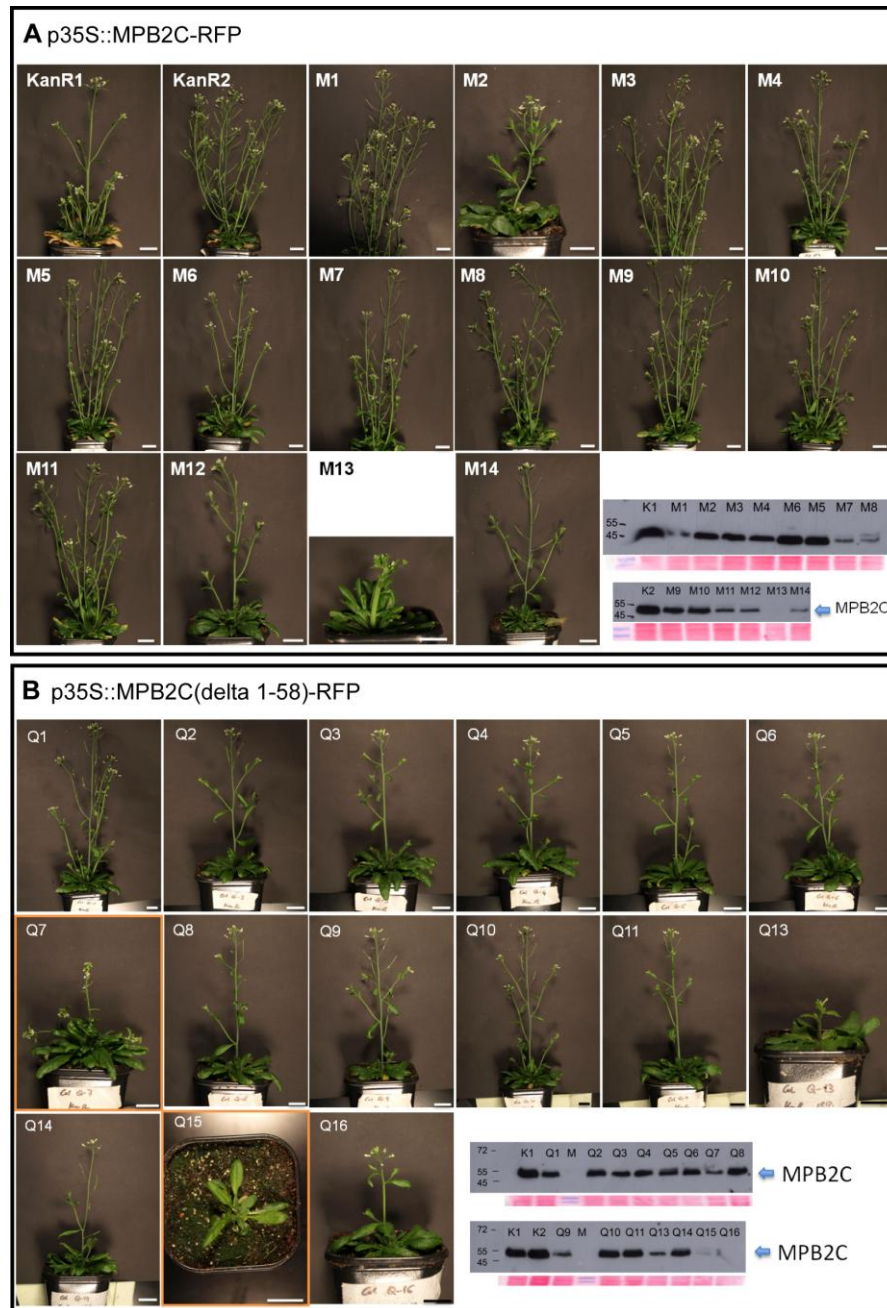


Figure 35: Phenotype and endogenous MPB2C protein levels in independent T1 plants from lines M and Q
Seven week old T1 plants after kanamycin selection on plates and transfer to soil. 14 plants transgenic for *p35S::MPB2C-RFP* (A) and 15 plants transgenic for *p35S::MPB2C(delta 1-58)-RFP* (B) were recovered. Endogenous MPB2C protein levels in inflorescence tissues of these plants aged 8 1/2 weeks were detected via Western blots. Delayed bolting and fasciated stems were observed for plants M13 (A) and Q15 (B). Plants Q7 and Q15 (B) showed downward-pointing siliques and abnormal angles of side branches. Scale bars: 2cm; KanR1 (=K1) and KanR2 (=K2) are kanamycin-resistant control plants grown in parallel; M: marker.

3.6.4 Ectopic overexpression of *MPB2C(delta 1-58)* partially mimics the *bp-1/pny* phenotype

One T1 plant transgenic for *p35S::MPB2C(delta 1-58)-RFP* (Q7) and to a lesser extent a second T1 plant which also had a fasciated stem (Q15), showed downward-pointing flowers and siliques (Figure 34). Plant Q7 showed in addition an increased angle (almost approximating 90°) between the main shoot and side branches, shortened and bent pedicels so that siliques appeared as if twisted around the stem, and internodes were spaced irregularly ranging from prolonged internodes to almost absent internodes leading to clusters of siliques (Figure 34). This phenotype was heritable. Downward-pointing siliques were also observed in the next generation.¹⁶ During vegetative growth, no differences between these plants and other independent transgenic plants or the controls were observed. Downward-pointing siliques and shortened internodes are the characteristic phenotype of *knat1/brevipedicellus (bp)* mutants (Byrne, Simorowski et al. 2002; Venglat, Dumonceaux et al. 2002). A similar phenotype was observed in transgenic plants¹⁷ in which spontaneous silencing of *KNAT1* had occurred (Figure 34F- H). Clustered siliques were reported for *pennywise (pny)* mutants. *PNY* (also *BLH9*) is a BEL-like homeodomain protein that was shown to interact with *KNAT1* via the MEINOX domain (Smith and Hake 2003). However, interaction of *MPB2C* with BLH proteins was not detected (Winter, Kollwig et al. 2007), but *KNB1* in a yeast two-hybrid screen was shown to interact with BLH1 and BLH6, but not with BLH9 (Fichtenbauer 2011). This phenotype suggests once more a connection between *MPB2C* and homeodomain proteins involved in developmental processes.

3.6.5 The number of unfertilized ovules is increased in plants overexpressing *MPB2C*

In several attempts we were not able to identify *MPB2C* null mutants (see chapter 3.5), which might suggest early lethality in the absence of *MPB2C* expression. On the other hand no strong *MPB2C* overexpression lines could be obtained, so strong overexpression might also have negative effects on viability. Alternatively, the overexpressed *MPB2C* protein could be unstable so that increased expression might be counteracted by increased proteasome-mediated degradation (see chapter 3.4.1). In order to address the question of potential lethality of *MPB2C* misexpression, the seed development of transgenic plants was investigated. The number of intact embryos and unfertilized ovules or aborted embryos in the first five siliques on the main shoot was counted. Unfertilized ovules, which appeared as small white structures protruding from the funiculus (Meinke 1994), were observed frequently, whereas only few truly aborted embryos, which appeared as colorless or brown and withered seeds (Meinke 1994), were observed (Figure 36). Both categories were pooled for evaluation when viability was evaluated.

Seed viability was quantified in individual T1 plants transgenic for *p35S::MPB2C-RFP* (lines “M”) and *p35S::MPB2C(delta 1-58)-RFP* (lines “Q”) (Figure 36). Despite high variability between individual T1 plants (Figure 36C, D) significantly less viable seeds per silique in comparison to control plants were observed in independent transgenic plants for *p35S::MPB2C(delta 1-58)-RFP*. Table 7 lists the seed viability statistics in pooled T1 plants (Figure 36B).

¹⁶ Note added in proof: After this work was finished, in three independent T2 lines, additionally reduced apical dominance either in form of increased shoot numbers or in form of suppressed growth of the main stem and increased growth of side branches was observed (F.K. pers. comm.)

¹⁷ lines transgenic for pAtML1:: YFP-KNAT1, the binary vector was a kind gift from David Jackson (CSHL).

Line	Individual plants	Viable seeds per silique	Students T-test (unpaired, two-sided)
Control (KanR lines)	n=2	93.4% (+/- 6.34%)	
p35S::MPB2C-RFP (lines M)	n=13	57.9% (+/-24.42%)	p= 0,06836
p35S::MPB2C(delta 1-58)-RFP	n=13	53.8% (+/- 21.18%)	p= 0,02386

Table 7: Seed viability in *p35S::MPB2C-RFP* lines

Seed viability was also quantified in 17 individual plants from six independent lines transgenic for *p35S::MPB2C-TAP* (Figure 37). A correlation between *MPB2C-TAP* expression level and unfertilized ovules/aborted embryos could be observed: Plants with strong overexpression of *MPB2C-TAP* (judged from Western blots on inflorescence tissues) had approximately twice as many unfertilized ovules/aborted embryos than transgenic plants with low or no transgene overexpression. The variability between individual plants was high. Therefore average values do not represent the observed results properly. Table 8 shows observed maxima and minima and the respective median values. Transgenic plants with moderate *MPB2C-TAP* expression had similar rates of viable seeds per silique as did transgenic plants with no measureable *MPB2C-TAP* expression. Transgenic plants with strong overexpression of *MPB2C-TAP* had more often a decreased number of viable seeds.

MPB2C-TAP expression level	maximum % of viable seeds	minimum % of viable seeds	median
true overexpression n=5 plants	98, 28 %	0 %	91,75 %
same level as endogenous MPB2C n=6 plants	100 %	32,10 %	99,06 %
no MPB2C-TAP n=6 plants	100 %	27,85 %	97,29 %

Table 8: Viable seed per silique (in %) in *MPB2C-TAP* overexpressing plants

One of the analyzed plants showed a fasciated stem (marked with § in Figure 37). In this plant 37.2% of the seeds were viable in siliques from the fasciated stem compared to 91.75 % viable seeds in siliques from a non-fasciated stem of the same plant. This could be explained by differential *MPB2C* expression in these two shoots, caused e.g. by local silencing of the transgene.

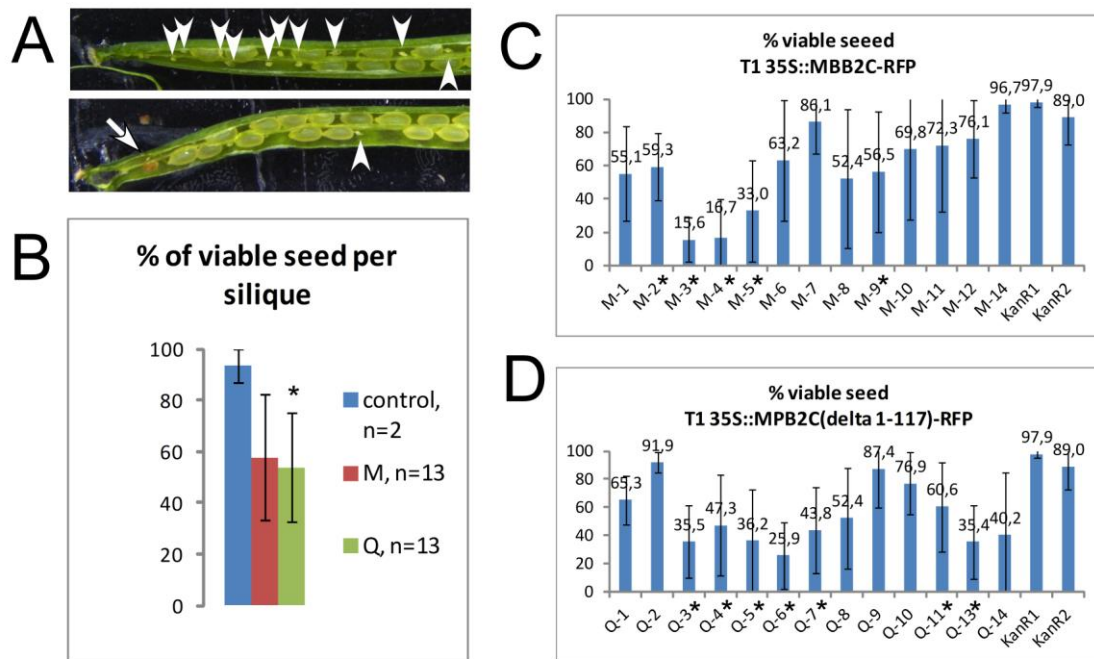


Figure 36: Embryo viability in lines M and Q

A: Exemplary pictures of siliques with unfertilized ovules (arrowheads) and aborted embryos (arrow) among viable seeds. **B:** The average embryo viability rate per silique (in %) of the first five siliques on the main inflorescence stem in independent transgenic T1 plants was reduced in plants overexpressing *MPB2C-tag* compared to control plants. n: independent transgenic T1 plants analyzed; M: *p35S::MPB2C-RFP*, Q: *p35S::MPB2C(delta 1-58)-RFP*, control: plants grown in parallel under same conditions. **C, D:** independent T1 lines pooled in diagram B were analyzed separately in order to determine statistical significance in relation to the control plants (KanR1, KanR2). Asterisks indicate statistically significant differences compared with control plants (Students t-test, unpaired, two-sided with p values <0.05).

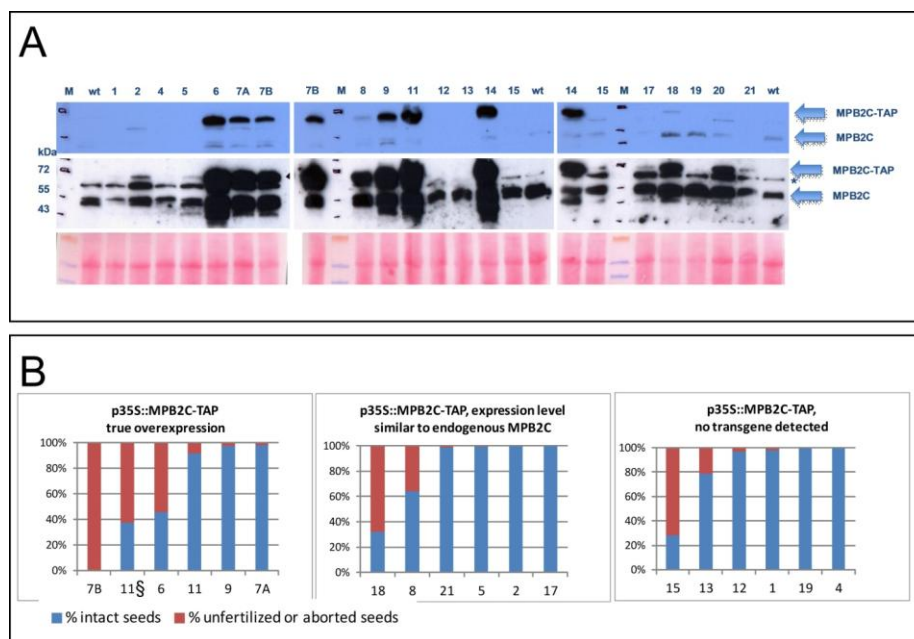


Figure 37: Embryo viability in *p35S::MPB2C-TAP* transgenic lines

A: Western blot on inflorescences of individual plants of *p35S::MPB2C-TAP Arabidopsis* lines. These plants were progeny of plants in which *MPB2C-TAP* expression had been confirmed via Western blot. The upper panel shows exposure on normal film, the middle panel shows prolonged exposure on sensitive film, and the lower panel shows Ponceau stained blots as loading control. Note the background band (*) appearing upon long exposure. **B:** Quantification of the average embryo

viability rate per silique (in %) in transgenic *p35S::MPB2C-TAP* plants. The first five siliques on the biggest secondary inflorescence stem were analyzed (except for plant #18, where siliques #4 to #8 were analyzed, because the first three siliques were degenerated). More plants with true *MPB2C* overexpression (first panel, compare also to A) had a lower number of viable seeds than plants with *MPB2C-TAP* levels similar to endogenous *MPB2C* levels (middle panel) or with no detectable *MPB2C-TAP* (right panel). In plant #11 viable seeds in the first five siliques on the biggest secondary shoot (11) and on a fasciated side branch (115) were quantified for comparison.

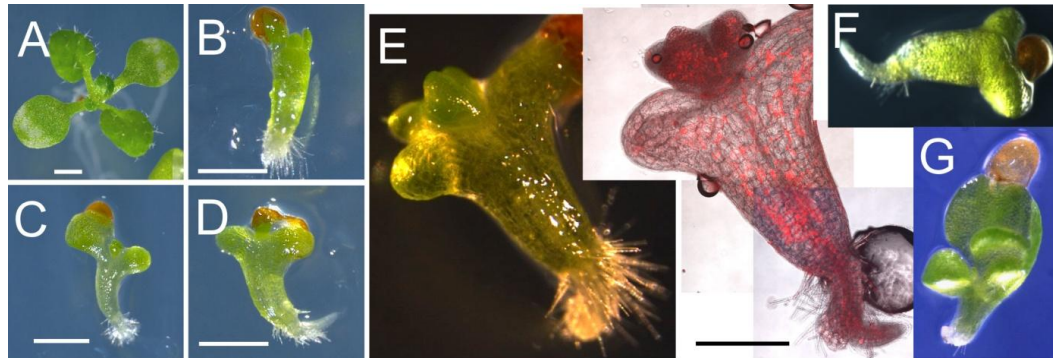


Figure 38: "Hydra"-like phenotype in *pG10-90::XVE>>pOlexA-46::MPB2C-Ala-mRFP1* lines

Estradiol- inducible *MPB2C-Ala-mRFP1* lines developed seedlings that stopped growth after germination and had only rudimentary and often radially symmetric leaf buds. Seedlings depicted had grown for ten days after germination on hygromycin B and 5µm estradiol-containing agar plates. **A:** Control plant grown under the same conditions. **B to E:** individual plants from line L1 of which 10% of the seedling in the T2 generation showed this phenotype. **E:** Fluorescence imaging (right picture) showed that *MPB2C-Ala-mRFP1* was expressed throughout the plant. A similar phenotype (but these were single events) was observed in one F1 plant resulting from a cross between *p35S::STM-GR* (Gallois, Woodward et al. 2002) and *p35S::MPB2C* (**F**) and in one inducible meristem subdomain promoter plant transgenic for *pKNAT1>>aMIR KNB1* (**G**). Scale bars: A to D: 1mm , E: 500µm.

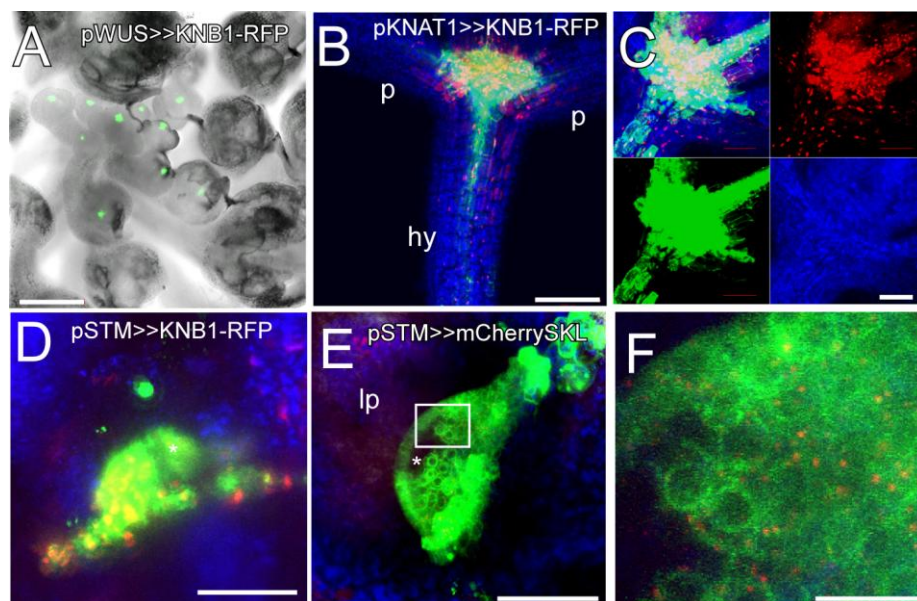


Figure 39: Meristem Subdomain Promoter Lines

Confocal fluorescence images confirmed promoter activity and specificity in meristem subdomains of transgenic *Arabidopsis* plants after ethanol induction. Promoter activity can be monitored via the green fluorescent reporter protein in all transactivation lines. **A:** In an induced inflorescence of a line transgenic for *pWUS>>KNB1-RFP* (line 77-41), the *WUS* promoter was active in single cells in the center of the inflorescence meristem and of young floral meristems (green channel and transmitted light only). *KNB1-RFP1* expression was verified in the SAM of seedlings in the next generation (not shown). **B:** In seedlings transgenic for *pKNAT1>>KNB1-RFP* (line 77-2), the *KNAT1* promoter was active in meristem between the two cotyledon petioles (p), and in the hypocotyl vasculature (hy). A magnified picture of the shoot apical meristem of line *pKNAT1>>KNB1-RFP* line 77-4 is shown in **C**. The three channels and the merged picture are shown separately. *KNB1-RFP* expression correlates with the sites of *pKNAT* activity. *KNB1-RFP* is also seen in nuclei of cells beyond the *pKNAT1* domain or in cells where the cytosolic GFP reporter is too weak for detection. **D:** In an *Arabidopsis* seedling transgenic for *pSTM>>KNB1-RFP* (line 77-5), promoter activity was seen in the shoot apical meristem (green) visible as a dome-shaped

structure. *pSTM* activity was excluded from sites of leaf initiation (asterisk). Nuclear expression of *KNB1-RFP* is seen in red. **E**: In the control line *pSTM>>mCherry-SKL* (line 84-2), the peroxisome-targeted red fluorescent protein (mCherry-SKL) is also seen in the SAM where the *STM* promoter is active (green, asterisk marks incipient leaf primordium). **F**: Magnification of boxed section in **E** shows mCherry-SKL-labeled peroxisomes. Scale bars: A, B: 200µm; C, D, E: 50µm; F: 10µm. Red: RFP, green: GFP, blue: chloroplast autofluorescence.

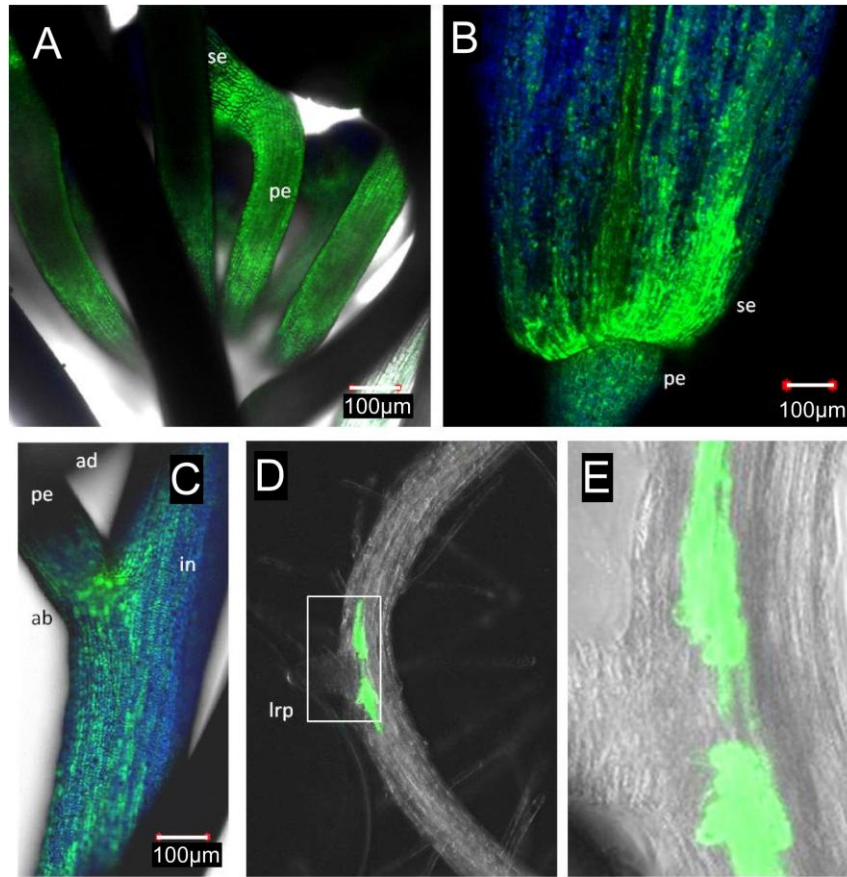


Figure 40: pKNAT1 promoter activity

Apart from expression in vegetative meristems (see Figure 39), the *pKNAT1>>GFP* driver line upon ethanol induction showed expression of the GFP reporter: **A**: in pedicels (pe) and sepals (se) of young floral organs in the inflorescence; **B**: at the transition from pedicel to flower and in basal sepals of young flowers; **C**: the *KNAT1* promoter was active in internodes (in) and pedicels (pe), and increased promoter activity can be seen in adaxial nodes. **D**: In roots, *KNAT1* was expressed in the vasculature at the flanks of lateral root primordia (lrp), marked section is magnified in **E**.

3.6.6 Embryo defects were observed in plants with altered *MPB2C* expression

Out of ten available independent lines harboring an estradiol inducible *MPB2C-RFP* construct (*G10-90::XVE>>pOlexA₄₆::MPB2C-Ala-mRFP1*, vector pMDC7, internal name: L), three lines produced a number of aberrant seedlings in the T2 generation (Figure 38). Germination rates were normal, but single plants remained arrested after germination, independent of the growth medium used. The aberrant plants had a normal basic body plan with primary roots, a hypocotyl and leaf-like organs. The roots appeared normal with root hair, but the hypocotyl was conical and thickened abnormally towards the shoot apical region. Cotyledons and the first two leaves were visible but often radially symmetric, and they did not elongate. Plants remained arrested at this stage and did not grow further. All aberrant plants showed RFP fluorescence under the confocal microscope (Figure 38E) even when not induced with estradiol. However, most plants that showed *MPB2C-RFP* expression appeared like wild type control plants and thus, *MPB2C-RFP* overexpression did not always trigger these embryo patterning defects. In the T2 generation of line L1 this phenotype occurred reproducibly and independent of estradiol-induction in several experiments with a frequency of

about 10% (in total: 14.7%, n= 136 plants, Figure 38B to E). Confirming that this phenotype was indeed a consequence of MPB2C-RFP overexpression, single plants with this defect were observed in two other independent transgenic lines (occurrence in the T2 generation: 2 out of 141 plants in line L7, and 1 out of 136 plants in line L10). Interestingly, in the following generations this phenotype was not observed. This suggests that the phenotype was dosage-dependent and / or was established in the previous generation. The basic plant body plan including cotyledons is established during embryogenesis. Therefore the embryo defects observed must occurred during seed maturation and not after germination. *In silico* data suggest low expression of *MPB2C* during embryogenesis (Figure 6), so higher expression levels of *MPB2C* in this stage might disturb normal patterning. It is possible that the parental plants had been exposed to inductive conditions or that spontaneous activation of the promoter had occurred during this phase. This is probably the reason why this phenotype was observed no matter if plants had germinated on inductive or non- inductive medium, and why it was not heritable to the next generation. A similar phenotype was observed for F1 plants of a cross between *p35S::STM-GR* (Gallois, Woodward et al. 2002) and *p35S::MPB2C-TAP* (Figure 38E), and in a single T2 plant transgenic for *pKNAT1>>aMIR KNB1* (Figure 38G). In addition a similar but less severe defect was observed in the T2 generation in one out of seven independent lines transgenic for *pKNAT1>>MPB2C* (see Figure 42). However, no further experiments with these plants could be done due to time constraints.

3.6.7 Expression of *MPB2C* from the *KNAT1/BP* promoter might cause embryo patterning defects

The set of ethanol-inducible, meristem subdomain promoter transactivation lines generated by (Deveaux, Peaucelle et al. 2003) allows fast establishment of transgenic lines in which a gene of interest can be expressed under strict spatial and temporal control. In brief, these plant lines harbor a cassette in which the ethanol-regulated transcription factor AlcR is expressed from various tissue-specific promoters. They also contain a reporter gene (GFP or GUS) under the *A. nidulans* alcA promoter which is activated by AlcR in the presence of ethanol. The gene of interest, too, is put under the control of alcA and a minimal 35S promoter in *trans*. Upon ethanol induction expression of the gene of interest is then activated from the respective tissue- specific promoter (see Figure 41). Hence, in contrast to strong constitutive ectopic expression via the viral 35S promoter, in this system expression of the gene of interest in specific tissues can be regulated in terms of time, duration and intensity.

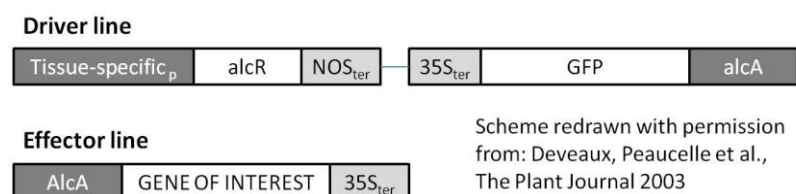


Figure 41 Inducible Meristem Subdomain Promoter Cassette

Various MPB2C and KNB1 constructs and artificial micro RNAs targeting *MPB2C* and *KNB1* were introduced into *pSTM*, *pWUS*, *pKNAT1* and *pAtML1* promoter driver lines (see Appendix D Transgenic Arabidopsis lines). First induction experiments in the T1 and T2 generation confirmed the functionality of the lines, e.g. showing GFP reporter activity and expression of *KNB1-RFP* from the KNAT1, WUS or STM promoter (examples given in Figure 39). Similar to the estradiol- inducible *MPB2C-RFP* lines, aberrant embryo patterning was observed in T2 plants in one out of eight tested

independent lines. In line *pKNAT1>>MPB2C* 78-5 on average 13.6% of plants (n= 228 in two independent experiments) had only one cotyledon or fused cotyledons, and they often lacked leaf primordia (Figure 42Error! Reference source not found.). Again this phenotype occurred upon growth on inductive and on non-inductive medium. Hence like for the estradiol- inducible plants induction during embryogenesis and not during germination might have been the cause. A similar phenotype was observed in one out of ten tested independent *pAtML1>>KNB1* lines (line *pAtML1>>KNB1* 77-2), see Figure 43.

3.7 Combined overexpression of *MPB2C* and *KNB1* does not alter shoot apex development

Overexpression of *KNB1* had no effect on the overall plant architecture or development (Fichtenbauer 2011). Promoter studies showed that *MPB2C* and *KNB1* are co- expressed in apical and vascular tissues (see chapter 3.1.7), and protein interaction between *MPB2C* and *KNB1* was shown in yeast-two hybrid interaction assays, plant co-expression studies (Fichtenbauer 2011), and in bimolecular fluorescence complementation assays (chapter 3.3.1). Hence both proteins together might be necessary for certain biological functions which neither protein alone can fulfill. Therefore the effect of co- overexpression of both genes on plant development was investigated.

However, crosses between *MPB2C-TAP* and *KNB1-RFP/-GFP* overexpression lines did not lead to altered seedling or shoot development in the F1 generation (Figure 44). Two independent *p35S::KNB1-RFP* and two independent *p35S::KNB1-GFP* lines were crossed with two independent *p35S::MPB2C-TAP* lines. Expression of *KNB1-GFP* or *KNB1-RFP* was confirmed via confocal microscopy during the seedling stage and after floral transition. Interestingly, *p35S::KNB1-RFP* or *-GFP* often was absent in plants at later stages despite a strong signal in the seedling stage. This might indicate that the lines either had a tendency to silence the transgene or that the overexpression of *MPB2C* affected the stability of *KNB1*. Expression of *MPB2C-TAP* was confirmed by Western blot assays on protein extracts from inflorescence tissues. Not only homozygous but also heterozygous parental lines were crossed, so that a segregating F1 was obtained. No phenotypic difference between plants showing expression of only one transgene and plants that did overexpress both transgenes was observed.

Despite the absence of any developmental aberrations, plants that co-overexpressed *MPB2C* and *KNB1* had an increased sensibility towards infection with *Oilseed Rape Mosaic Tobamovirus* (ORMV) (Fichtenbauer 2011). Interestingly, overexpression of *KNB1* alone had no effect on infection rates (Fichtenbauer 2011), and, as reported earlier, overexpression of *MPB2C* due to its interaction with the viral movement protein reduced the infection rates (Ruggenthaler, Fichtenbauer et al. 2009; Fichtenbauer 2011). A possible explanation could be that overexpression of *KNB1* leads to a destabilization of co-overexpressed and endogenous *MPB2C* therefore increasing viral susceptibility. This result together with data from yeast-three hybrid experiments (Fichtenbauer 2011) and co-infiltration (Winter 2007) strengthens the hypothesis that *MPB2C* and *KNB1* rather exert a negative effect on each other, either by subcellular re-localization upon interaction – as indicated by split YFP results, where interactions with *KNB1* occurred in the cytoplasm whereas *KNB1* alone was nuclear localized; and/or via promotion of proteasomal degradation of either one or both proteins. The observation that *MPB2C* is degraded via the proteasome pathway (see chapter 3.4.1) and the reduction of *KNB1* protein levels upon induction of *MPB2C* in yeast-three hybrid experiments

(Fichtenbauer 2011) indicates that both proteins might become susceptible to proteasomal degradation under certain conditions which still need to be characterized in detail.

3.8 Down-regulation of *MPB2C* in *KNB1*- overexpressing plants had no obvious effect on development

If both proteins were involved in the same biological process but they would negatively regulate each other, phenotypic changes were only expected if one gene was overexpressed and the other was absent or down-regulated. Therefore a *p35S::aMIR_MPB2C* line with confirmed down-regulation (line A6-32_6-28) was crossed with a *p35S::KNB1-GFP* line (line B2_4-1-1A-1A), see Figure 45. Down-regulation of *MPB2C* and expression of *KNB1-GFP* in inflorescences was confirmed via Western blot. Seven out of seven tested F1 plants had reduced endogenous *MPB2C* levels, and four of these seven plants did express *KNB1-GFP* in the adult stage as seen confirmed by Western blot. No phenotypic difference was observed between plants with and without *KNB1-GFP* expression or in comparison with the parental lines. The reduction of endogenous *MPB2C* levels via the artificial micro RNA in these plants might not have been sufficient to completely abolish *MPB2C* function. Yeast-three hybrid data support this hypothesis: In the interaction experiments, the effect of *MPB2C* on *KNB1-KNAT1* interaction was tested (Fichtenbauer 2011). The *MPB2C* construct was inducible, but even without induction, no positive interaction signal for *KNB1* and *KNAT1* was obtained. Western blot analysis revealed that the inducible construct had a weak background expression without induction, and minimal amounts of *MPB2C* were obviously sufficient to abolish the positive signal in the yeast-three-hybrid screen, which was elicited by *KNB1-KNAT1* interaction in the nucleus. Similar as with *MPB2C*, no null-mutant for *KNB1* could be verified or is available, so the phenotypic and developmental effects of the complete absence of one or both of these gene products could not be investigated *in planta*.

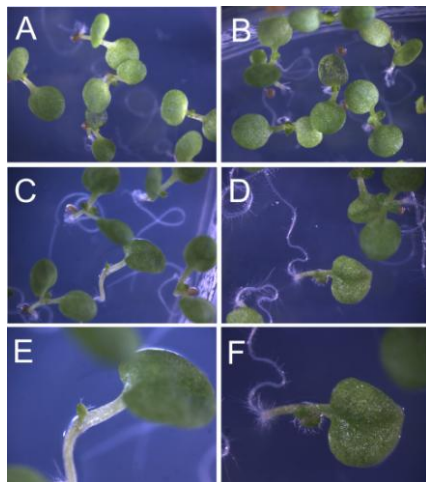


Figure 42: pKNAT1>>MPB2C transactivation plants
A, B: parental *pKNAT1::AlcR* line induced (**A**) and uninduced (**B**). No aberrant plants were observed. **C to F:** In the T2 of line *pKNAT1>>MPB2C* 78-5, 13.6% of the plants had only one cotyledon when ethanol- induced (**C**, close-up: **E**) and uninduced (**D**, close-up: **F**). Plants were grown on agar plates under long day conditions.

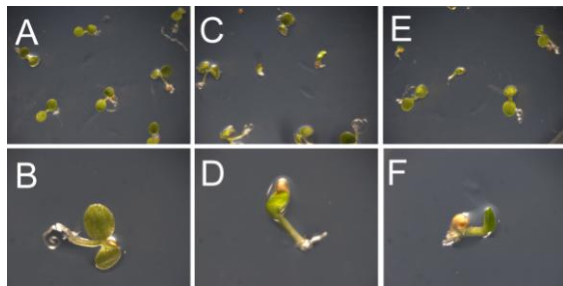


Figure 43: Seedling patterning defects in line *pKNAT1>>KNB1-RFP*
 In one out of ten independent lines transgenic for *pAtML1>>KNB1-RFP* seedlings in the T2 generation showed aberrant phenotypes when grown on agar plates under long day conditions. Pictures were taken three days after germination. **A, B:** *pAtML1>>KNB1-RFP* line 77-1 with no aberrant phenotypes (close-up is shown in **B**). **C to F:** Plants from line *pAtML1>>KNB1-RFP* 77-2 grown in parallel showed aberrant seedling phenotypes when ethanol-induced (**C, D**) but also when not induced (**E, F**) during germination. Plants enlarged in **D** and **F** did not grow further past this stage.

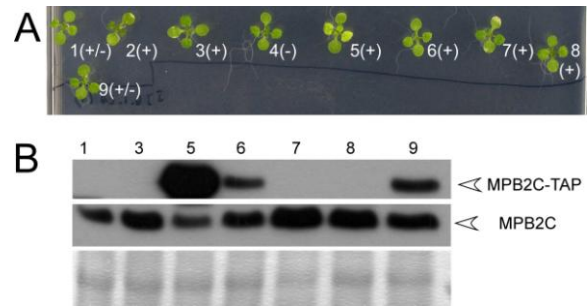


Figure 44: Co-overexpression of *MPB2C* and *KNB1* has no phenotypic effect in the F1
 Panel **A** shows individual F1 plants of the cross IIIH, i.e. ♀ *p35S::MPB2C-TAP* (plant I3_6-1-2A) x ♂ *p35S::KNB1-GFP* (plant B2_4-1A-1A), ten days after germination grown on non-selective agar plates under long day conditions. Panel **B** shows Western blots detecting the expression of MPB2C-TAP and of endogenous MPB2C (to confirm that no silencing occurred) in inflorescences from the same plants after transfer to soil. As a loading control the Ponceau-stained blot is shown below. Only plants that still expressed KNB1-GFP (judged from fluorescence microscopy) at this late stage were analyzed on the Western blot. Numbers represent protein extracts from individual plants shown in A, (+) indicates presence of the KNB1-GFP signal detected with the fluorescence microscope on a 10x magnification; (+/-) indicates a very weak KNB1-GFP signal, (-) indicates absence of a GFP signal.

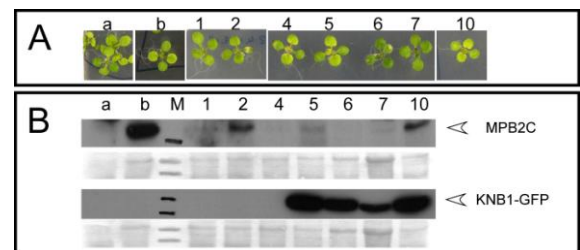


Figure 45: No phenotypic alterations in plants overexpressing *KNB1* and silencing *MPB2C*
A: F1 Seedlings of the cross IIIH, i.e. ♀ *35S::aMIR MPB2C* (plant A6-32_6-28) x ♂ *p35S::KNB1-GFP* (plant B2_4-1-1A-1A), ten days after germination grown on non-selective agar plates under long day conditions. **B:** Western blot on inflorescence tissues of the same plants after transfer to soil. The Ponceau-stained blot is shown below as loading control. Incubation with the anti-MPB2C antibody showed down-regulation of MPB2C to varying degrees in all seven plants. KNB1-GFP was detected in four out of seven F1 plants after floral transition. Note that plant b, offspring of the parental *p35S::KNB1-GFP* line, did not express KNB1-GFP in inflorescence tissues. The parental line showing strong overexpression had a tendency to silence KNB1-GFP at later developmental stages, which was also observed in F1 plants n°1, 2 and 4. Note that low levels of endogenous MPB2C were detected upon longer exposure in all aMIR-MPB2C-expressing plants. a:

3.9 Summary Results

MPB2C can be conceived as a linker protein mediating subcellular localization of interacting proteins by connecting them to larger complexes and/or to microtubules. Another level of regulation might be MPB2C providing a link to proteasomal degradation. The key features of MPB2C function in the context of regulation of cell-to-cell movement via plasmodesmata seem to be the following:

- MPB2C associates with microtubules;
- MPB2C is submitted to the proteasomal degradation pathway;
- MPB2C interferes with *Tobamovirus* infection;
- MPB2C interferes with homeodomain-mediated movement of KNOX I proteins;
- MPB2C is present in tissues where mobile homeodomain proteins are expressed;
- MPB2C overexpression resulted in a phenotype similar to the *bp/knat1* and *pny* mutant.

MPB2C is expressed throughout the plant life in tissues with meristematic activity. The susceptibility of the MPB2C protein to proteasomal degradation adds another level of flexibility in the regulation of protein amounts. In our miRNA and siRNA lines, we could still detect MPB2C protein although at lower levels. Even low levels of MPB2C might be sufficient for its biological function since effects were observed with minimal MPB2C amounts in yeast, and no apparent effect was observed *in planta* upon down-regulation of MPB2C.

Overexpression of an N-terminally truncated form of MPB2C less prone to form aggregates upon overexpression elicited a phenotype similar to *bp-1/pny* mutants. MPB2C might interfere with the function of KNAT1/BP and PNY by interfering with KNAT1 cell-to-cell movement. Cell-autonomous KNAT1 might not be able to function in the multicellular context in a similar way, as overexpression of movement-incompetent *GUS-KNAT1* did not elicit *KNAT1*-overexpression phenotypes. This hypothesis provides a basis for further work.

4 Discussion – Summary and Outlook

The aim of this work was to characterize the function of *MPB2C* in a developmental context. Expression domains of *MPB2C* in *Arabidopsis* were visualized via GUS reporter lines and *in situ* hybridization (see chapter 3.1.1); subcellular localization and protein-protein interactions of full-length *MPB2C* and *MPB2C* deletion constructs were compared *in planta* via bimolecular fluorescence complementation (BiFC) (see chapters 3.2.4 and 3.3); various transgenic *Arabidopsis* lines were established in order to analyze phenotypical changes upon altered constitutive or inducible expression of *MPB2C* (see Appendix D Transgenic Arabidopsis lines and chapter 3.6). Only moderate transgene expression levels could be attained - maybe because the MPB2C protein turnover is high. MPB2C was shown to be instable in cell extracts and seems to be sensitive to proteasome-mediated degradation (see chapter 3.4.1). On the other hand no null-mutants could be generated via artificial micro RNA, hairpin RNA silencing constructs or point mutations (TILLING), nor was such a mutant identified in available collections of T-DNA insertion lines (see chapter 3.5). These findings suggest that strong deregulation of *MPB2C* function might be lethal. Consistent with this, the rate of unfertilized ovules was increased in lines transgenic for *MPB2C-TAP* or *MPB2C-RFP* overexpression constructs (see chapter 3.6.5), and embryo patterning defects were observed in a transgenic line

with ectopic *MPB2C-RFP* expression (see chapter 3.6.6). These and other potential mutant phenotypes like stem fasciation (see chapter 3.6.3) were not stable over generations. However, ectopic expression of *MPB2C(delta1-58)-RFP* in two independent transgenic lines triggered a heritable phenotype similar to *bp-1 (knat1)/pny* mutants with downward-oriented and clustered siliques (see chapter 3.6.4), strengthening the idea that the observed interaction between MPB2C and KNOX proteins is of physiological importance (discussed in chapter 4.2).

Contrary to our expectations, MPB2C function seems to manifest phenotypically to a lesser extent in the vegetative or floral meristems themselves, where STM and KNAT1 are expressed; rather *MPB2C* seems to function not in meristems but in tissues where cells enter differentiation programs, like at the borders of the inflorescence meristem, where the inflorescence architecture (internode length, lateral organ spacing and orientation etc.) is established. There MPB2C seems to regulate KNAT1 activity/protein levels or cell-to-cell movement. *KNAT1* and *MPB2C* are co-expressed in these domains, and we could detect their interaction *in planta* in the BiFC system. It remains to be established whether the interaction between MPB2C and STM in the vegetative SAM or maybe during carpel patterning is of developmental importance. The endogenous expression of *MPB2C* beyond the shoot apical meristem in roots and in young leaves, as well as in carpels and in stomatal precursor cells (see Figure 8 and Figure 9) suggests that MPB2C in addition to the interaction with KNAT1 might play a hitherto unknown role in other patterning processes potentially interacting with other proteins as well. These observations will be discussed in the context of non-cell-autonomous KNOX I function and cell-to-cell transport via plasmodesmata. Based on my results I will propose and discuss a model in which MPB2C might play a role in a PD transport pathway involving membranes and potentially lipid rafts.

4.1 Phenotypic effects of altered *MPB2C* expression

4.1.1 Expected results upon altered *MPB2C* expression

The initial hypothesis was that MPB2C, as a microtubules-associated protein, regulates the cell-to-cell transport of mobile homeodomain proteins such as KN1, STM, and KNAT1/BP by recruiting them to the cytoskeleton. Therefore, in plants overexpressing *MPB2C* due to reduced STM or KNAT1 protein cell-to-cell trafficking, we expected to obtain phenotypes similar to *KNOX* gene mutants. Vice versa, we expected phenotypes resembling ectopic KNOX class I gene expression plants in lines with reduced or absent MPB2C, resulting from excessive movement of the respective KNOX proteins.

4.1.2 *MPB2C* down-regulation

If MPB2C plays an important role as a gatekeeper for mobile KNOX class I proteins at the borders of the shoot apical meristem – one would expect plants similar to KNOX I overexpression phenotypes upon reduction or absence of MPB2C. MPB2C down-regulation in the micro RNA lines was obviously not sufficient to trigger phenotypic alterations (see chapter 3.5.4). Indeed, yeast three-hybrid assays suggested that even minimal amounts of MPB2C have an influence on KNAT1: A strong negative effect on KNB1-KNAT1 interaction (or at least interaction readout) and KNB1 protein levels was observed even when MPB2C expression was not induced and the protein was barely detectable but not entirely absent, as the inducible promoter was leaky (Fichtenbauer 2011). No *MPB2C* knock-out plants could be identified or produced, neither could such lines be identified in T-DNA insertion collections (6 available lines, one examined in detail, see chapter 3.5.2) nor in the ordered TILLING point mutation lines (19 available lines, 2 examined in detail, see chapter 3.5.3), nor in plants

overexpressing an artificial miRNA (17 constitutive and 7 inducible independent lines, 10 tested in detail, see chapter 3.5.4). This suggests that MPB2C might be an essential protein, and that plants lacking MPB2C are not viable. Since *MPB2C* does not belong to a larger gene family in *Arabidopsis*, absence of MPB2C cannot be compensated. We therefore generated an inducible hairpin silencing construct in order to circumvent potential embryo lethality in the process of establishing transgenic plants. However, despite repeated floral dips and screening of millions of potential transgenic T1 seeds over a period of ten months, only three transgenic T1 plants could be recovered. Neither of these independent lines functioned in the expected way: One line did not respond to dexamethasone treatment (i.e. induction), and the other two lines showed paradox reactions by displaying increased instead of reduced MPB2C protein levels upon induction (see 3.5.5). The nature of the hairpin construct could resolve this paradoxon: The hairpin construct consisted of the entire *MPB2C* cDNA, which was inserted in sense direction and only after the spacer intron in antisense direction (Figure 31A). Thus, it could be that only the first part of the hairpin construct, namely *MPB2C* cDNA in the sense direction, was transcribed properly or remained stable as a transcript yielding a functional transcript and MPB2C protein instead of a silencing construct. Alternatively, T1 plants with very low basal expression of the functional hairpin construct could have died before being identified as being transgenic. Recently, a functional inverted repeat MPB2C silencing construct harboring three repeats of an about 200nt long stretch of the *NbMPB2C* gene was described. This construct yielded a five-fold reduction of MPB2C mRNA levels (Cho, Cho et al. 2012). This correlates well with the effects we obtained with our artificial micro RNA construct attaining a reduction to between 20% and 40% of wild type protein levels. However, the search for a true MPB2C loss of function mutant must go on in order to definitely prove the hypothesis that MPB2C is essential.

4.1.3 Expected effects of ectopic *MPB2C* expression

Ectopically expressed MPB2C might or might not have an effect on the phenotype. Obviously, if no mobile KNOX proteins binding to MPB2C were present in tissues with ectopic *MPB2C* expression, MPB2C would not exert any effect there (as long as MPB2C does not regulate the movement of other non-cell-autonomous proteins as well). Second, if KNOX I regulation by MPB2C indeed relied on third factors which are not co-expressed in these tissues there are two possible scenarios: First, ectopic expression of MPB2C could have no effect if these other regulators were needed for MPB2C function but not co-expressed in these ectopic tissues. Or, second, *MPB2C* ectopic expression could produce severe effects if these third factors would negatively regulate MPB2C function in endogenous expression domains (e.g. within the SAM in order to prevent MPB2C from interfering with STM and KNAT1 cell-to-cell movement). This might trigger phenotypes similar to KNOX I mutant plants, if KNOX I cell-to-cell movement became reduced or if MPB2C would trigger proteasomal degradation of the KNOX I proteins it interacts with. And finally a dosage effect might play a role when MPB2C is overexpressed in endogenous domains: Excess MPB2C molecules could out-compete the regulatory protein's numbers and hence escape negative or positive regulation and trigger or not aberrant phenotypes, respectively.

To sum it up, ectopic expression of *MPB2C* might either trigger no phenotype if MPB2C would require third factor(s) for its function, or STM or KNAT1 loss of function phenotypes would be observed. These could result either from excessive KNOX I degradation, if MPB2C was involved in promoting proteasomal degradation. Or, if MPB2C would only interfere with STM or KNAT1 movement, phenotypes similar to the phenotype of *pKNAT1::GUS-KNAT1/bp* plants (normal internode elongation but abnormal pedicel orientation) described by (Rim, Jung et al. 2009) would be

expected. Interestingly, we did indeed observe a very similar phenotype in plants transgenic for *p35S::MPB2C(delta 1-58) -RFP* (see results chapter 3.6.4 and discussion chapter 4.2.6).

4.1.4 *MPB2C* misexpression phenotypes manifest in different developmental stages

The phenotypes associated with *MPB2C* ectopic expression were generally observed in tissues where the endogenous *MPB2C* promoter is active. This supports the notion that *MPB2C* protein needs co-factors such as the interacting *KNB1* for its function. Ectopic expression in tissues without these hypothetical co-factors did not trigger phenotypic changes. The observed phenotypes indicate that *MPB2C* potentially plays a role in

- ovule development/fertilization (increased rates of unfertilized ovules, see chapter 3.6.5),
- embryo patterning (“hydra-like” phenotype, see chapter 3.6.6),
- shoot apical meristem size regulation or stem vascular patterning (fasciation, see chapter 3.6.3) and
- pedicel patterning (downward-oriented and clustered siliques, see chapter 3.6.4).

So far, no changes in root development were observed, despite that *MPB2C* promoter activity was detected in primary and lateral root tips, suggesting that *MPB2C* plays a role in these tissues as well (see Figure 8). In the above-ground parts of the plant fasciation and embryo patterning defects had a low penetrance; they occurred irregularly and unpredictably and in general were not heritable. Also the increase of unfertilized ovules per silique could not be statistically well correlated with *MPB2C* protein levels. Only the downward-pointing siliques and reduced apical dominance were reliably observed in subsequent generations. In the next section the different phenotypic changes observed will be discussed in the light of potential interaction between *MPB2C* and *KNOX I* proteins and maybe other *MPB2C* functions beyond the realm of *KNOX I* proteins.

4.2 *MPB2C* function in the context of homeodomain protein action

Since interaction of *MPB2C* with *KNOX I* proteins was observed in yeast two-hybrid, *in vitro*, and split YFP assays, the expression pattern of *MPB2C* was compared to *STM* and *KNAT1* expression patterns. Expression domains overlapped at certain stages and in some tissues in the course of development, but there were also differential expression patterns. The expression domain of *MPB2C* in the shoot apex and inflorescence meristem largely overlaps with the reported expression domain of *STM* (Long, Moan et al. 1996). *MPB2C* is expressed in regions overlapping with *KNAT1* domains in the shoot apex and in the abscission zone (Lincoln, Long et al. 1994). Thus the observed co-expression supports the notion that interaction between *MPB2C* and these homeodomain proteins detected in various experiments might fulfill a physiological role. Even more consistent than *MPB2C*–*KNOX* co-expression was the co-expression of *MPB2C* and *KNB1*, suggesting that these proteins are part of the same pathway.

KNAT3 (Serikawa, Martinez-Laborda et al. 1997) and *KNAT4* were reported to be expressed in guard cells (Zhao, Zhang et al. 2008), but interaction of *MPB2C* with those proteins awaits to be tested. In fact, if *MPB2C*–*KNOX* interaction was associated with regulation of *KNOX* cell-to-cell movement, interaction with *KNAT3* and *KNAT4* is rather unlikely, because at least *KNAT3* was not able to confer non-cell autonomy upon GFP-GL1 in the trichome rescue reporter line (Kim, Rim et al. 2005).

In roots, *STM* is not expressed and *KNAT1* is expressed at the base of lateral roots [(Truernit, Siemering et al. 2006), see also Figure 40 D and E] whereas *MPB2C* is expressed in the entire

emerging lateral root. Similar to the situation in the SAM, *MPB2C* and *KNAT1* expression overlap at the border of the meristematic region. This supports the notion of *MPB2C* being involved in boundary establishment between domains of unrestricted KNOX protein movement and adjacent domains where KNOX proteins are excluded.

4.2.1 Does *MPB2C* regulate *STM* or *KNAT1/BP* in the vegetative shoot apex?

In the vegetative phase *STM* (Long, Moan et al. 1996) and *KNAT1/BP* (Lincoln, Long et al. 1994) are expressed in the shoot apical meristem (SAM), but they are excluded from leaf primordia. *MPB2C* is expressed in a broader region throughout the shoot apex and in young leaf primordia. In leaves of the trichome rescue line, ectopically expressed *MPB2C* interfered with *KN1_{HD}*-mediated cell-to-cell movement (Winter, Kollwig et al. 2007). But in the cellular context of the SAM, this apparently does not apply, because it is known that *STM* and *KNAT1* are able to move between cells in all directions within the SAM (Kim, Yuan et al. 2003), a domain with relatively high endogenous *MPB2C* expression. Hence previous results from ectopic expression cannot be simply generalized - neither *STM* nor *KNAT1* are endogenously expressed in *Arabidopsis* leaves.

But why then is *MPB2C* expressed in the SAM? What is the function of *MPB2C* within the meristem? And why does the *MPB2C* expression domain extend beyond those of *STM* and *KNAT1*? Despite that no co-factor for direct *MPB2C*-KNOX interaction is required¹⁸, the effect of *MPB2C* interaction with KNOX I proteins might be dependent on the cellular environment: Regulatory co-factors such as *KNB1* or *KNOX* mRNAs (which are transported as well) might modulate the effects of interaction between *MPB2C* and *STM* or *KNAT1*. Hence, *MPB2C* might interfere with KNOX I protein movement only in certain tissues, whereas in other tissues *MPB2C* might even promote KNOX I access to plasmodesmata. Apart from affecting transport, together with *KNB1*, *MPB2C* might also affect KNOX protein stability by triggering proteasomal degradation. For instance in young leaf primordia, where expression of *STM* is repressed by *PCR1* and *PRC2* (Sang, Wu et al. 2009; Hay and Tsiantis 2010), and *KNAT1* expression is repressed by *AS1-AS2* and the chromatin remodeler *HIRA* (Guo, Thomas et al. 2008), *MPB2C* might act as a gatekeeper by preventing KNOX I homeodomain protein movement beyond their expression domain into these tissues and/or by triggering KNOX I protein degradation within preprimordial founder cells (P0) and in leaf primordia.

This model implies alternative regulation of *MPB2C* function within subdomains of the shoot apex. Alternative regulation of *MPB2C* function could be influenced either by the KNOX I proteins themselves or by third factors interacting with *MPB2C* and/or the KNOX I proteins such as *KNB1*. These two possibilities are not mutually exclusive. In the first scenario *STM* or *KNAT1* proteins might be modified during cell-to-cell transport so that in cells without endogenous KNOX I expression (such as leaf primordia) only the modified version existed. This modification could alter the effects of interaction with *MPB2C*. Or the presence of KNOX mRNA could be decisive: *MPB2C* might allow transport of a KNOX-KNOX mRNA ribonucleoprotein complex but prevent movement of KNOX proteins without their mRNA. In order to dissect the role of *MPB2C* within the expression domains of *STM* and *KNAT1* in the SAM and in the surrounding tissues, there are many questions to answer: Does *MPB2C* really interact with *STM* or *KNAT1* within the SAM? Is this interaction associated with proteasomal degradation or not? Are there other factors involved, and if so, which? In which subcellular compartment does this interaction take place? In the future, with the help of the meristem subdomain promoter lines (Deveaux, Peaucelle et al. 2003) we will test the effect of aMIR-

¹⁸ In yeast two-hybrid assays and ex vivo in protein overlay assays *MPB2C* directly interacted with *KN1* (Winter, Kollwig et al. 2007).

directed MPB2C down-regulation in meristem subdomains on STM and KNAT1. It would also be interesting to see whether ectopic co-overexpression of *MPB2C* with *KNOX* genes prevents *KNOX* overexpression phenotypes analogous to the results from *p35S::GUS-KNOX* lines (Kim, Yuan et al. 2003; Rim, Jung et al. 2009). In the second scenario the presence of KNB1 or other factors in tissues surrounding the SAM could direct a hypothetical *KNOX I-MPB2C* complex towards the proteasomal degradation pathway in order to ensure that *KNOX I* protein presence is limited to meristematic tissue. Adding another level of complexity, KNB1 itself is able to traffic beyond expressing cells in the SAM area (see Figure 39) and upon expression from the *KNAT1* promoter in roots [(Fichtenbauer 2011) and FK personal communication]. Thus, the mobile protein like *KNOX* proteins might be present domains beyond its own expression domain.

But let's step back and summarize: What is the evidence for a connection between MPB2C and proteasomal degradation?

4.2.2 MPB2C and the link towards proteasomal degradation

First, MPB2C itself was shown to be stabilized in cell extracts upon application of proteasome inhibitors MG132 and Epoxomicin (see Figure 27). If this instability of MPB2C also occurs *in planta* this might explain why *Arabidopsis* lines transgenic for *p35S::MPB2C* overexpression constructs showed only a moderate elevation of protein levels: due to of a high turnover rate of the MPB2C protein. Second, co-expression of MPB2C interfered with KNB1-KNAT1 interaction in a yeast three-hybrid screen, obviously by de-stabilizing KNB1. KNB1 protein levels were reduced even upon minimal *MPB2C* expression in the non-induced situation, and KNB1 was undetectable upon induction and subsequent high *MPB2C* expression in the yeast three-hybrid system (Fichtenbauer 2011). Third, attempts to transiently co-overexpress *MPB2C*, *KNB1* and *KNOX I* in *N. tabacum* and *A. thaliana* failed. In triple co-bombardments it was impossible to detect all three fluorescent fusion proteins in one cell. And even only co-bombardment of MPB2C and KNB1 yielded cells expressing each single construct, but both proteins were never observed together (F. Kragler, personal communication). The split YFP system showed, that at least upon transient agrobacterium-mediated co-expression MPB2C and KNB1 were present in the same cell. Triple co-infiltration of *MPB2C*, *KNB1* and *KNOX I* overexpression constructs in *N. benthamiana* led to lower KNB1 levels compared to co-infiltration of two constructs or single infiltration (see Figure 23). Hence a general destabilizing effect associated with *MPB2C* expression under certain conditions was observed. Ectopic expression of KNB1 was sufficient to rescue *p35S::GFP-KN1* expression phenotypes in *Arabidopsis* by abolishing the GFP-KN1 signal (Fichtenbauer 2011). Moreover, in the trichome rescue assay ectopic *KNB1* expression interfered with trichome development by causing degradation of the rescue construct (*pRbCS::GFP-GL1-KN1₂₅₆₋₃₂₆*) (Fichtenbauer 2011). Astonishingly this effect was observed even when direct interaction of KNB1 with the rescue construct was impossible, because KNB1 interacts with the MEINOX domain, which was absent in the rescue construct¹⁹. This suggests that the presence of endogenous MPB2C might have been necessary for KNB1-mediated degradation of the trichome rescue construct. Indeed, the rescue construct was visible (and hence not degraded) in tissues with *KNB1* ectopic overexpression but absence of endogenous *MPB2C* expression (Fichtenbauer 2011). Finally, co-expression of *MPB2C* and *KNB1* increased plant susceptibility to viral infection (Fichtenbauer 2011), which indicates that MPB2C – normally interfering with viral infection when overexpressed - might have been degraded in these plants.

¹⁹harboring amino acids 256-326 of KN1 (i.e. the NLS and the homeodomain but not the C-terminal MEINOX domain)

However, the details of interaction between MPB2C, KNB1 and KNOX proteins are still unknown. For example it was not unambiguous in the different experimental setups whether either KNB1 or MPB2C or KNOX protein levels were affected upon co-expression. This might be dependent on physiological conditions and on the method of ectopic (over-)expression used (yeast cells, bombardment, agrobacterium-mediated infiltration or transgenic plants). Endogenous situations might again deviate from these conditions. It also remains to be established whether MPB2C and KNB1 can bind KNOX I proteins at the same time or not. Since MPB2C interacts with the homeodomain (Winter, Kollwig et al. 2007) and KNB1 binds the MEINOX domain (Fichtenbauer 2011), a trimeric complex is theoretically feasible. This question will be addressed in the future via immuno co-precipitation assays in the presence of the third protein.

Which role could MPB2C play in respect to regulation of KNOX I proteins at the level of proteasomal degradation?

There is evidence for an indirect connection between KNOX proteins and proteasomes: Functional proteasomes seem to be necessary for the regulation of *KNOX* gene expression in leaves, since mutants in 26S proteasome subunits revealed ectopic expression of *KNOX* class I genes (Huang and Huang 2007). KNOX proteins also might be subject to proteasomal degradation directly; here is some evidence for this notion: KNOX proteins contain a conserved sequence rich in proline (P), glutamic acid (E), serine (S) and threonine (T), the so-called PEST motif, which increases protein turnover rate (Rogers, Wells et al. 1986). Deletion of the PEST domain resulted in more stable KNOX protein accumulation in several experiments [reviewed by (Hake, Smith et al. 2004)]. It was shown that application of the proteasome inhibitor MG132 was able to stabilize otherwise instable proteins with a PEST motif expressed in BY-2 cells (Adachi, Uchimiya et al. 2006), which indicates that PEST sequences probably mediate KNOX I protein instability via targeting them to proteasomes. However, nothing is known about the protein turnover rates of STM, KNAT1 and MPB2C in the shoot apex. Obviously STM and KNAT1 are able to function as transcriptional regulators within the SAM despite that MPB2C is co-expressed in the same tissue. Here again, modification due to movement of the KNOX I proteins or the presence of additional factors might modulate the consequences of interaction between MPB2C and STM or KNAT1.

Interestingly proteasomal degradation of the viral movement protein MP30 plays a positive role in the TMV infection cycle (Reichel and Beachy 2000). Viral spread was inhibited - but not completely abolished - in tobacco plants expressing a dysfunctional variant of ubiquitin (Becker, Buschfeld et al. 1993). Whether ubiquitination and proteasomal degradation have an impact on KNOX movement remains to be investigated. Since for now the involvement of the proteasomal pathway was only shown indirectly and *in vitro* in form of MPB2C stabilization upon application of proteasome inhibitors MG132 and Epoxomicin, the next experimental step will be to directly test ubiquitination of either protein in order to confirm that indeed the ubiquitin-dependent 26S proteasomal pathway is involved. Furthermore proteasome subunit mutant plants could be used to test whether *KNB1* overexpression still interferes with KN1 homeodomain movement or with *KNOX I* overexpression phenotypes in the absence of functional proteasomes. However, these results again rely on ectopic overexpression. The available inducible meristem subdomain promoter lines (Deveaux, Peaucelle et al. 2003) will be a valuable tool to dissect the interplay between MPB2C, KNB1 and the KNOX proteins in the different zones of the SAM. The potential effect of KNB1 on KNOX I degradation in the SAM could be investigated by expressing *KNB1* under the *STM* promoter and *KNAT1* from the *AtML1* promoter. Will the lobed leaves phenotype observed in *pAtML1::YFP-KNAT1* lines persist or will the

wild type phenotype be rescued if *KNB1* is expressed within the meristem subdomain and maybe mediates KNAT1 degradation?

4.2.3 Fasciation – a potential sign of cytokinin imbalance at the shoot apical meristem

Fasciation results from a loss of symmetry and deregulation of the shoot apical meristem size (Traas and Vernoux 2002). Many different causes can lead to fasciation, and they can be grouped into two classes: they are either of physiologic or of genetic origin (Iliev and Kitin 2011). Plants with enlarged meristematic domains caused by genetic effects are e.g. the *Arabidopsis* *CLAVATA* mutants which show fasciated growth due to an increased *WUSCHEL* expression domain (Clark, Running et al. 1993; Brand, Fletcher et al. 2000). The occasional occurrence of fasciation in *p35S::MPB2C-TAP* plants suggests a potential role of *MPB2C* in SAM size and/or border coordination. A constant stem cell pool size is crucial for coordinated plant growth and therefore it is regulated on several levels. This might explain why altered *MPB2C* expression did not always trigger this phenotype but rather seemed to increase the vulnerability for fasciation which itself was triggered only under certain circumstances. Alternatively fasciation might be a result of spontaneous silencing of *MPB2C* (see discussion below).

Fasciation was described to occur upon release of transcriptional *KNOX* gene suppression in *Atring1a*^{-/-} *Atring1b*^{-/-} double mutants (Xu and Shen 2008). We also observed fasciated growth in one plant transgenic for *pAtML1::YFP-STM* (but not in *pAtML1::YFP-KNAT1* lines) which showed other signs typical for *KNOX* gene overexpression like small lobed leaves and extreme apical dominance (one shoot only). Increased cytokinin levels favor fasciated growth, for instance in *amp1*²⁰ mutants known to accumulate elevated endogenous cytokinin levels and to develop enlarged meristems (Chaudhury, Letham et al. 1993; Helliwell, Chin-Atkins et al. 2001). Expression of cytokinin biosynthesis genes and cytokinin response factors is increased upon induction of *STM*, *KNAT1*, *KNAT2*, and *KN1* expression (Jasinski, Piazza et al. 2005; Yanai, Shani et al. 2005), and in turn elevated cytokinin biosynthesis might activate *KNOX* gene transcription in the SAM, as discussed by (Hay, Craft et al. 2004).

How can fasciation, as an indicator of *KNOX* class I gain of function, be explained in plants putatively overexpressing *MPB2C*, if *MPB2C* is thought to be a negative regulator of *KNOX* class I proteins? One plant line (Q15) showed at the same time fasciation (i.e. potential STM over-accumulation) and downward-oriented siliques (a sign of impaired KNAT1 cell-to-cell movement). Restricted movement could lead to over-accumulation of *KNOX* I proteins in cells where they are expressed, whereas they excluded from cells normally targeted by *KNOX* I movement. Alternatively this paradoxon and the random and non- inheritable nature of observed fasciation phenomena in *p35S::MPB2C-tag* plants could suggest that fasciation rather is the result of spontaneous silencing than that of *MPB2C* over-accumulation. Another possible explanation might be that *MPB2C* restricts *KNOX* I movement only under certain conditions or that *MPB2C* selectively inhibits movement of certain *KNOX* I proteins but not of all *KNOX* I proteins at the same time. *KNAT1* is expressed at the boundary of the meristem whereas *STM* is expressed within the meristem. *KNOX* proteins are able to form homo- and heterodimers with other proteins, albeit the significance of these interactions is not well understood (Hake, Smith et al. 2004). Hake and colleagues speculate that *KNOX*-*KNOX* interactions might regulate the amount of *KNOX* proteins in the cell available for heterodimerization with *BELL* homeodomain proteins, which mediates translocation of the heterodimer into the nucleus and enhances DNA binding affinity. Specific *KNOX* homo- or heterodimers might allow, and others might interfere with *MPB2C* interaction. Split YFP experiments suggest that interaction of *KNAT1* with

²⁰ AMP1 = ALTERED MERISTEM PROGRAM 1

MPB2C is stronger than interaction of STM with MPB2C. In plants with moderate levels of *MPB2C* overexpression from the viral 35S promoter, MPB2C might associate preferentially with KNAT1 whereby STM could escape the control of endogenous KNAT1 and of ectopic MPB2C and lead to fasciation. Moreover, if KNAT1 at the border of the meristem would limit the domain of STM function by forming KNAT1-STM heterodimers (so that STM can no longer bind its BEL1 partner and act in the nucleus), and if both, the homeodomain and the MEINOX domain are necessary for KNOX-KNOX interaction (Hake, Smith et al. 2004), then excess MPB2C associated with the KNAT1 homeodomain might prevent KNAT1-STM interaction. In turn, STM could move via plasmodesmata into the border regions of the meristem where KNAT1 would normally interfere with STM function. The consequence would be an enlarged meristematic region resulting in fasciated stem growth.

4.2.4 A role of MPB2C in female gametogenesis?

During reproductive growth *MPB2C* was expressed in the entire shoot apical domain, in inflorescence meristems and in floral meristems, although at very low levels. In this stage *STM* was highly expressed in meristematic zones (see Figure 11) and later in carpel primordia. *KNAT1* expression ceased gradually in the flower and inflorescence meristems, whereas high levels of *KNAT1* were observed in the cortex of the stem and in pedicels. In the abscission zone *KNAT1* and *MPB2C* expression overlapped. After floral transition, meristems are gradually losing their stem cell identity due to the expression of *AGAMOUS* which in turn inhibits *WUSCHEL*, a stem cell promoting factor (Lenhard, Bohnert et al. 2001; Liu, Kim et al. 2011). Inflorescence meristems produce flowers, and the floral organs in each flower grow from a floral meristem. *STM* is necessary for carpel development, and consequently *STM* expression is high in inflorescence and floral meristems and in developing carpels and placental tissues (Long, Moan et al. 1996; Long and Barton 2000). RNA *in situ* localization showed that *MPB2C* expression is low during early steps of floral patterning. This suggests that *MPB2C* seems not to be required for STM to fulfill its function in carpel patterning. However, *MPB2C* expression is high in carpels of young flowers where MPB2C might act to restrict or modulate STM function. Not only *STM* expression is important for carpel patterning, all other KNOX class I homeodomain proteins in *Arabidopsis*, such as BP, KNAT2 and KNAT6 also play a role in patterning of the gynoecium, especially during the establishment of the replum (Alonso-Cantabrana, Ripoll et al. 2007). The increased rates of unfertilized embryos in lines transgenic for *MPB2C* overexpression constructs suggest that MPB2C is involved in the development gametophytes. The *MPB2C* promoter is active in the funiculus and in ovule integuments (Winter, Kollwig et al. 2007) but never in stamens. *STM* itself is expressed in placental tissues but not in ovules (Long, Moan et al. 1996), neither are the other KNOX class I genes (Hamant and Pautot 2010). In contrast, the ectopic expression of *KNAT2* (Pautot, Dockx et al. 2001), *KNAT1/BP* (Truernit and Haseloff 2008) or *STM* (Schofield, Dewitte et al. 2007) had detrimental effects on ovule development. The TALE homeodomain protein BEL1 which among others interacts with STM, KNAT1, KNAT2, KNAT5 (Bellaoui, Pidkowich et al. 2001)²¹ is essential for ovule development (Robinson-Beers, Pruitt et al. 1992; Modrusan, Reiser et al. 1994; Ray, Robinson-Beers et al. 1994). In their model, Brambilla and colleagues (Brambilla, Kater et al. 2008) suggest that BEL1 interacts with *AGAMOUS* and *SEPALLATA* in order to prevent *WUSCHEL* expression in ovules. The presence of STM (and potentially other BEL1-interacting KNOX proteins) would interfere with this interaction and hence disturb ovule patterning. Although MPB2C is not able to interfere with STM-BEL1 interaction (Fichtenbauer 2011) and did not interact with BEL1 in a yeast two-hybrid assay (Fritz Kragler, personal communication), it could act as a guard in the funiculus between placental tissues (where STM is expressed) and developing ovules

²¹ or instead of KNAT5 with KNAT6 (Hackbusch, Richter et al. 2005)

by preventing STM cell-to-cell movement into these tissues and hence preclude the encounter of STM with BEL1 in ovules.

4.2.5 MPB2C function during embryo patterning – the “hydra”-like²² phenotype

The “hydra”-like plants observed in transgenic lines harboring an estradiol-inducible *MPB2C-mRFP* fusion construct indicate that excess MPB2C interfered with correct embryo patterning. *MPB2C-mRFP*-expressing plants with the hydra-like phenotype had a radicle, a hypocotyl and basal cotyledon-like structures (see Figure 38). The primary apical-basal body axis and the signaling pathways conferring shoot and root identity were obviously not disturbed. *MPB2C* overexpression seems to interfere with embryo patterning at the transition from radial to bilateral symmetry. Can this effect be explained by interaction of excess MPB2C with STM or KNAT1? If this phenotype was caused by altered regulation of *KNOX 1* genes, then embryo patterning defects in *MPB2C* overexpressing plants are more likely to be a result of MPB2C-STM rather than MPB2C-KNAT1 interaction, because the earliest stage of *KNAT1* expression is in the future hypocotyl of the late heart stage embryo (Long, Woody et al. 2002) – not in the shoot apical region and long after the time when cotyledon identity and polarity were established. During embryogenesis, the body axes and cotyledon identity are established even before the shoot meristem is defined in the heart stage. *STM* transcription is already initiated in the radially symmetric globular stage. *STM* expression is activated by **CUP SHAPED COTYLEDONS 3** (*CUC3*) whose expression in turn becomes limited to a stripe in the medial domain during the late globular embryo stage via auxin gradients [referenced by (Jenik, Gillmor et al. 2007)]. *STM* is first expressed in a single off-center cell in the late globular embryo and then the expression domain expands into the lateral regions of the presumptive SAM in form of a band separating the future cotyledons (Long and Barton 1998). Even severe *stm* mutants still have two cotyledons – which are, however, often not separated at their petioles (Clark, Jacobsen et al. 1996). This indicates that bilateral symmetry is initiated prior to *STM* expression in the globular stage.

But how can the radially symmetric phenotype of hydra-like plants be explained in terms of molecular interaction, when the break of radial symmetry precedes *STM* expression? Does MPB2C interact with other morphogens, too? Could MPB2C be involved in patterning processes which are independent of *KNOX 1* genes? Phenotypes similar to hydra-like plants were observed in mutants of **very long chain fatty acid** (VLCFA) biosynthetic genes. Such a potential connection between MPB2C function and VLCFAs in membrane-associated transport via plasmodesmata will be discussed later.

In hydra-like plants radial symmetry was maintained both in the cotyledon-like structures in regard to the shoot apex as well as within the cotyledon-like structures themselves: Often more than two such cotyledon-like buds protruded from the shoot apex. This might indicate that differentiation-initiating signals at the shoot apex of the globular embryo (e.g. auxin maxima) were less restricted. And the buds themselves as well as buds of true leaves - in case they had developed at all – were radially symmetric: they did not grow out to form a laminar shape with distinct adaxial and abaxial sides. Adaxial and abaxial identities are a matter of coordinated growth of many cells. This requires not only differential expression domains but also intercellular communication, e.g. via mobile small RNAs (Husbands, Chitwood et al. 2009). Blade outgrowth is promoted through *YABBY* genes in response to the establishment of adaxial and abaxial cell fates (Eshed, Izhaki et al. 2004). These cell fates might not be established in hydra-like plants, so that the signal for *YABBY* to promote blade

²² This internally used description for plants with this phenotype does not refer to the published Arabidopsis *hydra* mutants defective in Sterol biosynthesis Souter, M., J. Topping, et al. (2002). "hydra Mutants of Arabidopsis are defective in sterol profiles and auxin and ethylene signaling." *Plant Cell* **14**(5): 1017-31.

outgrowth – the juxtaposition of adaxial and abaxial cell fates - is missing. The next experimental steps will be to examine the identity of the epidermal cells on these leaf buds: are they differentiated or not? If so, do they have rather adaxial or abaxial identity? Is there polarity or not? Furthermore, the expression patterns of cell fate markers like class III homeodomain-leucine zipper (HD-ZIP III) genes (e.g. *PHABULOSA*, *PHAVOLUTA*, *REVOLUTA*) promoting adaxial cell fate or *KANADI* genes promoting abaxial cell fate could be monitored in hydra-like plants in order to determine at which stage of differentiation the arrest occurred.

KNAT1/BP plays a role in promoting differentiation of abaxial and lateral epidermal pedicel cells, which remain undifferentiated in *bp* mutants (Douglas and Riggs 2005). But in the vegetative shoot apex *KNAT1* or *STM* are not involved in lateral organ formation. Moreover, they are excluded from sites of organ initiation. So it seems not very likely that KNOX I homeodomain proteins are the cause for the hydra-like embryo patterning defects phenotype. However, as of yet a role for KNOX cannot be definitely excluded, because single plants with hydra-like phenotypes were also observed in two different transgenic plants where expression from KNOX promoters was altered:

- an F1 plant, the offspring of a cross between *pSTM::STM-GR* with *p35S::MPB2C-TAP*, which was phenotypically indistinguishable from hydra-like plants transgenic for estradiol-inducible *MPB2C-RFP* (see Figure 38F) and
- a plant in which an artificial micro RNA targeting *KNB1* was expressed via transactivation under the *KNAT1* promoter. This plant however had rudimentary leaf-like fused structures with a laminar shape (see Figure 38G).

Both plants were not analyzed further because only one such plant in these genetic backgrounds was observed and could not be reproduced in the time available. Detailed analysis of *MPB2C* and *KNB1* expression domains after fertilization and during the earliest stages of embryo development still await experimental characterization, and this will be crucial to explain the observed phenotypes.

4.2.6 A role for *MPB2C* during internode patterning and pedicel development

Two out of 15 *p35S::MPB2C(delta1-58)-RFP* plants had abnormal phenotypes with short and downward-oriented and occasionally clustered siliques, lateral shoots branching from the main stem with an angle approximating 90°, and reduced apical dominance (see Figure 34). In contrast to all other phenotypes observed in this work, this one was heritable and reliably observed in subsequent generations, and also in later generations of additional transgenic lines which sometimes developed fasciated stems as well (F. Kragler, pers. comm.). Abnormal internode patterning and pedicel orientation as a consequence of *MPB2C(delta1-58)* misexpression indicates that *MPB2C* might be important for the regulation of *KNAT1* movement during in these patterning processes.

Mutations in the *KNAT1/BP* locus result in plants with short pedicels (hence the name “*brevipedicellus*”), downward-pointing siliques, compact internodes, reduced apical dominance (Koornneef 1983; Douglas, Chuck et al. 2002; Venglat, Dumonceaux et al. 2002), increased and aberrant lignin production in the stem (Mele, Ori et al. 2003), and they form hyper-proliferative white-colored bulgy structures at the abscission zone between pedicel and silique (Wang 2006) leading to premature abscission (Shi, Stenvik et al. 2011). Mutations in the gene encoding the BEL1-like TALE homeodomain protein *PENNYWISE* (*PNY*) manifest in form of shorter inflorescence stems, partial loss of apical dominance and irregular internode patterning which causes silique clustering (Smith and Hake 2003). *PNY* is known to interact with *STM* and *KNAT1* (Smith, Boschke et al. 2002; Byrne, Groover et al. 2003). Interaction of *PNY* with *STM* ensures inflorescence meristem

maintenance whereas interaction of PNY with KNAT1 regulates internode patterning (Kanrar, Onguka et al. 2006). The *bp/pny* double mutant has an additive phenotype with reduced internode length, downward-oriented pedicels like *bp*, and clustered siliques like *pny* single mutants (Smith and Hake 2003). This phenotype resembles the observed phenotypes in the two independent *p35S::MPB2C(delta1-58)-RFP* T1 plants. Obviously STM seems to function normally in these plants, but KNAT1/BP and PNY function seems to be disturbed.

KNAT1 together with PNY restricts - probably at least partially via the transcription factors **BLADE-ON-PETIOLE** (BOP) 1 and 2 (Khan, Xu et al. 2012) - the expression of *KNAT2* and *KNAT6* to the junctions between pedicels and siliques and between pedicels and the stem (see model in Figure 4). In *bp* or in *pny* mutants, *BOP1* and *BOP2* expression around nodes is expanded (Khan, Xu et al. 2012). In *pny* mutants, *KNAT2* and *KNAT6* expression domains extend into pedicels, so PNY seems to repress *KNAT2* & *KNAT6* expression (Ragni, Belles-Boix et al. 2008). KNAT1 apparently represses but also activates *KNAT2* & *KNAT6* transcription, depending on the tissue context. In *bp* mutants, *KNAT6* is not expressed at the flower-pedicel junction but it is expressed in pedicels, mainly at the abaxial side, and *KNAT6* is highly expressed in the stem, whereas *KNAT2* is ectopically expressed in the distal parts of the pedicels and expression in the stem-pedicel junction is weaker than in the wild type (Ragni, Belles-Boix et al. 2008). *kmat2/kmat6* (Ragni, Belles-Boix et al. 2008) double mutants as well as *bop1/bop2* (Khan, Xu et al. 2012) double mutants can rescue the internode and pedicel patterning phenotypes in *bp* and in *pny* mutants. Crosses to GUS reporter lines and the nature of the involved genes (being transcription factors) suggest that this regulation takes place on a transcriptional level: PNY and KNAT1 seem to inhibit *BOP1* and *BOP2* expression, and *BOP1* and *BOP2* in turn are necessary for transcription of *KNAT6* (Khan, Xu et al. 2012). *KNAT2* expression seems not to be regulated via *BOP1* and *BOP2* (Khan, Xu et al. 2012) but still depends on functional KNAT1 and PNY.

MPB2C is endogenously expressed at the pedicel-silique junction in the abscission zone during and after abscission (see Figure 13), where it is co-expressed with *KNAT1*, *ATH1*, *KNAT2*, *KNAT6*, *BOP1*, *BOP2*, *IDA*, and *HAE/HSL2* in wild type plants. In young stems and pedicels with high KNAT1 expression, *MPB2C* is not expressed. In more mature stems and pedicels weak *MPB2C* expression was observed, although the exact developmental stages and the tissue specific localization of this expression domain need yet to be clearly defined. When expressed in internodes, *MPB2C* expression was observed in a gradient decreasing towards the inflorescence apex with local expression maxima at the adaxial side of nodes.

Judging from the phenotype in plants Q7 and Q15, the function of KNAT1 and PNY in pedicels seems to be disturbed when *MPB2C(delta1-58)-RFP* is ectopically overexpressed. Does *p35S::MPB2C(delta1-58)-RFP* mimic *bp*- and *pny*-like phenotypes by promoting KNAT1 (and maybe PNY) degradation in young pedicels where these proteins are needed to block *BOP1/2* and *KNAT2/6* expression? Or does ectopic *MPB2C(delta1-58)-RFP* block KNAT1 movement yielding an effect comparable to the situation in *pKNAT1::GUS-KNAT1/bp-3* plants (Rim, Jung et al. 2009)? The published plant photos show that the *bp-3* mutant as well as the partially rescued *pKNAT1::GUS-KNAT1/bp-3* plant still had an increased angle of side branches relative to the main stem resembling our *p35S::MPB2C(delta1-58)-RFP* plants. Rim et al. conclude that KNAT1 must move into domains beyond its endogenous expression domain (or be present in these domains upon ectopic expression via the 35S promoter) in order to exert its role in pedicel patterning²³. Abnormal clustering of siliques

²³ Note however, that the reported expression pattern of *pKNAT1::GUS-KNAT1/bp-3* differed from the one characterized as KNAT1 expression domain in earlier publications. *pKNAT1::GUS* showed a strong signal in

(the *pn*y phenotype) is not visible in these plants, so *p35S::MPB2C(delta1-58)-RFP* might not only affect KNAT1 movement but additionally have a negative effect on PNY function. Rim and colleagues showed that *pKNAT1::GFP-KNAT1* rescued the *bp-3* phenotype, and they concluded that this was possible because GFP in contrast to the GUS- tag did not abolish KNAT1 movement. This was inferred from the observation that in stems GFP-BP moved from the cortex to the epidermis whereas GUS-BP did not. The hypothesis that excess MPB2C in *p35S::MPB2C(delta1-58)-RFP* lines interferes with KNAT1 movement leading to the *bp*- like phenotype could be tested by ubiquitously expressing KNAT1 in our lines. A rescue of the patterning defect would be expected if MPB2C only interferes with KNAT1 movement, and no rescue would be expected if MPB2C mediates KNAT1 degradation. In either way I expect that ectopic overexpression of KNAT1 in these lines should not cause KNAT1-overexpression phenotypes.

Still, it remains to be established how *MPB2C(delta1-58)* interferes with PNY function. MPB2C interacts with the homeodomain, and since PNY is a member of the TALE homeodomain protein family, PNY seems to be a good a candidate for direct protein-protein interaction with MPB2C. But as mentioned previously, interaction of MPB2C with BEL1, another BLH protein, was not detected (F.K. personal communication). In contrast to MPB2C, KNB1 showed interaction with BEL1-like proteins (F.K. pers. comm.) and could be the missing link to MPB2C interfering with PNY function. How can the observed phenotypes be explained when the fluorescent fusion proteins MPB2C(delta 1-58)-RFP, MPB2C-RFP, and MPB2C-GFP could not be detected, neither via confocal microscopy nor via Western blots, in all tested transgenic plants? Most likely the protein levels were too low for detection due to the observed proteasome-mediated turnover of MPB2C. Nevertheless it will be necessary to correlate protein expression levels with phenotypes.

4.2.7 MPB2C without the N-terminal hydrophobic domain is functional

Why did full-length MPB2C not trigger such a *bp/pny*-like phenotype? Maybe simply because too few independent transgenic lines were screened in order to observe altered phenotypes. One plant transgenic for full-length MPB2C-RFP (plant M2) actually showed aberrant internode patterning similar to *p35S::SERRATE* plants (Prigge and Wagner 2001), see Figure 46. And another plant (M13) showed fasciation. But *p35S::MPB2C(delta 1-58)-RFP* plants showed stronger phenotypes. Why this?

pedicels and stems (Douglas et al. 2002, Figure 6E; Venglat et al. 2002, Figure 11E and F; Shi et al. 2011, supplemental Figure 3) whereas *pKNAT1::GUS-KNAT1/bp-3* showed no GUS signal in pedicels or stems, only at the abaxial junction between internode and pedicels and in the abscission zone (Rim, Jung et al. 2009 Figure 3D). All these reporter plants were in the same ecotype (Col), therefore a mutant *erecta* gene in the *Ler* background is not the cause for this discrepancy. Nevertheless, *KNAT1* promoter activity and KNAT1-GUS protein accumulation are obviously not identical. The lack of the GUS-KINAT1 signal despite KNAT1 promoter activity in pedicels and stems suggests that the fusion protein might be instable in pedicels and stems whereas it seems to remain stable at the junctions. Could this indicate that KNAT1/BP movement is required in order to balance a high protein turnover rate in pedicels and stems, or could a movement-associated modification stabilize the protein? By the way: Paradoxically BP-GUS seems to be present in very young pedicels where we never observed pMPB2C promoter activity.



Figure 46: *p35S::MPB2C-RFP* and *p35S::SERRATE* yield similar phenotypes

A: T1 plant (plant M2) transgenic for *p35S::MPB2C-RFP* shows a similar phenotype to a T3 plant transgenic for *p35S::SERRATE* [B, picture published by (Prigge and Wagner 2001)]. Both plants show aberrant inflorescence phyllotaxy.

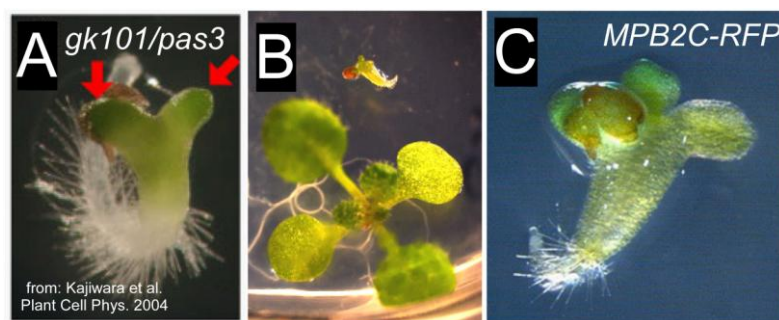


Figure 47: Similarity between *pas* mutants and "hydra"-like MPB2C-overexpressing plants

A: A six day old *gk-101/pas3* mutant plant developed bulges (arrows) instead of cotyledons. This picture was published by (Kajiware, Furutani et al. 2004). **B:** Ca. ten day old non-estradiol induced plants on hygromycin plates. Upper plant: - transgenic for *pGV10-90::XVE>>pOlexA-46::MPB2C-Ala-mRFP1*, line L1, RFP expression confirmed. Lower plant: control. **C:** The close-up of a plant from line L1 grown in parallel shows three bulges instead of cotyledons similar to the bulges observed in the *gk-101/pas3* mutant in A.

MPB2C(delta 1-58) showed an altered subcellular localization in transient expression assays (see chapter 3.2.5). The protein appeared less punctate and was observed more continuously in the cytoplasm and along microtubules, and it did not form large aggregates like the full-length protein. The large aggregates were obviously artifacts due to overexpression, because MPB2C localization via immunofluorescence had shown a pattern of small punctae along microtubules (Kragler, Curin et al. 2003). These aggregates might also develop in transgenic plants as a consequence of strong *MPB2C* overexpression and trigger degradation of the ectopic construct. So, the *delta (1-58)* construct lacking the hydrophobic N-terminal domain might even better effectuate a state of *MPB2C* overexpression because it better mimics endogenous *MPB2C* localization and does not form aggregates. Or MPB2C(delta 1-58) is simply more effective in binding target proteins. The effect of MPB2C(delta 1-58)-tag on KN1_{HD}-mediated cell-to-cell movement in the trichome rescue reporter line remains to be tested, as well as protein-protein interactions in the split YFP system. However, MPB2C(delta 1-58) interfered with KNAT1-KNB1 interaction the same way as did full-length MPB2C in yeast three-hybrid experiments (Daniela Fichtenbauer, personal communication). Additionally a similar deletion construct of *N. tabacum MPB2C* blocked MP30 cell-to-cell movement in transient

expression assays (F.K. personal communication). This suggests that MPB2C(delta 1-58) is functional regarding movement inhibition and has the potential to interact with KNAT1 and/or KNB1. Stomatal patterning defects had been observed in plants overexpressing *MPB2C* with an N-terminal GFP fusion (Ruggenthaler, Fichtenbauer et al. 2009). This fluorescent fusion protein was highly stable and detectable in transgenic plants, and it showed a subcellular localization at microtubules similar to MPB2C(delta 1-58) in transient expression, maybe because the N-terminal GFP tag masked the N-terminal hydrophobic domain. This fusion protein was at least partially functional because it interfered with ORMV infection (Ruggenthaler, Fichtenbauer et al. 2009). Stomatal patterning in *p35S::MPB2C(delta1-58)-RFP* lines needs to be examined.

Interestingly, one of the two subclades of MPB2C in monocots lacks the hydrophobic N-terminal domain. This adds weight to the idea that MPB2C without this domain is still functional and may even have assumed a specialized function.

4.3 MPB2C function in the context of *KNOX* genes - and beyond

Endogenous *MPB2C* is expressed in regions where neither *STM* nor *KNAT1/BP* promoters are active, e.g. in guard cells or seedling root tips. So the question arises whether *MPB2C* might be involved in processes beyond the interaction with these KNOX I proteins.

4.3.1 MPB2C, KONX and stomatal development

MPB2C was expressed in guard cell precursors and maturing guard cells of seedling cotyledons and true leaves (see Figure 9). The function of MPB2C in these tissues is not known, but the previously reported increase of stomatal clustering in *p35S::GFP-MPB2C* overexpression lines indicates a potential role for MPB2C in stomatal patterning (Ruggenthaler, Fichtenbauer et al. 2009). However, in our experiments, stomatal patterning in full-length *MPB2C-tag* overexpressing plants showing reduced trichome rescue in the KN1_{HD} movement reporter line was normal. But as discussed above, the N-terminal tag might modulate MPB2C function. In order to test this idea, stomatal patterning in *p35S::MPB2C(delta1-58)-RFP* plants should be analyzed. In fact, non-cell autonomous movement via PD is essential for correct stomatal patterning. But the mobile transcription factor SPEECHLESS (SPCH) (MacAlister, Ohashi-Ito et al. 2007) is a basic helix loop helix and not a homeodomain protein. Neither *STM* nor *KNAT1* are expressed in guard cell precursors or stomata. But *KNAT3* (Serikawa, Martinez-Laborda et al. 1997) and *KNAT4* (Zhao, Zhang et al. 2008) promoters are active in guard cells. These proteins belong to the KNOX class II family, and they are thought to be cell- autonomous. It remains to be tested whether MPB2C interacts with KNAT3 and KNAT4 or if MPB2C is involved in regulation of PD transport of other factors in guard cell precursors.

4.3.2 The function of MPB2C in roots remains elusive.

In our model MPB2C plays a role in border formation by limiting STM or KNAT1 cell-to-cell movement. In addition to regulation at the transcriptional level by other factors excluding *KNOX class I* gene expression from sites of leaf initiation, presence of *MPB2C* in these tissues could prevent the movement of homeodomain transcription factors beyond their expression domains into these tissues. In the root, *MPB2C* expression partially overlaps with *KNAT* gene expression (Dean, Casson et al. 2004; Truernit, Siemering et al. 2006). In the root tip with highest levels of *MPB2C* expression, no *KNAT* gene is expressed. But in the stele *MPB2C* expression partially overlaps with KNAT3, KNAT4, and KNAT6. *KNAT1* is expressed at the base of emerging lateral roots, and the *KNAT5* promoter is active in the proximal epidermis of emerging secondary roots, whereas *MPB2C* is expressed

throughout the entire lateral root primordium (see Figure 8). Furthermore, another *KNOX class I* gene, *KNAT6*, is involved in lateral root patterning (Dean, Casson et al. 2004). *KNAT6* was assigned as cell autonomous in the trichome rescue reporter screen in leaves (Kim, Rim et al. 2005), but there is evidence for non-cell autonomous *KNAT6* signaling in roots. First, *KNAT6* RNAi led to ectopic lateral root formation close to the root tip, although *KNAT6* expression was not detected in this zone in wild type plants (Dean, Casson et al. 2004). Second, *KNAT6* is expressed in the phloem and not in pericycle cells, but lateral roots are only initiated from pericycle cells overlying protoxylem but not phloem cells. The authors speculate that *KNAT6* might be part of a pathway preventing lateral root initiation maybe by increasing cytokinin levels or by influencing polar auxin transport. Or *KNAT6* could activate cell cycle inhibitors, which might act non-cell-autonomously like the cyclin-dependent kinase inhibitor KIPR1 (Weinl, Marquardt et al. 2005). Alternatively, *KNAT6* itself could move from cell to cell in roots. *KNOX class I* proteins are not the only transcription factors to act non-cell autonomously. In roots the GRAS family transcription factor SHORTROOT (SHR) moves, and SHR movement seems to depend on selective transport via plasmodesmata (Gallagher, Paquette et al. 2004). However, the regulation of cell-to-cell transport might be different in roots and shoots, because first, STM did not interact with the endosome-associated factor SHORT-ROOT INTERACTING EMBRYONIC LETHAL (SIEL), which mediates trafficking of SHR (Koizumi, Wu et al. 2011). And second, SHR did not interact with MPB2C or KNB1 in yeast two hybrid assays (Fritz Kragler, pers. comm.).

4.3.3 MPB2C and KNB1

MPB2C interaction with another *KNOX*-interacting protein, KNB1, was shown in split YFP assays (see chapter 3.3.1), and these two genes are co-expressed during plant life (compare Figure 7 to Figure 13 with Figure 14), albeit KNB1 in contrast to MPB2C seems to be excluded from meristematic domains. In our model, KNB1 could be the third factor to decide whether MPB2C interaction with STM or *KNAT1* leads to proteasomal degradation or not (Fichtenbauer 2011). The function of MPB2C and KNB1 beyond interaction with STM and *KNAT1*, as suggested by co-expression domains beyond sites of *KNOX I* transcription, remains to be investigated. The future identification of even more interaction partners of MPB2C and KNB1 might shed light on the physiological role of these proteins.

4.3.4 Is MPB2C involved in plant defense?

MPB2C interacts with the *TMV* movement protein MP30 (Kragler, Curin et al. 2003), and ectopic overexpression of *MPB2C* interferes with ORMV²⁴ infection in *Arabidopsis* (Ruggenthaler, Fichtenbauer et al. 2009; Fichtenbauer 2011). However, it is thought that viruses use existing endogenous transport mechanisms of the host plant for their intra- and intercellular movement (Nelson and Citovsky 2005). So interaction with MPB2C could occur just because MPB2C is part of that endogenous transport mechanism which is hijacked by *TMV* or ORMV movement proteins. This endogenous transport mechanism might also include negative regulation of transport via recruitment of non-cell-autonomous proteins or ribonucleoprotein complexes towards microtubules and preventing their access to PD under certain conditions. If MPB2C is a genuine plant defense gene, *MPB2C* expression – which is low in leaves – should be upregulated upon viral infection. This has not been shown until very recently: Cho and colleagues reported that the expression of *NbMPB2C* in *Nicotiana benthamiana* upon infection with *TMV* or *Potato virus X* was first down-regulated but after 36 hours increased twofold. Moreover, viral spread was increased in *NbMPB2C*

²⁴ *Oilseed Rape Mosaic Tobamovirus* (ORMV) is closely related to *Tobacco Mosaic Virus* (TMV) but infects *Arabidopsis*, which is not a good host for TMV.

silenced plants (Cho, Cho et al. 2012). Effects of viral infection on *MPB2C* expression in *Arabidopsis* have not yet been investigated.

MPB2C might have adopted the role of a plant defense gene in response to viral attacks. But other findings suggest that *MPB2C* might not primarily be a plant defense gene:

- its constitutive expression throughout plant life with increased expression levels in tissues where differentiation is initiated and patterning processes take place;
- low basal expression of *MPB2C* in leaf tissues which are exposed to viral attack;
- the reversal of *MPB2C*'s protective role against viral spread upon co-overexpression with *KNB1* (Fichtenbauer 2011). However, *KNB1* and *MPB2C* are co-expressed in most endogenous expression domains, which would rather favor viral spread than to prevent it.

4.4 *MPB2C* and apoplasmic transport - plant hormones

4.4.1 Auxin

Auxin is a small molecule derived from the amino acid tryptophan and plays a role in patterning and growth throughout plant life. It is involved in local and systemic signaling (Leyser 2011), and auxin maxima indicate sites of future organ outgrowth. In our experiments, *MPB2C* promoter activity was increased in plants grown on auxin-supplemented medium (see Figure 15). Online databases integrating results from expression profiling (e-FP Browser, AtGenExpress/Geneinvestigator, NASC Arrays Digital Northern) did not report altered *MPB2C* expression upon treatment with hormones (or under stress conditions). Maybe the endogenous *MPB2C* locus is more strictly regulated (e.g. via chromosome modifications) than the GUS-reporter transgene, which was inserted randomly into the genome. Alternatively, some additional elements within the *MPB2C* upstream regulatory sequence involved in fine-tuning the auxin response might not have been included in the promoter-GUS reporter construct. It is also conceivable that auxin could have an effect on endogenous *MPB2C* expression only in certain tissues, like e.g. in the root. In fact, *MPB2C* expression at the root tip and in lateral root primordia correlates quite well with local auxin maxima (Petersson, Johansson et al. 2009) (compare with Figure 8). However, a direct functional connection between *MPB2C* and auxin accumulation or polar auxin transport has not been reported so far. An indirect link via *KNOX* genes exists however:

Auxin accumulation is important for the regulation of *KNOX* gene expression: auxin is essential for the establishment of bilateral symmetry in the embryo and the subsequent correct localization of the *CUP SHAPED COTYLEDON (CUC)* expression domain. In turn, *CUC* genes initiate the expression of *STM* (Jenik, Gillmor et al. 2007). Later in the shoot apical meristem, auxin accumulates at sites of leaf initiation from which *STM* expression is excluded (Heisler, Ohno et al. 2005), and auxin together with *AS1* is required to repress *KNAT1* at the sites of leaf initiation (Hay, Barkoulas et al. 2006). In their review on the role of hormones in shoot apical meristem function, Eilon Shani and colleagues (Shani, Yanai et al. 2006) suggest that auxin might inhibit *KNOX* class I gene expression, and *KNOX* proteins in turn inhibit or negatively affect polar auxin transport. Consistent with this possibility, Scalon et al. (2002) have found that the *SEMAPHORE1 (SEM1)* gene of maize functions as a negative regulator of *KNOX* gene expression. Mutation of the gene leads to ectopic *KNOX* expression and, intriguingly, reduced polar auxin transport. This is associated with reduced lateral root formation in the *sem1* mutant (Scanlon, Henderson et al. 2002).

4.4.2 Gibberellins

Gibberellins (GAs) are diterpene plant hormones that control diverse aspects of growth and development. In *Arabidopsis*, GAs are essential for seed germination, leaf and root growth, floral induction under short-day conditions, inflorescence stem elongation, anther and petal development, fruit and seed development (Sun 2008; Yamaguchi 2008). GAs are absent from the shoot meristem.

Growth on gibberellic acid- supplemented plates induced *MPB2C* promoter activity in our experiments. This is interesting, because one function of KNOX proteins is to exclude GA from the meristem. *KNOX* genes act to repress the expression of gibberellic acid 20 oxidases, which catalyze the synthesis of bioactive gibberellins (Yamaguchi 2008), in *Arabidopsis* and tomato (Hay, Kaur et al. 2002), tobacco (Tanaka-Ueguchi, Itoh et al. 1998; Sakamoto, Kamiya et al. 2001), and potato (Chen, Banerjee et al. 2004). Furthermore STM increased the expression of *GA2ox2* and *GA2ox4*, gibberellic acid catabolic genes, in the meristem (Jasinski, Piazza et al. 2005). Hence *KNOX* gene products ensure the maintenance of a low GA regime in the shoot apical meristem by preventing GA biosynthesis and by counteracting GA diffusion into the meristematic zone by promoting GA degradation. If *MPB2C* expression in turn is induced via gibberellin, which is excluded from the shoot meristem via *STM*, this supports the notion that *MPB2C* might be relevant for border establishment at the boundary between meristem and differentiation zones. *MPB2C* expressed in GA rich domains immediately adjacent to the meristem would prevent cell-to-cell movement of STM into domains outside the meristem and hence protect GA outside the meristem from STM-mediated degradation. Results from our *in situ* *MPB2C* expression studies suggest, however, that in the vegetative shoot apex *MPB2C* is not expressed exclusively at sites with a high auxin and gibberellin regime, so these hormones might have a modulatory function but they do not seem to play a key role in the regulation of *MPB2C* expression.

4.4.3 Cytokinin

Cytokinins are adenine-derived plant growth regulators and play a role throughout development, from seed germination to tissue senescence. Cytokinins promote shoot growth (Skoog and Miller 1957; Estruch, Prinsen et al. 1991), leaf expansion (Devlin 1983), lateral bud release (Wickson 1958) and chloroplast development (Parthier 1979), they stimulate cell division and tumor formation (Akiyoshi, Klee et al. 1984), cause fasciations (Kenneth 1966; Crespi, Messens et al. 1992), they block root elongation (Ruzicka, Simaskova et al. 2009) and delay senescence (Noodén 1988).

Phenotypes strikingly similar to the here described hydra-like embryo patterning defect (in estradiol-inducible *MPB2C-mRFP* overexpression lines) and embryo lethality (occasionally observed in association with *MPB2C-tag* overexpression) have been described for *pasticcino* (*pas*) mutants, two of which are known to encode enzymes involved in the biosynthesis of **very long chain fatty acids** (VLCFA). These mutants showed severe embryo defects from the heart stage onwards with a short and wide hypocotyl and abnormal cotyledon patterning. They had a cell elongation defect combined with modified cell division patterns leading to the absence of the three distinct cell layers at the shoot apical meristem (Kajiwar, Furutani et al. 2004; Roudier, Gissot et al. 2010). Enlarged as well as almost absent SAMs were observed. Upon exogenous cytokinin application the *pas* mutants displayed hyper-proliferative SAMs with increased cell division rates (Faure, Vittorioso et al. 1998). In contrast to the hydra-like phenotype in plants overexpressing *MPB2C*, the *pas* mutants did not arrest development after germination, at least when grown on medium including 1% sucrose (Faure, Vittorioso et al. 1998). Sucrose as a carbon source can compensate for lacking photosynthetic capacity. All agar-grown plants in the here presented work (except for the hormone studies) were

cultivated on MS medium without sucrose, so it remains to be tested whether hydra-like mutants continue growth if sucrose is provided with the medium. It has not yet been tested whether *MPB2C* overexpressing plants have an altered response to exogenously applied cytokinin, but maybe there exists a functional connection between VLCFAs and *MPB2C* beyond cytokinin, see below.

4.4.4 The *pas* mutants –a connection between *MPB2C* and lipid rafts?

The striking similarity of hydra-like plants overexpressing *MPB2C* and *pasticcino* mutant plants with defective VLCFA biosynthesis (see Figure 47) might indicate that one of the cell-to-cell transport routes for macromolecules via plasmodesmata depends on vesicular transport and the compartmentalization of membranes into lateral domains or “rafts”. VLCFAs, consisting of 20 to 36 carbon atoms, are synthesized in the endoplasmic reticulum (ER). They serve as storage lipids and are membrane components in all eukaryotic cells. VLCFAs fulfill structural functions as protective lipids in skin and in the cuticular wax layer, and they influence the properties of cell membranes by facilitating the formation of membrane subdomains (so-called membrane rafts) or by inducing curvature in the lipid bilayer (Mouritsen 2011). More than being merely a structural component of the cell membrane, VLCFAs are involved in the secretory pathway and the synthesis of GPI lipid anchors (Bach, Michaelson et al. 2008). They are incorporated into sphingolipids, which are necessary for active vesicular fusion in the secretory pathway and play an essential role for cell plate formation and polar auxin transport (Markham, Molino et al. 2011). Sphingolipids are essential for embryo development (Chen, Han et al. 2006). VLCFAs are also involved in signaling during plant pathogen defense reactions, programmed cell death and guard cell closure (Lynch 2004; Bach, Michaelson et al. 2008; Bach, Gissot et al. 2011) (and references therein). Interestingly, plants with decreased sphingolipid biosynthesis have phenotypes similar to *KNOX* overexpressing plants, they are smaller and have altered leaf shapes (Chen, Han et al. 2006) and *KNOX* expression domains are enlarged in plants mutant for VLCFA biosynthesis.

Two of the three *PASTICCINO* (*PAS*) genes are known to encode enzymes involved in VLCFA biosynthesis. *PAS2* encodes an acyl-CoA dehydratase (Bach, Michaelson et al. 2008), which is one enzyme of the ER-localized VLCFA elongase multiprotein complex. *PAS3/GURKE/ACC1* encodes an acetyl-CoA carboxylase (Baud, Bellec et al. 2004; Kajiwarra, Furutani et al. 2004). The function of *PAS1*, an immunophilin, is less clear. It has been proposed to mediate nuclear import of a NAC-like transcription factor in dividing cells (Smoczynski, Roudier et al. 2006), and to be involved in fatty acid elongation, because it associated with the VLCFA elongase complex, and *pas1* mutants had reduced VLCFA levels (Roudier, Gissot et al.). *pas* mutants were either embryo lethal or displayed altered embryo, leaf and root development very similar to the observed *MPB2C* overexpressing hydra-like plants. The understanding of the role of VLCFAs in signal transduction is only at the beginning. Similar phenotypes in *pas* mutants and in mutants of the PD-transport regulator *MPB2C* might help to shed light on this field. *pas3* mutant embryos displayed a larger expression domain of *STM* than wild type plants (Kajiwarra, Furutani et al. 2004). Furthermore *KNAT2* and *KNAT6* but not *KNAT 1* expression was upregulated in either mutant of the three *PAS* genes (Harrar, Bellec et al. 2003). Nevertheless, no phenotypes similar to *pas* were ever described for *KNOX* overexpression lines (Hay and Tsiantis 2010) or for mutants in *ASYMMETRIC LEAVES1*, a negative regulator of *KNAT1* and *KNAT2* (but not of *STM*), which means that ectopic *KNOX* expression alone is not sufficient to elicit this phenotype. Indeed, not only *KNOX* domains but also expression domains of *WUSCHEL*, *AINTEGUMENTA* and *CUP SHAPED COTYLEDON1* were expanded in *pas1* (Roudier, Gissot et al. 2010). Roudier and colleagues sum it up:

"Thus, in the apex of pas1-3 embryos, the different cell territories required for proper organogenesis strongly overlap, leading to the coexistence of otherwise mutually exclusive cell fates." (Roudier, Gissot et al. 2010)

Interestingly, the strong *stm dgh6* allele is epistatic to *pas2* (Harrar, Bellec et al. 2003). The authors suggest that elevated *KNAT2* and *KNAT6* levels in the *pas* mutant background compensate for the lack of *STM* similar to the suppression of the *stm* phenotype in *stm/as1* double mutants (Byrne, Simorowski et al. 2002). Is the hydra-like phenotype in *MPB2C-mRFP* overexpressing plants caused by increased *KNOX* domains? According to our model, we would expect altered *KNOX* protein levels due to altered *KNOX* cell-to-cell transport and maybe altered protein stability but not altered expression domains, because *MPB2C* is not directly involved in the regulation of gene expression. Neither are the *PASTICCINO* genes *PAS2* and *PAS3*. Therefore it might still be informative to analyze *KNOX* expression domains in our hydra-like plants.

Roudier and colleagues suggest that polar auxin transport is disturbed in *pas* mutants because impaired vesicle trafficking interfered with the correct localization of the auxin efflux carrier PIN1. External application of VLCFAs could rescue PIN1 mislocalization (Roudier, Gissot et al. 2010). Polar auxin localization is essential for apical-basal patterning (Friml, Vieten et al. 2003) and the establishment of bilateral symmetry (Liu, Xu et al. 1993) during embryogenesis. The phenotypes of mutants in polar auxin transport have some aspects in common with the hydra-like mutants – growth arrest, conical hypocotyls, rudimentary roots – but they also differ from the hydra-like phenotypes: They do not develop true leaves, and their radialized cotyledons show abaxialization (cup shaped cotyledons) (Friml, Vieten et al. 2003) whereas hydra-like mutant cotyledons seem to have excess adaxial identity (cone-shaped cotyledons). The mechanisms that allow localized transport of proteins from vesicles to the plasma membrane are not well characterized in plants. Sorting seems to take place at the trans-Golgi network or in endosomes. Moreover, it is not known how differentially localized proteins remain at specific sites within the plasma membrane. Two possibilities exist: either there is a self-organizing scaffolding machinery or continual recycling occurs (Jürgens and Geldner 2002). Such a scaffold could be the lipid composition of membranes. The membrane raft hypothesis postulates the existence of special regions within membranes with an approximate diameter of 70nm displaying increased detergent resistance and enrichment in sphingolipids and sterols. They allow the accumulation of certain proteins and prevent lateral diffusion within the membrane due to their reduced fluidity (Mongrand, Stanislas et al. 2010).

Polar auxin transport is thought to be a vesicle-mediated process involving endosomes (Geldner, Friml et al. 2001; Geldner, Anders et al. 2003). The dependence on targeted vesicle transport and membrane anchoring via lipid rafts could be the common theme for similar phenotypes in polar auxin transport mutants, VLCFA biosynthesis mutants and *MPB2C* mutants. Excess *MPB2C* could interfere with correct vesicle sorting and hence disturb patterning processes. This could have a similar effect like defective biosynthesis of VLCFAs which could no longer provide certain vesicles with the lipids needed for correct localization and function of these vesicles.

4.4.5 Lipid rafts – a common feature in cell-to-cell transport of homeodomain proteins in animals and in plants?

Despite that TALE homeodomain proteins are conserved in all multicellular eukaryotes – animals, fungi and plants – and even must have existed in the last common eukaryotic ancestor (Burglin 1997; Derelle, Lopez et al. 2007), *MPB2C* homologs are not found in other kingdoms or in plants evolutionarily more ancient than land plants. In animals, too, some homeodomain proteins (which

are however not part of the TALE superfamily) such as ANTENNAPEDIA (ANTP) (Joliot, Pernelle et al. 1991) or ENGRAILED (ENG) (Joliot, Maizel et al. 1998) are non-cell autonomous. They lack conventional secretion peptides (Nickel 2003), and because they function both as mobile signals and as transcription factors, they have also been named “messenger proteins” (Prochiantz 2000). The homeoprotein domains mediating secretion and internalization have been characterized: Internalization is mediated by the third helix of the homeodomain (Derossi, Joliot et al. 1994) and this sequence is now used to increase transfection efficiency in biotechnology (Gadi, Ruthala et al. 2009). Secretion is mediated by a sequence in the homeodomain that harbors a nuclear export signal (Joliot, Maizel et al. 1998; Maizel, Bensaude et al. 1999). Here, like in plants, these motifs mediating cell-to-cell transport reside in (or close to) the homeodomain. The plant homeodomain protein KNOTTED1 moved between animal cells in culture (Tassetto, Maizel et al. 2005). Furthermore, co-expressed *MPB2C* inhibited cell-to-cell movement of the KN1 homeodomain in mammalian cell culture (F.K. unpublished). This suggests that there is a common mechanism for homeodomain protein cell-to-cell movement in plants and in animals, albeit animals have no plasmodesmata. How is this possible? Interesting is the observed association of nuclear-exported ENG with detergent insoluble membrane compartments enriched in sphingolipids and sterols (Joliot, Trembleau et al. 1997).

Detergent insolubility was the first defining feature of lipid rafts, the second feature was their special lipid composition – sphingolipids and sterols (Simons and Ikonen 1997). The concept of lipid rafts goes back to the 1970ies when scientists observed that lipids and proteins are not uniformly distributed across the cell membrane [reviewed by (Pike 2009)], and there has been much debate about that concept until the community agreed on the following definition:

“Membrane rafts are small (10–200 nm), heterogeneous, highly dynamic, sterol- and sphingolipid-enriched domains that compartmentalize cellular processes. Small rafts can sometimes be stabilized to form larger platforms through protein-protein and protein-lipid interactions.” (Pike 2006)

These membrane microdomains or lateral membrane compartments, which are less fluid and have characteristic lipid and protein contents have been described to occur in yeast and animals, and some time later they have also been found in plants [reviewed by (Simon-Plas, Perraki et al. 2011)]. In animals, these liquid ordered “islands” in the fluid membrane continuum are involved in signal transduction [reviewed by (Simons and Toomre 2000)] and pathogen interaction (Vieira, Correa et al. 2010). Plant lipid rafts play a role in the interaction between nitrogen fixing bacteria and legumes (Haney and Long 2009), intercellular virus movement (Raffaele, Bayer et al. 2009) or endocytotic turnover of membrane proteins (Tanner, Malinsky et al. 2011) [see also the review by (Grennan 2007)].

Typical proteins associated with plant lipid rafts are remorins. Proteomics on root, leaf and protoplast- derived lipid raft fractions identified among others vesicle trafficking proteins like clathrin, dynamins, ARF, tubulins, RAB and PRA proteins. In root lipid rafts also chaperons and ubiquitin or components of the ubiquitin ligase complex were identified (Lefebvre, Furt et al. 2007). Current models for plasmodesmal transport focus on the passage of molecules through the cytoplasmic sleeve, but many observations reveal the importance of membranes in the PD transport routes. PD not only provide a cytoplasmic continuity between cells, they also establish two types of membrane continuity, one in form of the cell membrane and the other via the appressed ER at the center of PD. The appressed ER is an evolutionary “invention” of land plants, like regulated transport

across PD and – coincidence or not – MPB2C. Proteins attached to the plasmalemma cannot diffuse laterally through PD, but molecules within the ER membrane can move from cell to cell via PD along the appressed ER membrane (Grabski, De Feijter et al. 1993; Martens, Roberts et al. 2006), and also small molecules inside the ER lumen can cross PD (Lazzaro 1996; Cantrill, Overall et al. 1999; Barton, Cole et al. 2011). Membranes are also essential for PD targeting. Many proteins and maybe even ribonucleoprotein complexes are thought to be transported via vesicle-mediated pathways towards PD [Karl Oparka in his review called it the “grab a Rab” imperative (Oparka 2004; Gallagher and Benfey 2005)]. Moreover in tomato the knock-down of *LeRab11a*, a GTPase potentially involved in vesicle docking and vesicle budding²⁵, triggered pleiotropic phenotypes resembling plants with misexpression of homeodomain proteins (Lu, Zainal et al. 2001). The authors speculate that homeodomain protein transport might be disturbed in these plants which would lead to HD protein accumulation in tissues where they are expressed and abnormally low levels in other tissues. However, the authors also concede that the observed effects might be caused by altered hormone levels (Lu, Zainal et al. 2001).

In our transient overexpression experiments, we often observed that STM or KN1 seemed to be localized to ER-like reticulate compartments [see also (Winter, Kollwig et al. 2007)], reminding of TMV MP, which is known to accumulate in the ER (Heinlein, Padgett et al. 1998; Reichel and Beachy 1998; Mas and Beachy 1999). Like homeodomain proteins, the viral movement proteins also seem to use “unconventional”²⁶ routes for their movement towards PD. A study on the triple gene block movement protein TGBp3 of *Poa semilatent virus* showed its intimate association with ER-derived membranes. But still, PD-targeting of TGBp3 was independent of a functional cytoskeleton, it was insensitive to brefeldin A treatment (which impairs Golgi-derived vesicle trafficking (Nebenfuhr, Ritzenthaler et al. 2002)), and PD targeting did not depend on COPII-mediated vesicle trafficking (Schepetilnikov, Solovyev et al. 2008). Apart from interaction with TMV MP30, MPB2C was also shown to interact with two out of three TGB movement proteins from *potato virus X* (PVX) (Cho, Cho et al. 2012). So, viruses like homeodomain proteins suggest that MPB2C might be part of this “unconventional” secretion pathway involved in PD-mediated cell-to-cell transport.

Is it conceivable that apart from the cytoplasmic transport pathway across PD there is also a membrane pathway which might include unconventional secretion with PD-associated lipid rafts involved? Not long ago, the presence of lipid rafts at plasmodesmata was inferred from the accumulation of remorin, a lipid raft-associated protein, at PD (Raffaele, Bayer et al. 2009), and this notion was discussed in recent reviews (Mongrand, Stanislas et al. 2010; Tilsner, Amari et al. 2011). Unconventional secretion associated with targeted vesicle transport guided or scaffolded by lipid rafts could be the common theme in homeodomain protein (and maybe also in viral) cell-to-cell movement in plants and animals.²⁷

²⁵ Whereas *Rab11* in *Drosophila* oocytes is involved polarized mRNA localization

²⁶ unconventional - at least from the perspective of the research community

²⁷ There has been a hype on lipid rafts with fierce discussions about their nature and physiological relevance, and much remains to be investigated. For now at least there seems to be a consensus that lipid rafts are no artifacts, but their definition is quite vague. Moreover different kinds of membrane rafts might coexist. Raft-defining lipids like sphingolipids in plants are different from those in animals (Mongrand, Stanislas et al. 2010). So, many details of this concept need to be refined. Similarly, the concept of “unconventional secretion” is anything else than a definition. It only says that this process differs from known signaling and transport processes, but it does not define a single pathway with known mechanisms. Rather, there might be many types of unconventional secretion like there might be many different kinds of lipid rafts.

The reader might keep in mind that MPB2C was isolated as MP30- interacting protein in a modified yeast two-hybrid screen, the Yeast Sos Recruitment System, where protein interaction takes place in a membranous environment (Kragler, Curin et al. 2003) rather than in the nucleus. Furthermore endogenous MPB2C protein accumulated in insoluble fractions when extracted from cells, and the intracellular localization of MPB2C resembles patterns observed with vesicle-associated factors. It would be interesting to identify the nature of the observed MPB2C punctae or bodies. Are they just protein clusters or are they vesicle-associated, and if so, what kind of vesicles would that be? Chemical treatment (e.g. with brefeldin A) or crosses into membrane sub- compartment marker lines like those in the WAVE collection established by Niko Geldner (Geldner, Denervaud-Tendon et al. 2009) will help to elucidate the nature of these bodies.

Recently a group reported that GFP-NbMPB2Cb was found not only in the punctate pattern but also at PD and that it was localized to the ER upon viral infection (Cho, Cho et al. 2012). Thus, despite that MPB2C does not have a transmembrane domain it seems to have the potential for membrane-association in the cell. This is one of many similarities MPB2C shares with **REMORINS** (REM) (Jacinto, Farmer et al. 1993; Bariola, Retelska et al. 2004; Raffaele, Mongrand et al. 2007). REMs are hydrophilic, vascular-plant-specific proteins. Some REMs have an N terminal hydrophobic domain and all have a C-terminal coiled-coil domain (Raffaele, Mongrand et al. 2007). They are associated with lipid rafts (Mongrand, Morel et al. 2004; Lefebvre, Furt et al. 2007) and located at plasmodesmata (Raffaele, Bayer et al. 2009; Fernandez-Calvino, Faulkner et al. 2011). The first REM was discovered as being phosphorylated upon challenge with oligogalacturonides, which are early defensive signaling molecules upon pathogen attack in plants (Jacinto, Farmer et al. 1993). REM have an influence on viral movement similar to MPB2C: *MPB2C* overexpression in *Arabidopsis* (Ruggenthaler, Fichtenbauer et al. 2009; Fichtenbauer 2011) or *N. benthamiana* (Cho, Cho et al. 2012) interfered with ORMV or *Potato Virus X* (PVX) infection, respectively, and REM overexpression delayed PVX infection of tomato plants (Raffaele, Bayer et al. 2009). MPB2C directly interacts with TMV MP (Kragler, Curin et al. 2003) and with two of the three PVX movement proteins TGBp1, and TGBp2 (Cho, Cho et al. 2012), whereas REM was shown to interact with the *Potato Virus X* movement protein TGBp1 (Raffaele, Bayer et al. 2009)²⁸. Despite that REMs play a role in plant-microbe interactions [reviewed by (Jarsch IK 2011)], many REMs are expressed ubiquitously and may serve house-keeping functions – similar to MPB2C. Some remorins were enriched in meristems, leaf primordia and root tips in potato and tomato (Retelska, Fleming et al. 2000) and accumulated in shoot apices including leaf primordia and in root apices (Bariola, Retelska et al. 2004) - tissues where *MPB2C* is also expressed. The expression of *AtREM1.3* (*AtDbp*) was upregulated upon auxin treatment (Alliotte, Tire et al. 1989), while we observed upregulation of MPB2C on auxin-supplemented plates. Last but not least misexpression of *REM* had no apparent phenotypic effect (Raffaele, Bayer et al. 2009) as did misexpression of *MPB2C* in most cases. So far attempts to knock out one or more of the remorin genes either failed or did not lead to an obvious phenotype (Reymond, Kunz et al. 1996; Bariola, Retelska et al. 2004) – which might of course be due to functional redundancy within the members of the REM gene family. And this is a difference between *MPB2C* and *REMs*: Remorins belong to a gene family of 16 genes in *Arabidopsis* (Raffaele, Mongrand

²⁸ TMV MP and the TGB proteins can mediate viral transport across plasmodesmata, although their targeting mechanisms differ slightly (Lucas, Ham et al., 2009; Niehl and Heinlein, 2011). However, TMV MP can complement the TGB-mediated movement function in hosts common to TMV and BSMV, a TGB-encoding virus. Solov'yev, A. G., D. A. Zelenina, et al. (1996). "Movement of a barley stripe mosaic virus chimera with a tobacco mosaic virus movement protein." *Virology* **217**(2): 435-41.

et al. 2007) whereas *MPB2C* is a single gene in *Arabidopsis*. Another difference is that REMs so far have not been detected to reside at microtubules.

However, it is tempting to speculate that MPB2C and REMs as scaffolding or adaptor proteins are part of a PD transport route involving membranes, which is usurped by some viral movement proteins and used for viral spread. In a model, MPB2C could guide vesicle-mediated transport towards plasmodesmal lipid rafts, where remorin takes over the cargo. Both proteins would function as adapter proteins between NCAPs and membranes and positively or negatively regulate macromolecular transport across PD. Interaction with MPB2C might either lead to proteasomal degradation or to access to a PD transport route. This might depend on MPB2C abundance (remember that MPB2C is able to dimerize), on the abundance and nature of the NCAP to be transported (whether RNA-associated or not, or maybe modified via phosphorylation etc.), and it might also depend on the presence of other interacting molecules such as KNB1. Intriguingly, KNB1 itself is non cell autonomous, and its role in PD transport seems to be the regulation of NCAP abundance and availability for transport (Fichtenbauer 2011).

In the PD transport model shown in Figure 2 A, MPB2C might be a vesicle-associated PD initial receptor (PD-IniR) or part of a vesicular PD transport complex (PD-TraC), whereas remorin might be a member of the PD docking complex, and CCT8 would be a refolding chaperone (RfC). Future research will show whether or not there is a connection between MPB2C and lipid rafts in general as well as between MPB2C and REMs in particular, and what role lipid rafts play in PD transport.

5 Material and Methods

5.1 DNA Protocols- Cloning

Cloning and PCR was done according to standard protocols (Sambrook, Fritsch et al. 1989) or according to the manufacturer's instructions. Most Plasmids were cloned using the GATEWAY® recombination technology (Invitrogen).

5.1.1 *E. coli* strains

For standard cloning procedures *E. coli* strain TOP10 (Invitrogen) was used. For propagation of Gateway plasmids containing the negative selection marker *ccdB* (that encodes a gyrase- inhibiting polypeptide (Bernard and Couturier 1992)) the *E. coli* strain DB3.1TM was used.

5.1.2 Bacterial growth

Bacteria were grown in liquid or solid cultures at 37°C in LB medium:

10g/l trypton, 5g/l yeast extract, 5g/l sodium chloride, 10g/l agar (for solid medium), pH 7, autoclaved for 20 min at 121 °C.

The following antibiotics (stored at -20 °C, working aliquots at 4°C) were used for selection:

Antibiotic	stock solution	solvent	conc. liquid	conc. on plate	comment
Ampicillin	100 mg/ml	50% EtOH	100 µg/ml	100 µg/ml	
Carbenicillin	100 mg/mg	H ₂ O	100 µmg/ml	100 µg/ml	
Chloramphenicol	34 mg/ml	EtOH	68 µl/ml	34 µg/ml	
Gentamycin	50 mg/ml	H ₂ O	50 µg/ml	50 µg/ml	
Kanamycin	50 mg/ml	H ₂ O	50 µg/ml	50 µg/ml	
Rifampicin	25 mg/ml	MeOH	100 µg/ml	100 µg/ml	
Spectinomycin	100 mg/ml	H ₂ O	100 µg/ml	100 µg/ml	
Streptomycin	10 mg/ml	H ₂ O	50 µg/ml	50 µg/ml	
Zeocin	50 mg/ml	H ₂ O	50 µg/ml	50 µg/ml	Agar must be low salt (5 g/l NaCl) and pH 7,5

5.1.3 *E. coli* transformation

E. coli was transformed via electroporation:

Preparation of electro- competent cells:

3 ml liquid overnight culture was diluted in 300 ml selective LB medium and grown 2- 4 hours until the exponential growth phase was reached (OD₆₀₀ was 0.8- 1.2). The culture was rapidly cooled to 4°C by shaking the flask in ice-water. From there on cells were kept on ice or at 4°C. Cells were harvested by centrifugation (7 500xg, 4°C, 12 min) and washed twice in one 300ml cold (4°C) sterile ddH₂O and once in 50 ml sterile ice-cold 10% glycerol. Cells were resuspend in 2- 5 ml cold 10% glycerol and split into 200µl aliquots in sterile Eppendorf tubes, shock frozen in liquid nitrogen and stored at -80°C until needed.

Electroporation:

30 minutes prior to transformation electro- competent cells were allowed to thaw on ice and electroporation cuvettes were cooled on ice whereas LB medium was pre-warmed to 37°C. 100- 500ng plasmid DNA per transformation reaction were placed into the cuvette (the volume should not

exceed 5µl; e.g. 5µl of 1:10 diluted ligation, 1µl of 1:500 diluted miniprep). A negative (water) and a positive control were always included. 100µl competent cells were added carefully, the exterior of the cooled cuvette was dried before the pulse was applied at 1.7 kV (or 0.85 kV for *Agrobacterium*), 25 µF, and 200 Ohms. Then 900µl LB medium were added, the bacteria were transferred to an Eppendorf tube and incubated shaking at 37°C for one hour before being plated onto selective medium. Electroporation cuvettes were cleaned with common soap, ethanol and 10 min UV treatment and re-used.

5.1.4 Plasmid isolation from *E. coli*

2ml selectively grown overnight culture was pelleted (centrifugation 2 min 14000 xg at room temperature) and resuspended in 300 µl buffer P1. 300µl of buffer P2 were added, tubes were inverted to mix, then 300 µl buffer P3 were added, tubes were inverted, and incubated 5 min on ice. Cell debris and chromosomal DNA were pelleted by centrifugation (14000xg rpm, 4C, 10min), and the supernatant was transferred to a fresh tube with 650 µl ice-cold isopropanol. The precipitated plasmid DNA was pelleted by centrifugation (14000rpm, 4C, 25min) and washed twice in 1ml 70% ethanol and then in ethanol absolute. The pellet was dried by incubation for 10 min at room temperature and resuspend in 30µl ddH₂O by incubation and shaking at 50°C for 10- 20 min.

Plasmids were stored at -20°C.

Buffer P1 (resuspension buffer):

50mM Tris, 10mM EDTA pH 8,0, 100µg/ml RNaseA (stored at 2-8°C).

Buffer P2 (lysis buffer):

200mM NaOH, 1% SDS (stored at room temperature).

Buffer P3 (neutralization buffer):

3M KoAc pH5.5 (stored at 2-8C or RT).

5.1.5 Cloning

Cloning of MPB2C-GFP (binary vector pEarleyGate 103) and MPB2C-TAP (binary vector pEarleyGate 205, (Earley, Haag et al. 2006) and cloning of the split YFP constructs (the binary vectors pCl112, N-YFP and pCl113, C-YFP were a kind gift from Martin Huelskamp, Institute of Botany, University of Cologne; (Wester, Digiuni et al. 2009)) was described earlier (Winter, Kollwig et al. 2007). Analogously, MPB2C deletion constructs were recombined into the respective binary vectors. MPB2C delta coiled-coil was generated by restriction digest of the Entry clone (in pENTR/D-TOPO) containing MPB2C cDNA with HindIII to remove 156 nucleotides spanning part of the predicted coiled-coil region and subsequent re-ligation. MPB2C delta 57aa was created by PCR on a MPB2C cDNA template (Entry vector) with Gateway primers FK339 + FK404 and subsequent recombination into pDONR/Zeo to obtain an Entry clone. MPB2C delta 1-117 aa was created by PCR on a MPB2C cDNA template (Entry vector) with Gateway primers FK696 + FK697 and subsequent recombination into pDONR/Zeo to obtain an Entry clone. These primers also insert a NotI and a BamHI restriction site, respectively. In order to generate MPB2C-RFP and MPB2C delta 57-RFP the respective entry clones were recombined with the binary Gateway® vector pBat-TL-K-RFP (a kind gift from Martin Huelskamp, Institute of Botany, University of Cologne). For the estradiol- inducible MPB2C-*Ala-mRFP1* construct, MPB2C cDNA was amplified with primers FK238 and FK239 introducing a BamHI and NcoI restriction site, respectively. The PCR fragment was used to replace KNB1 in the entry clone KNB1-*Ala-mRFP1_pENTR4* (Kollwig 2010). The binary vector was generated via Gateway®

recombination into vector pMDC7 (Curtis and Grossniklaus 2003). In order to generate the ethanol-inducible meristem subdomain promoter lines, the respective entry clones were recombined with vector pEC2 providing the following cassette *pAlcA::GW::t35S* (a kind gift from Patrick Laufs, INRA, France) to obtain a binary plasmid. This vector allows expression of the gene of interest in the presence of the transcription factor AlcR (see scheme in Figure 39). The reporter construct for MPB2C promoter activity *proMPB2C::MPB2C-GUS* was cloned by amplification of a 2.4 kb genomic fragment including the upstream region and the genomic sequence of MPB2C until just before the STOP codon with the primer pair FK518 + FK 554. The PCR product was recombined into pDONR/Zeo to obtain an Entry clone. Gateway® recombination into pKGWFS7 (Karimi, Inze et al. 2002) resulted in the respective binary plasmid. The inducible MPB2C silencing construct was generated by Gateway recombination of MPB2C cDNA into binary vector pOpOff2(hyg) (CSIRO; (Wielopolska, Townley et al. 2005)). In this vector two Gateway cassettes in opposite directions allow the dexamethasone-inducible expression of RNA hairpin constructs.

An artificial micro RNA against MPB2C was created as follows: A sequence specific for MPB2C was inserted into the backbone structure of miR164b in such a way that the resulting processed micro RNA is targeting the second exon of MPB2C mRNA. This artificial micro RNA precursor of 280nt length was synthetically produced and cloned via BamHI/EcoRI into pENTR4 to create an entry clone. The construct was recombined into the binary plasmid pMDC32 (Curtis and Grossniklaus 2003) for constitutive overexpression via the viral 35S promoter and into binary vector pEC2 (Patrick Laufs, INRA, France) for tissue-specific ethanol-inducible expression, see chapter 5.4.3.

A variant of MPB2C insensitive to a predicted endogenous micro RNA against MPB2C (genomic locul of targeting sequence: chr.1: 17699377-17699397 (Adai, Johnson et al. 2005; Lindow and Krogh 2005)) was generated by site-directed *in vitro* mutagenesis of the Entry vector. The primers FK576 and FK577 were designed to induce six silent mutations into the MPB2C ORF within the 21bp recognition site of the putative miRNA. Site-directed mutagenesis was done according to the manufacturer's instructions (Stratagene QuikChange™ II *Site-Directed Mutagenesis Kit*), and the result was verified by sequencing. Template for the mutagenesis was the Entry clone harboring the MPB2C genomic construct including the promoter region without STOP codon. This mutated construct was recombined into vector pKGWFS7.

5.2 RNA protocols

5.2.1 RNA extraction

RNA isolation was done on a protocol based on using Trizol (Invitrogen) and chloroform. In brief, fresh plant material was immediately frozen in liquid nitrogen, pulverized with mortar and pestle and resuspended in Trizol. After a centrifugation the supernatant was mixed with chloroform, centrifuged again, and subsequently RNA was precipitated from the upper aqueous phase with isopropanol and sodium acetate (linear acrylamide was added in order to precipitate small RNAs).

5.2.2 RNA *in situ* hybridization

RNA in situ hybridization was performed according to the protocol published by David Jackson (Jackson 1991) further optimized in his lab. Digoxigenin-11-UTP (Roche)- labeled RNA probes were generated by T7 RNA polymerase-mediated transcription on PCR products obtained from primers adding the T7 promoter sequence. The PCR fragment for MPB2C 5'-specific probes was designed to cover the first 602 nucleotides (probe M2, primers FK227 + FK621), the PCR fragment for **MPB2C** 3'-

specific probes covered the terminal 696 nucleotides, thus overlapping with the 5'probe for 320 nucleotides (probe M4, primers FK296 + FK421). A stronger signal was obtained with the 3'probe. Sense probes used as negative controls were designed to cover the 5'half of MPB2C (probe M1, primers FK284 + FK297) and the 3'half of the gene (probe M3, primers FK622 + FK228). For detection of **STM** mRNA a probe described by (Long, Moan et al. 1996) spanning amino acids 81 to 382 (including the homeodomain) was used (sense probe S1: primers FK623 + FK624, antisense probe S2: primers FK625 + FK626). For the detection of **KNAT1** mRNA the a probe covering 700bp at the the 5' portion of the gene lacking the homeobox was used as described by Lincoln (Lincoln, Long et al. 1994), (sense probe: FK627 + FK 628, antisense probe: FK629 + FK630). For detection of **KNB1** the probe was designed to cover the entire mRNA of 423 nucleotides from start codon to stop codon (sense probe: FK285 + FK178, antisense probe: FK177 + FK646).

A detailed protocol can be found in Appendix A: RNA *in situ* hybridization lab protocol

5.3 Protein Protocols

5.3.1 *In silico* Protein sequence analysis

In order to identify conserved regions in the MPB2C protein, a similarity search of the protein sequence was done against a database containing all non-redundant GenBank CDS translations+PDB+SwissProt+PIR+PRF excluding environmental samples from WGS projects with the standard settings (summarized in Table 9) of the web- based alignment tool BLASTP 2.2.25+ (Altschul 1997; Altschul 2005).

Search parameter name	Search parameter value
Program	BLASTp
Word size	3
Expect value	10
Hitlist size	100
Gapcosts	11,1
Matrix	BLOSUM62
Filter string	F
Genetic Code	1
Window Size	40
Threshold	11
Composition-based stats	2

Table 9: Search Parameters for alignment of MPB2C protein sequence against database

The resulting alignment was then restricted to plant proteins since there was a clear rise in the Expect value, a measure for the significance of the match in regard to the sequence length and the database size, to the fourth power (from $6e^{-04}$ to 1.3) between plant and non- plant sequences. Next, the protein sequences were screened for redundancy. It is possible that even non-redundant databases contain multiple entries for the same protein, e.g. two entries for Arabidopsis MPB2C were retrieved, one (GenBank Accession AAB38778.1) was only 209 amino acids short and that database entry might come from an incomplete cDNA sequence. This entry resulted from a publication in which a screen against an Arabidopsis cDNA library had been performed (Xia, Ramachandran et al. 1996), and therefore the truncated protein could result from an incomplete cDNA or from an alternatively spliced transcript. But since it is known that there is only one coding region for MPB2C in the Arabidopsis genome, this shorter protein sequence was omitted. In a similar way, four of six proteins retrieved from *Zea mays* were sorted out, and two out of four proteins from *Selaginella moellendorffii*.

The remaining 21 protein sequences were – in the order of decreasing similarity as retrieved from the BLAST search - aligned with ClustalW2, a multiple sequence alignment tool based on a pairwise alignment algorithm hosted by the European Bioinformatics Institute (EBI). The best result was achieved by using the default settings for the alignment with the protein weight matrix gonnet and the neighbor-joining clustering method. To get an impression of the quality of the alignment, the alignment result was uploaded to ClustalW2 Phylogeny, a web-based tool for phylogenetic tree generation. The resulting tree obtained with default settings did indeed roughly represent phylogenetic relationships. This very basic phylogenetic tree was adjusted for display by rotating some branches and rooted to the clade containing the homologs from *Physcomitrella* and *Selaginella*.

5.3.2 Antibodies

- Two antibodies against AtMPB2C are available. The polyclonal antibody raised in rabbit against an E. coli expressed full length MPB2C protein (Davids Biotechnologie GmbH, Regensburg, Germany) and purified against MPB2C immobilized on nitrocellulose filter paper by Friedrich Kragler.
- A peptide antibody targeting the 22 C-terminal amino acids of MPB2C (-DEESLVMAAQARAYLQSLAFTYY) was raised in rabbit and affinity purified via epoxy immobilized antigen (Davids Biotechnologie GmbH, Regensburg, Germany). The affinity purified IgG serum fraction (1.71 mg/ml in 100mM phosphate 100 mM sodium acetate buffer pH 6- 8 including 0.02% sodium azide) was stored at -80°C with 20% glycerol added, and working aliquots were stored at 4°C. For western blot a dilution of 1: 750 (1.82 µg/ml) was used.
- An antibody targeting the C-terminal 21 amino acids of KNB1 (-EETTSLLHNARYLIQNPSIEQ) was generated analogously and used in a dilution of 1: 750 (1.91 µg/ml).
- The anti- protein A antibody (P3775, Sigma Aldrich) from rabbit was used in a dilution of 1: 10 000.
- The monoclonal anti-Hemagglutinin tag antibody (a kind gift from Gotthold Schaffner, IMP Vienna) was obtained as supernatant from a mouse hybridoma cell line secreting the antibody. It was used in a dilution of 1: 750 in order to detect R-GUS in the protein stability assay.
- Secondary peroxidase-linked antibodies against rabbit IgG (NA 934) or against mouse IgG (Na 931) were purchased from GE Healthcare Life Sciences and both were used in a dilution of 1: 10 000.

5.3.3 Native Protein extraction with proteasome inhibitor

Plant material pre-treated with proteasome inhibitor (see chapter 5.5.4) was frozen in liquid nitrogen, macerated by shaking with metal beads in a TissueLyser (Qiagen) and thawed on ice in **native protein extraction buffer** with or without proteasome inhibitors MG132 and Epoxomicin. After incubation for 10 minutes at 21°C, samples were centrifuged for 10 minutes 16000xg at 4°C. Supernatants and pellets were separated. To detect MPB2C the pellet fraction was used, for the detection of the proteasome inhibitor reporter construct R-GUS the supernatant fraction was used.

Native protein extraction buffer: 50 mM Tris HCl pH 7.5, 150 mM NaCl, 2.5 mM MgCl₂, 5 % glycerol, 0.1% NP-40, 2mM DTT, 1 mM PMSF, 0.5 mM EDTA, 0.5 mM EGTA, 1x complete protease inhibitor (Roche)

Proteasome inhibitors in extraction buffer: 100µM MG132 (Sigma Aldrich) or instead the same volume of the solvent EtOH for mock-treated control, 5 µM Epoxomicin (Cayman Europe, Estonia) or the same volume of the solvent for Epoxomicin, DMSO, for the mock- treated control.

5.3.4 Protein extraction via Trizol and Acetone precipitation

100- 200 mg plant material was frozen in liquid nitrogen, broken up by shaking (3x 10 seconds, 30 shakes per second, always in a frozen state) with two metal beads in a TissueLyser (Qiagen) and thawed on ice in 500µl Trizol (Invitrogen). After mixing and incubation for 10 min at room temperature, the samples were centrifuged for 10 minutes 16000xg at 4°C. The supernatant was transferred into a fresh tube containing 100µl chloroform. The samples were mixed well and centrifuged for 15 minutes 16000xg at 4°C. The upper phase containing RNA was discarded, and 1ml of ice- cold acetone was added to the interphase and lower phase containing proteins. The samples were mixed and centrifuged for 10 minutes 16000 x g at 4°C. After a washing step with 1ml ice- cold acetone, the pelleted proteins were briefly dried and resuspended in phosphate buffer.

5.3.5 Western blot

Protein samples were mixed with **SDS loading dye** and boiled in a water bath for 10 minutes. After centrifugation at room temperature for 1 minute at 16000xg, samples were loaded onto a 7% SDS-Tricine polyacrylamide gel for electrophoresis and subsequently electro-blotted onto a PVDF membrane (Milipore). Incubation with primary antibodies was done overnight at 4°C in blocking solution (TBS, 0.1% Tween-20, 5% w/v dry milk), incubation with secondary antibodies from donkey against rabbit IgG coupled to horseradish peroxidase (GE Healthcare, NA934) or sheep anti- mouse- HRP (GE Healthcare, NA931) was done for one hour at room temperature in blocking solution. SuperSignal West Pico Chemiluminescent Substrate (Thermo Scientific) was used for detection of horseradish peroxidase activity. Weak signals were detected on Amersham Hyperfilm ECL (GE Healthcare).

SDS loading dye (final conc.): 2% SDS, 10% Glycerol, 50mM Tris pH 6.8, 0.2mg/ml bromphenol blue, 100mM DTT

SDS Tricine PAGE:

Anode Buffer: 200mM Tris-Cl pH 8.9

Cathode Buffer: 100mM Tris base, 100mM Tricine, 0.5% SDS, pH (Without adjusting: 8.3)

Stacking gel (4%): 750 mM Tris-Cl pH 8.45, 0.075% SDS, 4% acrylamide (acryl:bis = 37.5:1), 0.1% ammonium persulfate, 0.1% TEMED

Resolving gel (7%): 15% glycerol, 1M Tris-Cl pH 8.45, 0.1% SDS, 7% acrylamide (acryl:bis = 37.5:1), 0.05% ammonium persulfate, 0.05% TEMED

5.4 Plant Protocols

5.4.1 Plant growth conditions

Arabidopsis thaliana and *Nicotiana benthamiana* plants were grown on soil in a controlled environment with light intensities between 800 and 1000 µmolm⁻²s⁻¹ under long-day conditions (16 hours light/ 8 hours dark) or short day conditions (8 hours light/ 16 hours dark). If not stated otherwise, plants were grown under long day conditions. Growth temperature for *Nicotiana benthamiana* was 25°C +/- 5 day and 20°C +/- 5 night, humidity: 70% - 90%; for *Arabidopsis thaliana* the temperature was 22°C +/- 5 (or, if indicated: 17°C +/- 5), humidity: 60% +/- 20.

The soil mixture used for *Arabidopsis* was: 70 l "Max Planck" substrate (Stender AG, Schermbeck Germany) + 100g Osmocote Start (Scotts International B.V.) + 2 g Confidor (Bayer CropScience Austria) dissolved in 10l water. For growing *Nicotiana* plants the following soil mix was used: 5 parts Neuhaus N3 substrate + 1 part Perlite (Granuperl S 3-6, Knauf Perlit GmbH, Vienna) which was autoclaved before adding to 15 l soil mixture 75 g Osmocote (Substral Scotts Celaflor GmbH, Germany) + 0.3g Trianum (Microbial plant strengthener *Trichoderma* sp., Koppert Biological Systems B.V., The Netherlands) + 600µl Companion-G (*Bacillus subtilis* mixture, biohelp GmbH, Vienna, Austria) dissolved in 2 l water.

For growth on agar plates or selection of antibiotic-resistant *Arabidopsis* plants, dry seeds were sterilized by incubation for 10 minutes in a solution of 10% trichlor-isocyanurate (Chloriklar, Bayrol GmbH, Germany) in 90% ethanol. Subsequently they were washed at least three times in ethanol absolute and air-dried before spreading them on 0.6% agar plates with 1x Murashige Skoog medium including Gamborg B5 vitamins (Duchefa) adjusted to pH 5.7 (0.5 g/l MES, pH adjusted with KOH) and the according antibiotic (15 µg/ml Hygromycin B (Sigma) or 50 µg/ml Kanamycin (Sigma) or 25 µg/ml BASTA (Bayer CropScience, Austria). Note that in these experiments no sucrose was added to the plant medium, except for the hormone treatment experiments performed by Kornelija Pranjic (Figure 15).

5.4.2 Plant ecotypes

Arabidopsis thaliana ecotype Columbia was used for generating transgenic plants. The KNOX mutant lines *bp-1*, *stm11* and *stm-4* obtained from European Arabidopsis Stock Centre NASC were in Landsberg *erecta* background. The MPB2C SALK lines were in Columbia background, and the TILLING lines had the *erecta* mutation *er105* back-crossed to Columbia (Till, Reynolds et al. 2003).

5.4.3 Transgenic lines

Appendix D Transgenic Arabidopsis lines **Error! Reference source not found.** lists transgenic lines created during this work.

The ethanol-inducible (Deveaux, Peaucelle et al. 2003) meristem subdomain promoter transactivation driver lines (a kind gift from Patrick Laufs, INRA, France) in Columbia ecotype were homozygous for the respective transgene and for the selection marker Hygromycin B. These lines were transformed with binary vector pEC harboring the construct of interest to generate the ethanol-inducible meristem subdomain promoter transactivation lines.

Line R-GUS #8 was a kind gift from Andreas Bachmair (MFPL, University of Vienna) (Garzon, Eifler et al. 2007). This line harbors the transgenic construct pER::DHFR-3xHA-Ubi-R-GUS-1xHA: Driven from an estradiol-inducible promoter (pER) a fusion protein of dihydrofolate reductase (DHFR) with three hemagglutinin epitopes (HA) followed by the amino terminus of ubiquitin, an Arginine then residue by unstructured amino acids, a β glucuronidase gene (GUS) and one more HA epitope. Upon induction the fusion protein is expressed and immediately cleaved by ubiquitin-specific proteases into two proteins: the DHFR-3xHa-Ubi protein (ca 30 kDa) serves as reference protein whereas the R-GUS-1xHA protein (ca 90 kDa) is targeted to the proteasome according to the N-end rule – unless proteasomes are inhibited. R-GUS was detected with the anti-HA antibody.

Line 35S::STM-GR in Col0 was a kind gift from Robert Sablowski (John Innes Centre, Norwich) (Gallois, Woodward et al. 2002).

Line 35S::GFP-KN1 in Col0 as well as the binary plasmids 1229 (*pAtML1::YFP-STM*) and 1230 (*pATML1::YFP-KNAT1*) were a kind gift from David Jackson (Cold Spring Harbor, New York).

5.4.4 MPB2C SALK line

In this line T-DNA is inserted in an inverted manner exactly at the intron/exon border between the fourth exon and the fourth intron of MPB2C. The insertion point was confirmed via PCR and genomic sequencing. The T-DNA insertion could be tested via genomic PCR with three primers. Two primers were specific for MPB2C, one (FK 296) was 5', the other one (FK421) was 3' of the T-DNA insertion point, and the third primer was specific for the T-DNA left border (FK 447). Without T-DNA insertion an MPB2C-specific fragment of 933bp was amplified with primers FK296 and FK421. Whereas in the homozygous SALK line, a 470bp fragment was obtained with primers FK421 and 447. Due to the size of the T-DNA insertion, this PCR product is favored over a PCR product by primers FK296 and 421. Accession # SALK_090101C (NASC: N658803)

5.4.5 MPB2C TILLING lines

MPB2C TILLING (Targeting Induced Local Lesions in Genomes) lines were ordered at the Seattle Tilling Project (<http://tilling.fhcrc.org>), and seeds were obtained by the *A. thaliana* stock center. Two TILLING lines were closely analyzed. Point mutations in these lines led to significant amino acid changes in the MPB2C protein. In line TIL_CS94728 (ABRC Stock Nr. CS94728) the point mutation at bp 236 within exon 2 resulted in an amino acid exchange at position 79 of Glycine to Aspartic Acid (Gly79 -> Asp79) within a conserved region in the first third of MPB2C. In line TIL_CS91285 (ABRC Stock Nr. CS91285) harboring a point mutation at bp 428 in exon 3, Arginine at position 143 was replaced by Lysine (Arg143 -> Lys143) within a conserved domain being part of the predicted central coiled coil region of MPB2C.

Both TILLING lines could conveniently be genotyped via CAPS (Cleaved Amplified Polymorphic Sequence) markers. The mutations led to deletions of restriction enzyme cleavage sites, and thus the mutations could be verified via PCR amplification of the respective genomic region and subsequent restriction digest. The point mutation in line TIL_CS94728 led to destruction of an NlaIV restriction site: GGTTC (wt) -> GATTC (mut).

A 366bp PCR fragment obtained with primers FK293 + FK295 was cleaved by NlaIV into 236bp + 130bp in wild type genomic DNA, whereas the fragment remained uncleaved in line TIL_CS94728. In line TIL_CS91285 a DdeI site was destroyed: ACTAAG (wt) -> ACTAAA (mut). A PCR fragment of 317bp (primers FK296 + FK297) was cleaved twice in wild type into 139bp + 130bp + 48bp, and it was cleaved once in the tilling mutant TIL_CS91285 into 269bp + 48bp.

5.5 Agrobacterium strain

Agrobacterium strain AGL1 was used for all transformations. The strain harbors Rifampicin (25 µg/ml) and Ampicillin/Carbenicillin (100 µg/ml) resistance markers.

AGL1 Genotype: AGL0 recA::bla pTiBo542(delta)T Mop+ CbR (Lazo, Stein et al. 1991)

5.5.1 Agrobacterium-mediated transformation of *Arabidopsis thaliana*

Plant transformation (floral dip) was done using *Agrobacterium tumefaciens* strain AGL-1 according to the standard protocol (Clough and Bent 1998). In brief, an Agrobacterium strain harboring the binary plasmid with the gene of interest was grown in selective LB medium at 28°C until OD₆₀₀ 0.8- 1

and resuspended to OD₆₀₀ 0.8 in 0,5x MS [1x MS: 325mM sorbitol, 2.5mM MES, pH 5.5, filter sterilized with 0.01% silwet L-77 (Lehle Seeds)]. Inflorescences were dipped for 30 seconds into the agrobacterium solution, subsequently covered with plastic bags to avoid loss of humidity and kept protected from light for 12 hours. The procedure was repeated after 10 to 14 days to increase the transformation rate.

5.5.2 Agrobacterium infiltration of *Arabidopsis thaliana*

Infiltration of young leaves on *Nicotiana benthamiana* plants was done using *tumefaciens* strains AGL-1 or LBA4404. Agrobacterium strains harboring the binary plasmid of interest were grown in selective LB medium at 28°C until OD₆₀₀ 0.8- 1 and resuspended in **infiltration medium** to OD₆₀₀ of 0.3. After infiltration plants were covered to avoid loss of humidity and kept protected from light for 12 hours. Expression of fluorescent proteins usually could be detected 36 to 48 hours after infiltration.

Infiltration medium: 10mM MgSO₄, 10mM MES, 150μM Acetosyringone

5.5.3 Genomic DNA isolation from *Arabidopsis*

Extraction Buffer:

chemical	final	ml	of stock	...if you prefer to weigh
Tris	200mM	20 ml	1M	2.423g
NaCl	250mM	25 ml	1M	1.461g
EDTA	25mM	5 ml	0.5M	0.9306g
SDS	0.5 %	2.5 ml	20%	0.5g

ad pH 8.8

water to the final volume of 100 ml

- macerate 20- 200mg leave material with tiny glass beads or with a micro pistil
- add 700μl Extraction Buffer
- vortex for 5'', centrifuge for 1' (18 000 rpm or maximum)
- transfer 600μl supernatant into a new 1,5 ml microcentrifuge tube
- add 600μl isopropanol, vortex briefly
- centrifuge 5' (max speed)
- discard supernatant, wash 2 times with EtOH (70% then 100%)
- dry pellet, dissolve in 100μl H₂O

5.5.4 Plant pre-treatment with proteasome inhibitor

Inflorescences of mature *Arabidopsis* plants were dipped into a solution containing 10μM estradiol, 100μM MG132, 5μM Epoxomicin (or an equal volume of the respective solvents ethanol and DMSO for mock-treated samples) and 0.01% silwet L-77 (Lehle seeds) six hours prior to protein extraction. Estradiol was used to induce expression of the proteasome activity reporter fusion protein DHFR-HA-ub-Arg-lacI-3HA-GUS (Garzon, Eifler et al. 2007) which allowed to monitor proteasome-mediated protein degradation.

5.5.5 Induction of plants with ethanol

Every second day plants were induced for 2- 3 hours. On plate (the plates sealed with Parafilm M): Plates were placed together with 50 ml 10% EtOH in an open beaker into a tightly sealable plastic box (ca. 28 x 18 x 16 cm). Induction on soil: 100 ml 10% EtOH were placed in an open beaker on the plant tray, which was then covered with an autoclave bag and sealed.

5.6 Histology

5.6.1 GUS staining

Plant samples were taken in the afternoon for GUS staining.

Fixation of fresh tissue in ice-cold 80% Acetone: vacuum- infiltration (length dependent on tissue), incubation for 60 min at -20°C. Tissue was rinsed twice in **100mM Sodium Phosphate Buffer pH 7.0**, then incubated in **GUS staining solution**, vacuum infiltrated for 10 min and incubated overnight in the dark at 37°C.

Fixation: Tissue was rinsed in **1x PIPES buffer pH 6.8**, subsequently incubated in ice-cold **Triple Fix** solution and vacuum infiltrated for 15 min. Triple fix solution was replaced, and the tissue was incubated in Triple fix for 24 hours at 4°C, protected from light.

Dehydration: Tissue was rinsed twice in 1x PIPES buffer pH 6.8 and subsequently dehydrated in an ethanol series, 30 min each, at 4°C: 10% ethanol - 30% ethanol - clearing solution (50% ethanol 50% acetic acid) – 70% ethanol

Paraffin embedding: Automatic wax infiltration was done with the Shandon Excelsior tissue processor (Thermo Electron Corporation, Thermo Fisher Scientific Inc.) Embedding was done by using the Paraffin embedding center Shandon Histo Centre 3 (Thermo Electron Corporation, Thermo Fisher Scientific Inc.).

100mM Sodium Phosphate Buffer pH 7.0: 100mM sodium phosphate buffer made from 200mM stock solutions of Na₂HPO₄ and NaH₂PO₄ according to standard protocols (Sambrook, Fritsch et al. 1989).

1x PIPES buffer: 100mM PIPES, 10mM EGTA, 2mM MgSO₄, pH 6.8 (KOH)

GUS staining solution: 50mM Sodium phosphate buffer pH 7.0, 2mM K₃(Fe(CN)₆) Potassium Ferricyanide, 2mM K₄(Fe(CN)₆) Potassium Ferrocyanide, 0.1% Triton-X-100, 20mM 5-bromo-4-chloro-3-indolyl-β-D-glucuronic acid (X-Gluc, Fermentas)

Triple Fix: 1.5% Glutaraldehyde, 1% Formaldehyde, 2% Acrolein, 0.05% Tween-20 in 1x PIPES buffer

5.7 Microscopy

5.7.1 Fluorescence microscopy

A Leica TCS-SP2 spectral confocal laser scanning microscope (Leica Microsystems, Heidelberg) and a Zeiss LSM 510 META Scanning microscope (Carl Zeiss AG) were used. Probes were used without preparation: fresh plant material was cut with a razor blade and placed onto a microscope slide, and a 10% glycerol solution was added between the specimen and the cover slip. The excitation wavelength was 476/488nm and 568nm (ArKr Laser, Leica) or 488nm and 561nm (Diode Laser, Zeiss) for GFP/YFP and RFP, respectively. Fluorescence was detected at 500- 520nm (GFP), 525-580 nm (YFP), and 610- 630nm (RFP). Chloroplast autofluorescence was detected at 680- 710nm. Multiple channels were always scanned sequentially to avoid false-positive signals caused by bleed-through.

5.7.2 Light microscopy

Microscopes used were a Leica MZ16 FA Fluorescence Stereomicroscope with a LeicaDFC300FX color camera and the Leica Application Suite Software or a Zeiss Zoom SteREO Discovery.V12 stereomicroscope or a ZEISS Axio Imager microscope. Pictures from Zeiss microscopes were documented with a Zeiss AxioCamMRc 5 Zeiss color camera and AxioVision software.

5.7.3 Scanning electron microscopy

Fresh tissue samples were snap-frozen in liquid nitrogen and with no further processing examined in a Hitachi TableTop-Mikroskop TM-1000. Pictures were recorded and processed with the associated TM-1000 software.

5.7.4 Digital Photography

Photos were acquired with a digital Olympus E-410 camera, objectives used were: Olympus Zuiko Digital (35mm 1:3.5 Macro, Ø 52) or Olympus Digital (14-42mm 1:3.5-5.6).

5.8 Software

For *in silico cloning* the plasmid editor **ApE** vs.1.17 by M. Wayne Davis was used, often in combination with the online tool The Sequence Manipulation Suite(Stothard 2000).

Genome annotation was done with **GBrowse-TAIR**. GBrowse is a web-based server application developed by the Generic Model Organism Database project (GMOD). <http://gmod.org>

Sequence alignments against Databases or pairwise alignments were done with the NCBI Basic Local Alignment Search Tool **BLAST** (<http://blast.ncbi.nlm.nih.gov>) (Altschul 1997) or with the EMBL Pairwise Sequence Alignment Tool (<http://www.ebi.ac.uk/Tools/psa/>), respectively.

For alignment of homologous proteins and **ClustalW2** at EBI was used (Larkin 2007, Goujon 2010) and phylogenetic tree display was done with **TREEVIEW** (Page 1996) and **Mesquite** (Maddison 2011).

For working with confocal microscope pictures **ImageJ** vs. 1.45i by Wayne Rasband with the LOCI Bio-formats plugin by Curtis Rueden and Melissa Linkert was used. For pictures acquired by the Zeiss confocal microscope also the **LSM Image Browser** was used.

The ImageJ software gel quantification analysis tool was used for quantification Western blot signals.

6 Appendix A: RNA *in situ* hybridization lab protocol

I want to dedicate this detailed protocol, the heritage of the great researchers named below and probably of others more, to the scientific community, and I hope it can help others to establish this technique in their labs easily.

This protocol is optimized for *Arabidopsis* shoot tissue; it is based on the protocols of David Jackson²⁹, the EMBO course, Jeff Long, the Bowman lab and the Kidner & Timmermans protocol³⁰. This manual was written and applied for the RNA *in situ* hybridization experiments in the work for this thesis under the guidance of Alexander Goldshmidt and David Jackson in the CSHL, New York, 2009.

RNase considerations:

Most critical steps:

- sample fixation
- sectioning
- incubation with probes

Less critical:

- after hybridization of probe

Work as clean as possible:

- dedicate workspace to RNA work only, clean with soap and ethanol
- change gloves often
- use DEPC- treated water (100µl in 1l, stir o/n, autoclave)
- bake glassware for 2 hours at 150°C
- soak plastic ware in 0,2N NaOH, rinse with DEPC-H₂O to neutralize
- if experiment will be repeated: dedicate one plastic container for each solution, store RNase-free (i.e. in a specially dedicated place)
- for solutions, dishwashed glass bottles will be fine, but prefer baked glass wherever possible
- you can measure liquid amounts in falcon tubes

- pH adjustments with Lackmus paper rather than pH-meter
- pipettes dedicated to RNA work, RNase- free tips
- use chemicals specially dedicated to RNA work (or freshly opened containers)

Probe preparation

Material:

1. PCR reagents
2. Agarose gel
3. PCR purification kit
4. Ambion T7 Megascript kit³¹
5. Roche Digoxigenin-11-uridine-5'-triphosphate (Cat# 11209256910, 250nmol (10mM, 25µl) 227.50€)
6. 50 ml 2X Carbonate Buffer (80mM NaHCO₃, 120mM Na₂CO₃)
prepare with DEPC water, store aliquoted into 1.5ml tubes at -20°C
7. 50ml 10% acetic acid (= stop solution)
8. 100ml 3M NaOAc, pH5.2 or 4M LiCl, store aliquoted into 1.5ml tubes at -20°C
9. 100 mg/mL of transfer RNA (tRNA)(Roche; cat. no. 109541).
dilute to 20mg/ml, store aliquoted at -20°C
10. deionized formamide (Sigma F9037, store at 4°C)

Probe design

split gene of interest into ~500nt regions
include UTRs (UTR only can sometimes give better signal than coding region)
probes covering different regions can be mixed
avoid conserved regions (BLAST check)

for PCR- generated probes:

order primers including T7 RNA pol site:

5' **TAATACGACTCACTATA**GGG – gene specific sequence

sense probe (= neg. control): T7-5'gene3'gene

antisense probe (= probe): 5'gene3'-T7

Template production

PCR (2x 100µl)

gel purify PCR product (check 1µl on gel, Nanodrop for concentration)

²⁹ Jackson, D. (1991) *In situ* hybridization in plants. In: *Molecular Plant Pathology: A Practical Approach* (Bowles, D. J., Gurr, S. J., and McPherson, M., eds.), Oxford University Press, Oxford, pp. 163–174.

adaptation for non-radiolabeled probes:

Coen, E. S., J. M. Romero, et al. (1990). "floricaula: a homeotic gene required for flower development in *antirrhinum majus*." *Cell* **63**(6): 1311-22.

³⁰ "Hybridization as a Tool to Study the Role of MicroRNAs in Plant Development" by Catherine Kidner and Marja Timmermans in: *MicroRNA Protocols, Methods in Molecular Biology*, 2006, Volume 342, 159-179, DOI: 10.1385/1-59745-123-1:159

³¹ alternatively use Roche DIG-labeling kit or : Digoxigenin (DIG) RNA-labeling kit (Roche, Indianapolis, IN; cat. no. 1-175-025).

RNasin or RNase-out

T7 RNA polymerase, Roche

RNase-free deoxyribonuclease (DNase) (RQ1) (Promega, Madison, WI; cat. no. M610A).

Labeling reaction version A (modified from Ambion kit manual):

- Heat DNA template at 55°C for 2- 3 minutes, put on ice.
- Thaw reaction components; if buffer is thawed, keep at room temperature.
- Assemble reaction at RT (because Spermidine in reaction buffer would precipitate DNA on ice)

200ng	PCR
1µl	ATP
1µl	CTP
1µl	GTP
UTP/Dig-UTP	50/50
1µl	buffer
1µl	enzyme mix
total: 10µl	

- in parallel, dilute PCR product to the same conc. as used in the reaction; this will be the loading control on the agarose gel the next day
- incubate overnight at 37°C
- next day: add 0.5µl Turbo DNase (from kit)
- incubate 15min at 37°C
- add 20µl DEPC water (add 20µl DEPC water to DNA control)
- load 1µl on 2% TBE agarose gel (RNase-free) to check reaction efficiency next to each transcription reaction load same amount of template DNA as used in the reaction (i.e. 200ng PCR prod. in 30µl H₂O)
- Compare size: RNA should run a little smaller on gel.
- Compare band intensity of DNA vs. RNA, RNA should be stronger.

Carbonate Hydrolysis

calculate time for hydrolysis:

$$T = (Li - Lf) / (K \times Li \times Lf)$$

T... time in min
Li... initial length in kb
Lf... final length in kb
K... 0.11kb/min

e.g.: 1.5kb probe $t = (1.5 - 0.15) / (0.11 \times 1.5 \times 0.15) = 54.5$ min

NaOAc precipitation (Timmermanns)

1. adjust volume of RNA to 100µl with DEPC H₂O
2. add 100µl 2x Carbonate Buffer
3. incubate at 60°C for the calculated time
4. stop reaction by neutralizing with 10µl 10% acetic acid
5. precipitate RNA
 - a. add 1µl 100mg/ml tRNA
 - b. add with 1/10 vol 3M NaOAc (Ph 5.2) + 2 vol EtOH o/n at -20°C
 - c. centrifuge 30min at 4°C
 - d. wash pellet with 70% EtOH
6. resuspend RNA in 50% deionized formamide to a final concentration of 50ng/kb/µl

Most probes are used at a final concentration of 0.5ng/kb/µl probe complexity, so this gives a 100X stock for making up the hybridization solution.

Hybridizations are performed with 100µl per slide. Thus, if a probe is 0.5-kb long, the probe should be resuspended at a concentration of 25ng/µL (50ng ↔ 1µL ↔ 0.5kb) to obtain a 100x stock. If the probe is 1-kb long, 50ng/µL probe will make a 100X stock. Probes can be stored for months at -80°C, allowing the same probe to be used as a control in different experiments.

Probe Labeling reaction version B (David Jackson using Roche materials):

1. prepare 5x nucleotide stock:
each unlabeled nucleotide is 100mM, DIG-UTP is 10mM

ATP	1.25µl
GTP	1.25µl
CTP	1.25µl
UTP	0.625µl
DIG-UTP	6.25µl
DEPC-H ₂ O	39.375µl
	50.0µl

store in aliquots at -20°C

2. DNA template, use per reaction:
1µg linearized plasmid or
200ng purified PCR product

- heat template 2- 3 min at 55°C
- put on ice
- assemble:

10x buffer (Roche)	2.5µl
5x nuc + DIG-UTP	5µl
RNase out	0.7µl
T7 pol	0.5µl
DNA (1µg)	x µl
DEPC-H ₂ O	to 25µl

- 3- 5 hours 37°C
- then + 0.5µl T7 pol
- leave o/n at 37°C

3. DNase digest: add 1µl DNase
 incubate 60 min @ 37°C

4. check 1µl on gel (control: diluted DNA, see above)

5. Carbonate hydrolysis
add 25µl 2x Carbonate buffer
incubate 40 min at 65°C (or calculate and incubate at 60°C as described below)

if no carbonate hydrolysis is done, add 25 µl DEPC-H₂O

6. precipitate RNA
add 2.5µl stop solution
add 10µl 4M LiCl
add 5µl tRNA (20 mg/ml)
add 30µl EtOH
mix and freeze at -20°C for at least 15 min
spin 20min @ 4°C
wash pellet with 70% EtOH
resuspend in 100µl 50% deionized formamide

Fixation:

Material:

1. ice
2. 15ml falcon tubes or 20ml disposable glass scintillation vials
3. 10x PBS, autoclave
4. 2N NaOH
5. fixative (prepare fixative fresh each day)
4% Paraformaldehyde (Sigma 6148) in phosphate buffered saline (PBS)
you may add: DMSO up to 4%
Triton-X 100 up to 0.3%
Tween-20 up to 0.1%

1. prepare 10x PBS
use DEPC-treated water.
Prepare 10x PBS

10x PBS	1x PBS		mw	ad 1 l
1.3M	130mM	NaCl	58.44	76 g
70mM	7mM	Na2HPO4	141.96	9.937g
30mM	3mM	NaH2PO4	119.98	3.6g
		NaH2PO4 x H2O	137.99	4.13g

pH should be 7.0. If necessary, the pH can be adjusted with H3PO4 or NaOH. Check the pH with pH paper.

autoclave.

2. prepare fixative: 4% formaldehyde in PBS
dilute 10x PBS to 1x
adjust pH to 11 with NaOH (2N, few drops for 100ml, ~2 pellets for 500ml)
heat to ~60°C in microwave
under chemical fume hood:
add PFA³², mix, cool to RT
adjust pH back to 7 with H2SO4³³ conc. (1 droplet for 100ml)
add DMSO (up to 4%), Triton-X (up to 0,3%)
and/or Tween-20 (up to 0,1%)

Fixation

1. Harvest samples and place quickly into cold fixative in 15ml falcon tubes or scintillation vials. If dissection is required, do this in fixative on ice. Use ~10ml fixative for 10- 15 seedlings, or 10 Arabidopsis apices.
2. Vacuum infiltrate tissues: Tissue should be cooled during vacuum (on ice or at 4°C). Formaldehyde fumes are released, so apply vacuum under chemical fume hood. Tissue should be fully submerged (use grid if necessary). Apply vacuum (25mm Hg) 10min, release carefully, repeat until tissue sinks.

32 PFA (polymer, solid) is converted to FA (COH2 monomer, gas) during this procedure; weigh PFA like that: put in falcon tube under hood, weigh, repeat if necessary

33 no HCl: releases highly toxic fumes

3. Replace fixative with a large excess of fresh fixative (fill entire tube), incubate gently shaking at 4°C overnight.

Embedding

Material:

1. 1x PBS, cold
 2. 100% EtOH, cold
 3. DEPC water for EtOH gradient (30%- 100%, pre- cool solutions)
 4. (1 L 8.5% NaCl.)
 5. Eosin Y (Sigma E-4382)
 6. HistoClear (National Diagnostics, Atlanta, GA; cat. no. HS-200).
 7. Tissuepath paraplast X-tra (Fisher, Pittsburg, PA; cat. no. 23-021-401).
- Paraplast contains plastic polymers and DMSO that shall facilitate infiltration and sectioning. These additives are unstable at temperatures higher than 62°C. Therefore wax should be freshly melted before use, in an oven at 58°C to 60°C. This might take several hours. However, prolonged heating above 60°C should be avoided.
8. Base moulds (EMS, Fort Washington, PA; cat. no. 62352-15 or Richard Allan Scientific, 15x15mm Cat# 58950).
 9. Embedding rings (Fisher; cat. no. 22-038-197).
 10. tweezers, spirit lamp, peanut butter cups (aluminum) or weighing boats

Embedding procedure

pre- cool solutions.

all steps are performed at 4°C with gentle agitation.
0.85% NaCl can be added to this EtOH series to avoid excessive swelling and shrinking of the tissue.
eosin may be added to better visualize the samples.

day 1:

1. 30 min 1x PBS
2. 30 min 1x PBS
3. 60 min 30% EtOH
4. 60 min 40% EtOH
5. 60 min 50% EtOH
6. 60 min 60% EtOH
7. 60 min 70% EtOH

----- samples may be stored in 70% EtOH for several months at 4°C -----

8. 60 min 85% EtOH
9. overnight 95% EtOH + eosin

day 2:

move tissues to glass vials if falcon tubes were used before

all steps are done at room temperature with gentle³⁴ agitation

1. 30 min 100% EtOH + eosin
2. 30 min 100% EtOH + eosin
3. 60 min 100% EtOH + eosin

³⁴ tissue gets brisk during treatment

4. 60 min 100% EtOH + eosin
----- work in the hood with HistoClear -----
5. 60 min 1 vol HistoClear : 2 vol EtOH
6. 60 min 2 vol HistoClear : 1 vol EtOH
7. 60 min 100% HistoClear
8. 60 min 100% HistoClear
9. overnight 100% HistoClear + ½ vol
paraplast chips

prepare RNase-free bake glass beaker for the wax
(caution: beaker will never be clean again afterwards)

day 4:

Keep in mind that wax solidifies fast at RT, so keep samples warm if wax should remain liquid: use heated Put Paraplast chips in RNase-free beaker and incubate at 60°C to melt wax; constantly add wax as you use it up during the following steps.

1. place vials to 56°C- 60° until paraplast chips melt (ca 60 min)
2. replace wax/HistoClear solution (in the hood) with freshly melted wax
3. change wax in the evening, incubate overnight at 60°C

day 5:

1. replace wax in the morning
2. replace wax in the evening

day 6:

1. replace wax in the morning
2. pre-warm desiccator to 60°C before second wax change
3. replace wax in the afternoon
4. vacuum-treat samples to prevent air bubbles between tissues:
in pre-heated desiccator, pull vacuum for 5 min, incubate (with vacuum) in desiccator 60 min at 60°C
5. place tissue in molds:
prepare working space with
 - melted wax
 - hotplate
 - spirit lamp (to pre-warm tweezers)
 - tweezers
 - aluminum pie dishes or weighing boats
 - embedding rings
 - embedding molds

Pour sample in weighing boats on hotplate, put embedding rings on molds, fill to the top with wax, place single tissues into embedding rings, tissue should be placed to the bottom, arrange for sectioning

Alternatively, leave bulk of samples in weighing boats or pie cups, arrange so that they can be separately be removed from the block later. Still take care of orientation as good as possible – this will simplify steps afterwards greatly.

allow to cool slowly at RT (1/2 day)
put to 4°C before sectioning
store in plastic bags at 4°C for 1 year or longer

Sectioning

* RNase-sensitive*

Material:

1. Probe-on-plus slides (Fisher; cat. no. 15-188-52).
2. 0.2 N NaOH.

Sectioning can be tricky in very dry conditions, in which case static becomes a problem, or in warmer temperatures, in which case the ribbon may buckle in the heat. The wax blocks can be sectioned from cold and grounding the microtome with a wire sometimes helps to reduce static electricity. Slides used are Probe-On Plus from Fisher Biotechnology. They are pre- cleaned and charged. They also have a white paint label that provides a capillary space when two slides are sandwiched together.

1. Pre- warm the slide warmer to 42°C. Clean the microtome and slide warmer by wiping with 0.2M NaOH. Lay clean filter paper next to the microtome on which to place the wax ribbons.
2. Trim the block into a trapezoid shape, leaving approx 2 mm of wax around the plant tissue. Place the block into the microtome such that the longer of the two parallel faces is at the bottom. Cut through the region of interest. Sections 8- to 10-µm thick are reasonable, depending on the size of the cells in the tissue. The sections should make long wax ribbons.
3. Place a Probe-On Plus slide on the slide warmer and apply several drops of DEPC-treated water. Slides can be marked with pencil, because pencil marks will not dissolve in later EtOH incubations.
4. Float the wax ribbon on the water, shiny side down (the bottom side as the ribbon comes off of the microtome). Let the ribbon warm for approximately a minute to allow it to flatten out completely.
5. Before the edges of the wax contact the warm slide, tip off the water carefully but in one smooth movement, so the ribbon is lowered down onto the slide. Hold the slide upright and use a twist of tissue to drain off any excess water from the edge of the ribbon.
6. Leave the slides at a slight angle on the slide warmer at 42°C overnight so that the tissue adheres. Sectioned tissue can be stored in a box with silica desiccant for several weeks at 4°C.

In Situ Hybridization

* RNase-sensitive*

Material:

The following general stock solutions should be prepared. Again, all solutions are prepared using RNase-free chemicals and DEPC-treated dH₂O. In addition, approximately 12 L of DEPC-treated dH₂O is needed, part of it in 1-L RNase-free bottles for diluting stock solutions.

- 1 L of 10X PBS, pH 7.0., see table above
- 500 mL 0.5 M EDTA, pH 8.0
(EDTA x2H₂O mw: 372.24 --> 93.06 g/500ml, add 10g NaOH pellets or more until dissolved, adjust the pH with NaOH).
- 1 L of 1 M Tris-HCl solution,
 - pH 9.5
 - pH 8.0
 - pH 7.5

(Tris base mw: 121.14 --> 121.14 g/l, adjust the pH with concentrated HCl, check with pH paper)

Tris-HCl contains an amino group, which inactivates DEPC, so it is best made up with Tris base powder from a dedicated clean stock and dissolved in DEPC-treated water.

- 500 ml of 5 M NaCl
(NaCl mw: 58.44 -> 146.105g/500ml)
- 500 ml of 1M NaH₂PO₄
(NaH₂PO₄xH₂O mw: 137.99 --> 68.995g/500ml)
- 500 ml of 1M Na₂HPO₄
(Na₂HPO₄ mw: 141.96 --> 70.98g/500ml)
- 1 M Phosphate buffer, pH 6.8.

51ml	1M NaH ₂ PO ₄
49mL	1M Na ₂ HPO ₄
100mL	DEPC dH ₂ O

- 500ml of 1 M MgCl₂
(MgCl₂ x 6H₂O mw: 203.3 --> 101.65g/500ml)
- 20x SSC

20x SSC		mw	ad 1 l
3M	NaCl	58.44	175.32g
300mM	Na ₃ Citrate x 2H ₂ O	294.19	88.23g

Stir bars, spatulas, and glass measuring cylinders baked at 250°C overnight.

Plastic disposable pipettes, individually wrapped.

Disposable plastic Pasteur pipettes.

Section Pretreatment and Hybridization

Material :

before you start, see also section timing!

- slide rack
- 21 containers (250 ml) for slide rack
- 2 flat tightly sealing Tupperware containers (for hybridization of slide sandwiches and antibody incubation)
- saran wrap
- magnetic stirrer in fume hood
- Histoclear

- 1l 100% ethanol
- 250 ml 1x PBS
- 100 ml 20x SSC
- 40 mg/ml pronase (Sigma type XIV)
Dissolved in water and predigested to remove nucleases by incubating at 37°C for 4 h.
Aliquots (1 ml) are stored at -20°C or -80°C.
Alternatively: 10 mg/ml proteinase K. Proteinase K does not need to be predigested.
- 10x pronase buffer
 - 0.5M Tris Cl pH 7.5 (100ml 1M)
 - 0.05M EDTA (20ml 0.5M)
 - 80ml H₂O
- 250 ml 2mg/ml glycine in PBS (fresh)
0.5g glycine in 250 ml PBS
(you can prepare 10x stock and store at -20°C)
- 4% paraformaldehyde in PBS, made fresh, as detailed in section "Fixation"
- triethanolamine (Sigma T1377) store at RT
- acetic anhydride (Sigma A6404) store dry at RT
- HCl
- 10x in situ salts (store at RT or for convenience together with 50% Dex & 50x Den & tRNA at -20°C)

from stock solutions		
3M	NaCl	30ml 5M
0.1M	Tris pH 8	5ml 1M
0.1M	NaPhosphate pH 6.8	5ml 1M
50mM	EDTA	5ml 0.5M
	DEPC H ₂ O	5ml

- 40 ml 50% dextrane sulfate (mw > 500.000) Sigma D8906-5G
heat to 80°C to dissolve,
store in aliquots at -20°C
- 50x Denhardt's reagent Sigma D2532³⁵
store in aliquots at -20°C
- yeast tRNA (20µg/ml) Roche 109541
- 50% deionized formamide
- formamide (not deionized)

Timing

prepare before you start:

prepare 80°C water bath for probe denaturation
prepare 53°C oven (constant temperature for hybridization)
prepare 37°C incubator for pronase treatment

put on ice to thaw:

- pronase stock
- 10x in situ salts
- 50% deionized formamide
- 50% dextrane sulfate
- 50x Denhardt's reagent
- yeast tRNA (20µg/ml)

prepare containers with 250 ml each:

2x	Histoclear
1x	100% EtOH (A)
1x	100% EtOH (B)
1x	95% EtOH

³⁵ or self-made: 1% Ficoll, 1% Polyvinylporrolidone, 1% BSA, DEPC H₂O to 25 ml, filter sterilize

1x 85% EtOH
 1x 80% EtOH
 1x 70% EtOH
 1x 50% EtOH
 1x 30% EtOH
 1x DEPC-H₂O
 1x PBS (A)
 1x PBS (B)
 1x 1x Pronase buffer, pre-warm to 37°C
 1x 2 mg/ml glycine in PBS
 1x 4% formaldehyde: pH → heat →
 dissolve → put on ice
 1x Triethanolamine box with stir bar

start re-hydration and continue
 during pronase step adjust pH of 4% formaldehyde to 7
 during PBS steps after formaldehyde treatment prepare
 0.1 M triethanolamine-HCl, pH 8.0
 whenever you feel bored

- label tubes for probe denaturation, prepare
1.25 µl probe in 48.75 µl 50% deionized
formamide
- prepare master mix of hybridization solution (=
hyb sol w/o probe) can also be stored at -20°C)
- prepare humid chamber for hybridization
(paper towel wetted with 2x SSC 50%
formamide (not deionized) elevated with
disposable pipettes

Section Pretreatment

label slides with pencil: tissue & probe
 put in rack
 de-paraffinize and re-hydration:

at RT:

2x	10 min	Histoclear
2x	2 min	100% EtOH (A, then B;
discard A and replace with fresh EtOH)		
1x	30 sec	95% EtOH
1x	30 sec	85% EtOH
1x	30 sec	80% EtOH
1x	30 sec	70% EtOH
1x	30 sec	50% EtOH
1x	30 sec	30% EtOH
1x	30 sec	DEPC-H ₂ O
2x	15- 20 min	PBS (A, then B)

at 37°C:

30min Pronase treatment
 add pronase directly before slides to pre-
 warmed buffer
 781 µl of 40 mg/ml stock in 250 ml buffer →
 final 0.125 mg/ml
 timing: adjust pH of FA

at RT:

1x 2 min glycine (2 mg/ml) in PBS (to stop pronase)
 2x 5 min PBS

in hood:

1x 10 min 4% formaldehyde: pH → heat → dissolve → put
 on ice
 2x 5 min PBS

*timing: prepare 0.1M triethanolamine-HCl pH
 8.0 while stirring in hood:

245.75	ml	DEPC H ₂ O
3.25	ml	Triethanolamine
		(viscous!)
1.0	ml	HCl conc.

1x 10 min Acetic Anhydride (not stable
 in water):
 immediately before you out rack into
 solution add 1.3 ml acetic anhydride to
 triethanolamine pH 8.0, mix well,
 insert slide rack, continue stirring slowly (do not
 crash slides)

at RT (bench):

2x	5 min	PBS
1x	2 min	30% EtOH
1x	2 min	70% EtOH
1x	2 min	80% EtOH
1x	2 min	85% EtOH
1x	2 min	95% EtOH
2x	2 min	100% EtOH

dry slides completely at RT on paper towel, protected
 from RNases

if you need more time: store slides in container with
 100% EtOH on bottom for several hours at 4°C.

Hybridization

prepare mastermix
 solution is very viscous due to dextran sulfate, warm to
 mix better

	1x	5x
10x in situ salts	25 µl	125
deionized formamide	100 µl	500
50% dextran sulfate	50 µl	250
50x Denhardt's	5 µl	25
20 µg/ml yeast tRNA	12.5 µl	62.5
DEPC-H ₂ O	7.5 µl	37.5
total	200 µl	400

prepare probe:

48.75 µl 50% deionized formamide
 1.25 µl probe

 50 µl

- mix,
- incubate 2 min at 80°C
- immediately put on ice
- spin down to collect at bottom when cold
- keep on ice
- add 200 µl master mix to 50 µl denatured
probe
- mix
- put onto slide
- sandwich 2 slides carefully together (no air
bubbles)

be careful not to cross-“contaminate” slides with
 different probes:

- change gloves between probes

- keep sandwiches well separated
- incubate overnight (at least 16 hours) at 53°C (50°C to 55°C possible, but keep temperature you chose constant) in humid chamber elevated over towel wetted with 50% formamide in 2x SSC, keep aerosol-tight: use Tupperware for humid chamber, seal additionally with saran wrap between lid and container
- prepare 1.5 l 0.2x SSC, put to 55°C for next day

Post Hybridization treatment

no RNase worries anymore

Material:

1. 55°C shaking water bath
2. magnetic stir, 2 stir bars
3. microwave
4. plastic containers for wash:
 - a. 1 that holds 600 ml,
 - b. smaller flat ones for wash steps (can also be pipette tip container boxes, one holds 4 slides)
 - c. sealable Tupperware for antibody treatment
5. 1% Boehringer blocking reagent (or Roche 1096176 in TBS)
6. BSA (Sigma A7096)
7. 1M Tris pH 7.5
8. 1M Tris pH 9.5
9. 5M NaCl
10. 10N NaOH
11. HCl
12. Triton-X
13. 1M MgCl
14. Anti-DIG-AP Fab fragments (Roche 1093274) NBT/BCIP (Nitroblue tetrazolium plus bromochloroindolyl phosphate) mix Roche 1681451
15. Cysoseal (EMS 18006).

Solutions

prepare fresh

1. at least 1 hour before needed prepare 1% Boehringer blocking solution:

100 mM Tris pH 7.5	20ml (1M)
150 mM NaCl	6ml (5M)
1% Boehringer block	2g
H2O	ad 200ml

heat 1.5 min in microwave
stir until completely dissolved (remains cloudy)
if particles remain: add 10N NaOH until dissolved, re- adjust pH to 7.5 with HCl
cool to RT

2. BSA block solution:

100 mM Tris pH 7.5	30ml (1M)
150 mM NaCl	9ml (5M)
1% BSA	3g

0.3% Triton-X	900µl
H2O	ad 300ml

3. Anti-Dig Antibody:
1:1250 in BSA block solution (4 µl /5 ml)

4. for detection:

100mM Tris pH 9.5	10ml (1M)
100 mM NaCl	2ml (5M)
50 mM MgCl2	5ml (1M)
H2O	ad 100ml

5. 1x TE to stop reaction

10X TE:

100mM Tris pH 7.5 10ml (1M)
10mM EDTA pH 8.0 2ml (0.5 M)
H2O ad 100ml

Procedure

- set water bath to 55°C
- disassemble slide sandwiches in 300ml 0.2x SSC pre-warmed to 55°C:
- as soon as sandwich encounters the liquid it will start to disassemble
- (manipulate slides with clean gloves)
- put slides into rack
- put rack into fresh container with 600ml 0.2x SSC pre-warmed to 55°C
- incubate 60 min in shaking water bath at 55°C
- change 0.2x SSC (600ml pre-warmed)
- incubate 60 min in shaking water bath at 55°C

5 min at RT with 1x PBS (can be stored o/n at 4°C in PBS)

transfer slides into flat container tissue facing up to minimize volume of liquids used, incubate shaking at RT

45 min 200 ml 1% Boehringer block
45 min 50 ml 1% BSA

pour 5 ml diluted anti-DIG antibody into weighing dish
dry slides briefly on paper towel
re-assemble slide sandwiches by putting 2 slides together in weighing dish, allowing capillary forces to pull up antibody solution between slides; avoid bubbles

incubate 2 hours at RT in humid chamber (paper towel soaked with water on bottom)

- disassemble sandwich
- drain slides on paper towel
- wash 4x 15 min in 50ml 1% BSA blocking solution, rocking
- rinse 1x with Tris/NaCl/MgCl2
- 10 min incubation in Tris/NaCl/MgCl2

prepare substrate solution (very light sensitive and also toxic) immediately before using:

100µl NBT/BCIP into 5 ml Tris/NaCl/MgCl2

- re-assemble sandwiches as described for anti-dig antibody by dipping into substrate solution,
- incubate in humid box in complete darkness for 1- 3 days

- stop reaction by draining slides on paper and rinsing slides in 1x TE,
- wash with H₂O
- dry slides completely
- mount using 12 drops of Cytoseal
- store slides at RT

7 Appendix B – Protein Sequences used for alignment

7.1 Species relation of MPB2C homologs

Species	Classification
<i>Arabidopsis thaliana</i>	Tracheophyta-Angiosperms-Eudicots-Rosids-Eurosids II-Brassicales- Brassicaceae
<i>Arabidopsis lyrata</i>	Tracheophyta-Angiosperms-Eudicots-Rosids-Eurosids II-Brassicales- Brassicaceae
<i>Populus trichocarpa</i>	Tracheophyta-Angiosperms-Eudicots-Rosids-Eurosids I-Malpighiales-Salicaceae
<i>Ricinus communis</i>	Tracheophyta-Angiosperms-Eudicots-Rosids-Eurosids I-Malpighiales-Euphorbiceae
<i>Glycine max</i>	Tracheophyta-Angiosperms-Eudicots-Rosids-Eurosids I-Fabales-Fabaceae
<i>Vitis vinifera</i>	Tracheophyta-Angiosperms-Eudicots-Rosids-Vitales-Vitaceae
<i>Nicotiana benthamiana</i>	Tracheophyta-Angiosperms-Eudicots-Asterids-Solanales-Solanaceae
<i>Nicotiana tabacum</i>	Tracheophyta-Angiosperms-Eudicots-Asterids-Solanales-Solanaceae
<i>Hordeum vulgare</i>	Tracheophyta-Angiosperms-Monocots-Commelinids-Poales-Poaceae
<i>Oryza sativa</i>	Tracheophyta-Angiosperms-Monocots-Commelinids-Poales-Poaceae
<i>Sorghum bicolor</i>	Tracheophyta-Angiosperms-Monocots-Commelinids-Poales-Poaceae
<i>Zea mays</i>	Tracheophyta-Angiosperms-Monocots-Commelinids-Poales-Poaceae
<i>Picea glauca</i>	Tracheophyta-Gymnosperms-Pinophyta-Pinales-Pinaceae
<i>Picea sitchensis</i>	Tracheophyta-Gymnosperms-Pinophyta-Pinales-Pinaceae
<i>Selaginella moellendorffii</i>	Tracheophyta-Lycopodiophyta-Selaginellales- Selaginellaceae
<i>Physcomitrella patens</i>	Bryophytes-Bryopsida-Funariales-Funariaceae

7.2 Protein Sequences used for Alignment:

Sequences were retrieved from a BLAST search with AtMPB2C (first sequence) as input

>Arabidopsis_thaliana_NP_196429.1

MYEQQQHFMDLQSDSGFGDDSSWLAGDDDLRLSPHQSAAGTNSGNNLDRRLKDLVEMVPLIEHYMEHKERSSSFRRGSMIYTKMPSKE
SLSRGRNASQTPGRKKRDQEGNDDVMNNSREDENAKALAGAEKEEMSRLREQVNDLQTKLSEKEEVLKSMEMSKNQVNEIQEKLEAT
NRLVAEKDMLIKSMQLQLSDTKIKLADKQAALKTQWEAKTTGTRAIKLQEQLDAVEGDISTFTRVFETLAKTDSKKPDRDYDAVPYEFDHLPYL
DDVDETDLRKMEEARLAYVAAVNTAKEREDEESLVMAAQARAYLQSLAFTY

>Arabidopsis_lyrata_XP_002873341.1

MYEQQQHFMDLQSDSGFGDDSSWLAGDDDLRLSPHQSAAGTNSGNNLDRRLKDLVEMVPLIEHYMEHKERSSSFRRGSMIYTKMPSKE
SLSRGRNASQTPGRKKRDQEGNDDVMNNSREDGENATLSGAEKEELSRLREQVNDLQTKLFEKEEVLKSMEMSKNQVNDIQEKLEATN
RLVAEKEMLIKSMQLQLSDTKIKLADKQAALKTQWEAKTTGTRAIKLQEQLDAVQGDISTFTRVFETLAKTDSKKPDRDYDATPYEFDHLPYLD
DDETDLRKIEEARLAYVAAVTTAKERENEESLAMAQARAYLQSLAFT

>Populus_trichocarpa_XP_002305296.1

MYEAQRFVDLQQNSSNGDPKSWLSEDSNSNSPHTHPNHSQLASSAGGNVDRVLFNDLVEMVPLVQSLIDRKVSTSFTRRGSVIYTKTPSRE
SLSKKIDPRGRNTCQSIPTKKKMDHGDQKGTANDNQDADSFALSSRAVPTGKDAEELIALREQVEDLQRKLEKDELLKSAEVSQNM
NAVHAEFDEVKLQVAEKDSLKSTQLQLSNAKIKLADKQAALKEKLQWEAMTSNQKVETLQQLDSIQGGISSFMLVFENLTNNIPYAEYDIK
PCYLDQLPIDDLDDREMQMEEAREYIAAVASAKEKQDEKSIAAASARLHLQSFVF

>Ricinus_communis_XP_002514605.1

MYDPNQHFVDLQENSSFGDTKSWLLDDDDKNNNSPTLRLTHSNSASTAGTTGNIDPVLNNIVEMVPLIESLIHRKGNSSFTRRGSMIYTKTP
SRDSLYKKMTDPKGRNASQSIPTKKKKEHGDKDRGSGGNNQSDNFSIFSSRLASEKDIEELVTLREQVEDLQRKLAEKDELLKSAEISKQNM
NDVHGKLDLKHQAAEKDSLKSIQLQLSDAKIKLADKQAALKEIRWEAMTSNTKVEKLQEELDSKQGDISSMMLLFEGLTNESTKIAEDYDVNP
RYLDYLPIDDDMDIEMQEMEEARQAYIAAVATAKEKQDEESIAAASARLHLQSFVLRNAGNAGNVYLNNGGVSPSYRAYVH

>Vitis_vinifera_XP_002273093.1

MFEPQHFMDLHDNSSLGDPKSWLSGDDNSSIPIHRTQSSLSSASAAGTAANVDRLLFNDLVEIVPLVQSLIDRKASSSFTRVGAVTYTKTPSRE
SLSRFSELKGRNTAQSIPTKKRRDHGEKQGRNGSNNQDGCADGFSLFSSRAVASEKDEELIALREQVEDLQRKLAEKDELLKSAEISKQMS
AVHDKLDLQQAQAEKDSLKSTQLQLSDAKIKLADKQAALKEIQWEAMTSNRKVEKLQEDLESMQADISSFMLLFEGLTKNDSTIRSESYDTP
YHLGHLPPIDDLDEIGAQKMEEARLAYVAAVAAAKENQDEESIALAANSRLHLQSFVFKNNHMDVSRASPDVRIAGAPVGAVAH

>Nicotiana_benthamiana_ABB97536.1

MYEAQQLLDLQDNNNGFGGGADSRWSLGEDRSPTLRRTDSSLSNSAAGNVDRMLFNDLVEIVPLVQSLIDRKTKSSFSRRGSMTYTKTPPKE
SLYKKTSEAKGRNAAQSTATKKHRGQNKNVGSNQDGCTENFMISSRSPLEKDREELMALREQVEDLHKKLSEKDELLKEVEIAKNEMASICA
KLDEMCKEYAEKDSLLKSTQVQLSDAKVILADKQAAVEKLEWEAMTSSKKVDKLQNDLDVVRQEIAWFMQFVQKLTNGSRALAEYDAIPY
LCDKNLETDHPNKTGMQELEMAREAYLAAIAAAKENQDEASFSAAAKARLYLQSLVLRT

>Nicotiana_tabacum_AF326729_1

MALAFDNGGTDPSCWLSHENEISRTDSSLSNNVDPLLFNDLVQIVPLVQSLIDRKEKSSFTRRGSMTYTKMPSRESLYKKTSEVKGRNAGQSTA
TKKHRDQKNVSSSQDGYAENFSTPSSTSSLTEKDREELMTLREKVEDLQKKLLEKDELLKEAEILKNEITATNAELDEMKKDISEKDFLVKTTQV
QLSDALVKLADKKAAVEKLEWEAMTSSKKVERLQEDLDLLQGEISSFIQFVHALTGNDSDSAEECNVIPYPWDQNVEIDKLNEDLQKMEAA
REAYIAAVAAAKENPDEASLSAASTARSYLQSLVLRT

>Zea_mays_ACG39104.1

MHDRSHKPQPAEAGNGGPAGEGGGGNVDRVLFKNLVMVPLVESLMDRRVNPAYSRRASLVYTPAPPKASDLKSVKLPQSVSAKKRRDPG
DIAKSTPDSNGDNGSVVPLSLGAENMPKDEVAVLSEQINDLQKKLLEKEEALRSAESSVTEMNAAAYATIDELRRLVADKEALIRSTNSQLHDA
KIMLADKQASLEKLEWEVKMSNKKVEDLQGDMSNMGFEISLMVFFEKISENVSGDSYDDIIPSSYELETQSMSEIDKIEVDKDKERVYAEA
LAAARENPDDEHLNIAAEARSRLQVLVL

>Sorghum_bicolor_XP_002436879.1

MHDRSYKPQPAEAGSGGTAGDGGGGGGNVDRVLFKNLVMVPLVESLMDRRVNPAYSRRASLVYTPAPPKASDLKSVKLPQSVSAKKRRD
PGDAAKKSAPDSNGDSGSVVPFSLGAENMPKDEVAMLREQIDDLQKKLLEKEEALRSAESSVAEMNAAAYATIDELRRLVADKEALIRSTNSQL
HDAKIMLADKQASLEKLEWEVKMSNKKVEDLQGDMSNMGFEISLMVFFEKISENVSSDSYDDTIPLSHELEALQSTSEIDKIEVDKIEQERMM
YAEALAAARENPDDEHLNIAAEARSRLQVLVL

>Oryza_sativa_Japonica_NP_001057401.1

MLDRSLRPPQPQAAAAEAGPGGGGGGGNVDRVLFKNLVMVPLVESLMDRRSNPSYSRRASLVYTPAPAKKGSCLKSVKLPQSVSVKRR
RDPGETGKKSTADSNGENGAVAPVGLLGGENKPKDKDEIVLLREQIEELQKTLEKEEALKSAESLVGEMNTLYSTVDELRRQVADKEGLIKSINS
QLHNAKIMLADKQASLEKLEWEVKTSNKKVEDLQGDVSNMEFEIGSLMALFEKISENVSGELQDGSPLSSFELEALQSTSEIDKIEVEKIEQEA
YAEALAAARENPNEEQLNIAAEARLRLQVLVL

>Glycine_max_ACU19600.1

MQHFMDLQANSELGESNSWLSVKEQSGAAPNTNLDRLVFNLDLVEIVSLVQSLIDRKASRSFTRRGSMIYTKPTRESLSKRVTDSKSRNVAPSIP
AKKKRDHGEKEQKGKNSNDADNYSMFSSRTLASEKDIEELGMLKEQVEELQRKLEKDELLKSAENTRDQMNVFNAKLDELKHQASEKESLLK
YTQQQLSDAKIKLADKQAALERYNGKR

>Hordeum_vulgare_BAK00114.1

EAGAGAAGPGERRGDVLLVKDLEAMVPLVESLMDRRNTNPSYSRRASLVYTPAPPKGGDLKSAKTPQTVSAKKRRDPDGTGNKNTPDNSG
ENGSVAPMTQSAENKTKDKDEIGLLREQVDELQKQLVEKEDALRSAESTVSEMNAYSTVDGLKRQVAEKEALIKYANSQQLQNAKVMMLADK
QASLEKLEWEVKTSNKKVEDLQGDVSSMEFEISSFTLFEKISENVSGSDHGSIPSVDLEALQSAEIDKIEVDRIEERTTYAEALAAARANPNE
EHLSSVAEARSRLQVLVVQ

>Zea_mays_NP_001149293.1

MAEKPAGPTPRTRIRGGLAASAPSSRRLSSVSFTAAPSKIKKVPDPPKAVRPSRATPAKKRPQVDQAQKRREEVAALQEQLNGLQSLHEKDEA
LRSANLIGRVTAANEAVDGLRSQLSEKELLIESTGSELHGAKIMLAEKQAALKLEWEANVSSTKVEELQADVASMDEVSALMKLFRKITESD
RAPPPRDRNDLSLECEPVHDDTVDDIDLEKMEKEMSAYVSALSAKENPTDEFMRVADARLRLQAVVL

>Sorghum_bicolor_XP_002460396.1

MAEKPAGPTPRTRIRGGLAASAPSSRRLSSISFTAAPNQSKKVPDPPKAVRPTATPVKKRPQVDQAQKRREEIAALQEQLSGLQRLHEKDEA
LRSANLIGRITAANEAVDGLRSQLSEKELLIESTGSELHGAKIMLAEKQAALKLEWEANVSSTKVEELQVDVASMDEVSALMKLFRKITEND
RAPPPRDRNTDLSLECEPVQLDDTVNDIDVEKMEQEMSAYASALAAAKENPTDEFMRVATEARLRLQAVVL

>Hordeum_vulgare_BAK04980.1

MAEKTAGPASRSRIRGLAPSAPSSRRVVSMAFYAAPHQAKKVPPEKVVKPTRTPAKRRQPDQGGQKQREERAALQEQLSGLQDKLLEKDE
ALRSAENLIGRVSAANEAVDELRSQNDKESLVESTGSELHGAKIMLAEKQAALKLEWEAKMSSTKVEELKVDVASMDEVSALMKVFRKITE
NNRASHPTDRPDSSLECEPIQLDDTVGDIDTEKMEQEMSAYVTALAAAKDNPTTEFLKAVTEARLRLQAFVL

>Oryza_sativa_Japonica_NP_001063462.1

MAEKAVGHGPRTRIRGGGLAAAPTAPSAARRLSAVSYTAAPNLTKKVPDPKVVKPAKTPPVKKRPQVDQAQKQREELAALQEQLSGLQKK

LLEKDEALRSAEHLISRISAANAAVDELRGQLTEKESQIESTGSELHGAKIQLAEKQAALEKLEWEAKVSSTKVEELQVDVASMDVEISALMKLFR
KITENDRAPYSRERADDSSLECEPVQLDDMVGDIDMEKMEQEMSAYATALAAAKDNPTDEFLKAVTEARLRLQAFVL

>Picea_glauca_BT116589.1

MESNSSMGMDDQHFFRESWKDVRGYGGMHDMGYLAAGLGSPPSSPVSSQTNGHVDKDLRYDLVEMVPLVQSLMDYRVNKSFSHYSTLVY
TPTPTPRDLSARKMQDQNAKTPQTTRGTQKRAPKEGLSDNCKNNNVEYQGQFPDEVICSSRSSVGHEENMVDGNKAETLSSGNSAELL
QLQNQIEVLEKKLVEKEDELLKSAENSAIKMEAMQMKVEELQWQIQEKDSLIIAAHLQLCHKKNELADVKSLLKKAEDSKASKGKLQKLEEDL
NGLRCQIAAFISFFQTAEDKTATSGMHGVQSPEDLDVDPDFSSQASHLNSSYMVDLQDEIEHDHMAFTQSDKKEEEDLEQARRMYLAAIIA
AKNNPGEESLCLAAGLRVQLQQFLLRPTLENTLNDKLSIQALSFPAS*

>Picea_sitchensis_BT122738.1

MESNSSMGMDDQHFFRESWKDVRGYGGMHDMGYLAAGLGSPPSSPVSSQTNGHVDKDLRYDLVEMVPLVQSLMDYRVNKSFSHYSTLVY
TPTPTPRDLSARKMQDQNAKTPQTTRGTQKRAPKEGLSDNCKKKKK

>Selaginella_moellendorffii_XP_002984304.1

MATAASAVAAVKVRANLPRIRQEREILTPALDSSPRSSALFHSSPKKNARAFRATGRGGARRPAAEVVRPRIGQDLLPDISAWSSTPDGS
MLLPFGAPGSRSSNVGSGAAPRASISGRRCEGSLGEEELGKSRDTDFGVAMSVEDWSGLPPPAGIDKTIYQNLVEMIMPLMESFMEQKGRRG
FTRHASMVYTPAPPRDASSVKVSDSPLKSKKNKQQAQVAKDAKDEISAIWDEQENILRRVDQDESGVEYTESQNLIKLNREELVQLQAQIDLL
KKQVWEKDSMLETVRSEFAEAAREEELVELKKKMEEVQKSLRDRERFAQAVQSQLTEKHKDLVNMEAMVARMQREVMQKNDAAARMR
EELSHLQVQFSAQFQAQLQNMDFDDEPEAGVATDRDEAERIIAGLVPSETMPGNDKQLETARRMYLGAVITAKQKPGAESIALAAALRK
ELEAFLAHPYLCGGAGGDGESLCSFRHKAVGALPLI

>Selaginella_moellendorffii_XP_002985614.1

MPVPRRSELYASDSPSTPNAAGSDSPSVAGNSQFLSSDCSSNGECCSSGMAPWELDEVDPGARSTDKEMIPMTQIFMDRAGNDHR
AFTHRGRVLVYTRAPAQKALNCPARLKKNKQLNAEEVLQPKPIEQSVRDEPDLSMKLNKVELLKLQSQVEELKLVKRDKEGLLSQKSAQSDIKL
LEEAEISDLRNKVDLHTELLRRDFLVHSLQHLSEKHVEMGNMKLLIQGLQNELAKREHKHSQMESDMDLRFVAALRYENQIAGSPHFVP
QPDQMMIMSCERKTNPQRNQ

>Physcomitrella_patens_XP_001764087.1

MSFKLFEGVVKVCRVDEGERRRRTKKDADERKRNLGEQERRRSGSADKVVMAFRGPAGAMAGSSGVSPVDPALYRNLMVIMPLMETFME
QQGSRTSMFGRQASMIYTPAPLPKYLYKSYENPLKSKRVPMSPKLEPSHEDSKEECTWEESENILRRIDRPAQEDFNQDSRHLEEEELKQKL
WEKDCLLETGLQSLNQTLCQSQSQTDAVNQTSSSQFKSTEGNGLQEALFECNSKPGKHASHGNGAVQSKDEKHEDMKLLQAQIDQLRQKL
EKDSYIQAQLELREHQGLGELNLLLEQAERGIVKRSHKASSMEAEELTLRCQVLTTRYQLDAVEAAGLVDASQSEQLNTAREGPPHRVDM
VSSISSEARQKTTFLVSTPAPNGEEQVSSGSEGSKEEKELELARRKYLAAIMAARQMPLKESLAMVAECRNQLNTFLKDIPTLHCLGAE

7.3 (TAIR) Accession numbers

Gene	Species	TAIR accession	GenBank mRNA	GenBank Protein	RefSeq Protein
MPB2C	<i>A. thaliana</i>	At5g08120		AED91249.1	NP_196429.1
KNB1	<i>A. thaliana</i>	At5g03050		AAO39951.1	
KNAT1/BP	<i>A. thaliana</i>	AT4G08150			
KNAT2	<i>A. thaliana</i>	AT1G70510			
KNAT3	<i>A. thaliana</i>	AT5G25220			
KNAT4	<i>A. thaliana</i>	AT5G11060			
KNAT5	<i>A. thaliana</i>	AT4G32040			
KNAT6	<i>A. thaliana</i>	AT1G23380			
KNAT7	<i>A. thaliana</i>	AT1G62990			
STM	<i>A. thaliana</i>	AT1G62360			
MPB2C (putative)	<i>A. lyrata</i>				XP_002873341.1
MPB2C (putative)	<i>Glycine max</i>			ACU19600.1	
MPB2C (putative)	<i>Hordeum vulgare</i>			BAK00114.1	
MPB2C (putative)	<i>Hordeum vulgare</i>			BAK04980.1	
NtMPB2C	<i>N. tabacum</i>		AF326729.1		
NbMPB2Ca	<i>N. benthamiana</i>		DQ297413	ABB97536	
NbMPB2Cb	<i>N. benthamiana</i>			ADR32211	
MPB2C (putative)	<i>Oryza sativa Japonica</i>				NP_001057401.1
MPB2C (putative)	<i>Oryza sativa Japonica</i>				NP_001063462.1
MPB2C (putative)	<i>Physcomitrella patens</i>				XP_001764087.1
MPB2C (putative)	<i>Picea glauca</i>		BT116589.1		
MPB2C (putative)	<i>Picea sitchensis</i>		BT122738.1		
MPB2C (putative)	<i>Populus trichocarpa</i>				XP_002305296.1

MPB2C (putative)	<i>Ricinus communis</i>	XP_002514605.1
MPB2C (putative)	<i>Selaginella moellendorffii</i>	XP_002984304.1
MPB2C (putative)	<i>Selaginella moellendorffii</i>	XP_002985614.1
MPB2C (putative)	<i>Sorghum bicolor</i>	XP_002436879.1
MPB2C (putative)	<i>Sorghum bicolor</i>	XP_002460396.1
MPB2C (putative)	<i>Vitis vinifera</i>	XP_002273093.1
MPB2C (putative)	<i>Zea Mays</i>	NP_001116341.1
MPB2C (putative)	<i>Zea Mays</i>	ACG39104.1
MPB2C (putative)	<i>Zea Mays</i>	NP_001149293.1

8 Appendix C Primers used

Name	Sequence	used for
FK177	A ATG GAA GAA GAC GCA GGG AAT GGA GGA T	KNB1 antisense probe 5' primer
FK178	CCT CAT TGC TCA ATG CTA GGA TTC TGA AT	KNB1 sense probe 3' primer
FK227	C ACC ATG TAT GAG CAG CAG CAA C	For PCR atMPB2C ORF 5' primer for gateway system cassette A TOPO entry vector
FK238	CGG ACC ATG GAA TAT GAG CAG CAG CAA C	5' primer for PCR of AtMPB2C and NcoI/BamHI cloning into RFP vector
FK239	CGGCGG ATC CGC delta stop ATA TGT AAA GGC TAG TGA	3' primer for PCR of AtMPB2C and NcoI/BamHI cloning into RFP vector
FK284	TAATACGACTCACTATAGATGTATGAGCAGCAGCAAC	T7 pol AtMPB2C + strand RNA synthesis
FK285	TAATACGACTCACTATAGATGGAAGAAGACGCGAGGG	KNB1 sense probe 3' primer + T7
FK293	GGT TTC GAG GGG ATT GCA G	TILLING 728 genotyping 5' primer
FK295	CCT ATG CAA CCA AGC TAC AG	TILLING 728 genotyping 3' primer
FK296	GGA AGA AAT GCT TCT CAA AC	AtMPB2C genomic primer 5' exon 1004- 1023, tilling
FK296	GGA AGA AAT GCT TCT CAA AC	TILLING 285 genotyping 5' primer
FK297	GTG TCC GAT AAT TGT AAC TG	AtMPB2C genomic primer 3' exon 1301- 1320), tilling
FK297	GTG TCC GAT AAT TGT AAC TG	TILLING 285 genotyping 3' primer
FK338	GGGG ACA AGT TTG TAC AAA AAA GCA GGC TAT ATG TAT GAG CAG CAG CAA CAT TTC	BP cloning 5' AtMPB2C
FK339	GGGG ACA AGT TTG TAC AAA AAA GCA GGC TAT ATG GTT CCC CTT ATC GAG CAT TAC	BP cloning 5' delta N (bp 1-171) AtMPB2C
FK404	GGGG AC CAC TTT GTA CAA GAA AGC TGG GTC ATA ATA TGT AAA GGC TAG TGA TTG	3' MPB2C BP gateway primer w/o stop
FK421	TAATACGACTCACTATAG TTA ATA TGT AAA GGC TAG TGA TTG	3' AtMPB2C primer for – strand T7 RNA production
FK447	ATTTTGCCGATTTCCGGAAC	SALK genotyping left border primer
FK518	GGGG ACA AGT TTG TAC AAA AAA GCA GGC T CTC CAA AAA TGT ATA TAT AGA TAT ATA GAT TC	5' primer BP cloning of AtMPB2C genomic (Promoter+ terminator)
FK519	GGGG AC CAC TTT GTA CAA GAA AGC TGG GTC CCG CCG CTG CGT CTC TCG TTC	3' primer BP cloning of AtMPB2C genomic (Promoter+ terminator)
FK554	GGGG AC CAC TTT GTA CAA GAA AGC TGG GTT TAT ATG TAA AGG CTA GTG ATT G	BP 3' MPB2C w/o stop reading frame for pKGWFS7
FK577	gccaggagctatcgTCGCCGAAGCTGAGTCCCTTgcaaatcc	mutagenesis primer for miR insensitive MPB2C
FK586	ggatttgcaAAGGGACTCAGGCTTCGGCGAcgatagctctctggc	mutagenesis primer for miR insensitive MPB2C
FK621	TAATACGACTCACTATAGGG GTGTCCGATAATTGTAAC TG	MPB2C in situ 3' part antisense probe = FK297 + T7 site
FK622	TAATACGACTCACTATAGGG CAG TTA CAA TTA TCG GAC AC	MPB2C in situ 5' part sense probe 5' primer = FK297rc + T7 site
FK623	GTTGCTTCTTCTTCTTCTCTTC	STM sense probe 3' primer
FK624	TAATACGACTCACTATAGGGGTTGCTTCTTCTTCTTCTCTTC	STM sense probe 5' primer + T7
FK625	GAGAAAGAGGAAGGTGAGGATAG	STM antisense probe 3' primer
FK626	TAATACGACTCACTATAGGGGAGAAAGAGGAAGGTGAGGATAG	STM antisense probe 5' primer + T7
FK627	TAATACGACTCACTATAGGGATGGAAGAATACCAGCATGACAAC	KNAT1 sense probe 5' primer + T7
FK628	GAGGAGGCAGAGACAGACG	KNAT1 sense probe 3' primer
FK629	TAATACGACTCACTATAGGGGAGGAGGCAGAGACAGACG	KNAT1 antisense probe 5' primer + T7
FK630	ATGGAGCCGCCACAGCATCA	KNAT1 antisense probe 3' primer
FK646	TAATACGACTCACTATAGGG T TGC TCA ATG CTA GGA TTC TGA AT	KNB1 antisense probe 3' primer + T7
FK696	GGGG ACA AGT TTG TAC AAA AAA GCA GGC TAT GCG GCC GCA atg aac aat tct agg gaa gat g	5' BP MPB2C delta 1-117 + NotI site
FK697	GGG GAC CAC TTT GTA CAA GAA AGC TGG GTC GGA TCC ATA ATA TGT AAA GGC TAG TGA TTG	3' BP MPB2C delta STOP + BamHI site

9 Appendix D Transgenic Arabidopsis lines

Working Name	Promoter	Gene	Tag	Binary Vector	R	GB	#	Phenotype	Expr. v.
I3	p35S	MPB2C cDNA	TAP	pEarleyGate 205	B	Col	40	fasciation	pos.: Western blot
I3	p35S	MPB2C cDNA	TAP	pEarleyGate 205	B	Ws	11	no	n.d.
I3	p35S	MPB2C cDNA	TAP	pEarleyGate 205	B	Ler	7	no	n.d.
I3	p35S	MPB2C cDNA	TAP	pEarleyGate 205	B	TR	23	less trichomes	n.d.
H4	p35S	MPB2CcD NA	GFP	pEarleyGate 103	B	Col	13	no	neg.: confocal, Western
H4	p35S	MPB2CcD NA	GFP	pEarleyGate 103	B	TR	7	less trichomes	pos.: RT, neg.: Western, confocal
M	p35S	MPB2C cDNA	RFP	pBat-TL-K RFP	K	Col	14	M13 (T1): fasciation; T2: reduced apical dominance	neg. RFP (confocal), no fusion protein (Western); RT PCR pos. (Fritz Golm)
Q	p35S	MPB2C (delta 1-58)	RFP	pBat-TL-K RFP	K	Col	16	Q7 (T1): <i>pnv/bp</i> -like, Q15 (T1): <i>bp</i> -like, fasciation; T2: strongly reduced apical dominance	neg. RFP (confocal), no fusion protein (Western); RT PCR pos. (Fritz Golm)
L	<i>pG10-90::XVE>>pOlexA</i> -46	MPB2C cDNA	mRFP 1	pMDC7	H	Col	10	L1 (T2): 10% embryo patterning defects L7, L10 (T2): ca 1% embryo patterning defects; reduced apical dominance	pos.: confocal; promoter leaky!
55	p35S	MPB2C (delta 178-229)	GFP	pEarleyGate 103	B	Col	6	55-1: fasciation, 55-37:bushy	neg. GFP (confocal), no fusion protein (Western)
55	p35S	MPB2C (delta 178-229)	GFP	pEarleyGate 103	B	gl1	11	no	pos.: Western blot (W27): 55-2, 55-27
55	p35S	MPB2C (delta 178-229)	GFP	pEarleyGate 103	B	TR	14	less trichomes: T1 leaves 1- 4: on average 28.73% compared to TR parental line (=100%)	n.d.
55	p35S	MPB2C (delta 178-229)	GFP	pEarleyGate 103	B	Ler	28	no	n.d.
56	p35S	MPB2C (delta 178-229)	TAP	pEarleyGate 205	B	Col	19	no	pos.: Western blot (W27): 56-1, 56-22
56	p35S	MPB2C (delta 178-229)	TAP	pEarleyGate 205	B	gl1	18	no	neg.: Western blot (W27)
56	p35S	MPB2C (delta 178-229)	TAP	pEarleyGate 205	B	TR	24	less trichomes: T1 leaves 1- 4: on average 25.09% compared to TR parental line (=100%)	n.d.

Working Name	Promoter	Gene	Tag	Binary Vector	R	GB	#	Phenotype	Expr. v.
66	<i>pG10-90::XVE>>pOlexA</i> -46	MPB2C (delta 178-229)	none	pMDC7	H	Col	18	66-3 (T1) bushy, round leaves, almost no seed	n.d.
73	p35S	MPB2C (delta 1-117)	GFP	pEarleyGate 103	B	Col	T1 seed	no resistant plants!	n/a
74	p35S	MPB2C (delta 1-117)	TAP	pEarleyGate 205	B	Col	T1 seed	no resistant plants!	n/a
75	p35S	MPB2C (delta 1-117)	RFP	pBat TL-K RFP	K	Col	T1 seed	no resistant plants!	n/a
A6-30	pHsp70	aMIR MPB2C	none	pMDC30	H	Col	12	no	n/a
A6-32	p35S	aMIR MPB2C	none	pMDC32	H	Col	10	no	pos.: Northern (miR), Western: reduction of MPB2C
A6-32	p35S	aMIR MPB2C	none	pMDC32	H	Ler	7	T1: 3 of 7 plants look like Col, not like Ler	n.d.
85	<i>pG10-90::XVE>>pOlexA</i> -46	aMIR MPB2C	none	pMDC7	H	Col	7	no	n.d.
42	p35S::GR>>pOp6	MPB2C cDNA	hairpin	pOpOff2 Kan	K	Col	6	no	n.d.
47	p35S::GR>>pOp6	GUS	hairpin	pOpOff2 Kan	K	Col	4	no	pos.: GUS stain
43	p35S::GR>>pOp6	MPB2C cDNA	hairpin	pOpOff2 Hyg	H	Col	3	no	GUS pos.: 43-1 & 43-3, Western: no reduction of MPB2C
48	p35S::GR>>pOp6	GUS	hairpin	pOpOff2 Hyg	H	Col	3	no	n.d.
54	pMPB2C	genom. MPB2C + 3'UTR + 5'UTR	none	pMDC123	B	TIL LIN G 728	17	2(TIL):3(wt):2(„elephantiasis“)	n.d.
58	pMPB2C	genom. MPB2C + 5'UTR delta STOP	(GFP) -GUS	pKGWFS7	K	Col	ca 64	58-8 (T2): 50% severely dwarfed fused/bumpy rosette leaves when grown on SD, strong GUS in internodes; 58-14 (T1): internode elongation blocked, long pedicels, no GUS; 58-18 (T2): dwarfed, bumpy rosette leaves	pos. GUS stain
62	pMPB2C	genom. miR-insens. MPB2C + 3'UTR + 5'UTR	none	pMDC123	B	Col	T1 seed	n/a	n/a
63	pMPB2C	genom. miR-insens. MPB2C delta STOP + 5'UTR	(GFP) -GUS	pKGWFS7	K	Col	ca 100	63-12, delayed bolting 63-13: no apical dominance, bushy; 63-86: extreme bushy, reduced fertility, mostly terminal flowers; 63-72: fasciation;	pos. GUS stain: 18 of 48 T1 inflorescences (stem, pedicel, carpels)
pWUS>>7	pWUS::AlcR>>AlcA	KNB1 cDNA	Ala-mRFP 1	pEC2	K/B	Col	45	embryo patterning defects	pos.: RFP (confocal)
pWUS>>8	pWUS::AlcR>>AlcA	MPB2C cDNA	none	pEC2	K/B	Col	19	no	n.d.
pWUS>>84	pWUS::AlcR>>AlcA	mCherry	none	pEC2	K/B	Col	14	no	n.d.

Working Name	Promoter	Gene	Tag	Binary Vector	R	GB	#	Phenotype	Expr. v.
pKNAT1>>76	pKNAT1::AlcR>>AlcA	KNB1 genomic	none	pEC2	K/ B	Col	4	no	n.d.
pKNAT1>>77	pKNAT1::AlcR>>AlcA	KNB1 cDNA	Ala-mRFP 1	pEC2	K/ B	Col	16	no	pos.: RFP in roots (confocal)
pKNAT1>>78	pKNAT1::AlcR>>AlcA	MPB2C cDNA	none	pEC2	K/ B	Col	32	embryo patterning defects	n.d.
pKNAT1>>79	pKNAT1::AlcR>>AlcA	MPB2C (delta 178-229)	none	pEC2	K/ B	Col	24	no	n.d.
pKNAT1>>81	pKNAT1::AlcR>>AlcA	aMIR MPB2C	none	pEC2	K/ B	Col	18	no	n.d.
pKNAT1>>82	pKNAT1::AlcR>>AlcA	aMIR KNB1	none	pEC2	K/ B	Col	16	embryo patterning defects	n.d.
pKNAT1>>84	pKNAT1::AlcR>>AlcA	mCherry	none	pEC2	K/ B	Col	9	no	n.d.
pSTM>>>76	pSTM::AlcR>>>AlcA	KNB1 genomic	none	pEC2	K/ B	Col	9	no	n.d.
pSTM>>>77	pSTM::AlcR>>>AlcA	KNB1 cDNA	Ala-mRFP 1	pEC2	K/ B	Col	9	no	pos.: RFP (confocal)
pSTM>>>78	pSTM::AlcR>>>AlcA	MPB2C cDNA	none	pEC2	K/ B	Col	10	no	n.d.
pSTM>>>79	pSTM::AlcR>>>AlcA	MPB2C (delta 178-229)	none	pEC2	K/ B	Col	4	no	n.d.
pSTM>>>80	pSTM::AlcR>>>AlcA	MPB2C (delta 1-117)	none	pEC2	K/ B	Col	17	no	n.d.
pSTM>>>81	pSTM::AlcR>>>AlcA	aMIR MPB2C	none	pEC2	K/ B	Col	10	no	n.d.
pSTM>>>82	pSTM::AlcR>>>AlcA	KNB1 cDNA	Ala-mRFP 1	pEC2	K/ B	Col	6	no	n.d.
pSTM>>>83	pSTM::AlcR>>>AlcA	MPB2C cDNA-	Ala-mRFP 1	pEC2	K/ B	Col	43	no	neg.: RFP (confocal)
pSTM>>>84	pSTM::AlcR>>>AlcA	mCherry	none	pEC2	K/ B	Col	15	no	pos. RFP (confocal)
pAtML1>>76	pAtML1::AlcR>>AlcA	KNB1 genomic	none	pEC2	K/ B	Col	12	no	n.d.
pAtML1>>77	pAtML1::AlcR>>AlcA	KNB1 cDNA	Ala-mRFP 1	pEC2	K/ B	Col	12	embryo patterning defects	pos. RFP (confocal)
pAtML1>>78	pAtML1::AlcR>>AlcA	MPB2C cDNA	none	pEC2	K/ B	Col	12	no	n.d.
pAtML1>>79	pAtML1::AlcR>>AlcA	MPB2C (delta 178-229)	none	pEC2	K/ B	Col	12	no	n.d.
pAtML1>>80	pAtML1::AlcR>>AlcA	MPB2C (delta 1-117)	none	pEC2	K/ B	Col	12	no	n.d.
pAtML1>>81	pAtML1::AlcR>>AlcA	aMIR MPB2C	none	pEC2	K/ B	Col	14	no	n.d.
pAtML1>>82	pAtML1::AlcR>>AlcA	aMIR KNB1	none	pEC2	K/ B	Col	8	no	n.d.
pAtML1>>84	pAtML1::AlcR>>AlcA	mCherry	none	pEC2	K/ B	Col	6	no	n.d.

Table 10: Transgenic *Arabidopsis* lines

Abbreviations: Tag: Fusion protein; R: Resistance Marker; B: Basta, H: Hygromycin, K: Kanamycin; GB: Genomic background, ecotype; #: Number of transgenic lines; Expr. v. Expression verified;

10 Appendix E: Raw data trichome count

T1 plants from soil, Basta sprayed

TR wt grown on soil in same chamber

10-02-14 trichome count p35S::MPB2C (delta178-229)-TAP in TR

	leaf 1	leaf 2	leaf 3	leaf 4
55-1	1	0	0	4
55-2	0	0	0	2
55-3	0	0	0	11
55-4	0	0	2	2
55-5	0	0	3	7
55-6	0	1	12	16
55-7	0	1	6	12
55-8	0	1	5	7
55-9	1	1	7	9
55-10	0	0	0	0
55-11	0	0	0	1
55-12	0	2	3	7
55-13	0	0	0	0
55-14	0	0	2	5
avg.	0,14	0,43	2,86	5,93
standard dev.	0,4	0,6	3,6	4,9

10-02-14 trichome count 35S::MPB2C (delta178-229)-TAP in TR

	leaf 1	leaf 2	leaf 3	leaf 4	
56-1	0	2	4	2	
56-2	0	0	6	10	
56-3	0	0	0	0	
56-4	0	0	11	12	
56-5	3	4	10	13	
56-6	0	1	6	17	
56-7	1	1	8	8	
56-8	0	0	3	5	
56-10	0	0	0	0	
56-11	0	0	0	1	
56-12	0	0	2	5	
56-13	0	0	0	8	
56-14	0	0	0	0	later trichomes
56-15	0	0	0	1	
56-16	0	0	1	1	
56-17	0	0	0	0	yellow, dying leaves
56-18	0	0	5	5	strange leaf form - picture!
56-19	0	0	0	0	glabrous!
56-20	0	1	1	7	
56-21	0	0	0	0	almost glabrous
56-22	0	0	4	7	
56-23	0	0	0	0	glabrous!
56-24	0	0	0	0	glabrous!
56-25	0	0	0	1	
avg.	0,17	0,38	2,54	4,29	
standard dev.	0,64	0,92	3,45	4,97	

* 55-9: leaves destroyed, not countable

TR wild type

	leaf 1	leaf 2	leaf 3	leaf 4
TR wt 1	1	0	13	26
TR wt 2	2	1	16	21
TR wt 3	2	1	1	8
TR wt 4	0	0	8	14
TR wt 5	1	0	16	15
TR wt 6	0	2	9	17
TR wt 7	1	1	17	15
TR wt 8	0	1	11	6
TR wt 9	0	3	14	16
TR wt 10	0	2	10	21
TR wt 11	3	3	11	14
TR wt 12	1	1	6	12
TR wt 13	0	1	4	14
TR wt 14	1	1	12	32
avg.	0,86	1,21	10,57	16,50
std dev.	0,95	0,97	4,69	6,78

	TR wt, n=14	TR 55, n=14	TR 56, n=24
leaf 1	0,86	0,14	0,17
leaf 2	1,21	0,43	0,38
leaf 3	10,57	2,86	2,54
leaf 4	16,50	5,93	4,29

T test

	55 - wt	56 - wt
leaf1	0,02	0,02508451
leaf 2	0,01956287	0,01481201
leaf 3	5,1983E-05	1,435E-05
leaf 4	8,3503E-05	7,4245E-06

11 References

GBrowse.

- Adachi, S., H. Uchimiya, et al. (2006). "Expression of B2-type cyclin-dependent kinase is controlled by protein degradation in *Arabidopsis thaliana*." *Plant Cell Physiol* **47**(12): 1683-6.
- Adai, A., C. Johnson, et al. (2005). "Computational prediction of miRNAs in *Arabidopsis thaliana*." *Genome Res* **15**(1): 78-91.
- Aida, M., T. Ishida, et al. (1999). "Shoot apical meristem and cotyledon formation during *Arabidopsis* embryogenesis: interaction among the CUP-SHAPED COTYLEDON and SHOOT MERISTEMLESS genes." *Development* **126**(8): 1563-70.
- Akiyoshi, D. E., H. Klee, et al. (1984). "T-DNA of *Agrobacterium tumefaciens* encodes an enzyme of cytokinin biosynthesis." *Proc Natl Acad Sci U S A* **81**(19): 5994-8.
- Alliotte, T., C. Tire, et al. (1989). "An Auxin-Regulated Gene of *Arabidopsis thaliana* Encodes a DNA-Binding Protein." *Plant Physiol* **89**(3): 743-52.
- Alonso-Cantabrana, H., J. J. Ripoll, et al. (2007). "Common regulatory networks in leaf and fruit patterning revealed by mutations in the *Arabidopsis* ASYMMETRIC LEAVES1 gene." *Development* **134**(14): 2663-71.
- Alonso, J. M., A. N. Stepanova, et al. (2003). "Genome-wide insertional mutagenesis of *Arabidopsis thaliana*." *Science* **301**(5633): 653-7.
- Altschul, S. F., W. Gish, et al. (1990). "Basic local alignment search tool." *J Mol Biol* **215**(3): 403-10.
- Aoki, K., F. Kragler, et al. (2002). "A subclass of plant heat shock cognate 70 chaperones carries a motif that facilitates trafficking through plasmodesmata." *Proc Natl Acad Sci U S A* **99**(25): 16342-7.
- Bach, L., L. Gissot, et al. (2011). "Very-long-chain fatty acids are required for cell plate formation during cytokinesis in *Arabidopsis thaliana*." *J Cell Sci* **124**(Pt 19): 3223-34.
- Bach, L., L. V. Michaelson, et al. (2008). "The very-long-chain hydroxy fatty acyl-CoA dehydratase PASTICCINO2 is essential and limiting for plant development." *Proc Natl Acad Sci U S A* **105**(38): 14727-31.
- Bais, H. P., S. W. Park, et al. (2004). "How plants communicate using the underground information superhighway." *Trends Plant Sci* **9**(1): 26-32.
- Barany-Wallje, E., S. Keller, et al. (2005). "A critical reassessment of penetratin translocation across lipid membranes." *Biophys J* **89**(4): 2513-21.
- Bariola, P. A., D. Retelska, et al. (2004). "Remorins form a novel family of coiled coil-forming oligomeric and filamentous proteins associated with apical, vascular and embryonic tissues in plants." *Plant Mol Biol* **55**(4): 579-94.
- Barton, D. A., L. Cole, et al. (2011). "Cell-to-cell transport via the lumen of the endoplasmic reticulum." *Plant J* **66**(5): 806-17.
- Barton, K. P., S. (1993). "Formation of the shoot apical meristem in *Arabidopsis thaliana*: an analysis of development in the wild type and in the shoot meristemless mutant." *Development* **119**(823-831).
- Baud, S., Y. Bellec, et al. (2004). "gurke and pasticcino3 mutants affected in embryo development are impaired in acetyl-CoA carboxylase." *EMBO Rep* **5**(5): 515-20.
- Becker, F., E. Buschfeld, et al. (1993). "Altered response to viral infection by tobacco plants perturbed in ubiquitin system." *The Plant Journal* **3**(6): 875-881.
- Bellaoui, M., M. S. Pidkowich, et al. (2001). "The *Arabidopsis* BELL1 and KNOX TALE homeodomain proteins interact through a domain conserved between plants and animals." *Plant Cell* **13**(11): 2455-70.
- Belles-Boix, E., O. Hamant, et al. (2006). "KNAT6: an *Arabidopsis* homeobox gene involved in meristem activity and organ separation." *Plant Cell* **18**(8): 1900-7.

- Benitez-Alfonso, Y., M. Cilia, et al. (2009). "Control of Arabidopsis meristem development by thioredoxin-dependent regulation of intercellular transport." *Proc Natl Acad Sci U S A* **106**(9): 3615-20.
- Benitez-Alfonso, Y., C. Faulkner, et al. (2010). "Plasmodesmata: gateways to local and systemic virus infection." *Mol Plant Microbe Interact* **23**(11): 1403-12.
- Benning, U. F., B. Tamot, et al. (2012). "New aspects of Phloem-mediated long-distance lipid signaling in plants." *Front Plant Sci* **3**: 53.
- Bernard, P. and M. Couturier (1992). "Cell killing by the F plasmid CcdB protein involves poisoning of DNA-topoisomerase II complexes." *J Mol Biol* **226**(3): 735-45.
- Bhatt, A. M., J. P. Etchells, et al. (2004). "VAAMANA--a BEL1-like homeodomain protein, interacts with KNOX proteins BP and STM and regulates inflorescence stem growth in Arabidopsis." *Gene* **328**: 103-11.
- Bonner, J. T. (1998). "The origins of multicellularity." *Integrative Biology* **1**: 28-36.
- Bouyer, D., F. Geier, et al. (2008). "Two-dimensional patterning by a trapping/depletion mechanism: the role of TTG1 and GL3 in Arabidopsis trichome formation." *PLoS Biol* **6**(6): e141.
- Brambilla, V., M. Kater, et al. (2008). "Ovule integument identity determination in Arabidopsis." *Plant Signal Behav* **3**(4): 246-7.
- Brand, U., J. C. Fletcher, et al. (2000). "Dependence of stem cell fate in Arabidopsis on a feedback loop regulated by CLV3 activity." *Science* **289**(5479): 617-9.
- Burch-Smith, T. M. and P. C. Zambryski (2012). "Plasmodesmata paradigm shift: regulation from without versus within." *Annu Rev Plant Biol* **63**: 239-60.
- Burglin, T. R. (1997). "Analysis of TALE superclass homeobox genes (MEIS, PBC, KNOX, Iroquois, TGIF) reveals a novel domain conserved between plants and animals." *Nucleic Acids Res* **25**(21): 4173-80.
- Butenko, M. A., S. E. Patterson, et al. (2003). "Inflorescence deficient in abscission controls floral organ abscission in Arabidopsis and identifies a novel family of putative ligands in plants." *Plant Cell* **15**(10): 2296-307.
- Butenko, M. A., C. L. Shi, et al. (2012). "KNAT1, KNAT2 and KNAT6 act downstream in the IDA-HAE/HSL2 signaling pathway to regulate floral organ abscission." *Plant Signal Behav* **7**(1): 135-8.
- Byrne, M. E., A. T. Groover, et al. (2003). "Phyllotactic pattern and stem cell fate are determined by the Arabidopsis homeobox gene BELLRINGER." *Development* **130**(17): 3941-50.
- Byrne, M. E., J. Simorowski, et al. (2002). "ASYMMETRIC LEAVES1 reveals knox gene redundancy in Arabidopsis." *Development* **129**(8): 1957-65.
- Cande, W. Z. and P. M. Ray (1976). "Nature of cell-to-cell transfer of auxin in polar transport." *Planta* **129**(1): 43-52.
- Cantrill, L. C., R. L. Overall, et al. (1999). "Cell-to-cell communication via plant endomembranes." *Cell Biol Int* **23**(10): 653-61.
- Cao, X., K. Li, et al. (2005). "Molecular analysis of the CRINKLY4 gene family in Arabidopsis thaliana." *Planta* **220**(5): 645-57.
- Carraro, N., A. Peaucelle, et al. (2006). "Cell differentiation and organ initiation at the shoot apical meristem." *Plant Mol Biol* **60**(6): 811-26.
- Carroll, S. B. (2001). "Chance and necessity: the evolution of morphological complexity and diversity." *Nature* **409**(6823): 1102-9.
- Chan, R. L., G. M. Gago, et al. (1998). "Homeoboxes in plant development." *Biochim Biophys Acta* **1442**(1): 1-19.
- Chaudhury, A. M., S. Letham, et al. (1993). "amp1 - a mutant with high cytokinin levels and altered embryonic pattern, faster vegetative growth, constitutive photomorphogenesis and precocious flowering." *The Plant Journal* **4**(6): 907-916.
- Chen, H., A. K. Banerjee, et al. (2004). "The tandem complex of BEL and KNOX partners is required for transcriptional repression of ga20ox1." *Plant J* **38**(2): 276-84.

- Chen, M., G. Han, et al. (2006). "The essential nature of sphingolipids in plants as revealed by the functional identification and characterization of the Arabidopsis LCB1 subunit of serine palmitoyltransferase." *Plant Cell* **18**(12): 3576-93.
- Chen, M. H., J. Sheng, et al. (2000). "Interaction between the tobacco mosaic virus movement protein and host cell pectin methylesterases is required for viral cell-to-cell movement." *EMBO J* **19**(5): 913-20.
- Cho, S. K., C. T. Larue, et al. (2008). "Regulation of floral organ abscission in Arabidopsis thaliana." *Proc Natl Acad Sci U S A* **105**(40): 15629-34.
- Cho, S. Y., W. K. Cho, et al. (2012). "Cis-acting element (SL1) of Potato virus X controls viral movement by interacting with the NbMPB2Cb and viral proteins." *Virology* **427**(2): 166-76.
- Christensen, N. M., C. Faulkner, et al. (2009). "Evidence for unidirectional flow through plasmodesmata." *Plant Physiol* **150**(1): 96-104.
- Chuck, G., C. Lincoln, et al. (1996). "KNAT1 induces lobed leaves with ectopic meristems when overexpressed in Arabidopsis." *Plant Cell* **8**(8): 1277-89.
- Cilia, M. L. and D. Jackson (2004). "Plasmodesmata form and function." *Curr Opin Cell Biol* **16**(5): 500-6.
- Clark, S. E., S. E. Jacobsen, et al. (1996). "The CLAVATA and SHOOT MERISTEMLESS loci competitively regulate meristem activity in Arabidopsis." *Development* **122**(5): 1567-75.
- Clark, S. E., M. P. Running, et al. (1993). "CLAVATA1, a regulator of meristem and flower development in Arabidopsis." *Development* **119**(2): 397-418.
- Clark, S. E., R. W. Williams, et al. (1997). "The CLAVATA1 gene encodes a putative receptor kinase that controls shoot and floral meristem size in Arabidopsis." *Cell* **89**(4): 575-85.
- Clough, S. J. and A. F. Bent (1998). "Floral dip: a simplified method for Agrobacterium-mediated transformation of Arabidopsis thaliana." *Plant J* **16**(6): 735-43.
- Clouse, S. D. (2011). "Brassinosteroid signal transduction: from receptor kinase activation to transcriptional networks regulating plant development." *Plant Cell* **23**(4): 1219-30.
- Cole, M., C. Nolte, et al. (2006). "Nuclear import of the transcription factor SHOOT MERISTEMLESS depends on heterodimerization with BLH proteins expressed in discrete sub-domains of the shoot apical meristem of Arabidopsis thaliana." *Nucleic Acids Res* **34**(4): 1281-92.
- Cook, M., L. Graham, et al. (1997). "Comparative ultrastructure of plasmodesmata of Chara and selected bryophytes: toward an elucidation of the evolutionary origin of plant plasmodesmata." *Am J Bot* **84**(9): 1169.
- Crawford, K. M. and P. C. Zambryski (1999). "Plasmodesmata signaling: many roles, sophisticated statutes." *Curr Opin Plant Biol* **2**(5): 382-7.
- Crawford, K. M. and P. C. Zambryski (2000). "Subcellular localization determines the availability of non-targeted proteins to plasmodesmatal transport." *Curr Biol* **10**(17): 1032-40.
- Crawford, K. M. and P. C. Zambryski (2001). "Non-targeted and targeted protein movement through plasmodesmata in leaves in different developmental and physiological states." *Plant Physiol* **125**(4): 1802-12.
- Crespi, M., E. Messens, et al. (1992). "Fasciation induction by the phytopathogen Rhodococcus fascians depends upon a linear plasmid encoding a cytokinin synthase gene." *EMBO J* **11**(3): 795-804.
- CSIRO_Website. (2012). "hairpinRNAi vectors for plants." Retrieved 01.12.2011, from <http://www.pi.csiro.au/rnai/vectors.htm>.
- Curtis, M. D. and U. Grossniklaus (2003). "A gateway cloning vector set for high-throughput functional analysis of genes in planta." *Plant Physiol* **133**(2): 462-9.
- de Felippes, F. F., F. Ott, et al. (2011). "Comparative analysis of non-autonomous effects of tasiRNAs and miRNAs in Arabidopsis thaliana." *Nucleic Acids Res* **39**(7): 2880-9.
- De Smet, I., S. Lau, et al. (2010). "Embryogenesis - the humble beginnings of plant life." *Plant J* **61**(6): 959-70.
- Dean, G., S. Casson, et al. (2004). "KNAT6 gene of Arabidopsis is expressed in roots and is required for correct lateral root formation." *Plant Mol Biol* **54**(1): 71-84.

- Derelle, R., P. Lopez, et al. (2007). "Homeodomain proteins belong to the ancestral molecular toolkit of eukaryotes." *Evol Dev* **9**(3): 212-9.
- Derossi, D., A. H. Joliot, et al. (1994). "The third helix of the Antennapedia homeodomain translocates through biological membranes." *J Biol Chem* **269**(14): 10444-50.
- Deveaux, Y., A. Peaucelle, et al. (2003). "The ethanol switch: a tool for tissue-specific gene induction during plant development." *Plant J* **36**(6): 918-30.
- Devlin, R. M., Witham, F. (1983). "Plant Physiology." 4.
- Dievart, A. and S. E. Clark (2004). "LRR-containing receptors regulating plant development and defense." *Development* **131**(2): 251-61.
- Dockx, J., N. Quaedvlieg, et al. (1995). "The homeobox gene ATK1 of Arabidopsis thaliana is expressed in the shoot apex of the seedling and in flowers and inflorescence stems of mature plants." *Plant Mol Biol* **28**(4): 723-37.
- Dolan, L., K. Janmaat, et al. (1993). "Cellular organisation of the Arabidopsis thaliana root." *Development* **119**(1): 71-84.
- Dorokhov, Y. L., K. Makinen, et al. (1999). "A novel function for a ubiquitous plant enzyme pectin methylesterase: the host-cell receptor for the tobacco mosaic virus movement protein." *FEBS Lett* **461**(3): 223-8.
- Douglas, S. J., G. Chuck, et al. (2002). "KNAT1 and ERECTA regulate inflorescence architecture in Arabidopsis." *Plant Cell* **14**(3): 547-58.
- Douglas, S. J. and C. D. Riggs (2005). "Pedicel development in Arabidopsis thaliana: contribution of vascular positioning and the role of the BREVIPEDICELLUS and ERECTA genes." *Dev Biol* **284**(2): 451-63.
- Duckett, C. M., K. J. Oparka, et al. (1994). "Dye-coupling in the root epidermis of Arabidopsis is progressively reduced during development." *Development* **120**(11): 3247-3255.
- Dupont, E., A. Prochiantz, et al. (2007). "Identification of a Signal Peptide for Unconventional Secretion." *J. Biol. Chem.* **282**(12): 8994-9000.
- Earley, K. W., J. R. Haag, et al. (2006). "Gateway-compatible vectors for plant functional genomics and proteomics." *Plant J* **45**(4): 616-29.
- Ecole, D. (1970). "Premie`res observations sur la fasciation chez le Celosia cristata L. (Amarantace`es)." *C R Acad Sci Paris* **270**: 477-480.
- Ehlers, K. and R. Kollmann (2001). "Primary and secondary plasmodesmata: structure, origin, and functioning." *Protoplasma* **216**(1-2): 1-30.
- Endrizzi, K., B. Moussian, et al. (1996). "The SHOOT MERISTEMLESS gene is required for maintenance of undifferentiated cells in Arabidopsis shoot and floral meristems and acts at a different regulatory level than the meristem genes WUSCHEL and ZWILLE." *Plant J* **10**(6): 967-79.
- Epel, B., van Lent, JWM, Cohen, L, Kotlitzky G, Katz, A, Yahalom, A (1996). "A 41 kDa protein isolated from maize mesocotyl cell walls immunolocalizes to plasmodesmata." *Protoplasma* **191**: 70-78.
- Epel, B. L. (1994). "Plasmodesmata: composition, structure and trafficking." *Plant Mol Biol* **26**(5): 1343-56.
- Escobar, N. M., S. Haupt, et al. (2003). "High-throughput viral expression of cDNA-green fluorescent protein fusions reveals novel subcellular addresses and identifies unique proteins that interact with plasmodesmata." *Plant Cell* **15**(7): 1507-23.
- Eshed, Y., A. Izhaki, et al. (2004). "Asymmetric leaf development and blade expansion in Arabidopsis are mediated by KANADI and YABBY activities." *Development* **131**(12): 2997-3006.
- Estruch, J. J., E. Prinsen, et al. (1991). "Viviparous leaves produced by somatic activation of an inactive cytokinin-synthesizing gene." *Science* **254**(5036): 1364-7.
- Faulkner, C., O. E. Akman, et al. (2008). "Peeking into pit fields: a multiple twinning model of secondary plasmodesmata formation in tobacco." *Plant Cell* **20**(6): 1504-18.
- Faulkner, C. and A. Maule (2011). "Opportunities and successes in the search for plasmodesmal proteins." *Protoplasma* **248**(1): 27-38.
- Faure, J. D., P. Vittorioso, et al. (1998). "The PASTICCINO genes of Arabidopsis thaliana are involved in the control of cell division and differentiation." *Development* **125**(5): 909-18.

- Fernandez-Calvino, L., C. Faulkner, et al. (2011). "Arabidopsis plasmodesmal proteome." *PLoS One* **6**(4): e18880.
- Ferrandiz, C., S. Pelaz, et al. (1999). "Control of carpel and fruit development in Arabidopsis." *Annu Rev Biochem* **68**: 321-54.
- Fichtenbauer, D. (2011). KNB1 - A novel regulator of TALE proteins. *Department of Biochemistry*. Vienna, University of Vienna. **PhD**: 133.
- Fichtenbauer, D., X. M. Xu, et al. (2012). "The chaperonin CCT8 facilitates spread of tobamovirus infection." *Plant Signal Behav* **7**(3).
- Fletcher, J. C., U. Brand, et al. (1999). "Signaling of cell fate decisions by CLAVATA3 in Arabidopsis shoot meristems." *Science* **283**(5409): 1911-4.
- Friml, J., A. Vieten, et al. (2003). "Efflux-dependent auxin gradients establish the apical-basal axis of Arabidopsis." *Nature* **426**(6963): 147-53.
- Gadi, J., K. Ruthala, et al. (2009). "The third helix of the Hoxc8 homeodomain peptide enhances the efficiency of gene transfer in combination with lipofectamine." *Mol Biotechnol* **42**(1): 41-8.
- Gallagher, K. L. and P. N. Benfey (2005). "Not just another hole in the wall: understanding intercellular protein trafficking." *Genes Dev* **19**(2): 189-95.
- Gallagher, K. L., A. J. Paquette, et al. (2004). "Mechanisms regulating SHORT-ROOT intercellular movement." *Curr Biol* **14**(20): 1847-51.
- Gallois, J. L., C. Woodward, et al. (2002). "Combined SHOOT MERISTEMLESS and WUSCHEL trigger ectopic organogenesis in Arabidopsis." *Development* **129**(13): 3207-17.
- Garzon, M., K. Eifler, et al. (2007). "PRT6/At5g02310 encodes an Arabidopsis ubiquitin ligase of the N-end rule pathway with arginine specificity and is not the CER3 locus." *FEBS Lett* **581**(17): 3189-96.
- Gehring, W. J., M. Affolter, et al. (1994). "Homeodomain proteins." *Annu Rev Biochem* **63**: 487-526.
- Geldner, N., N. Anders, et al. (2003). "The Arabidopsis GNOM ARF-GEF mediates endosomal recycling, auxin transport, and auxin-dependent plant growth." *Cell* **112**(2): 219-30.
- Geldner, N., V. Denervaud-Tendon, et al. (2009). "Rapid, combinatorial analysis of membrane compartments in intact plants with a multicolor marker set." *Plant J* **59**(1): 169-78.
- Geldner, N., J. Friml, et al. (2001). "Auxin transport inhibitors block PIN1 cycling and vesicle trafficking." *Nature* **413**(6854): 425-8.
- Gifford, M. L., S. Dean, et al. (2003). "The Arabidopsis ACR4 gene plays a role in cell layer organisation during ovule integument and sepal margin development." *Development* **130**(18): 4249-58.
- Golz, J. F. and A. Hudson (2002). "Signalling in plant lateral organ development." *Plant Cell* **14 Suppl**: S277-88.
- Gomez-Mena, C. and R. Sablowski (2008). "ARABIDOPSIS THALIANA HOMEODOMAIN GENE1 establishes the basal boundaries of shoot organs and controls stem growth." *Plant Cell* **20**(8): 2059-72.
- Goujon, M., H. McWilliam, et al. "A new bioinformatics analysis tools framework at EMBL-EBI." *Nucleic Acids Res* **38**(Web Server issue): W695-9.
- Grabski, S., A. W. De Feijter, et al. (1993). "Endoplasmic Reticulum Forms a Dynamic Continuum for Lipid Diffusion between Contiguous Soybean Root Cells." *Plant Cell* **5**(1): 25-38.
- Greener, M. (2008). "It's life, but just as we know it." *EMBO Rep* **9**(11): 1067-9.
- Grennan, A. K. (2007). "Lipid rafts in plants." *Plant Physiol* **143**(3): 1083-5.
- Guo, M., J. Thomas, et al. (2008). "Direct repression of KNOX loci by the ASYMMETRIC LEAVES1 complex of Arabidopsis." *Plant Cell* **20**(1): 48-58.
- Guseman, J. M., J. S. Lee, et al. (2010). "Dysregulation of cell-to-cell connectivity and stomatal patterning by loss-of-function mutation in Arabidopsis chorus (glucan synthase-like 8)." *Development* **137**(10): 1731-41.
- Ha, C. M., J. H. Jun, et al. (2007). "BLADE-ON-PETIOLE 1 and 2 control Arabidopsis lateral organ fate through regulation of LOB domain and adaxial-abaxial polarity genes." *Plant Cell* **19**(6): 1809-25.
- Ha, C. M., G. T. Kim, et al. (2003). "The BLADE-ON-PETIOLE 1 gene controls leaf pattern formation through the modulation of meristematic activity in Arabidopsis." *Development* **130**(1): 161-72.

- Hacham, Y., N. Holland, et al. (2011). "Brassinosteroid perception in the epidermis controls root meristem size." Development **138**(5): 839-48.
- Hackbusch, J., K. Richter, et al. (2005). "A central role of Arabidopsis thaliana ovate family proteins in networking and subcellular localization of 3-aa loop extension homeodomain proteins." Proc Natl Acad Sci U S A **102**(13): 4908-12.
- Hake, S. and M. Freeling (1986). "Analysis of genetic mosaics shows that the extra epidermal cell divisions in Knotted mutant maize plants are induced by adjacent mesophyll cells." Nature **320**(6063): 621-623.
- Hake, S., H. M. Smith, et al. (2004). "The role of knox genes in plant development." Annu Rev Cell Dev Biol **20**: 125-51.
- Hamann, T., U. Mayer, et al. (1999). "The auxin-insensitive bodenlos mutation affects primary root formation and apical-basal patterning in the Arabidopsis embryo." Development **126**(7): 1387-95.
- Hamant, O. and V. Pautot (2010). "Plant development: a TALE story." C R Biol **333**(4): 371-81.
- Haney, C. H. and S. R. Long (2009). "Plant flotillins are required for infection by nitrogen-fixing bacteria." Proc Natl Acad Sci U S A **107**(1): 478-83.
- Harrar, Y., Y. Bellec, et al. (2003). "Hormonal control of cell proliferation requires PASTICCINO genes." Plant Physiol **132**(3): 1217-27.
- Hasunuma, T., E.-i. Fukusaki, et al. (2004). "Expression of fungal pectin methylesterase in transgenic tobacco leads to alteration in cell wall metabolism and a dwarf phenotype." Journal of Biotechnology **111**(3): 241-251.
- Hay, A., M. Barkoulas, et al. (2006). "ASYMMETRIC LEAVES1 and auxin activities converge to repress BREVIPEDICELLUS expression and promote leaf development in Arabidopsis." Development **133**(20): 3955-61.
- Hay, A., J. Craft, et al. (2004). "Plant hormones and homeoboxes: bridging the gap?" Bioessays **26**(4): 395-404.
- Hay, A., H. Kaur, et al. (2002). "The gibberellin pathway mediates KNOTTED1-type homeobox function in plants with different body plans." Curr Biol **12**(18): 1557-65.
- Hay, A. and M. Tsiantis (2010). "KNOX genes: versatile regulators of plant development and diversity." Development **137**(19): 3153-65.
- Haywood, V., F. Kragler, et al. (2002). "Plasmodesmata: pathways for protein and ribonucleoprotein signaling." Plant Cell **14 Suppl**: S303-25.
- Heinlein, M. (2002). "Plasmodesmata: dynamic regulation and role in macromolecular cell-to-cell signaling." Curr Opin Plant Biol **5**(6): 543-52.
- Heinlein, M. and B. L. Epel (2004). "Macromolecular transport and signaling through plasmodesmata." Int Rev Cytol **235**: 93-164.
- Heinlein, M., H. S. Padgett, et al. (1998). "Changing patterns of localization of the tobacco mosaic virus movement protein and replicase to the endoplasmic reticulum and microtubules during infection." Plant Cell **10**(7): 1107-20.
- Heisler, M. G., C. Ohno, et al. (2005). "Patterns of auxin transport and gene expression during primordium development revealed by live imaging of the Arabidopsis inflorescence meristem." Curr Biol **15**(21): 1899-911.
- Helariutta, Y., H. Fukaki, et al. (2000). "The SHORT-ROOT gene controls radial patterning of the Arabidopsis root through radial signaling." Cell **101**(5): 555-67.
- Helliwell, C. A., A. N. Chin-Atkins, et al. (2001). "The Arabidopsis AMP1 gene encodes a putative glutamate carboxypeptidase." Plant Cell **13**(9): 2115-25.
- Hepworth, S. R., Y. Zhang, et al. (2005). "BLADE-ON-PETIOLE-dependent signaling controls leaf and floral patterning in Arabidopsis." Plant Cell **17**(5): 1434-48.
- Hruz, T., O. Laule, et al. (2008). "Genevestigator v3: a reference expression database for the meta-analysis of transcriptomes." Adv Bioinformatics **2008**: 420747.
- Huang, W. and H. Huang (2007). "A Novel Function of the 26S Proteasome in Repressing Class-1 KNOX Genes During Leaf Development." Plant Signal Behav **2**(1): 25-7.

- Huang, Z., V. M. Andrianov, et al. (2001). "Identification of arabidopsis proteins that interact with the cauliflower mosaic virus (CaMV) movement protein." *Plant Mol Biol* **47**(5): 663-75.
- Husbands, A. Y., D. H. Chitwood, et al. (2009). "Signals and prepatterns: new insights into organ polarity in plants." *Genes Dev* **23**(17): 1986-97.
- Iliev, I. and P. Kitin (2011). "Origin, morphology, and anatomy of fasciation in plants cultured in vivo and in vitro." *Plant Growth Regul* **63**: 115-129.
- Ishige, F., M. Takaichi, et al. (1999). "A G-box motif (GCCACGTGCC) tetramer confers high-level constitutive expression in dicot and monocot plants." *The Plant Journal* **18**: 443.
- Jacinto, T., E. E. Farmer, et al. (1993). "Purification of Potato Leaf Plasma Membrane Protein pp34, a Protein Phosphorylated in Response to Oligogalacturonide Signals for Defense and Development." *Plant Physiol* **103**(4): 1393-1397.
- Jackson, D. (1991). In situ hybridization in plants. In: *Molecular Plant Pathology: A Practical Approach*. D. J. Bowles, Gurr, S. J., and McPherson, M., eds., Oxford University Press: 163- 174.
- Jackson, D., Veit, B., Hake, S. (1994). "Expression of maize KNOTTED1 related homeobox genes in the shoot apical meristem predicts patterns of morphogenesis in the vegetative shoot." *Development* **120**: 405-413.
- Jarsch IK, O. T. (2011). "Perspectives on Remorin Proteins, Membrane Rafts, and Their Role During Plant–Microbe Interactions." *Molecular Plant Microbe Interactions* **24**: 7-12.
- Jasinski, S., P. Piazza, et al. (2005). "KNOX action in Arabidopsis is mediated by coordinate regulation of cytokinin and gibberellin activities." *Curr Biol* **15**(17): 1560-5.
- Jefferson, R. A., T. A. Kavanagh, et al. (1987). "GUS fusions: beta-glucuronidase as a sensitive and versatile gene fusion marker in higher plants." *Embo J* **6**(13): 3901-7.
- Jenik, P. D., C. S. Gillmor, et al. (2007). "Embryonic patterning in Arabidopsis thaliana." *Annu Rev Cell Dev Biol* **23**: 207-36.
- Jinn, T. L., J. M. Stone, et al. (2000). "HAESA, an Arabidopsis leucine-rich repeat receptor kinase, controls floral organ abscission." *Genes Dev* **14**(1): 108-17.
- Joliot, A., A. Maizel, et al. (1998). "Identification of a signal sequence necessary for the unconventional secretion of Engrailed homeoprotein." *Curr Biol* **8**(15): 856-63.
- Joliot, A., C. Pernelle, et al. (1991). "Antennapedia homeobox peptide regulates neural morphogenesis." *Proc Natl Acad Sci U S A* **88**(5): 1864-8.
- Joliot, A., A. Trembleau, et al. (1997). "Association of Engrailed homeoproteins with vesicles presenting caveolae-like properties." *Development* **124**(10): 1865-75.
- Jürgens, G. and N. Geldner (2002). "Protein secretion in plants: from the trans-Golgi network to the outer space." *Traffic* **3**(9): 605-13.
- Jun, J. H., C. M. Ha, et al. (2010). "BLADE-ON-PETIOLE1 coordinates organ determinacy and axial polarity in arabidopsis by directly activating ASYMMETRIC LEAVES2." *Plant Cell* **22**(1): 62-76.
- Kajiwarra, T., M. Furutani, et al. (2004). "The GURKE gene encoding an acetyl-CoA carboxylase is required for partitioning the embryo apex into three subregions in Arabidopsis." *Plant Cell Physiol* **45**(9): 1122-8.
- Kanrar, S., O. Onguka, et al. (2006). "Arabidopsis inflorescence architecture requires the activities of KNOX-BELL homeodomain heterodimers." *Planta* **224**(5): 1163-73.
- Karimi, M., D. Inze, et al. (2002). "GATEWAY vectors for Agrobacterium-mediated plant transformation." *Trends Plant Sci* **7**(5): 193-5.
- Kenneth, V., Thiman, K. V., Sachs, T. (1966). "The role of cytokinin in the "fasciation" disease caused by *Corynebacterium fascians*." *American Journal of Botany* **53**: 731-739.
- Khan, M., P. Tabb, et al. (2012). "BLADE-ON-PETIOLE1 and 2 regulate Arabidopsis inflorescence architecture in conjunction with homeobox genes KNAT6 and ATH1." *Plant Signal Behav* **7**(7).
- Khan, M., M. Xu, et al. (2012). "Antagonistic interaction of BLADE-ON-PETIOLE1 and 2 with BREVIPEDICELLUS and PENNYWISE regulates Arabidopsis inflorescence architecture." *Plant Physiol* **158**(2): 946-60.
- Kim, I., E. Cho, et al. (2005). "Cell-to-cell movement of GFP during embryogenesis and early seedling development in Arabidopsis." *Proc Natl Acad Sci U S A* **102**(6): 2227-31.

- Kim, I., F. D. Hempel, et al. (2002). "Identification of a developmental transition in plasmodesmatal function during embryogenesis in *Arabidopsis thaliana*." Development **129**(5): 1261-72.
- Kim, I. and P. C. Zambryski (2005). "Cell-to-cell communication via plasmodesmata during *Arabidopsis* embryogenesis." Curr Opin Plant Biol **8**(6): 593-9.
- Kim, J. Y., Y. Rim, et al. (2005). "A novel cell-to-cell trafficking assay indicates that the KNOX homeodomain is necessary and sufficient for intercellular protein and mRNA trafficking." Genes Dev **19**(7): 788-93.
- Kim, J. Y., Z. Yuan, et al. (2002). "Intercellular trafficking of a KNOTTED1 green fluorescent protein fusion in the leaf and shoot meristem of *Arabidopsis*." Proc Natl Acad Sci U S A **99**(6): 4103-8.
- Kim, J. Y., Z. Yuan, et al. (2003). "Developmental regulation and significance of KNOX protein trafficking in *Arabidopsis*." Development **130**(18): 4351-62.
- Kirk, D. L. (2005). "A twelve-step program for evolving multicellularity and a division of labor." Bioessays **27**(3): 299-310.
- Kloepper, T. H., C. N. Kienle, et al. (2008). "SNAREing the basis of multicellularity: consequences of protein family expansion during evolution." Mol Biol Evol **25**(9): 2055-68.
- Kobayashi, K., M. S. Otegui, et al. (2007). "INCREASED SIZE EXCLUSION LIMIT 2 encodes a putative DEVH box RNA helicase involved in plasmodesmata function during *Arabidopsis* embryogenesis." Plant Cell **19**(6): 1885-97.
- Koizumi, K., S. Wu, et al. (2011). "An Essential Protein that Interacts with Endosomes and Promotes Movement of the SHORT-ROOT Transcription Factor." Curr Biol.
- Kollwig, G. (2010). How to bridle a homeodomain protein: characterization of At KNB36 and At MPB2C. University of Vienna. Vienna, Vienna. **Mag**.
- Kong, D., R. Karve, et al. (2012). "Regulation of plasmodesmatal permeability and stomatal patterning by the glycosyltransferase-like protein KOBITO1." Plant Physiol **159**(1): 156-68.
- Koornneef, M., Eden, J. van, Hanhart, C.J., Stam, P., Braaksma, F.J., Feenstra, W.J. (1983). "Linkage map of *Arabidopsis thaliana*." The Journal of Heredity **74**: 265-272.
- Koshland, D. E., Jr. (2002). "Special essay. The seven pillars of life." Science **295**(5563): 2215-6.
- Kragler, F. (2007). Plasmodesmata: Protein Transport Signals and Receptors. Plasmodesmata, Blackwell Publishing Ltd: 53-72.
- Kragler, F., M. Curin, et al. (2003). "MPB2C, a microtubule-associated plant protein binds to and interferes with cell-to-cell transport of tobacco mosaic virus movement protein." Plant Physiol **132**(4): 1870-83.
- Kragler, F., W. J. Lucas, et al. (1998). "Plasmodesmata: dynamics, domains and patterning." Annals of Botany **81**: 1-10.
- Kragler, F., J. Monzer, et al. (1998). "Cell-to-cell transport of proteins: requirement for unfolding and characterization of binding to a putative plasmodesmal receptor." The Plant Journal **15**(3): 367-381.
- Kragler, F., J. Monzer, et al. (2000). "Peptide antagonists of the plasmodesmal macromolecular trafficking pathway." Embo J **19**(12): 2856-68.
- Kumar, R., K. Kushalappa, et al. (2007). "The *Arabidopsis* BEL1-LIKE HOMEODOMAIN proteins SAW1 and SAW2 act redundantly to regulate KNOX expression spatially in leaf margins." Plant Cell **19**(9): 2719-35.
- Kurata, T., T. Ishida, et al. (2005). "Cell-to-cell movement of the CAPRICE protein in *Arabidopsis* root epidermal cell differentiation." Development **132**(24): 5387-98.
- Kurata, T., K. Okada, et al. (2005). "Intercellular movement of transcription factors." Curr Opin Plant Biol **8**(6): 600-5.
- Lander, E. S., L. M. Linton, et al. (2001). "Initial sequencing and analysis of the human genome." Nature **409**(6822): 860-921.
- Laux, T. (2003). "The Stem Cell Concept in Plants: A Matter of Debate." Cell **113**(3): 281.
- Lazo, G. R., P. A. Stein, et al. (1991). "A DNA transformation-competent *Arabidopsis* genomic library in *Agrobacterium*." Biotechnology (N Y) **9**(10): 963-7.

- Lazzaro, M. D. a. T., W.W. (1996). "The vacuolar-tubular continuum in living trichomes of chickpea (*Cicer arietinum*) provides a rapid means of solute delivery from base to tip." Protoplasma **193**: 181-190.
- Lee, J. H., H. Lin, et al. (2008). "Early sexual origins of homeoprotein heterodimerization and evolution of the plant KNOX/BELL family." Cell **133**(5): 829-40.
- Lee, J. S., T. Kuroha, et al. (2012). "Direct interaction of ligand-receptor pairs specifying stomatal patterning." Genes Dev **26**(2): 126-36.
- Lee, J. Y., J. Colinas, et al. (2006). "Transcriptional and posttranscriptional regulation of transcription factor expression in Arabidopsis roots." Proc Natl Acad Sci U S A **103**(15): 6055-60.
- Lee, J. Y., K. Taoka, et al. (2005). "Plasmodesmal-associated protein kinase in tobacco and Arabidopsis recognizes a subset of non-cell-autonomous proteins." Plant Cell **17**(10): 2817-31.
- Lee, J. Y., B. C. Yoo, et al. (2003). "Selective trafficking of non-cell-autonomous proteins mediated by NtNCAPP1." Science **299**(5605): 392-6.
- Lefebvre, B., F. Furt, et al. (2007). "Characterization of lipid rafts from *Medicago truncatula* root plasma membranes: a proteomic study reveals the presence of a raft-associated redox system." Plant Physiol **144**(1): 402-18.
- Lenhard, M., A. Bohnert, et al. (2001). "Termination of stem cell maintenance in Arabidopsis floral meristems by interactions between WUSCHEL and AGAMOUS." Cell **105**(6): 805-14.
- Lenhard, M. and T. Laux (2003). "Stem cell homeostasis in the Arabidopsis shoot meristem is regulated by intercellular movement of CLAVATA3 and its sequestration by CLAVATA1." Development **130**(14): 3163-73.
- Leyser, O. (1992). "Characterisation of three shoot apical meristem mutants of *Arabidopsis thaliana*." Development **116**: 397-403.
- Leyser, O. (2011). "Auxin, self-organisation, and the colonial nature of plants." Curr Biol **21**(9): R331-7.
- Li, J. and J. Chory (1997). "A putative leucine-rich repeat receptor kinase involved in brassinosteroid signal transduction." Cell **90**(5): 929-38.
- Li, Y., L. Pi, et al. (2011). "ATH1 and KNAT2 proteins act together in regulation of plant inflorescence architecture." J Exp Bot **63**(3): 1423-33.
- Lin, W. C., B. Shuai, et al. (2003). "The Arabidopsis LATERAL ORGAN BOUNDARIES-domain gene ASYMMETRIC LEAVES2 functions in the repression of KNOX gene expression and in adaxial-abaxial patterning." Plant Cell **15**(10): 2241-52.
- Lincoln, C., J. Long, et al. (1994). "A knotted1-like homeobox gene in Arabidopsis is expressed in the vegetative meristem and dramatically alters leaf morphology when overexpressed in transgenic plants." Plant Cell **6**(12): 1859-76.
- Lindow, M. and A. Krogh (2005). "Computational evidence for hundreds of non-conserved plant microRNAs." BMC Genomics **6**: 119.
- Liu, C., Z. Xu, et al. (1993). "Auxin Polar Transport Is Essential for the Establishment of Bilateral Symmetry during Early Plant Embryogenesis." Plant Cell **5**(6): 621-630.
- Liu, X., Y. J. Kim, et al. (2011). "AGAMOUS terminates floral stem cell maintenance in Arabidopsis by directly repressing WUSCHEL through recruitment of Polycomb Group proteins." Plant Cell **23**(10): 3654-70.
- Long, J. and M. K. Barton (2000). "Initiation of axillary and floral meristems in Arabidopsis." Dev Biol **218**(2): 341-53.
- Long, J. A. and M. K. Barton (1998). "The development of apical embryonic pattern in Arabidopsis." Development **125**(16): 3027-35.
- Long, J. A., E. I. Moan, et al. (1996). "A member of the KNOTTED class of homeodomain proteins encoded by the STM gene of Arabidopsis." Nature **379**(6560): 66-9.
- Long, J. A., S. Woody, et al. (2002). "Transformation of shoots into roots in Arabidopsis embryos mutant at the TOPLESS locus." Development **129**(12): 2797-806.
- Lu, C., Z. Zainal, et al. (2001). "Developmental abnormalities and reduced fruit softening in tomato plants expressing an antisense Rab11 GTPase gene." Plant Cell **13**(8): 1819-33.

- Lucas, W. J., Biao Ding, et al. (1993). "Tansley Review No. 58. Plasmodesmata and the Supracellular Nature of Plants." *New Phytologist* **125**(3): 435-476.
- Lucas, W. J., S. Bouché-Pillon, et al. (1995). "Selective Trafficking of KNOTTED1 Homeodomain Protein and Its mRNA Through Plasmodesmata." *Science* **270**(5244): 1980-1983.
- Lucas, W. J., B. K. Ham, et al. (2009). "Plasmodesmata - bridging the gap between neighboring plant cells." *Trends Cell Biol* **19**(10): 495-503.
- Lucas, W. J. and J. Y. Lee (2004). "Plasmodesmata as a supracellular control network in plants." *Nat Rev Mol Cell Biol* **5**(9): 712-26.
- Lucas, W. J., B. C. Yoo, et al. (2001). "RNA as a long-distance information macromolecule in plants." *Nat Rev Mol Cell Biol* **2**(11): 849-57.
- Lupas, A. (1996). "Coiled coils: new structures and new functions." *Trends Biochem Sci* **21**(10): 375-82.
- Lupas, A., M. Van Dyke, et al. (1991). "Predicting coiled coils from protein sequences." *Science* **252**(5010): 1162-4.
- Lynch, D. V., Dunn, Theresa M. (2004). "An introduction to plant sphingolipids and a review of recent advances in understanding their metabolism and function." *New Phytologist* **161**(3): 677-702.
- MacAlister, C. A., K. Ohashi-Ito, et al. (2007). "Transcription factor control of asymmetric cell divisions that establish the stomatal lineage." *Nature* **445**(7127): 537-40.
- Macklem, P. T. (2008). "Emergent phenomena and the secrets of life." *J Appl Physiol* **104**(6): 1844-6.
- Maddison, W. P. a. D. R. M. (2011). Mesquite: a modular system for evolutionary analysis. .
- Magnani, E. and S. Hake (2008). "KNOX lost the OX: the Arabidopsis KNATM gene defines a novel class of KNOX transcriptional regulators missing the homeodomain." *Plant Cell* **20**(4): 875-87.
- Maizel, A., O. Bensaude, et al. (1999). "A short region of its homeodomain is necessary for engrailed nuclear export and secretion." *Development* **126**(14): 3183-90.
- Malamy, J. E. and P. N. Benfey (1997). "Organization and cell differentiation in lateral roots of Arabidopsis thaliana." *Development* **124**(1): 33-44.
- Marchler-Bauer, A., J. B. Anderson, et al. (2009). "CDD: specific functional annotation with the Conserved Domain Database." *Nucleic Acids Res* **37**(Database issue): D205-10.
- Markham, J. E., D. Molino, et al. (2011). "Sphingolipids containing very-long-chain Fatty acids define a secretory pathway for specific polar plasma membrane protein targeting in Arabidopsis." *Plant Cell* **23**(6): 2362-78.
- Martens, H. J., A. G. Roberts, et al. (2006). "Quantification of plasmodesmatal endoplasmic reticulum coupling between sieve elements and companion cells using fluorescence redistribution after photobleaching." *Plant Physiol* **142**(2): 471-80.
- Mas, P. and R. N. Beachy (1999). "Replication of tobacco mosaic virus on endoplasmic reticulum and role of the cytoskeleton and virus movement protein in intracellular distribution of viral RNA." *J Cell Biol* **147**(5): 945-58.
- Matsubayashi, Y. (2003). "Ligand-receptor pairs in plant peptide signaling." *J Cell Sci* **116**(Pt 19): 3863-70.
- Maule, A., C. Faulkner, et al. (2012). "Plasmodesmata "in Comunicado". " *Front Plant Sci* **3**: 30.
- Maule, A. J. (2008). "Plasmodesmata: structure, function and biogenesis." *Curr Opin Plant Biol* **11**(6): 680-6.
- Maule, A. J., Y. Benitez-Alfonso, et al. (2011). "Plasmodesmata - membrane tunnels with attitude." *Curr Opin Plant Biol* **14**(6): 683-90.
- Mayer, K. F., H. Schoof, et al. (1998). "Role of WUSCHEL in regulating stem cell fate in the Arabidopsis shoot meristem." *Cell* **95**(6): 805-15.
- McDonnell, A. V., T. Jiang, et al. (2006). "Paircoil2: improved prediction of coiled coils from sequence." *Bioinformatics* **22**(3): 356-8.
- McKay, C. P. (2004). "What is life--and how do we search for it in other worlds?" *PLoS Biol* **2**(9): E302.
- McKim, S. M., G. E. Stenvik, et al. (2008). "The BLADE-ON-PETIOLE genes are essential for abscission zone formation in Arabidopsis." *Development* **135**(8): 1537-46.
- Meinke, D. (1994). Seed Development in Arabidopsis thaliana. *Arabidopsis*. C. R. S. Elliot M. Meyerowitz. New York, CSHL Press: 253ff.

- Mele, G., N. Ori, et al. (2003). "The knotted1-like homeobox gene BREVIPEDICELLUS regulates cell differentiation by modulating metabolic pathways." *Genes Dev* **17**(17): 2088-93.
- Micheli, F. (2001). "Pectin methylesterases: cell wall enzymes with important roles in plant physiology." *Trends Plant Sci* **6**(9): 414-9.
- Miller, S. M. (2010). "Volvox, Chlamydomonas, and the Evolution of Multicellularity." *Nature Education* **3**(9): 65.
- Modrusan, Z., L. Reiser, et al. (1994). "Homeotic Transformation of Ovules into Carpel-like Structures in Arabidopsis." *Plant Cell* **6**(3): 333-349.
- Mongrand, S., J. Morel, et al. (2004). "Lipid rafts in higher plant cells: purification and characterization of Triton X-100-insoluble microdomains from tobacco plasma membrane." *J Biol Chem* **279**(35): 36277-86.
- Mongrand, S., T. Stanislas, et al. (2010). "Membrane rafts in plant cells." *Trends Plant Sci* **15**(12): 656-63.
- Morvan, O., Quentin, M, Jauneau, A, Mareck, A, Morvan, C (1998). "Immunogold localization of pectin methylesterases in the cortical tissues of flax hypocotyl." *Protoplasma* **202**: 175-184.
- Mouritsen, O. G. (2011). "Lipids, curvature, and nano-medicine." *Eur J Lipid Sci Technol* **113**(10): 1174-1187.
- Muller, J., Y. Wang, et al. (2001). "In vitro interactions between barley TALE homeodomain proteins suggest a role for protein-protein associations in the regulation of Knox gene function." *Plant J* **27**(1): 13-23.
- Nagasaki, H., T. Sakamoto, et al. (2001). "Functional analysis of the conserved domains of a rice KNOX homeodomain protein, OSH15." *Plant Cell* **13**(9): 2085-98.
- Nakajima, K., G. Sena, et al. (2001). "Intercellular movement of the putative transcription factor SHR in root patterning." *Nature* **413**(6853): 307-11.
- Nebenfuhr, A., C. Ritzenthaler, et al. (2002). "Brefeldin A: deciphering an enigmatic inhibitor of secretion." *Plant Physiol* **130**(3): 1102-8.
- Nelson, R. S. and V. Citovsky (2005). "Plant viruses. Invaders of cells and pirates of cellular pathways." *Plant Physiol* **138**(4): 1809-14.
- Nickel, W. (2003). "The mystery of nonclassical protein secretion. A current view on cargo proteins and potential export routes." *Eur J Biochem* **270**(10): 2109-19.
- Niehl, A. and M. Heinlein (2011). "Cellular pathways for viral transport through plasmodesmata." *Protoplasma* **248**(1): 75-99.
- Noodén, L. D., Leopold, A.C. (1988). *Senescence and Aging in Plants*. San Diego., Accademic Press.
- Oparka, K. J. (2004). "Getting the message across: how do plant cells exchange macromolecular complexes?" *Trends Plant Sci* **9**(1): 33-41.
- Oparka, K. J., A. G. Roberts, et al. (1999). "Simple, but not branched, plasmodesmata allow the nonspecific trafficking of proteins in developing tobacco leaves." *Cell* **97**(6): 743-54.
- Ori, N., Y. Eshed, et al. (2000). "Mechanisms that control knox gene expression in the Arabidopsis shoot." *Development* **127**(24): 5523-32.
- Overall, R. and L. Blackman (1996). "A model of the macromolecular structure of plasmodesmata." *Trends in Plant Science* **1**: 307.
- Page, R. D. (1996). "TreeView: an application to display phylogenetic trees on personal computers." *Comput Appl Biosci* **12**(4): 357-8.
- Pare, P. W. and J. H. Tumlinson (1999). "Plant volatiles as a defense against insect herbivores." *Plant Physiol* **121**(2): 325-32.
- Parthier, B. (1979). "The role of phytohormones (cytokinins) in chloroplast development." *Biochem Physiol Pflanz* **174**: 173-214.
- Patterson, S. E. (2001). "Cutting loose. Abscission and dehiscence in Arabidopsis." *Plant Physiol* **126**(2): 494-500.
- Pautot, V., J. Dockx, et al. (2001). "KNAT2: evidence for a link between knotted-like genes and carpel development." *Plant Cell* **13**(8): 1719-34.

- Peaucelle, A., R. Louvet, et al. (2008). "Arabidopsis phyllotaxis is controlled by the methylesterification status of cell-wall pectins." *Curr Biol* **18**(24): 1943-8.
- Peaucelle, A., R. Louvet, et al. (2011). "The transcription factor BELLRINGER modulates phyllotaxis by regulating the expression of a pectin methylesterase in Arabidopsis." *Development* **138**(21): 4733-41.
- Pelloux, J., C. Rusterucci, et al. (2007). "New insights into pectin methylesterase structure and function." *Trends Plant Sci* **12**(6): 267-77.
- Perbal, M. C., G. Haughn, et al. (1996). "Non-cell-autonomous function of the Antirrhinum floral homeotic proteins DEFICIENS and GLOBOSA is exerted by their polar cell-to-cell trafficking." *Development* **122**(11): 3433-41.
- Perte, M. and S. L. Salzberg (2010). "Between a chicken and a grape: estimating the number of human genes." *Genome Biol* **11**(5): 206.
- Petersson, S. V., A. I. Johansson, et al. (2009). "An auxin gradient and maximum in the Arabidopsis root apex shown by high-resolution cell-specific analysis of IAA distribution and synthesis." *Plant Cell* **21**(6): 1659-68.
- Phelps-Durr, T. L., J. Thomas, et al. (2005). "Maize rough sheath2 and its Arabidopsis orthologue ASYMMETRIC LEAVES1 interact with HIRA, a predicted histone chaperone, to maintain knox gene silencing and determinacy during organogenesis." *Plant Cell* **17**(11): 2886-98.
- Pike, L. J. (2006). "Rafts defined: a report on the Keystone Symposium on Lipid Rafts and Cell Function." *J Lipid Res* **47**(7): 1597-8.
- Pike, L. J. (2009). "The challenge of lipid rafts." *J Lipid Res* **50** Suppl: S323-8.
- Prigge, M. J. and D. R. Wagner (2001). "The arabidopsis serrate gene encodes a zinc-finger protein required for normal shoot development." *Plant Cell* **13**(6): 1263-79.
- Prochiantz, A. (2000). "Messenger proteins: homeoproteins, TAT and others." *Curr Opin Cell Biol* **12**(4): 400-6.
- Quaedvlieg, N., J. Dockx, et al. (1995). "The homeobox gene ATH1 of Arabidopsis is derepressed in the photomorphogenic mutants cop1 and det1." *Plant Cell* **7**(1): 117-29.
- Raffaele, S., E. Bayer, et al. (2009). "Remorin, a solanaceae protein resident in membrane rafts and plasmodesmata, impairs potato virus X movement." *Plant Cell* **21**(5): 1541-55.
- Raffaele, S., S. Mongrand, et al. (2007). "Genome-wide annotation of remorins, a plant-specific protein family: evolutionary and functional perspectives." *Plant Physiol* **145**(3): 593-600.
- Ragni, L., E. Belles-Boix, et al. (2008). "Interaction of KNAT6 and KNAT2 with BREVIPEDICELLUS and PENNYWISE in Arabidopsis inflorescences." *Plant Cell* **20**(4): 888-900.
- Ragni, L., E. Truernit, et al. (2007). "KNOXing on the BELL: TALE Homeobox Genes and Meristem Activity." *International Journal of Plant Developmental Biology* **1**(1): 42-48.
- Raikhel, N. (1992). "Nuclear targeting in plants." *Plant Physiol* **100**(4): 1627-32.
- Ray, A., K. Robinson-Beers, et al. (1994). "Arabidopsis floral homeotic gene BELL (BEL1) controls ovule development through negative regulation of AGAMOUS gene (AG)." *Proc Natl Acad Sci U S A* **91**(13): 5761-5.
- Reichel, C. and R. N. Beachy (1998). "Tobacco mosaic virus infection induces severe morphological changes of the endoplasmic reticulum." *Proc Natl Acad Sci U S A* **95**(19): 11169-74.
- Reichel, C. and R. N. Beachy (2000). "Degradation of tobacco mosaic virus movement protein by the 26S proteasome." *J Virol* **74**(7): 3330-7.
- Retelska, D., A. Fleming, et al. (2000). Overexpression of remorin leads to cell defense and cell death in tobacco. *Plant Biology*.
- Reymond, P., B. Kunz, et al. (1996). "Cloning of a cDNA encoding a plasma membrane-associated, uronide binding phosphoprotein with physical properties similar to viral movement proteins." *Plant Cell* **8**(12): 2265-76.
- Rim, Y., L. Huang, et al. (2011). "Analysis of Arabidopsis transcription factor families revealed extensive capacity for cell-to-cell movement as well as discrete trafficking patterns." *Mol Cells* **32**(6): 519-26.

- Rim, Y., J. Jung, et al. (2009). "A non-cell-autonomous mechanism for the control of plant architecture and epidermal differentiation involves intercellular trafficking of BREVIPEDICELLUS protein." *Functional Plant Biology* **36**(3): 280-289.
- Robards, A. (1975). "Plasmodesmata." *Annual Review of Plant Physiology* **26**: 13-29.
- Robards, A., Lucas, WJ (1990). "Plasmodesmata." *Annual Review of Plant Physiology and Plant Molecular Biology* **41**: 369-419.
- Roberts, J. A., K. A. Elliott, et al. (2002). "Abscission, dehiscence, and other cell separation processes." *Annu Rev Plant Biol* **53**: 131-58.
- Robinson-Beers, K., R. E. Pruitt, et al. (1992). "Ovule Development in Wild-Type Arabidopsis and Two Female-Sterile Mutants." *Plant Cell* **4**(10): 1237-1249.
- Roeder, A. H., C. Ferrandiz, et al. (2003). "The role of the REPLUMLESS homeodomain protein in patterning the Arabidopsis fruit." *Curr Biol* **13**(18): 1630-5.
- Rogers, S., R. Wells, et al. (1986). "Amino acid sequences common to rapidly degraded proteins: the PEST hypothesis." *Science* **234**(4774): 364-8.
- Rojo, E., V. K. Sharma, et al. (2002). "CLV3 is localized to the extracellular space, where it activates the Arabidopsis CLAVATA stem cell signaling pathway." *Plant Cell* **14**(5): 969-77.
- Rose, A., S. Manikantan, et al. (2004). "Genome-Wide Identification of Arabidopsis Coiled-Coil Proteins and Establishment of the ARABI-COIL Database." *Plant Physiol.* **134**(3): 927-939.
- Rose, A. B. and J. A. Beliakoff (2000). "Intron-mediated enhancement of gene expression independent of unique intron sequences and splicing." *Plant Physiol* **122**(2): 535-42.
- Roudier, F., L. Gissot, et al. (2010). "Very-long-chain fatty acids are involved in polar auxin transport and developmental patterning in Arabidopsis." *Plant Cell* **22**(2): 364-75.
- Ruggenthaler, P., D. Fichtenbauer, et al. (2009). "Microtubule-associated protein AtMPB2C plays a role in organization of cortical microtubules, stomata patterning, and tobamovirus infectivity." *Plant Physiol* **149**(3): 1354-65.
- Ruiz-Medrano, R., B. Xoconostle-Cazares, et al. (2004). "The plasmodesmatal transport pathway for homeotic proteins, silencing signals and viruses." *Curr Opin Plant Biol* **7**(6): 641-50.
- Rutjens, B., D. Bao, et al. (2009). "Shoot apical meristem function in Arabidopsis requires the combined activities of three BEL1-like homeodomain proteins." *Plant J* **58**(4): 641-54.
- Ruzicka, K., M. Simaskova, et al. (2009). "Cytokinin regulates root meristem activity via modulation of the polar auxin transport." *Proc Natl Acad Sci U S A* **106**(11): 4284-9.
- Ryan, C. A. and G. Pearce (2001). "Polypeptide hormones." *Plant Physiol* **125**(1): 65-8.
- Sakamoto, T., N. Kamiya, et al. (2001). "KNOX homeodomain protein directly suppresses the expression of a gibberellin biosynthetic gene in the tobacco shoot apical meristem." *Genes Dev* **15**(5): 581-90.
- Sambrook, J., E. F. Fritsch, et al. (1989). "Molecular Cloning. A Manual." *Cold Spring Harbor Laboratory Press*.
- Sanderfoot, A. (2007). "Increases in the number of SNARE genes parallels the rise of multicellularity among the green plants." *Plant Physiol* **144**(1): 6-17.
- Sang, Y., M. F. Wu, et al. (2009). "The stem cell--chromatin connection." *Semin Cell Dev Biol* **20**(9): 1143-8.
- Santner, A. and M. Estelle (2009). "Recent advances and emerging trends in plant hormone signalling." *Nature* **459**(7250): 1071-8.
- Scanlon, M. J., D. C. Henderson, et al. (2002). "SEMAPHORE1 functions during the regulation of ancestrally duplicated knox genes and polar auxin transport in maize." *Development* **129**(11): 2663-73.
- Schepetilnikov, M. V., A. G. Solovyev, et al. (2008). "Intracellular targeting of a hordeiviral membrane-spanning movement protein: sequence requirements and involvement of an unconventional mechanism." *J Virol* **82**(3): 1284-93.
- Schlereth, A., B. Moller, et al. (2010). "MONOPTEROS controls embryonic root initiation by regulating a mobile transcription factor." *Nature* **464**(7290): 913-6.
- Schoelz, J. E., P. A. Harries, et al. (2011). "Intracellular Transport of Plant Viruses: Finding the Door out of the Cell." *Mol Plant*.

- Schrödinger, E. (1944). What is life? The Physical Aspect of the Living Cell & Mind and Matter, Cambridge University Press.
- Scofield, S., W. Dewitte, et al. (2007). "The KNOX gene SHOOT MERISTEMLESS is required for the development of reproductive meristematic tissues in Arabidopsis." Plant J **50**(5): 767-81.
- Scofield, S., W. Dewitte, et al. (2008). "A model for Arabidopsis class-1 KNOX gene function." Plant Signal Behav **3**(4): 257-9.
- Semiarti, E., Y. Ueno, et al. (2001). "The ASYMMETRIC LEAVES2 gene of Arabidopsis thaliana regulates formation of a symmetric lamina, establishment of venation and repression of meristem-related homeobox genes in leaves." Development **128**(10): 1771-83.
- Serikawa, K. A., A. Martinez-Laborda, et al. (1997). "Localization of expression of KNAT3, a class 2 knotted1-like gene." Plant J **11**(4): 853-61.
- Serikawa, K. A., A. Martinez-Laborda, et al. (1996). "Three knotted1-like homeobox genes in Arabidopsis." Plant Mol Biol **32**(4): 673-83.
- Sessions, A., M. F. Yanofsky, et al. (2000). "Cell-cell signaling and movement by the floral transcription factors LEAFY and APETALA1." Science **289**(5480): 779-82.
- Sexton, R., Roberts, JA (1982). "Cell Biology of Abscission." Annual Review of Plant Physiology and Plant Molecular Biology **33**: 133-162.
- Shani, E., O. Yanai, et al. (2006). "The role of hormones in shoot apical meristem function." Curr Opin Plant Biol **9**(5): 484-9.
- Shi, C. L., G. E. Stenvik, et al. (2011). "Arabidopsis class I KNOTTED-like homeobox proteins act downstream in the IDA-HAE/HSL2 floral abscission signaling pathway." Plant Cell **23**(7): 2553-67.
- Shiu, S. H. and A. B. Bleeker (2001). "Plant receptor-like kinase gene family: diversity, function, and signaling." Sci STKE **2001**(113): re22.
- Shpak, E. D., J. M. McAbee, et al. (2005). "Stomatal patterning and differentiation by synergistic interactions of receptor kinases." Science **309**(5732): 290-3.
- Simon-Plas, F., A. Perraki, et al. (2011). "An update on plant membrane rafts." Curr Opin Plant Biol **14**(6): 642-9.
- Simons, K. and E. Ikonen (1997). "Functional rafts in cell membranes." Nature **387**(6633): 569-72.
- Simons, K. and D. Toomre (2000). "Lipid rafts and signal transduction." Nat Rev Mol Cell Biol **1**(1): 31-9.
- Simpson, C., C. Thomas, et al. (2009). "An Arabidopsis GPI-anchor plasmodesmal neck protein with callose binding activity and potential to regulate cell-to-cell trafficking." Plant Cell **21**(2): 581-94.
- Skoog, F. and C. O. Miller (1957). "Chemical regulation of growth and organ formation in plant tissues cultured in vitro." Symp Soc Exp Biol **11**: 118-30.
- Smith, H. M., I. Boschke, et al. (2002). "Selective interaction of plant homeodomain proteins mediates high DNA-binding affinity." Proc Natl Acad Sci U S A **99**(14): 9579-84.
- Smith, H. M. and S. Hake (2003). "The interaction of two homeobox genes, BREVIPEDICELLUS and PENNYWISE, regulates internode patterning in the Arabidopsis inflorescence." Plant Cell **15**(8): 1717-27.
- Smith, H. M., N. Ung, et al. (2011). "Specification of reproductive meristems requires the combined function of SHOOT MERISTEMLESS and floral integrators FLOWERING LOCUS T and FD during Arabidopsis inflorescence development." J Exp Bot **62**(2): 583-93.
- Smyczynski, C., F. Roudier, et al. (2006). "The C terminus of the immunophilin PASTICCINO1 is required for plant development and for interaction with a NAC-like transcription factor." J Biol Chem **281**(35): 25475-84.
- Solovyev, A. G., D. A. Zelenina, et al. (1996). "Movement of a barley stripe mosaic virus chimera with a tobacco mosaic virus movement protein." Virology **217**(2): 435-41.
- Souter, M., J. Topping, et al. (2002). "hydra Mutants of Arabidopsis are defective in sterol profiles and auxin and ethylene signaling." Plant Cell **14**(5): 1017-31.
- Steeves, T. A. and I. M. Sussex (1989). Patterns in Plant Development, Cambridge University Press.

- Stenvik, G. E., M. A. Butenko, et al. (2006). "Overexpression of INFLORESCENCE DEFICIENT IN ABSCISSION activates cell separation in vestigial abscission zones in Arabidopsis." Plant Cell **18**(6): 1467-76.
- Stenvik, G. E., N. M. Tandstad, et al. (2008). "The EPIP peptide of INFLORESCENCE DEFICIENT IN ABSCISSION is sufficient to induce abscission in arabidopsis through the receptor-like kinases HAESA and HAESA-LIKE2." Plant Cell **20**(7): 1805-17.
- Stonebloom, S., T. Burch-Smith, et al. (2009). "Loss of the plant DEAD-box protein ISE1 leads to defective mitochondria and increased cell-to-cell transport via plasmodesmata." Proc Natl Acad Sci U S A **106**(40): 17229-34.
- Stothard, P. (2000). "The sequence manipulation suite: JavaScript programs for analyzing and formatting protein and DNA sequences." Biotechniques **28**(6): 1102, 1104.
- Strasburger, E. (1882). Ueber den bau und das wachsthum der zellhäute. Jena, G. Fisher.
- Sun, T.-P. (2008). "Gibberellin Metabolism, Perception and Signaling Pathways in Arabidopsis." The Arabidopsis Book **6**.
- Takano, S., M. Niihama, et al. (2010). "gorgon, a novel missense mutation in the SHOOT MERISTEMLESS gene, impairs shoot meristem homeostasis in Arabidopsis." Plant Cell Physiol **51**(4): 621-34.
- Tanaka-Ueguchi, M., H. Itoh, et al. (1998). "Over-expression of a tobacco homeobox gene, NTH15, decreases the expression of a gibberellin biosynthetic gene encoding GA 20-oxidase." Plant J **15**(3): 391-400.
- Tangl, E. (1884). Zur Lehre von der Continuität des Protoplasmas im Pflanzengewebe. Wien.
- Tangl, E. (1885). Studien Über das Endosperm einiger Gramineen. Wien.
- Tanner, W., J. Malinsky, et al. (2011). "In plant and animal cells, detergent-resistant membranes do not define functional membrane rafts." Plant Cell **23**(4): 1191-3.
- Taoka, K. I., B. K. Ham, et al. (2007). "Reciprocal Phosphorylation and Glycosylation Recognition Motifs Control NCAPP1 Interaction with Pumpkin Phloem Proteins and Their Cell-to-Cell Movement." Plant Cell.
- Tassetto, M., A. Maizel, et al. (2005). "Plant and animal homeodomains use convergent mechanisms for intercellular transfer." EMBO Rep **6**(9): 885-90.
- Taylor, J. E. and C. A. Whitelaw (2001). "Tansley Review No. 127. Signals in Abscission." New Phytologist **151**(2): 323-339.
- Thomas, C. L., E. M. Bayer, et al. (2008). "Specific targeting of a plasmodesmal protein affecting cell-to-cell communication." PLoS Biol **6**(1): e7.
- Tian, G. W., M. H. Chen, et al. (2006). "Pollen-specific pectin methylesterase involved in pollen tube growth." Dev Biol **294**(1): 83-91.
- Tian, Q., L. Olsen, et al. (2007). "Subcellular localization and functional domain studies of DEFECTIVE KERNEL1 in maize and Arabidopsis suggest a model for aleurone cell fate specification involving CRINKLY4 and SUPERNUMERARY ALEURONE LAYER1." Plant Cell **19**(10): 3127-45.
- Till, B. J., S. H. Reynolds, et al. (2003). "Large-scale discovery of induced point mutations with high-throughput TILLING." Genome Res **13**(3): 524-30.
- Tilney, L. G., T. J. Cooke, et al. (1991). "The structure of plasmodesmata as revealed by plasmolysis, detergent extraction, and protease digestion." J Cell Biol **112**(4): 739-47.
- Tilsner, J., K. Amari, et al. (2011). "Plasmodesmata viewed as specialised membrane adhesion sites." Protoplasma **248**(1): 39-60.
- Torii, K. U., N. Mitsukawa, et al. (1996). "The Arabidopsis ERECTA gene encodes a putative receptor protein kinase with extracellular leucine-rich repeats." Plant Cell **8**(4): 735-46.
- Traas, J. and T. Vernoux (2002). "The shoot apical meristem: the dynamics of a stable structure." Philos Trans R Soc Lond B Biol Sci **357**(1422): 737-47.
- Truernit, E. and J. Haseloff (2008). "Arabidopsis thaliana outer ovule integument morphogenesis: ectopic expression of KNAT1 reveals a compensation mechanism." BMC Plant Biol **8**: 35.
- Truernit, E., K. R. Siemerling, et al. (2006). "A map of KNAT gene expression in the Arabidopsis root." Plant Mol Biol **60**(1): 1-20.

- Turgeon, R. and S. Wolf (2009). "Phloem transport: cellular pathways and molecular trafficking." *Annu Rev Plant Biol* **60**: 207-21.
- Ung, N., S. Lal, et al. (2011). "The role of PENNYWISE and POUND-FOOLISH in the maintenance of the shoot apical meristem in Arabidopsis." *Plant Physiol* **156**(2): 605-14.
- Vaten, A., J. Dettmer, et al. (2011). "Callose biosynthesis regulates symplastic trafficking during root development." *Dev Cell* **21**(6): 1144-55.
- Venglat, S. P., T. Dumonceaux, et al. (2002). "The homeobox gene BREVIPEDICELLUS is a key regulator of inflorescence architecture in Arabidopsis." *Proc Natl Acad Sci U S A* **99**(7): 4730-5.
- Venter, J. C., M. D. Adams, et al. (2001). "The sequence of the human genome." *Science* **291**(5507): 1304-51.
- Vieira, F. S., G. Correa, et al. (2010). "Host-cell lipid rafts: a safe door for micro-organisms?" *Biol Cell* **102**(7): 391-407.
- Wada, T., T. Kurata, et al. (2002). "Role of a positive regulator of root hair development, CAPRICE, in Arabidopsis root epidermal cell differentiation." *Development* **129**(23): 5409-19.
- Waigmann, E., M. H. Chen, et al. (2000). "Regulation of plasmodesmal transport by phosphorylation of tobacco mosaic virus cell-to-cell movement protein." *EMBO J* **19**(18): 4875-84.
- Waigmann, E. and P. Zambryski (1995). "Tobacco mosaic virus movement protein-mediated protein transport between trichome cells." *Plant Cell* **7**(12): 2069-79.
- Wang, X.-Q. (2006). "Requirement of KNAT1/BP for the Development of Abscission Zones in Arabidopsis thaliana." *Journal of Integrative Plant Science* **48**(1): 15- 26.
- Weinl, C., S. Marquardt, et al. (2005). "Novel functions of plant cyclin-dependent kinase inhibitors, ICK1/KRP1, can act non-cell-autonomously and inhibit entry into mitosis." *Plant Cell* **17**(6): 1704-22.
- Wester, K., S. Digiuni, et al. (2009). "Functional diversity of R3 single-repeat genes in trichome development." *Development* **136**(9): 1487-96.
- White, R. G. and D. A. Barton (2011). "The cytoskeleton in plasmodesmata: a role in intercellular transport?" *J Exp Bot* **62**(15): 5249-66.
- Wickson, M., Tiemann, K. (1958). "The Antagonism of Auxin and Kinetin in Apical Dominance." *Physiologia Plantarum* **11**(1): 62-74.
- Wielopolska, A., H. Townley, et al. (2005). "A high-throughput inducible RNAi vector for plants." *Plant Biotechnol J* **3**(6): 583-90.
- Winter, D., B. Vinegar, et al. (2007). "An "Electronic Fluorescent Pictograph" browser for exploring and analyzing large-scale biological data sets." *PLoS One* **2**(8): e718.
- Winter, N. (2007). MPB2C a cytoplasmic protein involved in the control of macromolecular transport in plants via plasmodesmata. *Institute of Biochemistry*. Vienna, University of Vienna. **Mag.**
- Winter, N., G. Kollwig, et al. (2007). "MPB2C, a microtubule-associated protein, regulates non-cell-autonomy of the homeodomain protein KNOTTED1." *Plant Cell* **19**(10): 3001-18.
- Witthoft, J. and K. Harter (2011). "Latest news on Arabidopsis brassinosteroid perception and signaling." *Front Plant Sci* **2**: 58.
- Wolf, S., C. M. Deom, et al. (1989). "Movement protein of tobacco mosaic virus modifies plasmodesmatal size exclusion limit." *Science* **246**(4928): 377-9.
- Wolf, S., G. Mouille, et al. (2009). "Homogalacturonan methyl-esterification and plant development." *Mol Plant* **2**(5): 851-60.
- Wolfe-Simon, F., J. Switzer Blum, et al. (2011). "A bacterium that can grow by using arsenic instead of phosphorus." *Science* **332**(6034): 1163-6.
- Wu, S. and K. L. Gallagher (2011). "Mobile protein signals in plant development." *Curr Opin Plant Biol* **14**(5): 563-70.
- Wu, S. and H. Smith (2012). "Out of step: The function of TALE homeodomain transcription factors that regulate shoot meristem maintenance and meristem identity." *Frontiers in Biology* **7**(2): 144-154.

- Wu, X., J. R. Dinneny, et al. (2003). "Modes of intercellular transcription factor movement in the Arabidopsis apex." *Development* **130**(16): 3735-45.
- Xia, G., S. Ramachandran, et al. (1996). "Identification of plant cytoskeletal, cell cycle-related and polarity-related proteins using *Schizosaccharomyces pombe*." *Plant J* **10**(4): 761-9.
- Xoconostle-Cazares, B., Y. Xiang, et al. (1999). "Plant paralog to viral movement protein that potentiates transport of mRNA into the phloem." *Science* **283**(5398): 94-8.
- Xu, J. and N. H. Chua (2010). "Processing bodies and plant development." *Curr Opin Plant Biol* **14**(1): 88-93.
- Xu, L. and W. H. Shen (2008). "Polycomb silencing of KNOX genes confines shoot stem cell niches in Arabidopsis." *Curr Biol* **18**(24): 1966-71.
- Xu, L., Y. Xu, et al. (2003). "Novel as1 and as2 defects in leaf adaxial-abaxial polarity reveal the requirement for ASYMMETRIC LEAVES1 and 2 and ERECTA functions in specifying leaf adaxial identity." *Development* **130**(17): 4097-107.
- Xu, M., E. Cho, et al. (2012). "Plasmodesmata formation and cell-to-cell transport are reduced in decreased size exclusion limit 1 during embryogenesis in Arabidopsis." *Proc Natl Acad Sci U S A* **109**(13): 5098-103.
- Xu, X. M. and D. Jackson (2010). "Lights at the end of the tunnel: new views of plasmodesmal structure and function." *Curr Opin Plant Biol* **13**(6): 684-92.
- Xu, X. M., J. Wang, et al. (2011). "Chaperonins facilitate KNOTTED1 cell-to-cell trafficking and stem cell function." *Science* **333**(6046): 1141-4.
- Yadav, R. K., T. Girke, et al. (2009). "Gene expression map of the Arabidopsis shoot apical meristem stem cell niche." *Proc Natl Acad Sci U S A* **106**(12): 4941-6.
- Yadav, R. K., M. Perales, et al. (2011). "WUSCHEL protein movement mediates stem cell homeostasis in the Arabidopsis shoot apex." *Genes Dev* **25**(19): 2025-30.
- Yahalom, A., R. D. Warmbrodt, et al. (1991). "Maize Mesocotyl Plasmodesmata Proteins Cross-React with Connexin Gap Junction Protein Antibodies." *Plant Cell* **3**(4): 407-417.
- Yamaguchi, N., A. Yamaguchi, et al. (2012). "LEAFY controls Arabidopsis pedicel length and orientation by affecting adaxial-abaxial cell fate." *Plant J* **69**(5): 844-56.
- Yamaguchi, S. (2008). "Gibberellin metabolism and its regulation." *Annu Rev Plant Biol* **59**: 225-51.
- Yanai, O., E. Shani, et al. (2005). "Arabidopsis KNOX1 proteins activate cytokinin biosynthesis." *Curr Biol* **15**(17): 1566-71.
- Yang, Y., A. Costa, et al. (2008). "Isolation of a strong Arabidopsis guard cell promoter and its potential as a research tool." *Plant Methods* **4**: 6.
- Zhao, Z., W. Zhang, et al. (2008). "Functional proteomics of Arabidopsis thaliana guard cells uncovers new stomatal signaling pathways." *Plant Cell* **20**(12): 3210-26.
- Zhong, R., C. Lee, et al. (2008). "A battery of transcription factors involved in the regulation of secondary cell wall biosynthesis in Arabidopsis." *Plant Cell* **20**(10): 2763-82.

12 Curriculum Vitae

Name: Nikola Winter
Birth date: January 8th 1981 in Vienna, Austria
Nationality: Austrian
Languages: German (native), English, French (basics)
Academic Degree: Mag.

Education:

2008 - 2012 Doctoral studies of Molecular Biology at the University of Vienna
2000 - 2007 Study of Molecular Biology at the University of Vienna
Graduation: October 16th 2007
1991 - 1999 Bundesgymnasium Zirkusgasse 48, Vienna
Graduation June 18th 1999

Publications:

Nikola Winter, Gregor Kollwig, Shoudong Zhang, and Friedrich Kragler: „MPB2C, a Microtubule-Associated Protein, Regulates Non-Cell-Autonomy of the Homeodomain Protein KNOTTED1“, The Plant Cell 19: 3001-3018; October 26, 2007

Oral presentations at international meetings:

- “Studying the Role of MPB2C in Homeodomain protein cell-to-cell transport in Arabidopsis”, Cold Spring Harbor Laboratories Course “Molecular Techniques in Plant Sciences”, 26/06/09 – 15/08/09, Cold Spring Harbor Laboratories, USA
- “Regulation of STM cell-to-cell movement” 07/10/09 – 09/10/09 International PhD School on Plant Development Retzbach, Germany
- „MPB2C - at the crossroad of cell-to-cell transport with defense and development” 21/03/10 – 26/03/10 Plasmodesmata Conference in Sydney, Australia

International Experience:

- 04/09/08 - 08/09/08: Advanced Workshop on Structure and Function of mRNP, University of Aarhus, Denmark
- 25/06/09 – 16/07/09: Course „Molecular Techniques in Plant Sciences“, Cold Spring Harbor Laboratories, New York, USA
- 22/08/09 – 13/09/09: Visiting researcher in the laboratory of David Jackson, Cold Spring Harbor Laboratories, New York, USA